Non-proteinaceous effectors of *Botrytis cinerea*

Contributions and modes of action during the interaction with hosts

Si Qin

Propositions

1. *Dicer-like* genes of *Botrytis cinerea* are inappropriate targets for spray-induced gene silencing to control the disease.
(this thesis)

2. Botrydial is the cell death-inducing effector that has a highest impact on the virulence among all known effectors of *Botrytis cinerea*.
(this thesis)

3. It is worthwhile to improve the quality of genome assemblies and annotations, especially for organisms that were among the first to be sequenced.

4. Scientists can better focus on addressing research questions and experimental designs when routine techniques are outsourced to external parties.

5. Scientists benefit from having hobbies in addition to research.

6. The requirement to provide propositions with a PhD thesis is outdated and bears no relevance for demonstrating the scientific qualifications of a PhD candidate.

Propositions belonging to the thesis, entitled

Non-proteinaceous effectors of *Botrytis cinerea*:

Contributions and modes of action during the interaction with hosts

Si Qin

Wageningen, 4 July 2023

Non-proteinaceous effectors of *Botrytis cinerea*:

Contributions and modes of action during the interaction with hosts

Si Qin

Thesis committee

Promotor
Dr J. A. L. van Kan
Associate professor, Laboratory of Phytopathology
Wageningen University & Research

Co-promotor
Dr J. J. B. Keurentjes
Associate professor, Laboratory of Genetics
Wageningen University & Research

Other members
Prof. Dr G. Smant, Wageningen University & Research
Dr P. M. Bleeker, University of Amsterdam
Dr L. Zhang, Eberhard Karls Universität Tübingen, Germany
Dr E. P. Benito, Universidad de Salamanca, Spain

This research was conducted under the auspices of the Graduate School
Experimental Plant Sciences

Non-proteinaceous effectors of *Botrytis cinerea*:

Contributions and modes of action during the interaction with hosts

Si Qin

Thesis

submitted in fulfilment of the requirements for the degree of doctor
at Wageningen University
by the authority of the Rector Magnificus,
Prof. Dr A.P.J. Mol,
in the presence of the
Thesis Committee appointed by the Academic Board
to be defended in public
on Tuesday 4 July 2023
at 1:30 p.m. in the Omnia Auditorium.

Si Qin
Non-proteinaceous effectors of *Botrytis cinerea*: Contributions and modes of action during the interaction with hosts,
233 pages.

PhD thesis, Wageningen University, Wageningen, the Netherlands (2023)
With references, with summary in English

ISBN 978-94-6447-696-5
DOI https://doi.org/10.18174/630135

Table of contents

Chapter 1

General introduction

Effectors of filamentous pathogens: an arsenal containing diverse molecules

***Botrytis cinerea* as a case study**

Introduction

Agricultural crops can be infected by filamentous plant pathogens, including pathogenic fungi and oomycetes, leading to huge pre- and post-harvest losses. Based on the different lifestyles of plant pathogens, they can be classified as biotrophs, necrotrophs or hemibiotrophs. Biotrophic microorganisms feed and complete their life cycle on living plant tissues; necrotrophic pathogens kill host cells and then take up nutrients from the dead tissues; and hemibiotrophs first colonize the living host with a biotrophic life style for a period and then switch to a necrotrophic behaviour and feed on dead tissues. Plant pathogens deploy multiple distinct strategies in order to enable them to colonize their hosts. Among these strategies, the secretion of molecules which are referred to as "effectors" can effectively facilitate the infection of the hosts by pathogens. However, the definition of effectors has been undergoing a dynamic evolution, which until today has not yet reached a consensus among biologists that study the molecular mechanisms in plant-pathogen interactions.

The term effector initially emerged in the field of plant-microbe interactions by the end of last century and started to become popular in the early 2000s (Hogenhout et al., 2009). In the beginning, small proteins delivered through the type III secretion system of gram-negative bacteria were found to trigger hypersensitive response (HR) in resistant plants, resulting in an "avirulence" effect. However, later on these proteins were shown to play a positive role in virulence on susceptible hosts. Therefore, the term effector arose, which resolved the conceptual limitation of "avirulence factor" or "virulence factor" and reflected the dual activities of such proteins. Hereafter, an increasing number of biologists adopted the term effector, in order to describe secreted proteins and other molecules produced by different plant-associated microbes, which can modulate the interactions between the microbes and their hosts. Undoubtedly, the term effector nowadays is well accepted and widely used in the fungal and oomycete research community. Hogenhout et al. (2009) defined effectors as "all pathogen proteins and small molecules that alter host-cell structure and function. These alterations either facilitate infection (virulence factors and toxins) or trigger defense responses (avirulence factors and elicitors) or both." The term was more narrowly defined by lo Presti et al. (2015) as "Effectors suppress plant defense responses and modulate plant physiology to accommodate fungal invaders and provide them with nutrients". In the light of the previous definitions of effectors though with minor modifications, the term effector in this chapter refers to any secreted molecules from the filamentous plant pathogens that suppress or induce plant defense responses and modulate plant physiology. There are also reports of effectors that indirectly affect the host

colonization by manipulating the microbial community on or in the host tissue (Snelders et al., 2018). Such effectors are not discussed in this chapter, in order to frame the interest only within bipartite interactions between pathogens and plants.

This chapter will discuss four different categories of effectors produced by filamentous plant pathogens, as well as the molecular basis of the interactions between effector molecules and their plant targets. Effectors of the model necrotrophic fungus *Botrytis cinerea* will be spotlighted, as the pathogen has an extremely broad host range and produces a functionally and structurally diverse pool of effectors. In the end, I will summarize the advances in studying and utilizing the effector biology of filamentous pathogens (especially *B. cinerea* as a model species), and also conjecture the future perspectives for development of plant natural resistant resources against these pathogens.

Effector proteins

The proteinaceous effectors are usually secreted, small and cysteine-rich proteins. They are the most extensively studied and considered as "classical" effectors. The first fungal effector gene Avr9 was cloned in 1991 from the tomato leaf mould fungus *Cladosporium fulvum* (van Kan et al., 1991). Later on, more *C. fulvum* Avr proteins, namely Avr2, Avr4, Avr4E and Avr5, were identified (Joosten et al., 1994; Mesarich et al., 2014; Rooney et al., 2005; Westerink et al., 2004). Even though *C. fulvum* Avr effectors all accumulate in the plant apoplast after being secreted by the fungus, their functions are quite diverse. Avr2 functions as an inhibitor of the tomato Rcr3 gene product which is an extracellular cysteine protease (Rooney et al., 2005) while Avr4 binds chitin which enables it to protect fungal cell walls from hydrolysis by plant chitinases (van den Burg et al., 2006) and the molecular functions of Avr4E, Avr5 and Avr9 remain elusive. Meanwhile, plants have evolved intricate defense mechanisms, one of which is the induction of HR. The Cf proteins in tomato plants recognize their matching Avr effectors, triggering HR which restricts the growth of the biotroph *C. fulvum* and thereby establishes host resistance. This phenomenon that the HR is elicited by the interaction between one resistance gene product from the plant and one effector gene product from the pathogen provided the conceptual evidence for the "gene-for-gene" model, which was initially proposed more than half a century ago, purely based on genetic information (Flor, 1954).

On the contrary, if the interaction between an effector from a necrotrophic pathogen and a receptor from the plant triggers plant programmed cell death, it may promote the disease development of the necrotroph that feeds on dead tissues. This is termed "inverse gene-for-gene" interaction (Friesen et al., 2007), and the induction of host cell death is considered to be the most common mode of action of the necrotrophic effectors. Molecular studies

have characterized a number of effector proteins from the model necrotrophic pathogen *B. cinerea* that induce host cell death. Two phytotoxic proteins that are homologous to a necrosis and ethylene-inducing protein (NEP) from *Fusarium oxysporum* were identified in *B. cinerea*, and referred to as BcNEP1 and BcNEP2 (Staats et al., 2007). A cerato-platanin family protein BcSPL1, and a highly abundant protein in the *B. cinerea* secretome BcIEB1 were shown to elicit cell death in host plants (Frías et al., 2011, 2016). None of the four above cell death inducing proteins possesses a known enzyme activity. However, even some enzymes secreted by *B. cinerea* display cell death-inducing activities that do not require their catalytic activity, such as the xylanases BcXyn11A (Noda et al., 2010) and BcXyl1 (Yang et al., 2018), the xyloglucanase BcXYG1 (Zhu, Ronen, et al., 2017), several polygalacturonases (PGs) (Zhang et al., 2014) and glucoamylase BcGs1 (Zhang et al., 2015). Among all *B. cinerea* effectors described above, the plant components that are required for their cell death inducing capacity have only partly been uncovered, specifically for BcNEP1/2, BcPGs and BcXyn11. The glycosylinositol phosphorylceramide sphingolipids present in plant plasma membranes were found to act as receptors for the necrosis and ethylene-inducing peptide 1–like (NLP) toxins which include BcNEP1 and BcNEP2 (Lenarčič et al., 2017). The Arabidopsis leucine-rich repeat receptor-like protein AtRLP42 was shown to be responsible for the recognition of BcPGs (Zhang et al., 2014). Two tomato *LeEIX* proteins (*LeEIX1* and *LeEIX2*) have been identified to be receptors for ethylene-inducing xylanase that induce cell death, but only LeEIX2 can transduce the signaling for the induction of HR and LeEIX1 attenuates the defense responses induced by the Eix/LeEIX2 interaction (Bar et al., 2010; Ron & Avni, 2004). It is possible that the *B. cinerea* xylanase BcXyn11A -induced HR can also be mediated via interacting with LeEIX2. Interestingly, the host programmed cell death (PCD) induced by BcXyl1 and BcXYG1 required the plant LRR receptor-like kinases (RLKs) BAK1 and SOBIR1 (Yang et al., 2018; Zhu, Ronen, et al., 2017), suggesting that the perception of BcXyl1 and BcXYG1 may be dependent on individual LRR-RLPs which require BAK1 and SOBIR1 for downstream signal transduction (van der Burgh & Joosten, 2019).

For hemibiotrophs, effectors expressed during the first biotrophic phase and the ones produced during the subsequent necrotrophic phase are likely to display different (maybe even opposite) effects on the host plant. These effectors should favor the infection by first helping the pathogen with escaping or suppressing plant defense in the biotrophic phase, and by inducing host cell death in the necrotrophic phase. For instance, the hemibiotrophic oomycete pathogen *Phytophthora infestans* produces the cell death-suppressing effector PiSNE1 during the early biotrophic growth on tomato (Kelley et al., 2010), while the gene encoding a necrosis-inducing NLP protein PiNPP1 is up-regulated during the necrotrophic stage (Kanneganti et al., 2006).

Small RNAs (sRNAs)

Besides proteins, the production by plant pathogenic microbes of small RNAs that function as effectors has come into the picture in the past decade. Weiberg et al. (2013) reported for the first time that sRNAs derived from *B. cinerea* can be translocated into host cells during infection. Among these *B. cinerea* secreted sRNAs, some of them were reported to suppress the expression of host target genes related to plant immunity, and thus these sRNAs produced by the pathogen were proposed to act as a novel class of fungal effectors that function through cross-kingdom RNA interference (ck-RNAi) (Weiberg et al., 2013). It was reported that deletion of Dicer-like (*Dcl*) genes in *B. cinerea* (namely *Bcdcl1* and *Bcdcl2*) almost abolished the production of sRNA molecules with the size of 20–26 nt (Wang et al., 2016). This *B. cinerea* mutant displayed a significant reduction in fungal virulence on Arabidopsis and tomato leaves (Weiberg et al., 2013), suggesting that the *B. cinerea* sRNAs generated through the DCL-dependent pathways are virulence factors. Later on, the same research group reported that a single *B. cinerea* small RNA Bc-siR37 was predicted to target at least 15 Arabidopsis genes, of which eight genes were down-regulated during *B. cinerea* infection. Besides, Arabidopsis mutants overexpressing Bc-siR37 exhibited enhanced susceptibility to *B. cinerea*. These observations collectively indicated that Bc-siR37 can suppress plant immunity by cross-kingdom RNAi (Wang et al., 2017).

The naturally occurring ck-RNAi is a relatively young topic in the field of plant-microbe interactions. At the start of this PhD project, there were no other studies showing that sRNA molecules from filamentous plant pathogens (other than *B. cinerea*) can function as effectors by targeting host genes for silencing. Nevertheless, this phenomenon is possibly a wide-spread mechanism in other pathosystems. For example, a genome-wide degradome study combined with sRNA sequencing revealed that the oomycete pathogen *Plasmopara viticola* produces a large number of sRNAs which may target transcripts in the host grapevine (Brilli et al., 2018).

Secondary metabolites and peptides

Phytotoxins, including phytotoxic secondary metabolites (SMs) and peptides, can be considered effectors if they are capable to induce PCD via interacting with plant components and subsequently triggering downstream signaling pathways. Phytotoxins are traditionally categorized into host-specific toxins (HSTs) and non-host specific toxins (nHSTs), depending on the spectrum of host species that are sensitive to a toxin, rather than on the chemical structures or properties of the toxin. By definition, HSTs are only toxic to a certain plant species or plant family and they function as essential determinants for host-specificity

of the pathogen (Wolpert et al., 2002). Opposite to HSTs, nHSTs are biologically active in a broad spectrum of host species and are not the determinants of host specificity of the pathogens that produce these toxins (Berestetskiy, 2008).

The cell death-inducing mechanism of most HSTs has not been characterized at the molecular level, despite that the HST-receptor model had been proposed six decades ago by Pringle & Scheffer (1964). There are two well characterized cases of HSTs that have been demonstrated to induce apoptosis. The AAL-toxin TA from the tomato pathotype of *Alternaria alternata* (*A. alternata* f sp *lycopersici*) induces apoptotic-like cell death in toxin-sensitive tomato, as proven by detection of several representative features of apoptosis including TUNEL-positive cells, DNA laddering and the formation of apoptotic-like bodies (Wang et al., 1996). The AAL toxin is chemically related to sphingosines and interferes with the activity of ceramide synthase in tomato cells, resulting in depletion of ceramide and accumulation of toxic sphingolipid intermediates which culminates in the induction of apoptosis (Michaelson et al., 2016). The HST victorin (a cyclic peptide) produced by the oat victoria blight fungus *Cochliobolus victoriae* was also found to induce apoptosis, demonstrated by the detection of relevant cellular hallmarks including DNA laddering, heterochromatin condensation, cell shrinkage and protease activation (Curtis & Wolpert, 2004; Navarre & Wolpert, 1999; Yao et al., 2001). The sensitivity to victorin and susceptibility to *C. victoriae* were first reported to be associated with a dominant allele at the oat *Vb* locus, the product of which was later shown to be a 100-kDa protein that binds to victorin (Wolpert et al., 1994; Wolpert & Macko, 1989). A later study identified an intracellular coiled-coil nucleotide-binding site-leucine rich repeat (CC-NBS-LRR) receptor, encoded by the *LOV1* gene in Arabidopsis, that confers the sensitivity to victorin and susceptibility to *C. victoriae* (Lorang et al., 2007). However, victorin does not bind directly to LOV1, but it physically interacts with a thioredoxin h5 (TRXh5) which regulates the activity of NPR1 (the central regulator of systemic acquired resistance) and TRXh5 is probably guarded by the LOV1 receptor (Gilbert & Wolpert, 2013; Wolpert & Lorang, 2016). Besides, it has been found that some other types of plant components can also function as targets for HSTs. The cyclic tetrapeptide HC-toxin produced by *C. carbonum* inhibits host histone-deacetylases and leads to H3 and H4 histone-hyperacetylation, such that transcript levels of many genes in maize are disturbed (Broschla et al., 1995). The linear polyketides T-toxin of *C. heterostrophus* race T and PM-toxin of *Mycosphaerella zeae-maydis* directly bind to the mitochondrial protein URF13, resulting in perforation of mitochondrial membranes (Rhoads et al., 1995; Yun et al., 1998). A number of perylenequinone toxins, including cercosporin from *Cercospora* spp. and elsinochromes from *Elsinoë* spp., are able to induce

the production of singlet oxygen and superoxide under light condition, which trigger plant cell death (Daub & Briggs, 1983; Liao & Chung, 2008).

In general, nHSTs show relatively mild phytotoxic effects, and act as quantitative virulence factors that do not determine the pathogenicity but only enhance disease severity. The knowledge about the mode of action of nHSTs is limited, but a few studies have reported nHSTs that can elicit PCD. The nHST tenuazonic acid produced by *Alternaria alternata* blocks the Q_B-binding site of photosystem II, leading to increased generation of singlet oxygen, which activates an EXECUTER proteins-dependent pathway and triggers a PCD response (S. Chen et al., 2015). The sesquiterpene botrydial produced by a number of *Botrytis* spp. was shown to induce PCD, as suggested by callose deposition, accumulation of ROS and phenolic compounds in leaf tissues that were treated with pure botrydial (Rossi et al., 2011). The botrydial-triggered PCD is influenced by plant hormone signaling pathways, as salicylic acid signaling-impaired Arabidopsis mutants were less sensitive while jasmonate-insensitive mutant were more sensitive to botrydial compared with wild type Arabidopsis (Rossi et al., 2011). Another major type of phytotoxin from *B. cinerea* is the polyketide botcinic acid and its derivatives, of which the mode of action is barely studied. Botrydial and botcinic acid, despite being chemically distinct, were reported to have functional redundancy in the virulence of *B. cinerea* (Dalmais et al., 2011). Oxalic acid produced by *Sclerotinia sclerotiorum* and related species such as *B. cinerea* can be considered as an effector as well. It is reported that oxalic acid plays a versatile role in the pathogen-plant interaction. Oxalic acid lowers the ambient pH, which provides a microenvironment that enhances the activities of some secreted enzymes from fungi (e.g., endo-PGs, aspartic protease and laccase) but inhibits the activity of PG-inhibiting proteins from the host plant (Favaron et al., 2004; Manteau et al., 2003; Nakajima & Akutsu, 2014; ten Have et al., 2002). Oxalic acid was also shown to inhibit the oxidative burst in the host plant (Cessna et al., 2000), and induce apoptotic-like PCD (K. S. Kim et al., 2008).

Genome analyses in plant pathogens have revealed that the capacity to produce SMs differs between microbes with distinct lifestyles. In general, obligate biotrophs contain a smaller number of (active) SM gene clusters as compared to necrotrophs and hemibiotrophs. For example, genes involved in secondary metabolism, such as dimethylallyl diphosphate tryptophan synthase, terpene cyclase, polyketide synthase (PKS) or nonribosomal peptide synthetase (NRPS), are either completely missing or rare in the genome of the barley powdery mildew *Blumeria graminis* f.sp. *hordei* (Raffaele et al., 2010) which is a Leotiomycete, phylogenetically related to the necrotroph *B. cinerea* that contains in its genome a total of 43 SM key biosynthetic genes (Amselem et al., 2011). Only a limited number of fungal SMs have a role in primary physiological processes, acting as UV-

protectant pigment or siderophore, while some are known to possess antibiotic activity that participates in microbial competition. For a significant number of SM biosynthetic gene clusters, their products have not been chemically identified and their biological function remains largely elusive. A number of such SMs might function as effector molecules and participate in virulence, provided that their corresponding biosynthetic genes are expressed during relevant stages of host infection. However, there are currently more examples of SMs that may have no contribution to the biotrophic colonization or even a negative impact on host infection. Biosynthetic genes of such SMs are usually down-regulated during infection, and otherwise these SMs may act as "avirulence factors". For example, the biotrophic tomato leaf mould *C. fulvum* possesses 23 core SM genes, including genes responsible for the production of cercosporin and elsinochrome, which are barely expressed or down-regulated during infection of tomato (Collemare et al., 2014). Another example of a gene that acts as an "avirulence gene" was described in the hemibiotrophic rice blast fungus *Magnaporthe oryzae*. The *ACE1* gene encodes an enzyme that contains both PKS and NRPS domains and produces an uncharacterized secondary metabolite which can be recognized by the Pi33 protein in resistant rice cultivars. The *ACE1* gene is exclusively expressed in appressoria during host surface penetration (Böhnert et al., 2004; Fudal et al., 2007). Such SMs acting as avirulence effectors may not only be expressed in the biotrophic phase of hemibiotrophs, but could also be present in strictly biotrophic pathogens.

Production by pathogens of plant hormones or molecules interfering with plant hormone signaling

Plant hormones are strongly linked to plant development and involved in triggering important signaling processes when encountering biotic and abiotic stresses (Chanclud & Morel, 2016). The plant hormones jasmonic acid (JA), salicylic acid (SA), ethylene (ET), abscisic acid (ABA) and cytokinins (CKs) have been described to function as important regulators in plant immunity (Denancé et al., 2013). Interestingly, several studies have revealed that microbial pathogens can also produce such plant hormones or molecules that mimic plant hormones, and thereby manipulate plant physiology to favor the invasion of these pathogens. Therefore, these pathogen-derived plant hormones can be classified as effectors regarding the term defined in this chapter, and below I review the (potential) roles of plant hormones produced by *B. cinerea* in plant-pathogen interactions.

The antagonistic crosstalk between SA and JA signaling pathways has been extensively studied, and these two hormones are major players in plant immunity (Gimenez-Ibanez et al., 2013). Traditionally, SA is considered to be required for immunity against biotrophic microorganisms, while JA is involved in plant defense against necrotrophic pathogens (Spoel

et al., 2007). SA or its derivatives can be produced by some plant pathogens, such as the hemibiotrophic cacao pathogen, *Moniliophthora perniciosa*. Although there has been no evidence that *B. cinerea* can produce SA directly, it was reported that an exopolysaccharide derived from *B. cinerea* acts as an elicitor of the SA pathway. In turn, the SA pathway antagonizes the JA signaling pathway, thereby allowing the fungus to promote disease in tomato (El-Oirdi et al., 2011). ET is a volatile phytohormone that induces fruit ripening and participates in multiple physiological processes ranging from senescence to vegetative growth (Bleecker & Kende, 2000). ET production was reported in many plant pathogens, including *B. cinerea* that produces ET both *in vitro* and in tomato fruits (Cristescu et al., 2002). However, the production of ET by *B. cinerea in vitro* requires high concentrations of free methionine as precursor and it is unlikely that such precursor concentrations can be achieved in a host plant environment. Thus, ET levels produced by *B. cinerea* are unlikely to be sufficient to make a meaningful impact on the plant-fungus interaction, and it remains to be investigated whether ET production by *B. cinerea* plays a role in the infection process.

Enhanced abscisic acid (ABA) levels in plants are known to be correlated with increased susceptibility to pathogens, and several pathogenic fungal genera have been reported to produce ABA (Crocoll et al., 1991; Dörffling et al., 1984; Mauch-Mani & Mauch, 2005). *B. cinerea* was the second fungus ever reported to produce ABA *in vitro* (Marumo et al., 1982), shortly after a similar report in *Cercospora rosicola* (Assante et al., 1977). Exogenous application of ABA to tomato plants increases susceptibility and ABA -deficient or ABA-insensitive plants are more resistant to *B. cinerea* (Audenaert et al., 2002; Lai et al., 2014), suggesting that the ABA production from *B. cinerea* might contribute to enhanced host susceptibility. The ABA biosynthetic gene cluster was cloned and turned out to be present in three isolates of *B. cinerea*, including B05.10 (Siewers et al., 2006), however, the contribution of ABA production by *B. cinerea* in virulence remains to be clarified.

CKs have been known to play an important role in plant growth for a long time, but the effects of CKs in plant-pathogen interactions are only recently being investigated more extensively. CKs produced by biotrophic and hemibiotrophic pathogens can act as virulence factors, as was illustrated in the biotrophs *U. maydis* (Morrison et al., 2017) and *Claviceps purpurea* (Hinsch et al., 2015; Kind et al., 2018), and in the hemibiotrophs *Colletotrichum graminicola* (Behr et al., 2012) and *M. oryzae* (Chanclud et al., 2016). By contrast, there are no reports of necrotrophic plant pathogens that secrete CKs during infection.

Effector biology in *B. cinerea* as a case study

Genomic, transcriptomic, secretomic and metabolomic techniques in combination with improved computational tools have eased the prediction and identification of

proteinaceous and non-proteinaceous effectors. The gapless genome assembly of *B. cinerea* (van Kan et al., 2017) has strongly stimulated the research on *B. cinerea* effector biology. Even when using the previous, inaccurate version of *B. cinerea* genome assembly as reference (Amselem et al., 2011), the number of predicted effector proteins by the computational tool EffectorP reached 183 which represented 18.4% of the *B. cinerea* secretome (Sperschneider et al., 2016). More than 40 gene clusters for the biosynthesis of SMs (polyketides, terpenes, nonribosomal peptides and alkaloids) were detected in the *B. cinerea* genome, indicating that there is potential for the fungus to produce many more SMs than the few that have been studied till now (I. G. Collado & Viaud, 2015). Transcriptomic analyses together with sRNA-sequencing profiles offered the insight that sRNAs from *B. cinerea* can be translocated into plant cells and silence plant genes and vice versa, during the *B. cinerea* – host interaction (Weiberg et al., 2013; Wang et al., 2016, 2017).

The model in Figure 1 illustrates that *B. cinerea* secretes diverse types of effector molecules that either modulate host immunity, tilt the balance of host hormone signaling, or induce plant PCD via hijacking host defense responses. The most extensively studied mechanism for the functioning of *B. cinerea* effectors is the induction of PCD, by interacting with plant targets to initiate the PCD signaling. *B. cinerea* infects an extremely broad spectrum of plant species by deploying a complex effector arsenal, which makes plant breeding for resistance to this notorious pathogen very challenging. Major genes conferring complete resistance to *B. cinerea* have not been reported, while mutation or deletion of particular susceptibility (*S*) genes might provide an effective alternative for obtaining resistance to *B. cinerea* (van Schie & Takken, 2014; Sun et al., 2017). Studying host targets of the *B. cinerea* PCD-inducing effectors might lead to the identification of *S* genes in host plants. Last but not least, prior to using an effector as a tool to identify *S* genes in the host, the contribution of such an effector to the virulence of the pathogen should be examined. Since not all effectors are necessarily virulence factors, the loss of function of a plant target of an effector that does not have impact on the fungal virulence will likely not alter plant resistance to the pathogen.

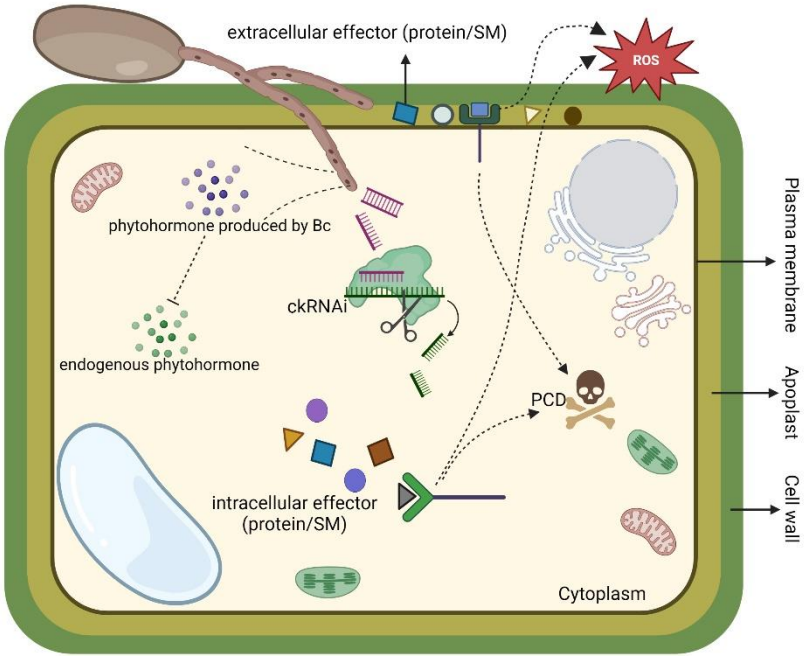

Figure 1. *B. cinerea* secretes diverse types of effector molecules, which include sRNAs produced by the fungus, extra-/intra-cellular proteinaceous/SM effectors and fungal production of phytohormones, into the host cell. For illustrating the effector molecules in more detail, the sizes of plant subcellular organelles and fungal effectors are not in real scales. The figure is created with BioRender.com.

Thesis outline

My thesis research focused on non-proteinaceous “atypical” effectors of *Botrytis,* specifically small RNAs and phytotoxic secondary metabolites (SMs). The role of these *Botrytis* effectors in fungal virulence as well as the molecular interactions between host plants and the effectors were studied.

To investigate the naturally occurring sRNA warfare between *B. cinerea* and tomato, we generated a sRNA/mRNA - sequencing dataset, with the aim to identify sRNAs produced by the fungus and the plant during early phases of the infection and to examine the expression of their predicted mRNA targets in the other organism. **Chapter 2** studies the effect of *B. cinerea* sRNAs on down-regulation of predicted target genes in tomato. We generated *B. cinerea mutants*, in which Dicer-like genes were deleted, to reduce sRNA production, and examined the consequence of this mutation on virulence on several plant species. In **Chapter 3**, we investigated the potential of plant sRNAs to suppress the expression of their predicted targets in *B. cinerea*. We generated a *B. cinerea* mutant in the *Bcspl1* gene in which the interaction between a tomato sRNA and its predicted target site in the *Bcspl1* mRNA would be abolished and examined the impact on the *Bcspl1* transcript level.

Chapter 4 describes the contribution of the phytotoxic sesquiterpene metabolite botrydial to the virulence of *B. cinerea* on different host species. Infection assays were performed to assess the virulence of the wild type *B. cinerea* and mutants that are unable to produce botrydial and another polyketide phytotoxin botcinic acid on Arabidopsis, tomato, *Nicotiana benthamiana*, French bean and cowpea plants. Besides testing the virulence of fungal mutants, we also tested the sensitivity to botrydial of a range of dicotyledons and monocotyledons.

A functional botrydial biosynthetic gene cluster is present in the genomes of the generalist *B. cinerea* and the lily-specific pathogen *B. elliptica*. In **Chapter 5** we show that *B. elliptica* can indeed produce botrydial *in vitro*, and we examined the expression of *B. elliptica* key genes for botrydial biosynthesis during the infection in lily. We studied the cell death responses to botrydial in four lily cultivars, both in leaves and petals, and compared the virulence of mutants that do not produce botrydial to the *B. elliptica* wild type strain.

In **Chapter 6** we describe that the *B. cinerea ΔBcbot2/ΔBcboa6* mutant which produces neither botrydial nor botcinic acid was almost non-virulent on tomato ("incompatible interaction”), when an inoculation medium was used in the virulence assay that differed from that used in Chapter 4 ("compatible interaction”). The virulence of the mutant was restored by supplementing yeast extract in the inoculation medium. An RNA sequencing

study was performed to investigate the changes in the fungal transcriptome between the incompatible and compatible interactions, to obtain insights into “backup” infection strategies of *B. cinerea* in the absence of botrydial and botcinic acid.

The PCD induced by botrydial has been reported to be mediated by SA/JA pathways, however, the underlying mechanism of the botrydial-induced PCD is largely unknown. In **Chapter 7** we applied genomic and genetic strategies to identify plant genes required for cell death induction by botrydial . On the one hand, we assessed the sensitivity to botrydial of Arabidopsis ecotypes belonging to a haplotype mapping population, and employed genome-wide association studies (GWAS) to pinpoint the allelic variations correlated with the sensitivity to botrydial. On the other hand, we crossed two Arabidopsis ecotypes that differed markedly in botrydial sensitivity and adopted a bulk-segregant analysis (BSA) to identify genetic loci correlated with insensitivity to botrydial. The results from both analyses were combined to select candidate genes for which T-DNA insertion mutants were tested.

Chapter 8 provides a general discussion of the key results in this project and future prospects of the effector biology studies in *B. cinerea* and other filamentous plant pathogens in a broader view.

Chapter 2

Molecular characterization reveals no functional evidence for naturally occurring cross-kingdom RNA interference in the early stages of *Botrytis cinerea*-tomato interaction

Si Qin[1*], Javier Veloso[1,2*], Guido Puccetti[1], Tim Bosman[1], Mirna Baak[3], Britt Boogmans[1], Xiaoqian Shi-Kunne[1], Sandra Smit[3], Robert Grant-Downton[4], Thomas Leisen[5], Matthias Hahn[5] and Jan A. L. van Kan[1]

[1]Laboratory of Phytopathology, Wageningen University, Netherlands

[2]FISAPLANT, University of A Coruña, Spain

[3]Bioinformatics Group, Wageningen University, Netherlands

[4]St. Peter's College, University of Oxford, UK

[5]Department of Biology, University of Kaiserslautern, Germany

[*] These authors equally contributed to this work

This chapter is published as:

Qin, S., Veloso, J., Baak, M., Boogmans, B., Bosman, T., Puccetti, G., Shi-Kunne, X., Smit, S., Grant-Downton, R., Leisen, T., Hahn, M. & van Kan, J. A. L. (2023). Molecular characterization reveals no functional evidence for naturally occurring cross-kingdom RNA interference in the early stages of *Botrytis cinerea*–tomato interaction. *Molecular Plant Pathology*, 24(1), 3-15.

Abstract

Plant immune responses are triggered during the interaction with pathogens. The fungus *Botrytis cinerea* has previously been reported to use small RNAs (sRNAs) as effector molecules capable of interfering with the host immune response. Conversely, a host plant produces sRNAs that may interfere with the infection mechanism of an intruder. We used high-throughput sequencing to identify sRNAs produced by *B. cinerea* and *Solanum lycopersicum* (tomato) during early phases of interaction and to examine the expression of their predicted mRNA targets in the other organism. A total of 7042 *B. cinerea* sRNAs were predicted to target 3185 mRNAs in tomato. Of the predicted tomato target genes, 163 were indeed transcriptionally down-regulated during the early phase of infection. Several experiments were performed to study a causal relation between the production of *B. cinerea* sRNAs and the down-regulation of predicted target genes in tomato. We generated *B. cinerea* mutants in which a transposon region was deleted that is the source of c.10% of the fungal sRNAs. Furthermore, mutants were generated in which both Dicer-like genes (*Bcdcl1* and *Bcdcl2*) were deleted and these displayed a >99% reduction of transposon-derived sRNA production. Neither of these mutants was significantly reduced in virulence on any plant species tested. Our results reveal no evidence for any detectable role of *B. cinerea* sRNAs in the virulence of the fungus.

Introduction

Grey mould caused by the fungus *Botrytis cinerea* is a disease that affects a wide range of hosts (Fillinger and Elad, 2016; van Kan et al., 2014). For many years, infection by *B. cinerea* was considered to mainly require production of phytotoxic metabolites and plant cell wall-degrading enzymes (van Kan, 2006). In the past decade it has become clear that *B. cinerea* also produces effector proteins with cell death-inducing capacity that may contribute to its virulence towards a broad range of host plants (Choquer et al., 2007; Noda et al., 2010; Zhu et al., 2017). An additional layer of complexity was revealed by the report that small RNAs (sRNAs) can act as a novel class of fungal effectors, which can be translocated into host cells and suppress the expression of host target genes by RNA interference (RNAi). A subset of these host genes is involved in immune responses, and their silencing by fungal sRNAs might thus facilitate invasion of the pathogen (Weiberg et al., 2013). It has been known for years that plant transgene-derived double-stranded RNAs (dsRNAs) could induce gene silencing in invading pathogens and pests (Baum et al., 2007; Iqbal et al., 2020; Nowara et al., 2010), a process referred to as host-induced gene silencing (HIGS). However, Weiberg et al. (2013) reported that a pathogen can also produce sRNAs that actively suppress host immune responses, indicative of a true RNA information warfare between *B. cinerea* and its host (Chaloner et al., 2016; Weiberg et al., 2014). This concept was later also demonstrated in other pathosystems. For instance, the parasitic plant *Cuscuta campestris* secretes microRNAs to silence plant genes involved in defense signaling to promote parasitism (Shahid et al., 2018). The pathogenic oomycete *Hyaloperonospora arabidopsidis* was also reported to deliver sRNAs to silence *Arabidopsis thaliana* defense genes and these sRNAs are important for virulence (Dunker et al., 2020). Moreover, Wong-Bajracharya et al. (2022) recently reported that small RNAs from the ectomycorrhizal fungus *Pisolithus microcarpus* can enter a host plant and regulate host transcripts in a symbiotic interaction. The first report that plant sRNAs are translocated to an invading fungal pathogen was in the cotton–*Verticillium dahliae* interaction (Zhang et al., 2016). Cai et al. (2018) demonstrated that a host plant can secrete exosome-like vesicles containing sRNAs that can subsequently be taken up by *B. cinerea* hyphae at the infection site. Another study by Hou et al. (2019) described how a plant can produce small interfering RNAs (siRNAs) to confer resistance to *Phytophthora capsici* through cross-kingdom RNAi, while inversely a *Phytophthora* effector can specifically inhibit the biogenesis of host siRNAs to facilitate infection. The delivery of host sRNAs can subsequently mediate silencing of genes in pathogens (Cai et al., 2018; Hou et al., 2019), indicating that sRNA translocation and RNAi induction between plants and microbial pathogens (fungi, oomycetes) is bidirectional. By contrast, Kettles et al. (2019) reported that RNAi-deficient *Zymoseptoria tritici* mutants were fully pathogenic to wheat

and *Z. tritici* was unable to take up external dsRNAs that were derived from transgenic wheat plants or artificially synthesized, suggesting that cross-kingdom RNAi may not occur in the wheat–*Z. tritici* pathosystem. Cross-kingdom RNAi seems to be confined to certain host–pathogen interactions and may not be a ubiquitous phenomenon.

Small RNAs are mostly cleaved products from non-coding double-stranded RNAs (dsRNAs) and single-stranded RNAs with hairpin structures, which are processed by the endoribonuclease activity of Dicer-like (DCL) proteins (Baulcombe, 2004; Ghildiyal & Zamore, 2009; Torres-Martínez & Ruiz-Vázquez, 2017). Complexes composed of sRNAs, Argonaute (AGO) proteins and auxiliary proteins conduct silencing of target mRNAs when the sRNAs are fully or partially complementary to their target (Novina & Sharp, 2004; Silvestri et al., 2019). Cross-kingdom RNAi caused by sRNAs generated by host and pathogens is considered a well-documented phenomenon that may have a significant effect on resistance or susceptibility during host–pathogen interactions (Dubey et al., 2019). For the first time, Weiberg et al. (2013) reported that the majority of sRNAs produced by *B. cinerea* during infection of *A. thaliana*, are derived from long terminal repeat (LTR) retrotransposons in the fungal genome. Interestingly, a recent study reported that retrotransposons can promote virulence of *B. cinerea,* as a fungal strain that carried only silenced transposon relicts and produced few sRNAs became more virulent by introduction of an exogenous active retrotransposon (Porquier et al., 2021). Retrotransposon-derived dsRNA molecules in *B. cinerea* are predominantly processed into sRNAs by two DCL proteins, BcDCL1 and BcDCL2 (Wang et al., 2016; Weiberg et al., 2013). It was reported that removal of both *Bcdcl1* and *Bcdcl2* genes in *B. cinerea* almost abolished the production of sRNA species with a size range of 20–26 nucleotides (nt) (Wang et al., 2016), and significantly reduced the virulence of *B. cinerea* on *A. thaliana* and *Solanum lycopersicum* (tomato) leaves (Weiberg et al., 2013). However, the *Δdcl1/Δdcl2* double mutant in the studies of Weiberg et al. (2013) and Wang et al. (2016) unexpectedly displayed reduced growth and aberrant sporulation phenotypes.

We aimed to establish in more detail the role of sRNAs in the early interaction between *B. cinerea* and tomato. Considering that the decisive processes in the interaction between *B. cinerea* and its host plants would occur within the first 24 hours post inoculation (hpi) (Veloso & van Kan, 2018), we generated a dataset from samples taken at 12 hpi (when penetration is just accomplished), 16 hpi (occurrence of first signs of cell death) and 24 hpi (onset of lesion expansion). Samples were sequenced at sufficient read depth to also analyze *B. cinerea* sRNAs and mRNAs at these early timepoints, when fungal biomass is low. We examined the data for occurrence of inverse correlations in transcript levels between

sRNAs and their corresponding (predicted) target transcripts from the pathogen and host. Subsequently, we performed functional analyses to evaluate whether the observed down-regulation of mRNAs could have been mediated by cross-kingdom RNAi. Neither the deletion of a retrotransposon region producing approx. 10 % of the total sRNAs from the *B. cinerea* genome nor the deletion of both Dicer-like genes impaired virulence on tomato and three other hosts. Our results suggest that natural production of sRNAs by *B. cinerea* may not contribute as much to virulence as previously reported.

Results

We extracted sRNA and mRNA samples from *B. cinerea*-infected tomato leaves harvested at 12, 16 and 24 hpi. Mock-inoculated tomato leaves at the same time points, as well as a *B. cinerea* liquid culture were included as controls. All samples were used for generating strand-specific libraries and sequenced at read depths varying from 4.2 M to 89 M per sample (Supplementary Table S1). For infected leaf samples, sRNA reads were mapped to the *B. cinerea* genome (van Kan et al., 2017) and the tomato genome (Hosmani et al., 2019) to identify whether they were of fungal or host-plant origin. sRNA reads that were mapped perfectly to both genomes (100% identity over the entire length) were eliminated from further analysis.

Many *B. cinerea* and tomato sRNAs and their predicted targets are expressed during early infection

The sRNA read length distribution in *B. cinerea* and tomato samples, grown separately, were different between the organisms (Figure 1A, B). The *B. cinerea* sRNA molecules showed a somewhat ragged distribution with two main peaks, at 25 and 33 nt. Because it was reported that sRNAs derived from LTR retrotransposons can contribute to fungal pathogenesis by hijacking the host RNAi machinery (Weiberg et al., 2013; Weiberg and Jin, 2015), we further dissected the sRNA reads that were mapped to transposable elements (TEs) in the *B. cinerea* genome. The TE-derived sRNA pool contained mainly 20-24 nt sRNA molecules with a peak at 22 nt (Figure 1A). Tomato sRNA sequences contained two sharp peaks, one at 24 nt and the other at 32 nt (Figure 1B). The peak at 32 nt consisted mainly of sequences representing half-size tRNA molecules, cut near the anticodon loop. The 24nt-sRNAs are related to cis-acting siRNAs (typically associated with RNA-dependent DNA methylation) or natural antisense transcript-derived siRNAs. The former is associated with transposon silencing and the latter with the regulation of stress-response genes (Ghildiyal & Zamore, 2009). Further analyses only focused on sRNA reads with sizes 20-24 nt because these are considered important in gene silencing (Kamthan et al., 2015), either by transcriptional or post-transcriptional gene silencing (Sijen et al., 2001). The entire dataset

of sRNAs from *B. cinerea* contained 27,918 unique sRNA molecules with lengths between 20 and 24 nt (Supplementary Table S2). These sequences predominantly originated from the ribosomal RNA repeat region (13,258 sRNAs, 47.5%) and TE loci (9,368 sRNAs; 33.5%). Other sources of sRNAs were tRNA loci, coding sequences as well as introns (Supplementary Table S2). The entire dataset of *B. cinerea* sRNAs of 20-24nt contains only 62 of the 73 sRNA sequences published by Weiberg et al. (2013), despite samples being sequenced at much greater read depths (Supplementary Table S2). The 11 absent sRNA sequences do not map on the latest version of the *B. cinerea* genome (van Kan et al., 2017).

A total of 33 transposon regions in the *B. cinerea* genome produced >100,000 sRNA reads each, with two regions on Chr14 being predominant sources of sRNAs: the Gypsy-type retrotransposon regions annotated as *ms3003* (coordinates Chr14: 1705089-1712486) and *ms3095-3099* (a complex array of multiple elements, Chr14: 253,000-283,000) of which *ms3095* and *ms3097* are transcriptionally active. Each of these regions produced >500,000 sRNA reads and each contributed roughly 10% to the total sRNA read counts (Supplementary Table S3) produced by TEs. Of the 27,918 unique sRNAs from *B. cinerea* with a length between 20 and 24 nt in the entire dataset, 5859 (21%) originated from these two regions. The total number of unique sRNAs molecules produced by tomato with a length between 20 and 24 nt was 934,159 (Supplementary Table S4), which predominantly originated from TE loci (573,727 sRNAs, 61%), annotated gene regions (324,294 sRNAs, 35%) and tRNA loci (2206 unique sRNAs, 0.2%). Due to the incomplete assembly and annotation of repeats in the tomato genome, these numbers are likely to be underestimated.

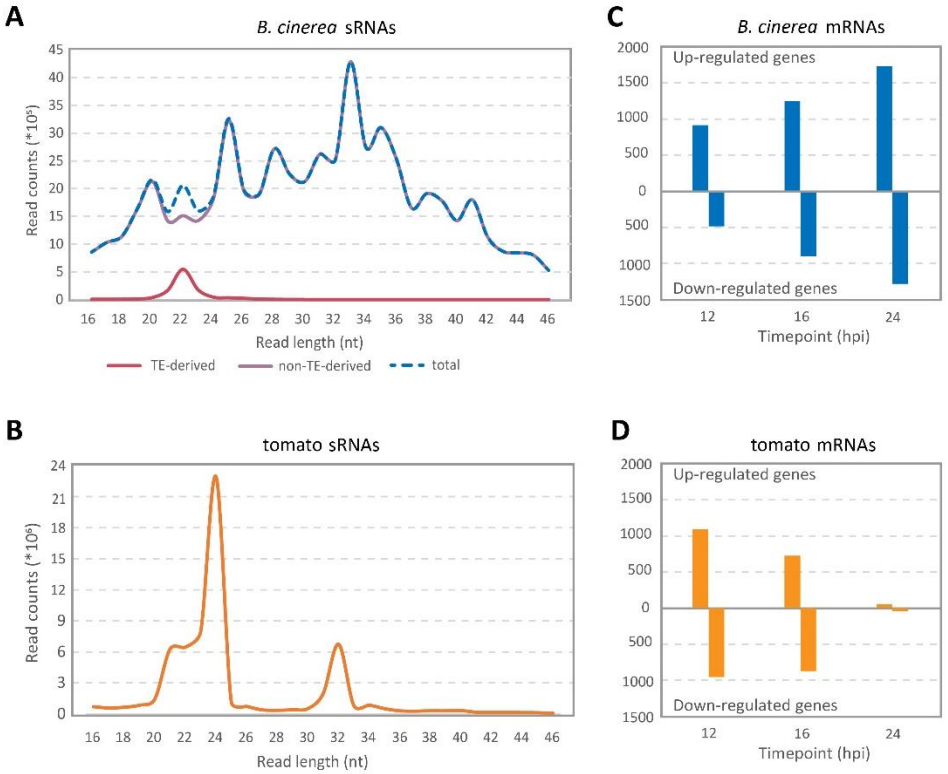

Figure 1. Small RNA (sRNA) profiles of tomato and *Botrytis cinerea* and differential expression of plant and fungal mRNAs during their interaction. **(A)** Read length distribution of unique sRNA sequences in *B. cinerea* liquid cultures. The pink line represents the transposable elements (TE) -derived *B. cinerea* sRNAs, the purple line shows the non-TE-derived *B. cinerea* sRNAs, and the blue-dashed line represents the total *B. cinerea* sRNAs. **(B)** Read length distribution of unique sRNA sequences in the compiled tomato mock-treated samples (orange line). The scale on the left in both (a) and (b) provides a read count for each read length of the samples. **(C)** Numbers of differentially expressed genes in *B. cinerea* at 12, 16 and 24 hours post inoculation (hpi). *B. cinerea* grown in liquid medium for 16 h was used as control for all three infection time-points for the analysis of differentially expressed fungal genes (blue bars). **(D)** Numbers of differentially expressed genes in tomato. Mock-treated leaves collected at 12, 16 and 24 hpi were used as the respective controls for *B. cinerea*-inoculated leaves collected at 12, 16, and 24 hpi for the analysis of differentially expressed tomato genes (orange bars).

B. cinerea and tomato genes down-regulated during interaction and potentially targeted by sRNAs from tomato and *B. cinerea*

After mapping mRNA reads on the fungal and tomato genomes, differential expression analyses were performed by comparing gene expression during *B. cinerea* infection of tomato with the respective controls, a *B. cinerea* liquid culture and the mock-inoculated tomato leaves. Differentially expressed genes of *B. cinerea* and tomato during the early

interaction (12, 16 and 24 hpi) were listed for each time point (Figure 1C, D). Many *B. cinerea* genes were up- or down-regulated during infection, as compared to growth in liquid culture, particularly at 24 hpi (>3000 genes, one quarter of the annotated genes) (Figure 1C). Among the most strongly up-regulated genes of *B. cinerea* were genes encoding polygalacturonases and other Carbohydrate-Active enZYmes (CAZymes), proteases and botcinic acid biosynthetic enzymes (Supplementary Table S5). Tomato genes that were up- or down-regulated during *B. cinerea* infection, as compared to the mock-treated samples, were identified predominantly at 12 hpi and 16 hpi (Figure 1D). Up-regulated tomato genes included genes encoding chitinases, peroxidases, and ethylene-responsive genes (Supplementary Table S6). To analyze whether down-regulation of tomato mRNAs could be mediated by *B. cinerea* sRNAs that participate in cross-kingdom gene silencing, a target gene prediction was performed. Sequences of *B. cinerea* sRNAs (Supplementary Table S2) were used as input to predict whether mRNAs of tomato could be targeted for silencing. Conversely, tomato sRNAs were used to predict target mRNAs in *B. cinerea*. Of the 27,918 unique sRNAs from *B. cinerea* with a length between 20 and 24 nt and coverage of at least 10 reads in the dataset, a quarter (7042 sRNAs) were predicted to potentially target 3185 distinct mRNAs in tomato. *B. cinerea* sRNAs with predicted target mRNAs in tomato originated from the ribosomal DNA repeat region on Chr4 (3279 sRNAs, 47%) and from TE loci on different chromosomes (2398 sRNAs, 34%) (Figure 2). Conversely, of 934,159 unique sRNAs molecules produced by tomato with a length between 20 and 24 nt, 114,011 had a predicted target mRNA in *B. cinerea* (11,434 distinct mRNAs, >97% of the fungal gene models).

A simulation was performed to evaluate the significance of the number of potential sRNA target transcripts. Three sets of 27,918 random sRNA sequences were generated with the same length distribution and GC content as the experimental *B. cinerea* sRNA dataset, and these random sequences were used as input for target prediction in tomato. The numbers of predicted target tomato transcripts for the three random sRNA sets were 6882, 6699 and 6798. Next, we generated a set of 934,159 random sRNA sequences with the same length distribution and GC content as the experimental tomato sRNA dataset, and used these random sequences as input for target site prediction in *B. cinerea*. The number of predicted target fungal transcripts was 11,331. These simulations indicate that the number of predicted target transcripts based on the biological samples was lower than or similar to the predicted targets based on randomly generated datasets.

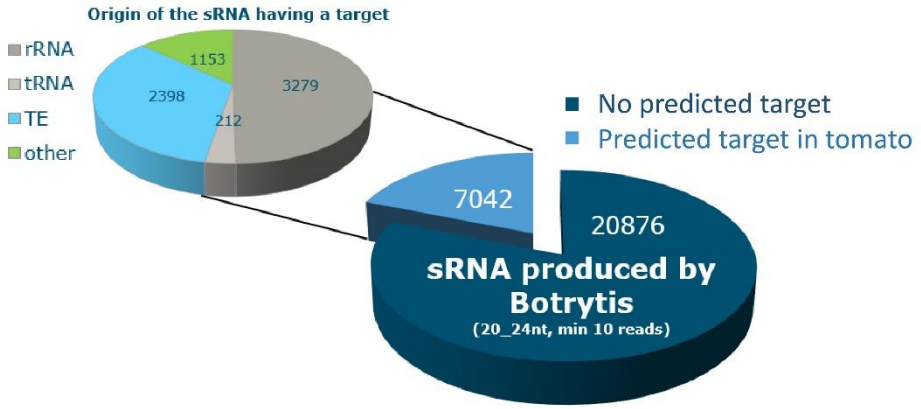

Figure 2. Number of unique small sRNAs (sRNAs) produced by *Botrytis cinerea* with a length of 20-24 nucleotides. The genomic origin of sRNAs predicted to have a target in tomato is shown: ribosomal RNA (rRNA), transfer RNA (tRNA), transposable elements (TE), and other origins.

Figure 3A illustrates relations between sRNAs originating from *B. cinerea* TE regions (fungal chromosomes in blue) and the genomic locations of their predicted target genes on tomato chromosomes (in orange). Predicted target mRNAs in tomato for each *B. cinerea* sRNA are listed in Supplementary Table S7. Of the 3185 tomato genes predicted to be targeted by *B. cinerea* sRNAs, 163 indeed displayed significantly lower transcript levels during the course of infection (Supplementary Table S8). Notably, also 158 tomato genes that were predicted to be targeted by *B. cinerea* sRNAs also displayed significantly higher transcript levels (Supplementary Table S8).

To evaluate the significance of obtaining a certain number of potential target genes in tomato that indeed were down-regulated during *B. cinerea* infection, a simulation was performed. From the entire set of tomato gene models, we selected random samples of 3185 genes (in 100 iterations) and recorded how many genes were down-regulated or up-regulated in the experimental dataset. The means of the number of up- and down-regulated genes in these 100 iterations were 131 and 153, respectively. The experimental observation of 163 down-regulated transcripts among 3185 predicted target genes did not significantly deviate from the number of down-regulated transcripts that one would expect by chance among a random set of genes.

Most of the sRNAs produced by tomato originated from 215 TE regions (Supplementary Table S9), with nine TEs producing more than 1 million sRNA read counts in the dataset. The total of 934,159 unique tomato sRNAs was predicted to target almost all 11,700 *B. cinerea*

genes (Figure 3B; predicted targets of tomato sRNAs listed in Supplementary Table S10). Most tomato TEs are located near the ends of chromosomes (Figure 3B). From the 114,011 tomato sRNAs that were predicted to have a target mRNA in *B. cinerea*, 70,189 were produced from TEs. The number of predicted *B. cinerea* target genes that displayed a significant down-regulation in at least one of the infection time points studied (12, 16 and 24 hpi) as compared to the liquid culture was 1713, which is about 15% of the *B. cinerea* genes (Supplementary Table S11).

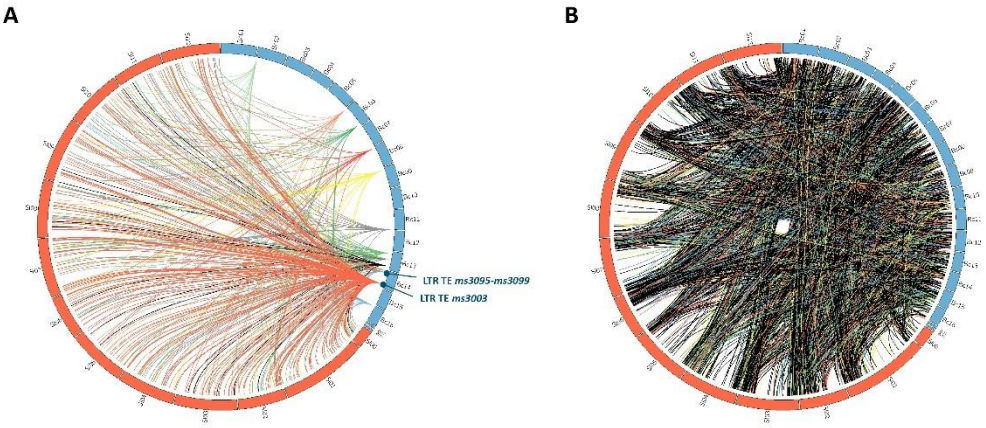

Figure 3. Genomic regions of small RNA (sRNA)-producing loci in *Botrytis cinerea* with their predicted target genes in tomato **(A)** and of sRNAs-producing loci in *Solanum lycopersicum* (tomato) with their predicted target genes in *B. cinerea* **(B)**. Blue boxes represent the 18 chromosomes of *B. cinerea*, whereas orange boxes represent the 12 chromosomes of tomato. *B. cinerea* chromosomes are oversized for illustration purposes. Only sRNAs produced by transposable element (TE) regions of *B. cinerea* **(A)** and of *S. lycopersicum* **(B)** are shown.

Correlation between the down-regulation of tomato mRNAs and levels of *B. cinerea* sRNAs that are predicted to target them

After analyzing data from *B. cinerea*- and mock-inoculated tomato leaves sampled at 12, 16 and 24 hpi, we aimed to validate the *in silico* prediction and establish more detailed sRNA – mRNA profiles during the early infection. New inoculations were performed and sampled at seven time points within the first 24 hpi for extraction of sRNA and mRNA. The expression levels of selected sRNAs and their matching target genes were quantified by reverse transcription-quantitative PCR (RT-qPCR). We selected 10 Bc-sRNAs (sRNAs from *B. cinerea*) together with their predicted nine Sl-mRNA targets (tomato transcripts) (Supplementary Table S12) for molecular validation. The selection of sRNA-mRNA pairs was based on the following criteria: (i) both the sRNA and target mRNA showed sufficient reads in the data at all time points; (ii) the predicted target mRNA was significantly down-regulated at one or

more time point(s) compared to a previous time point; (iii) at most two unique sRNAs were predicted to target a single mRNA in tomato; and iv) the target gene might participate in plant immune responses. Nine immune-related genes in tomato were selected as candidate targets (Supplementary Table S12), including three receptor-like kinases (named *LRR, RLK*, and *RLPK* in this study), one mitogen-activated protein kinase (*MAPK3*), a MAP kinase kinase kinase (*MAPKKK56*), a casein kinase (*CK*), and three transcription factors (*WRKY23*, *WRKY46*, and *WRKY50*).

Molecular quantification results from RT-qPCR indicated correlations between most tested Bc-sRNAs and their matching Sl-mRNA targets (Figure 4). The only exception was the mRNA from the tomato *CK* gene, which displayed stable levels at all time points analyzed (Supplementary Figure S1). For the tomato genes analyzed, transcript levels of *LRR* and *RLPK* decreased over time as infection progressed, *RLK*, *MAPK3*, *MAPKKK56*, *WRKY23* and *WRKY46*, genes showed fluctuating expression profiles within 24 h after *B. cinerea* inoculation, and the mRNA level of *WRKY50* strongly decreased at 16 and 20 hpi, then recovered to a level similar to the mock control at 24 hpi (Figures 4a and S1). Despite various expression profiles of predicted target genes, two main correlations were observed between the sRNAs and their predicted target mRNAs. The first type was a synchronized down-regulation of target mRNA with the high level of the corresponding sRNA in the other organism. Figure 4 shows the correlation between the tomato *RLK* transcript level and the Bc-sRNA_RLK level at 10 and 20 hpi, and similarly for the *MAPKKK56* transcript level and the Bc-sRNA_MAPKKK56 level at 12 and 14 hpi. In the second type of correlation, suppression of mRNA level was slightly delayed as compared to the time when sRNA was highly produced. For example, mRNA levels of *WRKY50* decreased between 12 hpi and 20 hpi, while the expression level of Bc-sRNA_WRKY50 was highest at 12 hpi and 14 hpi (Figure 4).

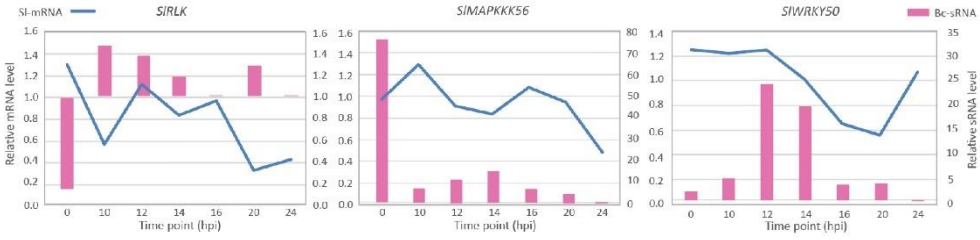

Figure 4. Correlations between production levels of small RNAs (sRNAs) and their predicted target mRNAs in *Botrytis cinerea* and tomato through seven sampling time points. Reverse transcription-quantitative PCR results showing dynamics in the production levels of three chosen Bc-sRNAs (pink bars) and the corresponding tomato transcripts (blue lines). The predicted target tomato genes are shown above each chart.

Effects of deleting a retrotransposon in *B. cinerea* on virulence

Approximately 10% of the total sRNAs produced by *B. cinerea* strain B05.10 originated from a retro-transposon region on Chr14 annotated as *ms3003* (Figure 3A, Supplementary Table S3). To verify whether sRNAs originating from *ms3003* contribute to fungal virulence, the entire *ms3003* region (c.12.5 kb) was deleted and virulence assays were performed with mutants. Three independent *Δms3003* knockout transformants were obtained by a CRISPR/Cas9-mediated system (Leisen et al., 2020) (Supplementary Figure S2). Infection assays on tomato leaves indicated that the *Δms3003* mutants caused lesions of equal sizes as the recipient B05.10 (Figure 5A, B). Furthermore, expression levels of three tomato genes, which were predicted targets of Bc-sRNAs derived only from ms3003, were quantified by RT-qPCR for six time points within the first 30 h after inoculation by B05.10 or *Δms3003*. As shown in Figure 5C, Sl05g014130, Sl06g074390 and Sl01g060030 displayed similar expression profiles in tomato leaves infected by B05.10 and *Δms3003*, although the levels of the corresponding Bc-sRNAs targeting Sl05g014130 and Sl01g060030 seemed to be lower (with no statistical significance) in the *Δms3003* mutant as compared to B05.10 (Figure 5C). We also attempted to delete a second TE region on Chr14 with a size of about 30 kb, designated *ms3095-3099* (Figure 3A), which has a complex tandem array of transposons, and is also the source of ~10% of the total sRNA reads (Supplementary Table S3). The deletion was partially successful: from multiple experiments, few transformants were obtained in which the 5'- or 3'-end of the region was replaced by a donor template, while the other side was retained. Despite numerous attempts, we failed to obtain transformants lacking the entire *ms3095-3099* region.

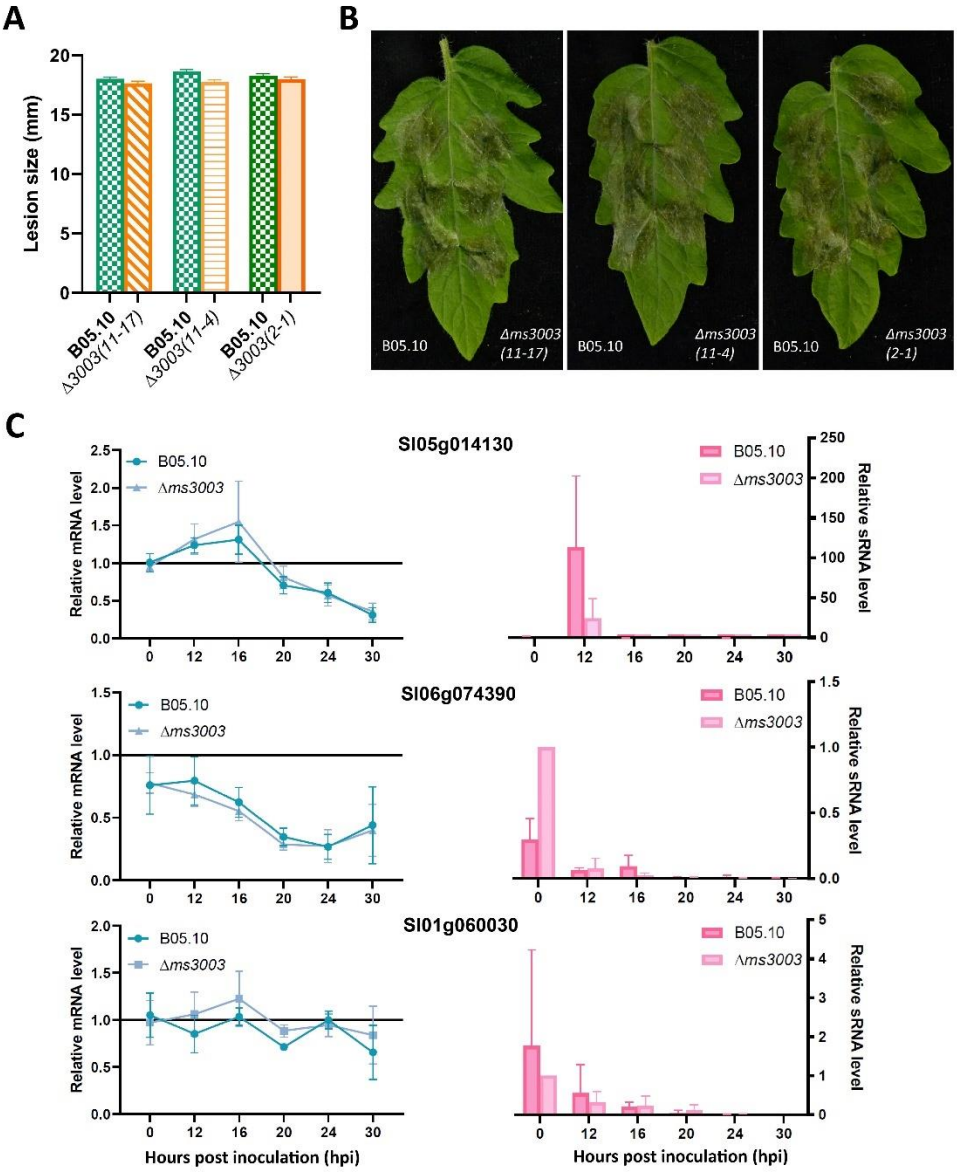

Figure 5. (A and B) The virulence of three *Δms3003* independent mutants compared with the wild-type B05.10 strain on tomato leaves, evaluated by lesion sizes in diameter (mm) at 3 days post inoculation (dpi). The measured data were plotted as a bar chart **(A)**. Error bars represent standard error of 72 datapoints from three experiments; statistical analyses by Student's t-test indicated no significant differences. Infected leaves were photographed at 3 dpi **(B)**. The virulence assay was performed three times, each with similar results. **(C)** Transcript profiles of three tomato genes (predicted targets of Bc-sRNAs derived from *ms3003*) during the infection of tomato leaves by B05.10 or a *Δms3003* mutant. Error bars represent standard error from four biological replicates and two biological replicates in the plot of relative mRNA level and small RNA level, respectively.

Deleting *B. cinerea Bcdcl1* and *Bcdcl2* eliminated transposon-derived sRNAs, but did not affect virulence

Generation of sRNAs in fungi requires the action of Dicer-like proteins, to cleave double-stranded replication intermediates generated from retrotransposon transcripts, into small interfering RNAs that can mediate gene silencing. Weiberg et al. (2013) reported that a *B. cinerea* double mutant that was defective in both *Bcdcl1* and *Bcdcl2* was reduced in virulence, presumably due to its inability to generate siRNAs with a size of 20 – 26 nt (Wang et al., 2016). However, the *ΔBcdcl1/ΔBcdcl2* double mutant in the studies of Weiberg et al. (2013) and Wang et al. (2016) displayed reduced mycelial growth and abnormal sporulation. Such phenotypes were not necessarily expected for such mutants, and we suspected the occurrence of additional pleiotropic mutations in this double mutant. Thus, we generated novel single and double mutants in the *Bcdcl1* and *Bcdcl2* genes. Initial attempts to generate knockout mutants in strain B05.10 as recipient resulted in the generation of several independent *ΔBcdcl2* mutants. However, the *ΔBcdcl1* mutant could never be obtained in the homokaryotic state, despite applying a few rounds of single-spore isolation. To overcome this issue, we chose as recipient mutant strain *Δku70*, in which nonhomologous end-joining repair is disturbed (Choquer et al., 2008; Pinedo et al., 2008), to facilitate homokaryotic deletion of *Bcdcl1* and *Bcdcl2* genes. At least three independent knockout strains were obtained for each single or double mutant (Supplementary Figure S3). To verify that the *ΔBcdcl1/ΔBcdcl2* double mutants were indeed defective in generating siRNAs, we sequenced the sRNA pool of recipient strain *Δku70* and three independent double mutants, grown in liquid culture**.** Indeed *ΔBcdcl1/ΔBcdcl2* double mutants showed reduced amount of sRNAs, specifically in the range between 20 and 24 nt (Figure 6A). The double mutants still contained a residual amount of sRNAs (Figure 6A). Mapping of the reads revealed that none of the unique sRNA sequences in the *ΔBcdcl1/ΔBcdcl2* double mutants was derived from TE regions (at a threshold of 10 reads) while in the recipient strain *Δku70*, 1409 of the 5996 unique sRNA sequences (23%) were derived from TE regions (Figure 6B). Two strains of each single mutant and three strains of the double mutant were tested for virulence and *in vitro* growth on two solid media. All *ΔBcdcl1, ΔBcdcl2,* and *ΔBcdcl1/ΔBcdcl2* mutants displayed similar radial growth and developmental behavior (sporulation and sclerotia formation) as the *Δku70* recipient and the wild-type strain B05.10 (Supplementary Figure S4). In multiple biological repetitions, we never observed any significant reduction in lesion size between the wild-type and mutants, on tomato (Figure 6C), *A. thaliana, Nicotiana benthamiana* or *Phaseolus vulgaris* (Supplementary Figure S5) despite testing multiple independent mutants for each gene, as well as multiple independent double mutants. These

results indicated that TE-derived 20-24nt sRNAs from *B. cinerea* played an undetectable role in the developmental behavior and aggressiveness on host plants of the fungus.

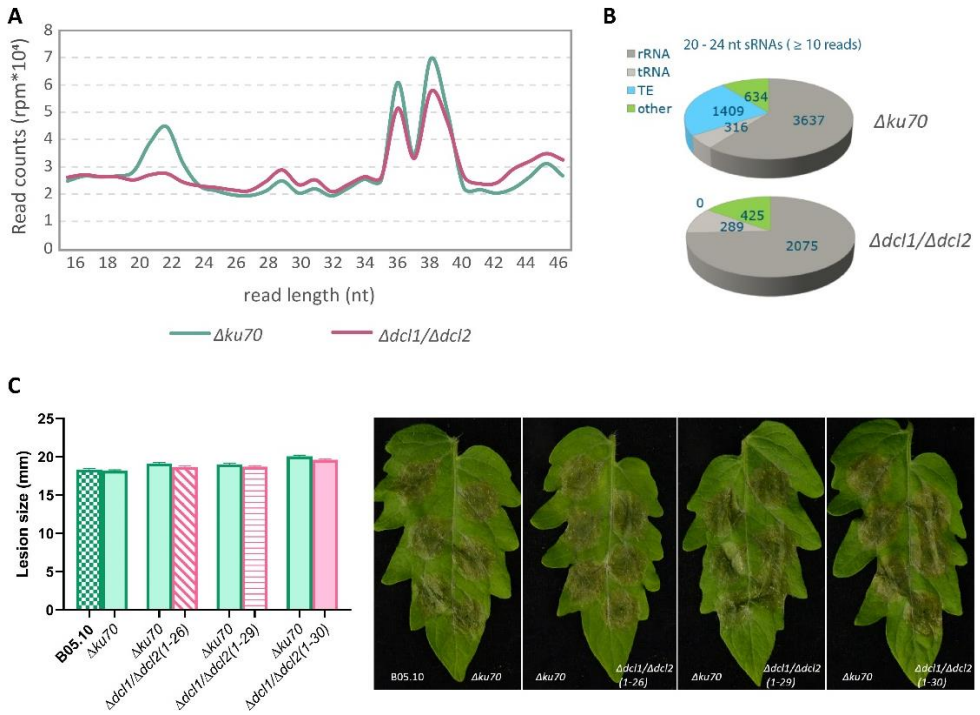

Figure 6. (A) Profile of normalized read counts (rpm) for total small RNA (sRNA) (length 16-46 nucleotides) produced in *Δku70* and *ΔBcdcl1/ΔBcdcl2* mutants. **(B)** The numbers of unique sRNAs produced by *B. cinerea Δku70* and *ΔBcdcl1/ΔBcdcl2* mutants with a length of 20-24 nt and their origin in the *B. cinerea* genome: ribosomal RNA (rRNA), transfer RNA (tRNA), transposable elements (TE), and other origins. The pie chart shows the results of three biological replicates. **(C)** The virulence of *ΔBcdcl1/ΔBcdcl2* compared with *Δku70*, and *Δku70* with wild-type B05.10 strain on tomato leaves. The diameter of lesions was measured at 3 days post inoculation (dpi), represented as a bar chart on the left side of panel **(C)**. Error bars represent standard error of 72 inoculations from three independent experiments, and there were no significant differences between each comparison (statistical analyses were performed by Student's t-test). Symptoms were photographed at 3 dpi, shown on the right side of panel **(C)**.

Discussion

Both plants and fungi produce various types of small RNAs through a number of pathways, and these sRNAs may have important regulatory functions in an organism by either mediating DNA methylation or RNA interference that result in transcriptional or post-transcriptional gene silencing, respectively. The studies by Weiberg et al. (2013) and Wang et al. (2017) reported that sRNAs can not only modulate transcript levels in the organism producing the sRNAs (Chang et al., 2012; Lax et al., 2020), but also reduce transcript levels in a different organism during a pathogenic interaction. On the one hand, sRNAs produced by *B. cinerea* could affect the transcript levels of *A. thaliana* genes involved in plant immunity (Weiberg et al., 2013), while on the other hand, sRNAs from a host plant could affect the transcript levels of fungal genes participating in the infection process (Cai et al., 2018; Wang et al., 2016). One crucial step in this RNA warfare obviously is the translocation of the sRNAs from the producing organism (either the plant or the fungus) to the opponent in the interaction. Extracellular vesicles were reported to be key players in the delivery of the sRNAs into the cells of the opponent. Studies by Cai et al. (2018) and He et al. (2021) revealed that not all sRNA molecules produced are effectively loaded into vesicles and thereby provided indications for the selectivity of sRNA translocation, although the mechanism of selectivity was not understood. Rutter and Innes (2020), however, have raised concerns about the conclusions of some recent studies on plant extracellular vesicles, because the experimental approaches may insufficiently distinguish *bona fide* vesicle cargo from merely co-purifying contaminants. Studies using a complementary approach (Wang et al., 2016) demonstrated that synthetic sRNAs that are topically applied to plant surfaces can be taken up in *B. cinerea* and lower the expression of target genes in the invading fungus, thereby reducing disease development.

The studies by Weiberg et al. (2013) and Wang et al. (2017) had a major shortcoming that we considered important from a biological perspective of the plant-pathogen interaction. The tissue samples analyzed in these studies were taken from 24 hpi onwards, at a moment when the interaction between *B. cinerea* and its host is already well advanced and the fate of the interaction is largely decided (Veloso and van Kan, 2018). Under commonly used laboratory conditions for inoculation, *B. cinerea* spores germinate within 3-4 hpi and infection structures are formed around 6-8 hpi. Fungal penetration is completed around 10-12 hpi and first signs of cell death become evident at 16 hpi. Therefore, sampling tissues at 24-72 hpi provides a snapshot of sRNA and mRNA profiles that does not reflect the decisive moments in this plant-fungus interaction. This consideration stimulated us to sample at earlier time points to explore the sRNA and mRNA profiles at three decisive moments: 12

hpi (following penetration, during the early biotrophic phase of the interaction); 16 hpi (around the transition from the biotrophic to the necrotrophic phase), and 24 hpi (when the necrotic lesion in a host is established and the fungus expands beyond the inoculation spot). The sRNA sequence data that we obtained were different from the data obtained by Weiberg et al. (2013), but difficult to compare. Not only were time points different, the read depth was also much deeper, and the reads could be mapped to more completely assembled and better annotated versions of the *B. cinerea* and tomato genomes (Hosmani et al., 2019; van Kan et al., 2017). The sRNA dataset from *B. cinerea* contained almost 28,000 unique sRNA sequences with a length of 20-24 nt, yet only 62 sRNAs from the 73 sequences described by Weiberg et al. (2013) were present in our data with a coverage of at least four reads. The 11 missing sRNAs of Weiberg et al. (2013) did not map to the recent version of the *B. cinerea* genome or were not detected in our dataset. The 28,000 *B. cinerea* sRNAs were predicted to target >3000 genes in the tomato genome, including hundreds of genes that could potentially participate in plant defence or immunity. Yet only 163 of the predicted tomato target mRNAs indeed showed significant down-regulation in the same tissue samples, while 158 potential tomato target mRNAs showed up-regulation.

We identified a set of genes related to plant immunity that were predicted to be targeted by *B. cinerea* sRNAs, and did indeed display a reduced mRNA level during infection, as compared to mock controls. A detailed RT-qPCR analysis was performed with sampling at seven time points between 0 and 24 hpi, to establish an association between the level of the Bc-sRNA and its target Sl-mRNA. The results in Figures 4 and S1 show that in some cases, there was an inverse correlation between the level of a Bc-sRNA and its predicted target in tomato, which might indicate that cross-kingdom RNAi was indeed operative to achieve this down-regulation. However, whether the production of a unique Bc-sRNA that is predicted to target a Sl-mRNA actually causes the downregulation of its target is difficult to establish. Firstly, many sRNAs are derived from transposons, some with multiple closely related, but non-identical copies, and it is genetically impossible to dissect the function of individual sRNAs. Second, many of the Bc-sRNAs are predicted to target multiple distinct Sl-mRNAs. Conversely, many Sl-mRNAs are predicted to be targeted by multiple distinct Bc-sRNA molecules from various genomic origins. Whether a predicted sRNA-mRNA interaction actually occurs in the plant-fungus interaction depends on multiple factors: the concentration of the sRNA within the (plant or fungal) tissue; the effective translocation of sRNA between fungus and plant, through vesicles or otherwise, the efficacy of sRNA-mRNA hybrid formation, dependent on the free energy; and the efficacy of the RNAi process that destroys the target mRNA. All these processes will have an impact on the outcome of the plant-fungus interaction only if they occur sufficiently rapidly and efficiently, and only if the

reduction of mRNA results in a notable reduction of the encoded protein that has a meaningful impact on the interaction. The reduction of transcript levels by, for example, 50% does not necessarily result in an equivalent reduction of the protein. Even if the protein levels were reduced to a similar extent as its transcript, this would only lead to physiological problems if the protein catalyzes a rate-limiting step in the biological process of interest. Furthermore, the overall consequences of differential expression of plant immunity genes, mediated by fungal sRNAs, are hard to predict and do not necessarily lead to increased susceptibility of the infected plant.

During the *B. cinerea*-tomato interaction, numerous fungal and plant genes were down-regulated over the course of the infection process (Figure 1C, D). Based on the observations of Weiberg et al. (2013) and Wang et al. (2016), and the identification of about 95,000 potential sRNA-mRNA interactions in our dataset (7,042 Bc sRNA-Sl mRNA interactions and 88,196 Sl sRNA-Bc mRNA interactions), it was tempting to consider that many changes in transcript levels were indeed caused by cross-kingdom RNAi. However, simulations indicated that similar, or even higher, numbers of predicted sRNA-mRNA interactions occur with randomly generated sRNA datasets, and the 163 down-regulated tomato mRNAs in the experimental dataset did not deviate from the number of down-regulated transcripts that one may expect in a random subset of 3185 tomato genes. Other explanations for down-regulation, besides cross-kingdom RNA interference, should therefore be considered. *B. cinerea* undergoes developmental transitions during early phases of infection that are associated with transcriptional reprogramming. To penetrate the host tissue, fungal germ tubes develop infection structures with their specific developmental and transcriptional program (Choquer et al., 2021; Leroch et al., 2013). Once infection structures have completed host surface penetration (10-14 hpi), they are redundant and the fungus switches to intercellular hyphal growth while suppressing host cell death (Veloso and van Kan, 2018). From about 16 hpi, host cells are triggered to undergo programmed cell death and the fungus is exposed to oxidative stress in dying host tissue (Choquer et al., 2007; Torres et al., 2006). On the plant side, tomato genes that are down-regulated on *B. cinerea* inoculation could be regulated by numerous physiological processes that are associated with defense responses and/or disease development, rather than by fungal sRNAs.

The majority of sRNAs produced by *B. cinerea* is derived from the rRNA repeat and a number of very active TEs of the Gypsy family. Two regions in chromosome 14 (*ms3003* and *ms3095-ms3097*) stood out as producers of massive amounts of sRNAs, with each of these regions producing c.10% of the total read counts (Figure 3A, Supplementary Table S3). These elements not only produced many reads, but also a great diversity of sRNAs, from a range of lengths and often overlapping in sequence. Production of such molecules is a random

"disposal process" to eradicate the replication intermediate and thereby modulate the activity of the retrotransposon. The fact that sRNAs are produced that may, in addition, silence transcripts in a host plant should thus be considered accidental and a "collateral benefit". The sheer number and diversity of sRNAs will inevitably have numerous (predicted) target genes within any given host plant, just by coincidence. If silencing of host immunity confers advantage to the fungus, *B. cinerea* genotypes that contain active retrotransposon copies are likely to be more successful than genotypes devoid of active transposons. Evolutionary selection will not operate at specific sequence level, but on the possession of such (active) elements. Studies on genetic diversity in the *B. cinerea* population revealed that a subset of isolates were considered to lack active transposons, and were referred to as "*vacuma*" isolates (Giraud et al., 1999; Martinez et al., 2003; Samuel et al., 2012). Such isolates were often reported to be less virulent on particular hosts (Martinez et al., 2003), but it was difficult to experimentally validate this correlation because of differences in the origin and genetic backgrounds of isolates. In a study by Porquier et al. (2021), a *vacuma* isolate was transformed with an LTR-type TE and became slightly but significantly more virulent than the recipient strain. We applied an inverse strategy and eliminated one TE region (*ms3003*, c,12.5 kb) that was responsible for the generation of c.10% of the sRNA population from the genome of the highly virulent strain B05.10 (Supplementary Figure S2). This is to our knowledge the first successful targeted deletion of a TE region from the *B. cinerea* genome and perhaps from any other fungus. We also attempted to delete a second TE region, designated *ms3095-3099*, with a size of c.30 kb, which also generates ~10% of the sRNA population. This locus has a complex tandem array of multiple transposons in direct or inverted repeat orientation, and we attempted to delete it by using CRISPR guide RNAs that would cut in the unique sequences flanking the TE region, and transforming with a donor template that would merge the two flanking regions by a selection marker cassette. In multiple experiments a few transformants were obtained, in which either the 5' -part or the 3'-part of the region was recombined with the donor template, but the recombination target site at the other end was retained. These mutants were not further analyzed as they did not contain the complete desired deletion. Despite the successful knockout of a c.12.5 kb TE region *ms3003*, the virulence of the mutants was not notably reduced (Figure 5). This was probably due to the presence of additional TEs, including the *ms3095-3099* region on Chr14, that compensate for the loss of the *ms3003* region. An alternative explanation would be that the cross-kingdom RNAi as such does not have a significant impact on the infection process to affect the virulence of mutants. This hypothesis was tested by generating double mutants that were defective in both Dicer-like genes *Bcdcl1* and *Bcdcl2*. The study by Weiberg et al. (2013) reported an almost absolute loss of virulence of such a mutant, but

their mutant displayed serious growth retardation and abnormal sporulation. By contrast, the *ΔBcdcl1/ΔBcdcl2* mutants that we generated independently displayed a >99% reduction in TE-derived sRNA production (of 20-24 nt length molecules), while the rDNA-derived sRNAs were largely unaffected by deletion of *Bcdcl1* and *Bcdcl2*. Three independent *ΔBcdcl1/ΔBcdcl2* mutants showed neither any pleiotropic phenotypes as reported by Weiberg et al. (2013), nor reduced virulence on any of four distinct host plants (Figure 6C).

This indicates that, in our view, the role of cross-kingdom RNAi at the level of single sRNA-mRNA interactions appears too small to be detected in the infection on leaves of several plant species under controlled laboratory conditions. These results are difficult to reconcile with reports that plant protection from *B. cinerea* infection can be achieved by applying onto plant surfaces sRNAs that can silence *B. cinerea* Dicer-like genes as reported by Wang et al. (2016). This study made use of single and double-stranded RNAs that target the *B. cinerea* Dicer-like genes, with the reasoning that silencing of *Bcdcl1* and *Bcdcl2* would prevent the fungus from producing sRNAs that can suppress plant immune responses and thereby trigger resistance. Our observation that *ΔBcdcl1/ΔBcdcl2* double mutants were equally virulent as the wild-type strain (Figures 6c and S5), despite depletion of an immense proportion of its sRNAs (Figure 6A, B), suggests that the protection conferred by sRNAs that target *B. cinerea* Dicer-like genes might operate through a different mechanism than merely the disruption of the fungal sRNA producing capacity. More recent publications have reported the topical application of a plethora of distinct sRNAs that confer resistance to *B. cinerea* (McLoughlin et al., 2018; Nerva et al., 2020; Spada et al., 2021). In these studies, the sRNAs were designed to target fungal genes with a role in growth (lanosterol C-14-α demethylase, chitin synthase, elongation factor EF2) or signal transduction required for virulence (MAP kinase BMP3). A very extensive study on *Sclerotinia sclerotiorum* (McLoughlin et al., 2018; Nerva et al., 2020; Spada et al., 2021) showed that 20 out of 59 sRNAs (targeting a range of physiological functions) applied on *Brassica napus* leaves could reduce *S. sclerotiorum* lesion development. Subsequent tests with sRNAs targeting the orthologs of five of these 20 genes from *B. cinerea* also conferred reduction of *B. cinerea* lesion development (McLoughlin et al., 2018; Nerva et al., 2020; Spada et al., 2021). Technically, the topical application of sRNAs to confer plant protection from disease falls under the definition of Spray-Induced Gene Silencing (SIGS) (Wang & Jin, 2017), and offers an attractive perspective for future crop protection strategies. However, the success of this method does not necessarily provide evidence for the importance of natural cross-kingdom RNA interference in the *B. cinerea*-host interaction as earlier proposed by Weiberg et al. (2013).

Materials and Methods

Fungal strains, plant material and growth conditions

B. cinerea strains used in this study (Table 1) were grown and spores collected as described in File S1. Tomato (*S. lycopersicum* cv. Moneymaker) and *Nicotiana benthamiana* were grown in a greenhouse at 20 °C. *A. thaliana* and French bean (*Phaseolus vulgaris*) were grown in a climate chamber at 21 °C and 19 °C for day and night temperature, respectively. The light had a photoperiod of 12 h/day and the chamber had 70% RH.

Table 1. *B. cinerea* strains used in this study.

***B. cinerea* strain**	**Description**	**Origin/Reference**
B05.10	wildtype *B. cinerea*	van Kan et al. (2017)
Δms3003 (#2-1, #11-4, #11-17)	*Bcms3003* knockout mutant generated from B05.10 background, Hygromycin resistant	this study
Δku70	*Bcku70* knockout mutant generated from B05.10 background, Hygromycin resistant	Choquer et al. (2008)
Δdcl1 (#5-2, #6-1)	*Bcdcl1* knockout mutant generated from *Δku70* background, Hygromycin and Fenhexamid resistant	this study
Δdcl2 (#5-4, #5-19)	*Bcdcl2* knockout mutant generated from *Δku70* background, Hygromycin and Nourseothricin resistant	this study
Δdcl1/Δdcl2 (#1-26, #1-29, #1-30)	*Bcdcl1 and Bcdcl2* double knockout mutant generated from *Δku70* background, Hygromycin, Fenhexamid and Nourseothricin resistant	this study

Tomato inoculations with *B. cinerea*

B. cinerea conidia were diluted in Potato Dextrose Broth (PDB, 12 g/l) medium to 1000 conidia/µl and inoculated on detached tomato leaves essentially as described byZhang & van Kan (2013). Details on the inoculation and sampling design are provided in File S1.

RNA extractions

Fungal mycelium or tomato leaf samples were frozen in liquid nitrogen and used for extraction of small RNA using the mirPremier® microRNA Isolation Kit (Sigma-Aldrich) while the mRNA fraction was isolated using the SV Total RNA Isolation System (Promega).

Generation and analyses of the RNAseq dataset

Single-end Illumina sequencing was applied to all sRNA and mRNA samples by Vertis Biotechnologie AG (Martinsried, Germany) on a strand-specific library with read length of 75 nt. Sequence processing and bioinformatic analyses of data are described in detail in File S1.

RT-qPCR quantification of mRNA and sRNA levels

Reverse transcription from mRNA was done using Superscript III reverse transcriptase (Invitrogen). For reverse transcription of sRNA, the qScript microRNA cDNA Synthesis kit (Quanta Bioscience) was used. 20 ng of each cDNA sample was input for performing RT-qPCR using SensiMix SYBR Hi-ROX Kit (Bioline). Primer combinations shown in Supplementary Table S13 were used to quantify levels of mRNAs and sRNAs. An actin gene from tomato was used to normalize plant mRNA levels, and the relative mRNA level of each time point was calculated by comparing with the mock inoculated sample at the same time point. A small RNA derived from *B. cinerea* 28S rRNA was used to normalize fungal sRNA levels. The threshold cycle (CT) values were determined by Bio-Rad CFX Manager 3.1 and fold-changes calculated using the $^{\Delta\Delta}$Ct method (Dorak, 2007).

***B. cinerea* transformation by CRISPR/Cas9-mediated approach**

B. cinerea mutant strains used in this study were generated by CRISPR/Cas9-mediated transformation, as described (Leisen et al., 2020) with modifications specified in File S1.

Data Availability Statement

The data of this project have been deposited in the NCBI database under Bioproject at www.ncbi.nlm.nih.gov/biopr oject/ with accession num-ber PRJNA496584. Raw sequence reads are deposited in the Sequence Read Archive at www.ncbi.nlm.nih.gov/sra/ project SRP166089 under accession numbers SRX4902781-SRX4902782, SRX4902789, SRX4902791-SRX4902800, SRX15228005 - SRX15228010, SRX15231189, SRX15231190, SRX19002251 (sRNAs) SRX4902771-SRX4902780 and SRX4902783-SRX4902787, SRX4902790, SRX15231192, SR X15231193, SR X190 02219 (mRNAs).

Supplementary Materials

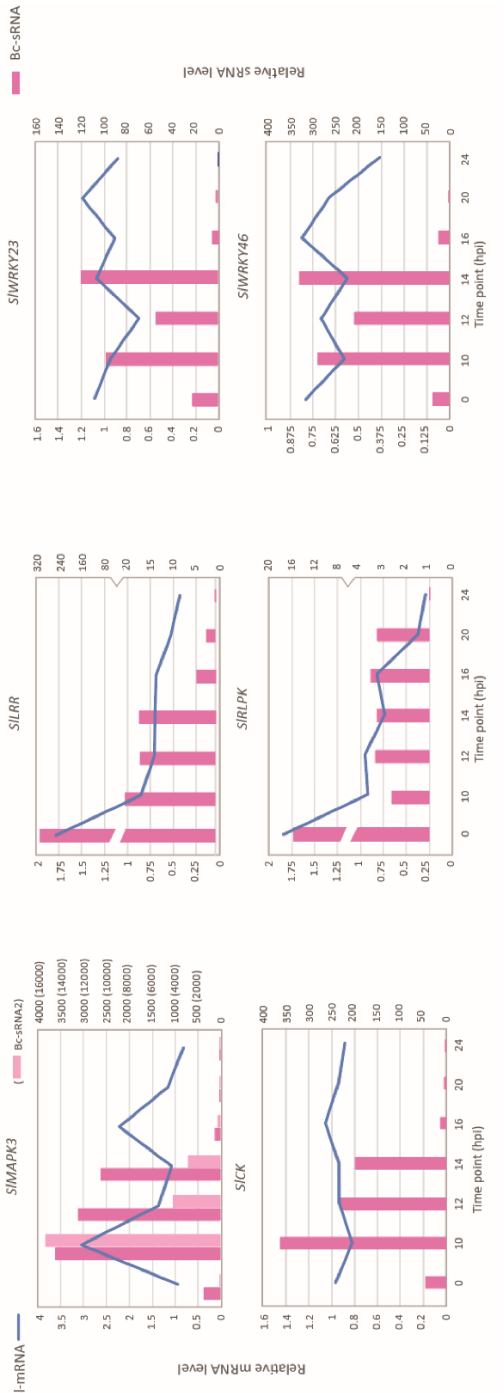

Supplementary Figure S1. Correlations between production levels of Bc-sRNAs and their predicted target mRNAs in tomato through seven sampling time points. Reverse transcription-quantitative-qPCR results showing dynamics in the production levels of six chosen Bc-sRNAs (pink bars) and the corresponding tomato transcripts (blue lines). The predicted target tomato genes are shown above each chart.

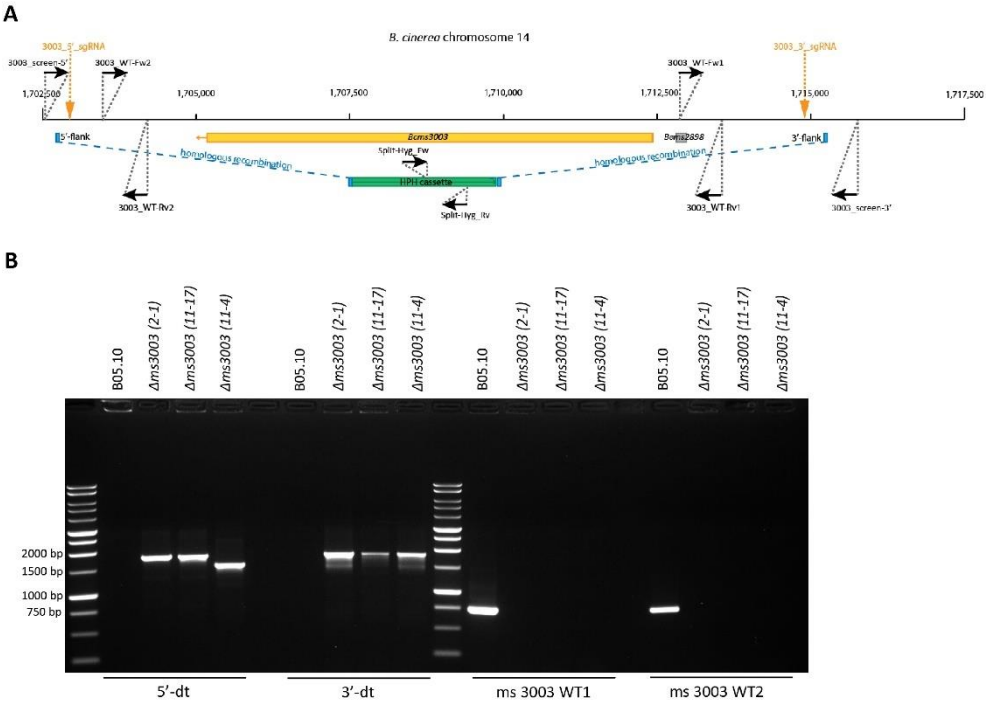

Supplementary Figure S2. (A) Schematic representation of the generation of *Δms3003* transformants via CRISPR/Cas9-mediated transformation with two sgRNAs and the primers used in genotyping the transformants. **(B)** Genotyping of *Δms3003* transformants by PCR, representing the target region was replaced by the donor template via homologous recombination on both 5'- and 3'- flanks. The same PCR reactions were performed with wild-type B05.10 as the non-transformed control.

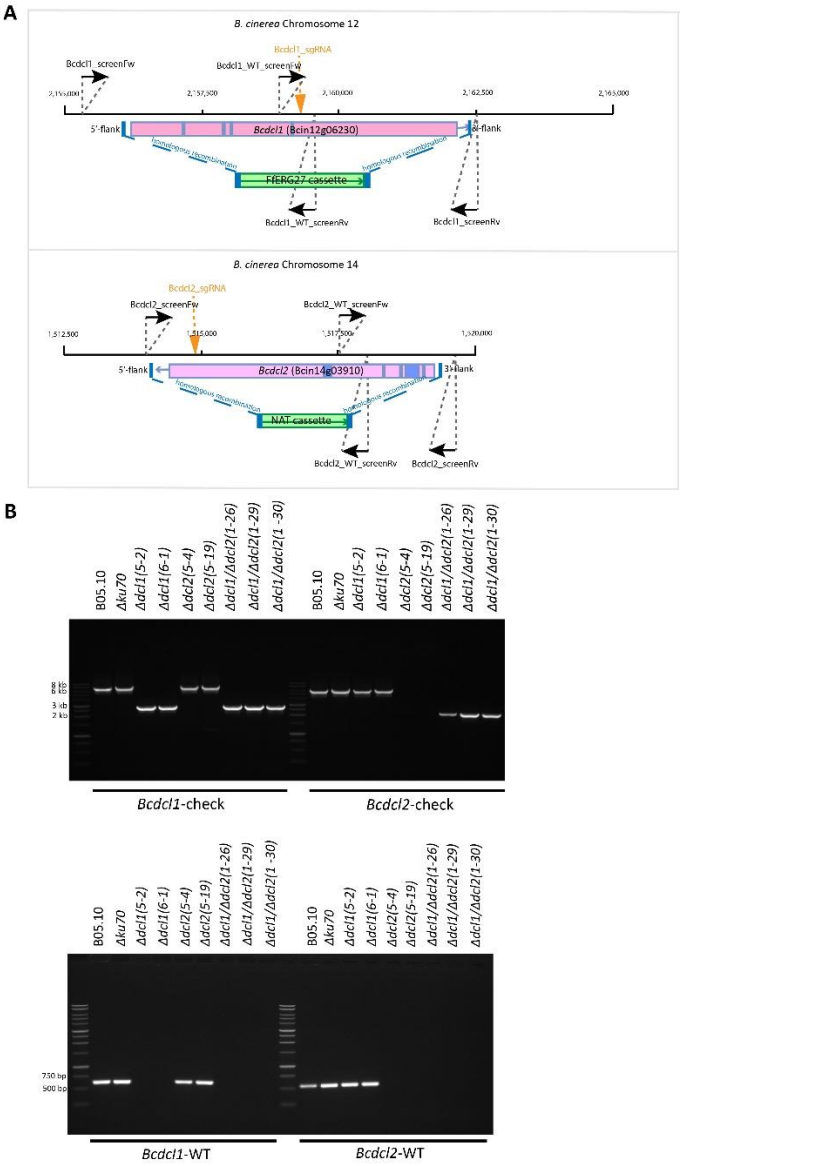

Supplementary Figure S3. (A) Schematic representation of the generation and characterization of *ΔBcdcl1, ΔBcdcl2,* and *ΔBcdcl1/ΔBcdcl2* transformants. **(B)** Genotyping of *ΔBcdcl1, ΔBcdcl2,* and *ΔBcdcl1/ΔBcdcl2* transformants by PCR with primers shown in **(A)** and File S1. For the *Bcdcl1*-check reaction, a band of 6.7 kb in B05.10 and *Δku70* indicates the wild-type *Bcdcl1* gene and a band of 2.7 kb in *ΔBcdcl1/ΔBcdcl2* mutants as the replacement of this gene by the donor template. Similarly, the *Bcdcl2*-check resulted in a product of 5.6 kb for B05.10 and *Δku70*, and one with the size of 2.0 kb for *ΔBcdcl1/ΔBcdcl2* mutants. For the *Bcdcl1*-WT reaction, only the B05.10, *Δku70* and *ΔBcdcl2* strains showed amplicons of the *Bcdcl*1 gene, while the *ΔBcdcl1* and *ΔBcdcl1/ΔBcdcl2* strains did not. Similarly, the *Bcdcl2*-reaction could only amplify the *Bcdcl2* fragment in the B05.10, *Δku70*, and *ΔBcdcl1* strains, but not in the *ΔBcdcl2* and *ΔBcdcl1/ΔBcdcl2* strains.

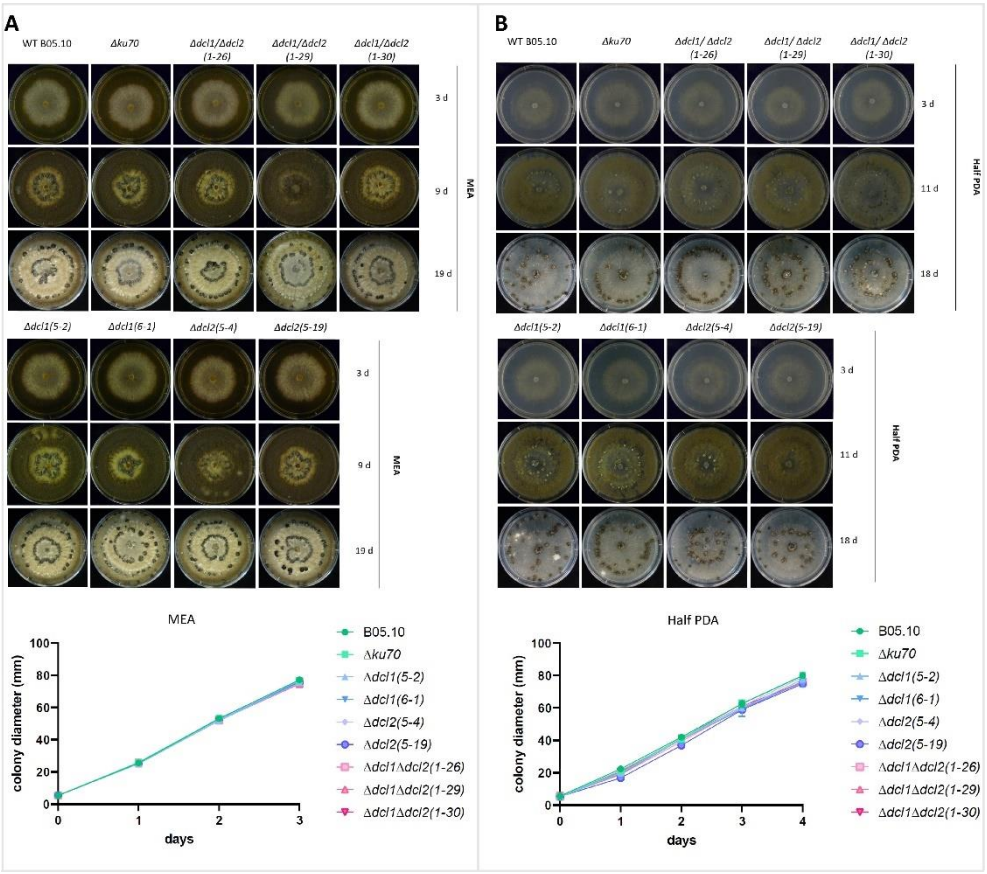

Supplementary Figure S4. *In vitro* mycelial growth, conidia formation, and sclerotial development of B05.10 wild-type (WT), *Δku70, ΔBcdcl1, ΔBcdcl2*, and *ΔBcdcl1/ΔBcdcl2* mutant strains on MEA **(A)** and PDA **(B)** plates. The line charts below the photos represent the mycelial growth rate of B05.10 WT, *Δku70, ΔBcdcl1, ΔBcdcl2*, and *ΔBcdcl1/ΔBcdcl2* mutant strains on MEA **(A)** and PDA **(B)** plates for 3 and 4 consecutive days, respectively.

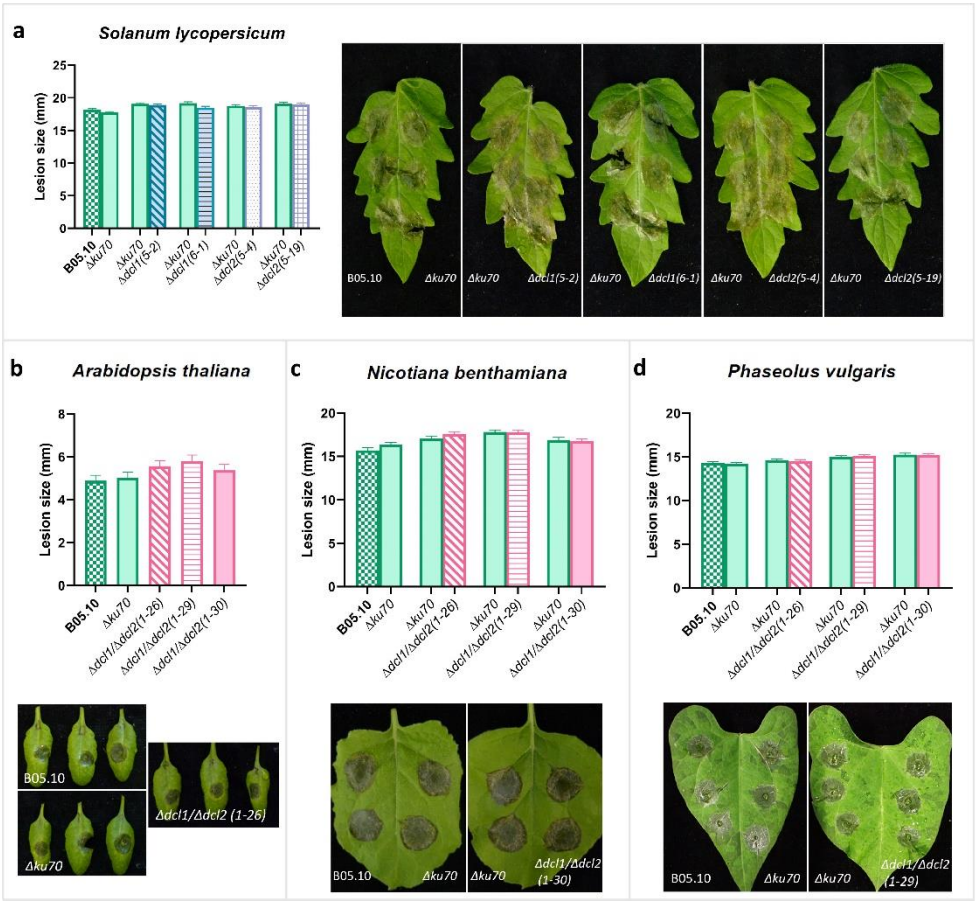

Supplementary Figure S5. (A) Virulence assays of *ΔBcdcl1* and *ΔBcdcl2* single mutants compared with *Δku70*, and *Δku70* compared with B05.10, which were performed with tomato leaves. **(B-D)** Virulence assays of *ΔBcdcl1/ΔBcdcl2* double mutant strains compared with *Δku70*, and *Δku70* compared with B05.10. The assays were performed with *Arabidopsis thaliana* **(B)**, *Nicotiana benthamiana* **(C)** and *Phaseolus vulgaris* **(D)**, represented as bar charts and photos. Error bars in the charts represent standard errors of 72, 72, and 120 datapoints from three experiments for *A. thaliana, N. benthamiana*, and *P. vulgaris,* respectively. No significant reduction in the virulence of *ΔBcdcl1, ΔBcdcl2*, and *ΔBcdcl1/ΔBcdcl2* compared with *Δku70*, and the same for *Δku70* compared with B05.10, statistically analyzed by Student's t test.

The following Supplementary materials are available to be downloaded from the "Supplementary materials_PhD thesis_Qin(2023).zip" file, and thus only legends are shown below.

Supplementary Table S1 Sequence read depth of the mRNA and small RNA samples.

Supplementary Table S2 Sheet 1: sequences of 27,918 unique small RNAs (sRNAs) from *Botrytis cinerea* with a length between 20 and 24 nucleotides, and their genomic origin: chromosome coordinates, ribosomal RNA repeat, transposable element loci, tRNA loci, gene regions. Sheet 2: correspondence of 73 sRNAs described by Weiberg et al. (2013) to our data.

Supplementary Table S3 Transposable elements (TEs) in *Botrytis cinerea* as sources of smalls RNAs. The list provides the genomic location (chromosome, start and end coordinates), the TE identifier from REPET annotation, the read counts for the entire repeat region as well as the percentage of the total read counts. Only repeat elements that generated at least 100 read counts are included.

Supplementary Table S4 Sequences of 934,154 unique small RNAs from tomato with a length between 20 and 24 nucleotides, and their genomic origin: chromosome coordinates, gene region, transposable element loci.

Supplementary Table S5 Differentially expressed genes of *Botrytis cinerea* during tomato leaf infection at different hours postinoculation (hpi) as compared to *in vitro* liquid culture. Each sheet provides the gene ID, the log2FC, the adjusted p value and a gene description. Sheet 1: expression at 12 hpi; sheet 2: expression at 16 hpi; sheet 3: expression at 24 hpi.

Supplementary Table S6 Differentially expressed genes of tomato during *Botrytis cinerea* infection at different hours postinoculation (hpi) as compared to mock-treated leaves at the same time point. Each sheet provides the gene ID, the log2FC, the adjusted p value and a gene description. Sheet 1: expression at 12 hpi; sheet 2: expression at 16 hpi; sheet 3: expression at 24 hpi.

Supplementary Table S7 Predicted target mRNAs in tomato for each of the 7,042 *Botrytis cinerea* small sRNAs (sRNAs). The sheet provides the sRNA sequence, its coordinates on the *B. cinerea* genome, the transposable (TE) origin, the gene ID of the predicted target gene, and a description of this gene.

Supplementary Table S8 Tomato genes predicted to be targeted by *Botrytis cinerea* small RNAs that display significant differential expression during *B. cinerea* infection, as compared to mock-inoculated leaves. Sheet contains both down-regulated and up-regulated genes.

Supplementary Table S9 Transposable elements in tomato as sources of small RNAs. The list provides the genomic location (chromosome, start and end coordinates), the transposable element (TE) identifier from REPET annotation, the read counts for the entire repeat region as well as the percentage of the total read counts. Only repeat elements that generated at least 30,000 read counts are included.

Supplementary Table S10 Predicted target mRNAs in *Botrytis cinerea* for each of 114,011 tomato small RNAs (sRNAs). The sheet provides the sRNA sequences, their coordinates on the tomato genome, the gene or transposable element (TE) origin, and the gene ID of the predicted target genes in *B. cinerea*.

Supplementary Table S11 *Botrytis cinerea* genes predicted to be targeted by tomato small RNAs that display significant down-regulation during infection, as compared to liquid culture controls.

Supplementary Table S12 Target genes from tomato and *Botrytis Cinerea* selected for detailed reverse transcription-quantitative PCR validation. The table contains the functional annotation of target genes, gene names used in this study, the gene ID (in tomato or *B. cinerea*), and small RNA (from *B. cinerea* or tomato) that is predicted to target the gene.

Supplementary Table S13 All primers used in this study.

Supplementary File S1 More detailed description of the experimental procedures.

Chapter 3

Molecular characterization of cross-kingdom RNA interference in *Botrytis cinerea* by tomato small RNAs

Si Qin[1*], Javier Veloso[1,2*], Guido Puccetti[1] and Jan A. L. van Kan[1]

[1]Laboratory of Phytopathology, Wageningen University, Netherlands

[2]FISAPLANT, University of A Coruña, Spain

[*] These authors equally contributed to this work

This chapter is published as:

Qin, S., Veloso, J., Puccetti, G., & Van Kan, J. A. L (2023). Molecular characterization of cross-kingdom RNA interference in *Botrytis cinerea* by tomato small RNAs. *Frontiers in Plant Science*, 14, 792.

Abstract

Previous studies have suggested that plants can modulate gene expression in pathogenic fungi by producing small RNAs (sRNAs) that can be translocated into the fungus and mediate gene silencing, which may interfere with the infection mechanism of the intruder. We sequenced sRNAs and mRNAs in early phases of the *Solanum lycopersicum* (tomato)-*Botrytis cinerea* interaction and examined the potential of plant sRNAs to silence their predicted mRNA targets in the fungus. Almost a million unique plant sRNAs were identified that could potentially target 97% of all fungal genes. We selected three fungal genes for detailed RT-qPCR analysis of the correlation between the abundance of specific plant sRNAs and their target mRNAs in the fungus. The fungal *Bcspl1* gene, which had been reported to be important for the fungal virulence, showed transient downregulation around 20 hours post inoculation and contained a unique target site for a single plant sRNA that was present at high levels. In order to study the functionality of this plant sRNA in reducing the *Bcspl1* transcript level, we generated a fungal mutant that contained a 5-nucleotide substitution that would abolish the interaction between the transcript and the sRNA without changing the encoded protein sequence. The level of the mutant *Bcspl1* transcript showed a transient decrease similar to wild type transcript, indicating that the tomato sRNA was not responsible for the downregulation of the Bcspl1 transcript. The virulence of the *Bcspl1* target site mutant was identical to the wild type fungus.

Introduction

Plants are continuously exposed to fungal pathogens but they are usually able to combat these pathogens and remain healthy. To achieve this, plants have evolved an array of defense mechanisms. One of the most extensively studied defense mechanisms is conferred by host programmed cell death (PCD) at the host-pathogen interaction site, which can subsequently restrict the invasion by biotrophic and necrotrophic pathogens. However, PCD does not necessarily stop the invasion of necrotrophic pathogens effectively. By contrast, necrotrophic fungal pathogens take advantage of the induction of host cell death for their infection as they feed on dead tissue. Plant PCD triggers a series of reactions in the host, such as fortification of the plant cell wall (by callose and lignin), local production of pathogenesis-related (PR) proteins, phytoalexins and production of reactive oxygen species (ROS) (Veloso and van Kan, 2018). Despite the induction of all these defense responses in the host plant, it cannot successfully halt the colonization by necrotrophs. It is thus relevant to study plant defense mechanism(s) which can successfully control plant diseases caused by necrotrophic fungi.

A novel insight in plant defense mechanisms has emerged in the past 15 years, demonstrating that plant transgene-derived double- stranded RNAs (dsRNAs) could induce gene silencing by RNA interference (RNAi) in invading pathogens and pests (Baum et al., 2007; Nowara et al., 2010; Iqbal et al., 2020), in a process referred to as host-induced gene silencing (HIGS). The proof of concept for exploiting HIGS to control a fungal pathogen was demonstrated by Nowara et al. (2010), who expressed a set of double-stranded RNAs in (stably or transiently) transformed plants that would target *Blumeria graminis* genes that encode either effector *Avra10* or 1,3-b-glucanosyltransferases involved in haustoria formation. The successful deployment of HIGS suggested the occurrence of trafficking of RNA molecules from a plant into a fungus that could induce RNAi in the fungus, and thus HIGS can be considered as an example of cross-kingdom RNAi (ckRNAi).

In later studies, it was reported that plant endogenous small RNAs (sRNAs) can be naturally translocated to parasitic organisms and trigger silencing of genes in the invaders through RNAi. This phenomenon provided an example of the natural occurrence of ckRNAi, and it was proposed to be an effective host defense strategy by several studies. The first case was in the cotton-*Verticillium dahliae* interaction, in which the production of two cotton microRNAs (miRNAs) increased upon infection by *V. dahliae* and the miRNAs were translocated to the fungal hyphae where they silenced specific *V. dahliae* genes (Zhang et al., 2016). Cai et al. (2018) demonstrated that Arabidopsis can secrete exosome-like vesicles containing sRNAs which can be taken up by *Botrytis cinerea* hyphae at the infection site. This

study described two small interfering RNAs (siRNAs) that selectively accumulate in fungal cells and are predicted to target *B. cinerea* genes that are involved in vesicle-trafficking pathways. A study by Hou et al. (2019) described that Arabidopsis produces increased amounts of secondary siRNAs upon infection by *Phytophthora capsici*. They observed that Arabidopsis mutants that are impaired in secondary siRNA biogenesis exhibited hyper-susceptibility to *P. capsici*. In several pathosystems, the naturally delivered host sRNAs have been proposed to contribute to plant immunity (likely) *via* silencing genes in the invading pathogens (Cai et al., 2018; Hou et al., 2019; Zhang et al., 2016). This process could contribute to plant defense against pathogens when the target genes that are silenced indeed have an important role in virulence or development of the pathogens.

We aimed to further explore the role of natural ckRNAi in defense of a model crop against a fungal pathogen. *Solanum lycopersicum* (tomato) is an important crop species that can be parasitized by many pathogenic microbes, resulting in considerable economic losses. The necrotrophic pathogen *B. cinerea* can infect different organs of the above-ground part of tomato plants, causing devastating damage for the crop during both pre- and post-harvest stages. *B. cinerea* was shown to be able to take up both sRNA and dsRNA molecules from the environment (Wang et al., 2016). The ability to take up exogenous sRNAs is one of the preconditions for the full function of RNAi triggered by sRNAs or dsRNAs present in the fungal environment. This feature of *B. cinerea* has been exploited in plant protection with spray-induced gene silencing (SIGS) by the application on plant surfaces of synthetic RNA molecules targeting genes involved in growth or in signaling required for virulence (McLoughlin et al., 2018; Nerva et al., 2020; Spada et al., 2021). Furthermore, a classical HIGS approach was also shown to enhance crop resistance against *B. cinerea* using transgenic potato lines expressing dsRNA that can target a *B. cinerea* gene which regulates cell growth and proliferation (Xiong et al., 2019). However, the efficacy of naturally occurring ckRNAi in the *B. cinerea*-crop interaction mediated by host-derived sRNAs is not fully conclusive.

In this study, we aimed to evaluate the role of endogenous sRNAs of the host plant in the early phases of the tomato - *B. cinerea* interaction. A sRNA and messenger RNA (mRNA) - sequence dataset were generated within the first 24 hours post inoculation (hpi). This dataset was described in a previous study (Chapter 2, Qin et al., 2023), in which we could not validate the contribution of *B. cinerea* sRNAs to fungal virulence. We turned our focus to the inverse side of the tomato – *B. cinerea* interaction, namely tomato sRNAs and their function in plant defense against *B. cinerea via* ckRNAi during a natural infection. Correlations were studied between the abundance of three selected tomato sRNAs and the transcript levels of their matching fungal genes. In an attempt to experimentally validate

the causal relation between the level of one tomato sRNA and its predicted single target mRNA in *B. cinerea*, we mutated a *B. cinerea* gene that was reported to contribute to fungal virulence and was predicted to be silenced by a single tomato sRNA. Substitutions in the target site neither altered the expression profile of the mutant transcript nor enhanced the fungal virulence by escaping the silencing effect by the tomato sRNA.

Results

B. cinerea genes down-regulated during infection and potentially targeted by sRNAs from tomato

Differential expression analyses of fungal genes were performed by comparing gene expression during infection of tomato leaves with a *B. cinerea* liquid culture, as described in Qin et al. (2023). More than 3000 *B. cinerea* genes (one quarter of the annotated genes) were differentially expressed at 24 hpi, as compared to growth in liquid culture, of which 1724 were up-regulated and 1282 were down-regulated (Supplementary Data 1). Among the up- regulated genes of *B. cinerea* at this time point of infection were genes encoding five polygalacturonases and 103 other carbohydrate-active enzymes (CAZymes), 51 proteases, 63 membrane transporters, 5 proteins involved in signaling and 12 putative transcription factors. Moreover, the cluster of *Bcboa* genes encoding biosynthetic enzymes for the production of the polyketide phytotoxin botcinic acid were upregulated at 24 hpi, as compared to the *in vitro* liquid culture. Meanwhile, the *in planta* down-regulated genes (at 24 hpi) included genes encoding 36 CAZymes, 27 proteases, 39 membrane transporters, 33 proteins involved in signaling and 93 putative transcription factors. Moreover, there was significant down-regulation *in planta* at 24 hpi of melanin biosynthetic genes (Schumacher, 2016), of the gene cluster encoding biosynthetic enzymes for production of the sesquiterpene phytotoxin botrydial (Porquier et al., 2016), as well as the non- ribosomal peptide synthase gene *Bcnrps8* and six polyketide synthase genes along with their flanking genes involved in synthesis of (yet unknown) secondary metabolites (Supplementary Data 1).

Within the entire dataset, approx. 15% of the *B. cinerea* genes (1713 genes) that were predicted targets of the tomato sRNAs indeed displayed significant down-regulation in at least one of the time points (12, 16 and 24 hpi) as compared to the liquid culture (Qin et al., 2023). These fungal transcripts were, on average, predicted to each be targeted by 19.3 unique tomato sRNAs (Supplementary Data 2). The list of *in planta* downregulated genes that are predicted to be silenced by tomato sRNAs includes genes encoding 63 CAZymes, 43 proteases, 46 membrane transporters, 46 proteins involved in signaling and 101 putative transcription factors (Supplementary Data 2). Only 30 fungal genes were predicted to be targeted by a single tomato sRNA, including transcripts encoding fumarase BcFUM1, glutathione S-reductase BcGST8, catalase BcCAT7, phosphatidylserine decarboxylase BcPSD, melanin biosynthetic enzyme BcBRN2 and the cell death- inducing effector BcSPL1.

Correlation between mRNA down- regulation in *B. cinerea* and levels of tomato sRNAs that are predicted to target them

After examining the *in silico* prediction of *B. cinerea* genes targeted by tomato sRNAs based on the sequencing dataset, we aimed to validate and establish in more detail the host sRNA – fungal mRNA profiles during the early infection. We performed new experiments to inoculate tomato leaves with *B. cinerea* and sampled at seven time points within the first 24 hpi. sRNA and mRNA were extracted from these samples, followed by quantification of the expression levels of selected tomato sRNAs (Sl-sRNAs) and their matching target mRNAs in *B. cinerea* (Bc- mRNAs) by reverse transcription-quantitative PCR (RT-qPCR). We selected three Sl-sRNAs and their predicted target Bc-mRNAs (Table 1) for molecular validation. The selection of sRNA-mRNA pairs was based on the following criteria: i) the predicted target mRNA showed sufficient reads in the sequencing dataset at all infection time points; ii) the predicted target mRNA was significantly down-regulated at one or more time point(s) as compared to the liquid culture; iii) the target gene might contribute to fungal infection; iv) the tomato sRNA was up- regulated in the early stages of infection and should be derived from a transposon locus. The following three *B. cinerea* genes were chosen for further analysis: the 5-oxoprolinase gene *Bcoxp1 is* a homolog of the *Fusarium graminearum oxp1* gene which was reported to be involved in development and virulence (Yang et al., 2018); the gene *Bccnd1*, encoding a secreted effector protein that is expressed in a calcineurin-dependent manner (Viaud et al., 2003) and is homologous to *GAS1* and *GAS2* effectors of *Magnaporthe grisea*, expressed in appressoria and required for full virulence (Xue et al., 2002); and the cerato-platanin gene *Bcspl1*, encoding an effector that induces plant cell death and is important for virulence (Frías et al., 2011).

Molecular quantification results from RT-qPCR indicated correlations between Sl-sRNAs and their matching Bc-mRNA targets (Figure 1). Expression levels of the three tested *B. cinerea* genes displayed upregulation at 12 hpi, and they reached their lowest level at 20 hpi but increased again at 24 hpi. The down- regulation of the three Bc-mRNAs coincided with, or followed shortly after, an increase of the levels of their corresponding Sl- sRNAs. Specifically, the lowest expression of the three Bc-mRNAs occurred at 20 hpi, while Sl-sRNAs levels were high at 14 hpi or 16 hpi (Figure 1). Interestingly, levels of these three selected Sl-sRNAs all displayed an approximate doubling in the early stage of fungal infection between 12 and 14 hpi, or between 14 and 16 hpi

Table 1. Selected predicted *B. cinerea* target genes and their corresponding Sl-sRNA sequences.

Annotation of target *B. cinerea* gene	Gene name	ID	Sl-sRNA – Bc-mRNA alignment	Free energy (kCal/Mol)
5-oxoprolinase	*Bcoxp1*	Bcin04g01040	BcOXP1: 5' acuAUUCAGUCUCCUCAACUCGAu 3' :|| :|||||||||||||| sRNA_1326: 3' ugcUGAGGUAGAGGAGUUGAGCUu 5'	-34.51
Calcineurin-dependent (CND) gene	*Bccnd1*	Bcin08g05540	Bccnd1: 5' gcUUUAUACAUCUUAAAUCUUUa 3' :|| | |||||||||||||| sRNA282: 3' uuGAACAGGUAGAAUUUAGAAAa 5'	-20.19
Cerato-platanin	*Bcspl1*	Bcin03g00500	spl1-wt: 5' acccaAGUCGACAAGAGUGCUUGU 3' |||| ||||||||:||||| sRNA1187: 3' caguaUCAGAUGUUCUCAUGAACA 5'	-28.41

Generation of *B. cinerea* mutant with synonymous substitutions at the target site in *Bcspl1*

From *B. cinerea* genes that were predicted to be targeted for silencing by tomato sRNAs, we selected one gene for experimental validation of a causal relation between the presence of the tomato sRNA and the down-regulation of its target *B. cinerea* mRNA. Selection of the gene was based on three criteria: its transcript should decrease at some time during infection, as compared to the previous time point(s) in the dataset; the transcript should be (predicted to be) targeted by a single tomato sRNA, in order to minimize the impact of multiple sRNA-mRNA interactions; the gene should participate in virulence of *B. cinerea.* The *Bcspl1* gene was selected as it is the predicted target of a single tomato sRNA (sRNA1187) and encodes a cell death inducing effector protein with a role in virulence (Frías et al., 2011). Only 30 genes were predicted to be targeted by a single tomato sRNA (Supplementary Data 2) and *Bcspl1* was the only gene in this list that had been reported to participate in virulence. During *B. cinerea* infection on tomato leaves, *Bcspl1* displayed a peak in transcript level at 12 hpi and was ~10-fold down-regulated at 20 hpi (Figure 1). The lower transcript level of *Bcspl1* coincided with a transient peak in the level at 16 hpi of the tomato sRNA1187 (Figure 1), which is produced from a transposable element on tomato

chromosome 6 (Figure 2A).

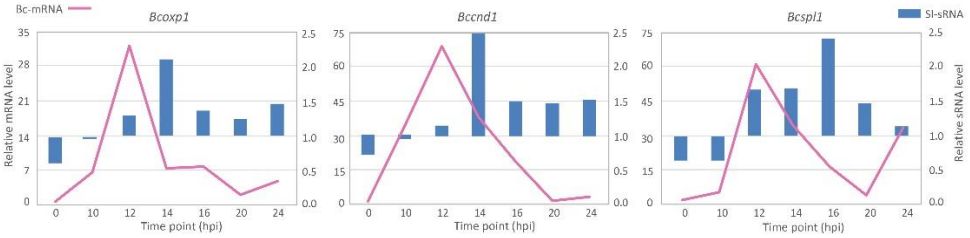

Figure 1. Quantification of production levels of three Sl-sRNAs (blue bars) and mRNA levels of their predicted target genes in *B. cinerea* (pink lines). The expression data were collected from four experiments, and the predicted target *B. cinerea* gene is indicated above each chart.

In order to disrupt the ability of *Bcspl1* mRNA to interact with sRNA1187, we aimed to generate a *B. cinerea* mutant carrying a *Bcspl1* allele with mutations in the sRNA target site. A substitution of five nucleotides would result in a change of free energy of the hybrid between sRNA1187 and the *Bcspl1* mRNA from -28 kCal/Mol (wild type) to -11 kCal/Mol (mutant), without changing the encoded protein (Figure 2B). The cut-off for free energy of RNA hybrids is -20 kCal/Mol (Marıńand Vanıç2011), implying that this substitution would fully abolish sRNA-mRNA hybrid formation. We checked that the synonymous substitutions in the *Bcspl1* target site would not result in a sequence that could inadvertently be targeted by different tomato sRNAs in the dataset. A gene replacement construct was generated that encompassed the entire *Bcspl1* gene (containing the desired five- nucleotide substitution) and a part of the downstream gene Bcin03g00510 with a hygromycin-resistance cassette (*hph*) inserted in the intergenic region (Figure 3A). Transformation of this construct to wild type *B. cinerea* strain B05.10 yielded seven transformants of which two contained the *hph* cassette in the target locus and five were ectopic transformants (Figure 3B). The *Bcspl1* gene from both transformants was amplified and sequenced. Transformant #5 contained the desired substitution and was named *spl1-5mnt.* Transformant #1 contained a wild type *Bcspl1* sequence, presumably as a result of recombination with the target locus downstream of the sRNA target site (orange dashed lines in Figure 3A). This transformant was designated *spl1-wt* and served asa control transformant to exclude an impact on transcript levels caused by introducing a *hph* cassette close to the *Bcspl1* locus.

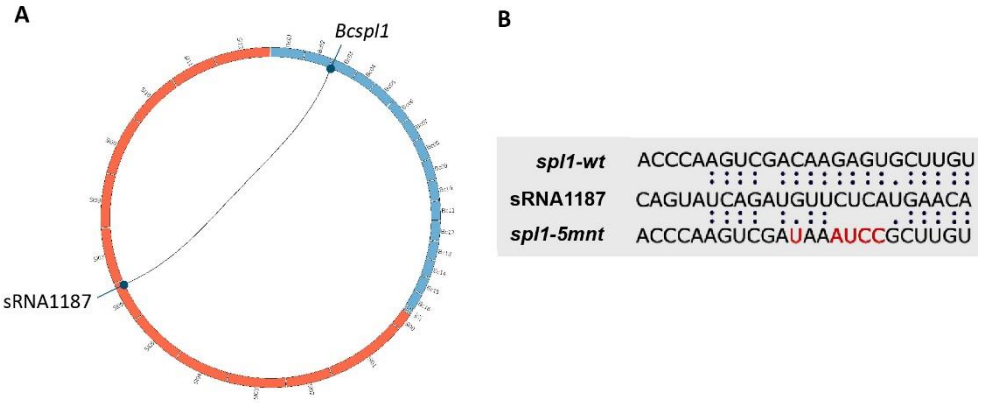

Figure 2. (A) Representation of the tomato genomic locus producing the sRNA1187 (tomato chromosomes presented as orange boxes) and the *B. cinerea Bcspl1* locus (*B. cinerea* chromosomes are presented as blue boxes). **(B)** Alignment of the sequences between tomato sRNA1187 and the wild type *Bcspl1* transcript or the mutated version designed to abolish interaction with the sRNA.

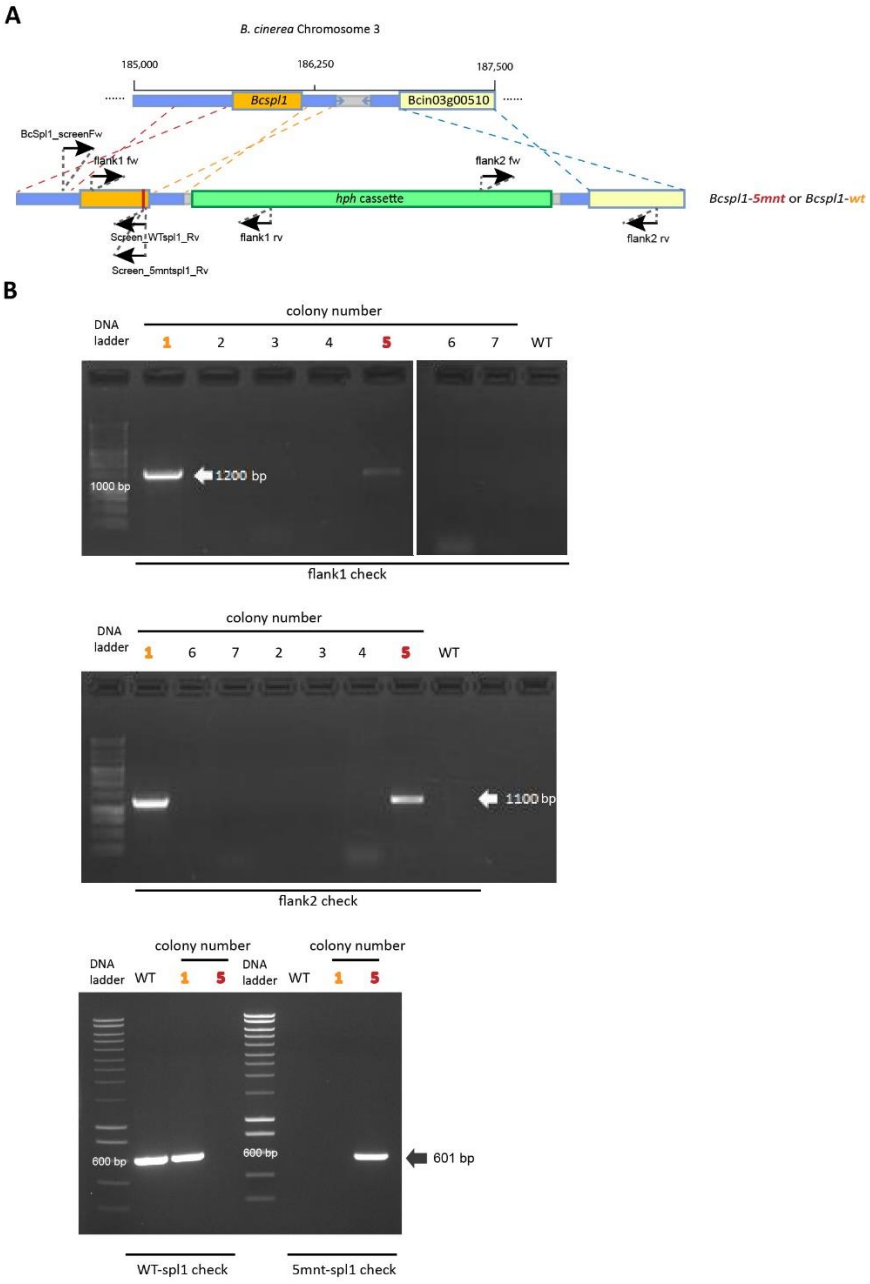

Figure 3. (A) Schematic representation of recombination events resulting in the generation of the transformants *spl1-5mnt* (red dashed lines) or *spl1-wt* (orange dashed lines). The blue dashed lines indicate the 3'-recombination event. The positions of primers used in genotyping the transformants are indicated. **(B)** Genotyping of transformants by PCR. Colony 1 (marked in orange) was the *spl1-wt* transformant while colony 5 (marked in red) was the *spl1-5mnt* mutant. Colonies 2-4 and 6-7 were ectopic transformants.

Effect of substitutions at the sRNA target site on *Bcspl*1 expression profile

We hypothesized that if the tomato sRNA would indeed participate in silencing of *Bcspl1* in *B. cinerea* during infection, the synonymous substitutions in the sRNA target site would result in a distinct *Bcspl1* transcript profile during infection, i.e., the downregulation between 16 and 24 hpi (as observed in Figure 1) would be abolished. This might result in a higher virulence of the fungal mutant if the increased production of BcSPL1 protein would enable the fungus to trigger host cell death more effectively.

We inoculated tomato leaves with both the *spl1-5mnt B. cinerea* mutant and the control *spl1-wt* transformant and sampled the tomato leaf samples at four timepoints between 12 and 36 hpi. RT-qPCR was performed to quantify the *Bcspl1* expression in *spl1- 5mnt* and *spl1-wt* mutants. Contrary to the hypothesis, the *Bcspl1* transcript profile in *spl1-5mnt* was similar to that in *spl1-wt* (Figure 4A), indicating that the downregulation of *Bcspl1* at 24 hpi was not abolished despite the substitution in the predicted target site for sRNA1187. Additionally, the level of tomato sRNA1187 was not significantly different between the leaf tissues infected by *spl1-wt* or *spl1-5mnt* isolates (Figure 4B). Infection assays were performed to compare the virulence of both transformants to each other and to wild type strain B05.10. As shown in Figure 5, there was neither a difference in virulence between *spl1-5mnt* and *spl1-wt*, nor between *spl1-wt* and wild type B05.10. These experiments did not provide any evidence for participation of tomato sRNA1187 in the downregulation of *Bcspl1* mRNA during infection.

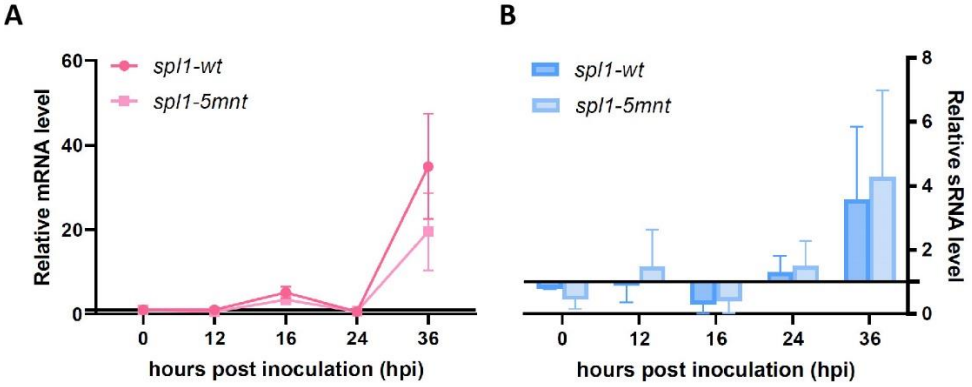

Figure 4. Expression levels of *Bcspl1* mRNA **(A)** and sRNA1187 **(B)** in *spl1-wt* and *spl1-5mnt* inoculated tomato leaves during the first 36 hpi. The expression data are shown by mean relative expression levels with standard error, either in a line chart **(A)** or a bar chart **(B)**, resulting from four independent inoculation assays.

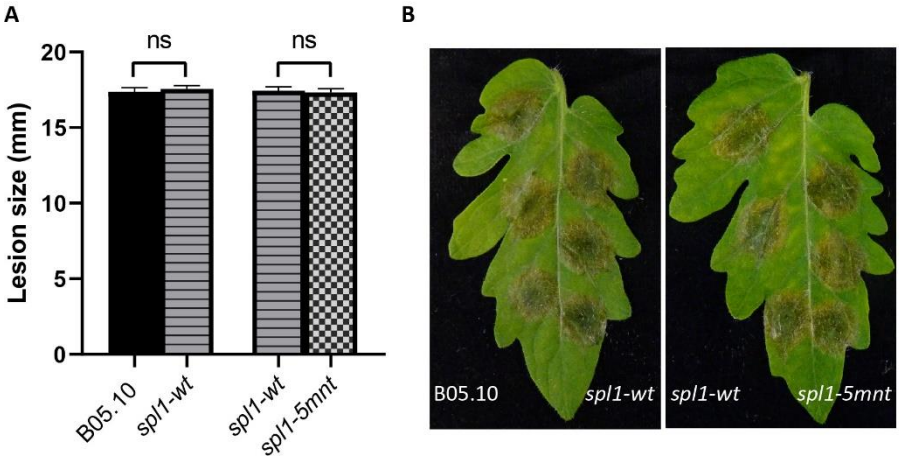

Figure 5. Virulence of *B. cinerea* WT B05.10*, spl1-wt* and *spl1-5mnt* transformants on tomato leaf, represented by a bar chart **(A)**; and disease symptoms photographed at 3 dpi **(B)**. The average lesion sizes and standard errors in the bar chart **(A)** resulted from 92 inoculations in three independent experiments, and statistical analysis was performed using t-test (ns indicates non-significance).

Discussion

In an earlier study (Chapter 2) we could not identify any evidence for the contribution of *B. cinerea* small RNAs to virulence through the induction of ckRNAi during infection. There are several examples that individual small RNAs, as those produced by *B. cinerea*, can indeed silence plant genes when expressed in stable or transiently transformed plants at high levels, as reported by Weiberg et al. (2013) and Wang et al. (2017). In a natural infection of *B. cinerea* on a host plant, however, the amount of fungal biomass is very low as compared to plant biomass at early time points of the interaction. As argued by Veloso and van Kan (2018), the decisive processes that determine success or failure in the *Botrytis*-host interaction occur around 16 hpi. In this phase of the interaction, our RNA samples typically contained ~1% fungal RNAs (both for the sRNA and mRNA pools) in the entire dataset. Fungal hyphae that penetrate the plant surface and enter the interior plant tissues are vastly outnumbered by plant cells. Furthermore, the fungal sRNA population consists of thousands of distinct unique sequences and their potency in silencing target mRNAs in a host plant is essentially defined by random chance (Chapter 2). If a specific fungal sRNA (at such low abundance) is able to target a plant mRNA and induce its silencing, it is unlikely that this will result in effective interference with crucial plant functions in the short time span of just a few hours. Indeed, our earlier study (Chapter 2) showed that *B. cinerea* mutants in which both Dicer- like genes were deleted did not produce any detectable transposon- derived sRNAs, and could infect four distinct host plant species as effectively as the wild type of fungus.

One can envisage that the inverse situation (plant sRNAs targeting fungal mRNAs) is distinct, as the abundance of plant RNAs largely exceeds that of fungal RNAs. In an early phase of the plant-fungus interaction, fungal hyphae that penetrate the host surface and enter the plant tissue are surrounded by a large number of plant cells, each of which may produce and release small RNAs. *B. cinerea* can take up sRNAs present in exocytotic vesicles that accumulate at the extracellular interface between the plant and fungal cells (Cai et al., 2018). Fungal appressoria and invasive hyphae could have a high propensity to take up host plant exocytotic vesicles containing sRNAs.

During the *B. cinerea*-tomato interaction, numerous fungal genes were downregulated over the course of the infection process. Based on observations of Weiberg et al. (2013) and Wang et al. (2016), and the identification of 88,196 potential, predicted Sl-sRNA – Bc-mRNA interactions in our dataset (Chapter 2), it was tempting to consider that many changes in fungal transcript levels were indeed caused by cross-kingdom RNAi. However, other explanations for down-regulation of fungal transcripts should also be taken into

consideration. *B. cinerea* undergoes infection-related developmental transitions during penetration of the host tissue, by forming either appressoria or infection cushions, each with their specific developmental and transcriptional program (Leroch et al., 2013; Choquer et al., 2021). Once these infection structures have completed host surface penetration (10-14 hpi), they become redundant and the fungus switches to an intercellular hyphal growth while suppressing host cell death (Veloso and van Kan, 2018). From ~16 hpi, host cells are triggered to undergo programmed cell death and the fungus is exposed to oxidative stress in dying host tissue (Torres et al., 2006; Choquer et al., 2007). These developmental transitions and changes in chemical environment are likely to have a much greater impact on fungal gene expression than the presence of any plant sRNAs.

We identified three *B. cinerea* genes related to fungal infection that were predicted to be targeted by tomato sRNAs and did indeed display a transient reduction of mRNA level during infection, as compared to liquid culture. RT-qPCR analysis was performed with sampling at seven time points between 0 and 24 hpi, in order to establish an association between the level of the sRNA and its target mRNA with a high resolution of the dynamics. We observed an inverse correlation between the level of each selected Sl-sRNA and its predicted target in *B. cinerea*, which suggested that ckRNAi possibly could have contributed to achieving this downregulation. However, whether the production of unique plant sRNA molecules able to target a fungal mRNA could actually cause the downregulation of its target was difficult to establish merely from the expression profiles.

We therefore introduced mutations in the target site of a *B. cinerea* gene, *Bcspl1*, aiming to establish a causal relation between the production of the unique tomato sRNA molecule and the downregulation of *Bcspl1* mRNA in *B. cinerea*. The *B. cinerea* transformant with the allelic variant of *Bcspl1* displayed a similar transcript profile and the same virulence as the control transformant with an unaltered target site. This result indicated that the transient downregulation of the *Bcspl1* transcript at 24 hpi was not mediated by the tomato sRNA, but possibly controlled by an intrinsic regulatory mechanism within the fungus, instead of resulting from cross-kingdom RNAi. Only a single pair of Sl-sRNA – Bc-mRNA was examined in this study due to the restriction by the criteria that we set. In order to study in more detail whether tomato sRNAs indeed play a role in plant defense against *B. cinerea*, two aspects should be taken into account. Firstly, many sRNAs are derived from transposons, some with multiple closely related, but non-identical copies, and it is genetically impossible to dissect the function of individual naturally-produced sRNAs from the host. In order to functionally eliminate the vast majority of tomato sRNAs, one should use a tomato mutant in which multiple Dicer-like (*DCL*) genes are knocked out. There are seven *DCL* genes in tomato

(*SlDCL1*, *SlDCL2a-d*, *SlDCL3* and *SlDCL4*) (Bai et al., 2012), and *SlDCL1* or *SlDCL3*-silencing mutant as well as single loss-of-function mutant of *SlDCL2b* or *SLDCL4* are available (Yifhar et al., 2012; Kravchik et al., 2014a; Kravchik et al., 2014b; Wang et al., 2018). Phenotypic characterization of these individual mutants proved that different SlDCL proteins are responsible for the production of different types of sRNAs. In order to abolish the biosynthesis of all sRNAs that potentially participate in cross- kingdom RNAi, multiple *SlDCLs*-knock-out mutants should be used. Such plants are, however, not available and research in Arabidopsis has shown that the deletion of multiple Dicer-like genes can have serious impact on plant viability and morphology (Bouchéet al., 2006). Besides, the host sRNAs which are naturally translocated into the fungus are only a small proportion of the total host sRNAs generated by DCL proteins. Many plants sRNAs have regulatory functions on endogenous genes by RNAi and influence developmental processes or resistance to stress. Therefore, an enhanced susceptibility of plant mutants lacking *DCL* genes would not directly prove the function of plant sRNAs in plant defense *via* ckRNAi, due to the numerous physiological roles of the *DCL* genes.

The natural occurrence and function of the ckRNAi from both sides of the plant-parasite interaction is a relatively young research topic. A number of studies concluded that ckRNAi is a naturally occurring phenomenon. There were also observations that specific plant sRNAs can play a role in plant defense against pathogens, however, mostly through indirect methods by either overexpressing these sRNAs in plants (Hou et al., 2019) or knocking out their predicted target genes in the pathogen (Zhang et al., 2016). The technical and biological challenges that we discussed above clearly limit the capacity to directly prove the occurrence and importance of natural ckRNAi. It thus remains debatable to what extent the natural occurrence of ckRNAi mediated by endogenous host sRNAs contributes to effective plant defense.

Materials and methods

Fungal strains, plant material and growth conditions

B. cinerea strains used in this study (Table 2) were grown and spores were collected as described in Zhang and van Kan (2013). Tomato (*S. lycopersicum* cv. Moneymaker) were grown in a greenhouse at 20°C for five to six weeks, and detached compound leaves were used for inoculation assays.

Table 2. *B. cinerea* strains used in this study.

B. cinerea **strain**	**Description**	**Reference**
B05.10	Wild type *B. cinerea*	van Kan et al. (2017)
spl1-5mnt	Strain containing synonymous substitutions of 5 nt in tomato sRNA target site in the *Bcspl1* coding sequence and a hygromycin-resistance cassette.	This study
spl1-wt	Strain containing wild type *Bcspl1* and a hygromycin-resistance cassette.	This study

Tomato inoculations with *B. cinerea*

B. cinerea conidia were diluted in Potato Dextrose Broth (PDB, 12 g/l) medium to 1000 conidia/ml and 2 ml droplets containing the conidia suspension were inoculated on detached tomato leaves essentially as described by Zhang and van Kan (2013). The inoculated compound leaves were inserted in wet floral foam and incubated in closed containers at 20°C with relative humidity of ~100% under natural light, before being examined for the virulence assay or sampled for further purposes. For the virulence assay, each tomato leaflet was inoculated with three droplets on every leaf half for one *B. cinerea* strain. For the sampling of *B. cinerea* (or mock) - infected tomato leaves that was used for mRNA and sRNA sequencing, 10 droplets of 2 ml conidia suspension (or only PDB) were inoculated on both leaf halves at ~1 cm from the central vein. Four leaflets of one compound leaf were inoculated at the same time, and one leaflet was sampled by excising the central vein and collecting the remaining leaf tissue at each defined time point (t=0; 12; 16 and 24 hpi). For the sampling *B. cinerea* (or mock) - infected tomato leaves that was used for the quantitative reverse transcription PCR (RT-qPCR), the leaflets were inoculated in six to eight

circular areas and area included five 2 ml droplets of conidia suspension (or only PDB). The inoculated areas were excised by a cork borer with a diameter of 15.6 mm at each time point (t=0; 12; 16, 24 and 36 hpi). More details on the inoculation and sampling design were described in Qin et al. (2023).

RNA extraction

Fungal mycelium or tomato leaf samples were frozen in liquid nitrogen and used for extraction of small RNA using the mirPremier® microRNA Isolation Kit (Sigma-Aldrich) while mRNA was isolated using the Maxwell® 16 LEV Plant RNA Kit (Promega).

Generation and bioinformatic analyses of the RNAseq dataset

Single-end Illumina sequencing was applied to all sRNA and mRNA samples by Vertis Biotechnologie AG (Martinsried, Germany) on a strand-specific library with read length of 75 nt. Sequence processing and bioinformatic analyses of data are described in Qin et al. (2023). Differentially expressed genes (DEGs) in the fungus were identified by comparing fungal mRNA levels in the infected tomato leaf tissues with a *B. cinerea* liquid culture, as described in our recent study (Chapter 2). Differentially produced sRNAs in tomato were analyzed by comparing tomato sRNA levels in the *B. cinerea*-infected tomato leaf tissues with the mock-inoculated leaf tissues at the same time point, as described in Qin et al. (2023). The thresholds for up- or down- regulation were calculated similarly for both mRNA and sRNA, using the DEseq2 algorithm through a negative binomial distribution to calculate the p-value. The significance was defined by thresholds that consisted of a p-value of lower than 0.05 and a log2 fold-change of higher than 1 or lower than -1 for up- or down-regulation, respectively. To determine the origin of the sRNA reads, the reads were mapped to both the *B. cinerea* and *S. lycopersicum* genomes. Bowtie was used as mapping tool with the constraint to only map reads without mismatches (-v 0). Reads that had a perfect match to the *B. cinerea* genome were also mapped to the *S. lycopersicum* genome and vice versa. Reads mapping perfectly on both genomes were labelled as 'shared reads' and were discarded, while reads that mapped to only one genome were labelled as 'unique reads'. Target prediction of sRNAs was performed using sRNAs extracted from the 'unique reads'. The tool psRNATarget was used to predict the plant sRNA targets on the fungal mRNA population (Dai et al., 2018), with settings adjusted to the default Schema V2 2017. The 'expectation' was set to match a free energy threshold of -20 kCal/mol (expectation 3). Both UTRs and CDS were tested for target sites. The sequences of the UTRs and CDS were obtained using the coordinates of the ASM83294v1 release-51 *B. cinerea* annotation. Predicted sRNA-target pairs were filtered by expression keeping only the sRNA-target pairs that

showed sRNA up- regulation and target mRNA down-regulation.

RT-qPCR quantification of mRNA and sRNA levels

Synthesis of cDNA from mRNA was performed using M-MLV reverse transcriptase (Promega). For reverse transcription of sRNA, the qScript microRNA cDNA Synthesis kit (Quanta Bioscience) was used. RT-qPCR was performed using SensiMix SYBR Hi-ROX Kit (Bioline). Primer combinations described in Supplementary Table 1 were used in RT-qPCR to quantify levels of mRNAs and sRNAs. The transcript level of a ribosomal protein encoding gene *Bcrpl5* from *B. cinerea* was used to normalize fungal mRNA levels. A sRNA of the tomato U6 spliceosomal RNA component was used to normalize plant sRNAs. The threshold cycle (Ct) values were determined by Bio-Rad CFX Manager 3.1 and fold-changes calculated using the $2^{-\Delta\Delta Ct}$ method (Pfaffl, 2006).

***B. cinerea* transformation**

B. cinerea mutant strains used in this study were generated by PEG-mediated protoplast transformation as described by (Kars et al., 2005) with minor modifications. The constructs of donor templates were made by the yeast recombination method as described by Schumacher (2012). For the construction of plasmids as well as the amplification of donor templates, PCR was performed with the primer sets shown in Supplementary Table S1 using the Expand™ High Fidelity PCR System (Sigma). After obtaining transformed colonies on hygromycin-selective plates, the screening of transformants was performed by PCR with primer sets indicated in Supplementary Table 1 using the GoTaq® G2 DNA Polymerase (Promega). The coding region of the *Bcspl1* gene from the mutants used in this study was sequenced to verify whether or not the sRNA target site contained the 5- nucleotide substitution.

Data availability statement

The datasets presented in this study have been deposited in the NCBI database under Bioproject at www.ncbi.nlm.nih.gov/ bioproject/ with accession number PRJNA496584. Raw sequence reads are deposited in the Sequence Read Archive at www.ncbi. nlm.nih.gov/sra/ project SRP166089 under accession numbers SRX4902781-SRX4902782, SRX4902789, SRX4902791-SRX4902800, SRX15228005-SRX15228010, SRX15231189, SRX15231190, SRX19002251 (sRNAs) SRX4902771-SRX4902780, SRX4902783-SRX4902787, SRX4902790, SRX15231192, SRX15231193, SRX19002219 (mRNAs).

Supplementary materials

The following Supplementary materials are available to be downloaded from the "Supplementary materials_PhD thesis_Qin(2023).zip" file, and thus only legends are shown below.

Supplementary Table S1. The list of DNA primers used in this study.

Supplementary Data S1. Differentially expressed *B. cinerea* genes during the infection of tomato leaves (sampled at 12, 16 and 24 hpi), as compared with a *B. cinerea in vitro* culture. The data contains four Excel sheets, which respectively provide all DEGs at 12/16/24 hpi *in planta*, and a summary sheet presenting the numbers of DEGs that are described to encode transporters, CAZymes, proteases, proteins involved in SM biosynthesis, signaling components and transcription factors (TFs) at different timepoints.

Supplementary Data S2. The data includes three sheets, i) the list of *B. cinerea* genes which were predicted to be targeted by tomato sRNAs, and the number of unique tomato sRNA sequences and merged sRNA sequences are shown together with their predicted matching single fungal gene; ii) the details of log2 fold-change and the adjusted p-value for each predicted target fungal gene which were significantly down-regulated at no less than one time point *in planta*, and iii) a legend that explains the headings in the columns of the former two sheets.

Chapter 4

The phytotoxin botrydial produced by *Botrytis cinerea* contributes to fungal virulence and triggers cell death in both dicotyledons and monocotyledons

Si Qin[1], Inmaculada Izquierdo-Bueno[2], Isidro González Collado[2] and Jan A. L. van Kan[1]

[1]Laboratory of Phytopathology, Wageningen University, Netherlands

[2]Departamento de Química Orgánica, Facultad de Ciencias, Universidad de Cádiz, Spain

Abstract

The necrotrophic plant pathogen *Botrytis cinerea* produces phytotoxic secondary metabolites during host infection. Until now, the contribution of the two major phytotoxins botrydial (BOT) and botcinic acid (BOA) to the virulence of *B. cinerea* is still disputable, since results from virulence assays using different mutants performed by separate research groups were inconsistent. In this study, we assessed the roles of BOT and BOA in virulence of *B. cinerea* on five distinct host species. We observed different levels of reduction in the virulence of *B. cinerea* mutants lacking the capacity to produce BOT and/or BOA as compared to the wild type fungus. Interestingly, BOT was indispensable for *B. cinerea* to successfully infect Arabidopsis*,* whereas deficiency in BOA production did not reduce the virulence of *B. cinerea* on this host. Lacking either BOT or BOA production in *B. cinerea* resulted in slightly reduced virulence on tomato, and eliminating both phytotoxins had an additive effect on lowering the virulence on this host. The same *B. cinerea* double mutant exhibited subtle though significant reduction in virulence on *Nicotiana benthamiana* and cowpea but not on French bean. Moreover, we validated the phytotoxic activity of BOT on different dicotyledons and report for the first time that monocotyledons are also sensitive to BOT. This study provides evidence that BOT could be used as a potential tool to explore host susceptibility to *Botrytis* in some plant species.

Introduction

Botrydial (BOT), botcinic acid (BOA) and their derivatives are the major phytotoxic secondary metabolites produced by the plant pathogen *Botrytis cinerea* (I. G. Collado et al., 2007). BOT is a bicyclic sesquiterpene, which requires a gene cluster containing seven genes (*Bcbot1-Bcbot7*) for its biosynthesis (Pinedo et al., 2008; Porquier et al., 2016). Deleting a key gene for synthesizing BOT in the *B. cinerea* strain T4 resulted in reduced virulence, while the *Δbot1 or Δbot2* mutants generated in other strains showed similar virulence as the wild type (WT) recipients (Pinedo et al., 2008; Siewers et al., 2005). The gene cluster responsible for the biosynthesis of the polyketide BOA includes 13 genes, named *Bcboa1-Bcboa13* (Porquier et al., 2019; van Kan et al., 2017). The two polyketide synthase genes *Bcboa6* and *Bcboa9* are both essential for the production of BOA in *B. cinerea*. Mutant strains lacking either *Bcboa6* or *Bcboa9* displayed no significant difference in virulence as compared to the WT *B. cinerea* strain B05.10, and the *Δbot2* mutant derived from B05.10 also showed no reduction in virulence on French bean (*Phaseolus vulgaris*) and tomato (*Solanum lycopersicum*) (Dalmais et al., 2011). Dalmais et al. (2011) also reported that *Δbot2Δboa6* double mutants, which produced neither BOT nor BOA, displayed reduced virulence compared with the WT B05.10 on these two hosts. However, a recent study from Leisen et al. (2020) showed no difference in virulence between the WT B05.10 and the *Δbot2Δboa6* mutant strain generated by CRISPR/Cas9-mediated transformation. Although these two studies independently generated *Δbot2Δboa6* mutant strains with the same recipient strain, different results were observed in infection assays for assessing the virulence of mutants. Generally, it seems that the role of BOT and BOA in the virulence of *B. cinerea* is debatable.

It is known that *B. cinerea* produces BOT both during fermentation *in vitro* (Rebordinos et al., 1996) and infection *in planta* (Deighton et al., 2001). BOT extracted from *B. cinerea* culture filtrate has been demonstrated to be phytotoxic to *Nicotiana tabacum* (Rebordinos et al., 1996) and French bean (Colmenares et al., 2002). A study by Rossi et al. (2011) showed that necrotic symptoms were detected on *A. thaliana* leaves at spots treated with BOT. Deighton et al. (2001) described for the first time that BOT was detected in different host tissues upon infection by *B. cinerea*, including ripe fruits of sweet pepper (*Capsicum annuum*), leaves of French bean and *Arabidopsis thaliana*. The highest concentration of BOT detected *in planta* reached 140 nmol/g in one of the tested French bean cultivars upon infection by the aggressive strain B05.10. Collectively, BOT is able to induce cell death in different plant species, and it can be produced in *in vitro* cultures as well as during plant infection by *B. cinerea*.

Until now, all published studies evaluated the toxicity of BOT in dicotyledonous plants, as *B. cinerea* mainly infect dicots. However, BOT can be produced not only by *B. cinerea* but also by several other *Botrytis* spp., including some which are specialized to single monocot taxa as their natural hosts (Valero-Jiménez et al., 2020). According to the genome annotations of different *Botrytis* spp., a fully functional BOT cluster is present in four species infecting *Allium* species (*B. aclada*, *B. porri*, *B. sinoallii* and *B. squamosa*), and in two species infecting monocotyledonous ornamentals (*B. deweyae* on daylily and *B. elliptica* on lily) (Elad et al., 2016; Valero-Jiménez et al., 2020). The function of maintaining the BOT gene cluster in different *Botrytis* spp. besides *B. cinerea* is under-investigated. Therefore, testing whether BOT is toxic to monocots, especially the species that are hosts of the *Botrytis* spp. possessing a BOT cluster, will allow us to gain insights in the potential function of BOT in these pathogens.

In this study, we first validated the role of BOT and BOA in fungal virulence of *B. cinerea* on different host species through infection assays using the WT strain B05.10 and mutants that are unable to produce BOT or/and BOA. Secondly, we examined the phytotoxic activity of BOT on several dicotyledon and monocotyledon plant species by applying pure BOT on leaf surfaces. We observed that BOT was able to induce cell death responses in all dicots and monocots tested, legitimizing the presence of functional BOT clusters in monocot-specific *Botrytis* species.

Results

BOT is essential for the virulence of *B. cinerea* on *A. thaliana*

In order to assess the contribution of BOT and BOA to the virulence of *B. cinerea*, we inoculated *A. thaliana* (Col-0) plants with the wild type (WT) strain B05.10, the *Δbot2#1* mutant that is unable to produce BOT, the *Δboa6#1* mutant that does not produce BOA, and the *Δbot2Δboa6#6* double mutant that produces neither BOT nor BOA. The WT B05.10 was able to cause macerated expanding lesions on inoculated leaves (Figure 1). The vast majority of inoculations with the *Δbot2#1* and *Δbot2Δboa6#6* strains resulted in water-soaked, necrotic lesions restricted to the inoculation area (Figure 1A&B), indicating that BOT production is essential for the virulence of *B. cinerea* on *A. thaliana*. The *Δboa6#1* single knockout mutant displayed similar virulence as the WT B05.10 (Figure 1), suggesting that BOA alone does not play a detectable role in the fungal virulence on *A. thaliana.*

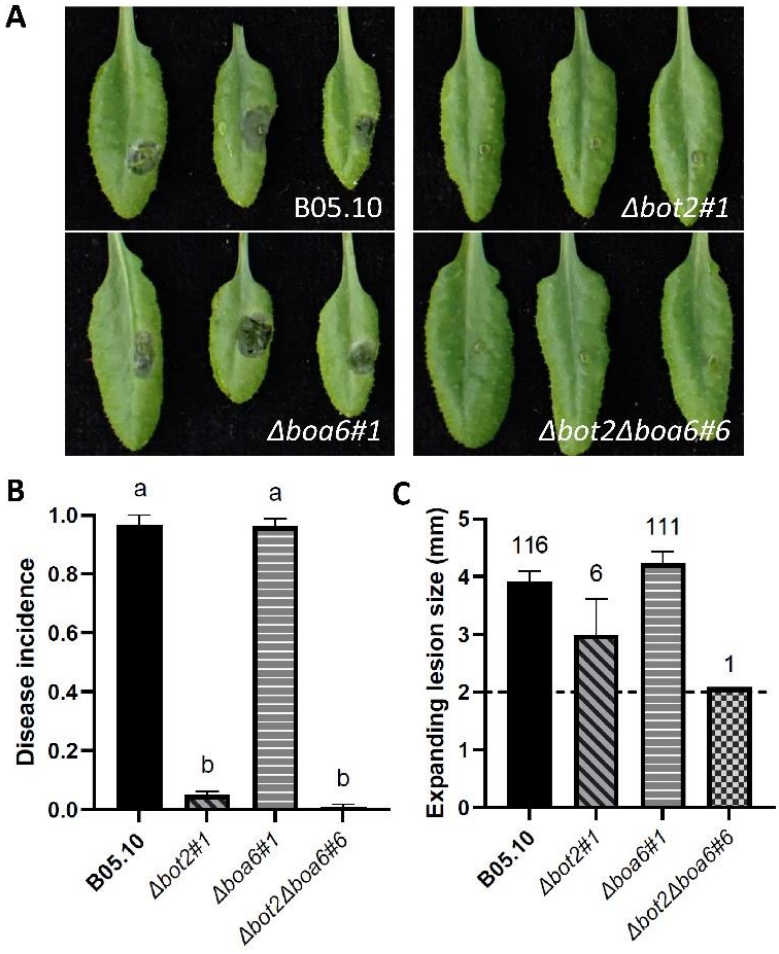

Figure 1. Virulence of WT B05.10, *Δbot2#1, Δboa6#1* and *Δbot2Δboa6#6* on *A. thaliana* (Col-0) leaves. **(A)** The symptoms on leaves inoculated with different *B. cinerea* strains were photographed at 3 days post inoculation (dpi). **(B)** Disease incidence (the ratio of the number of expanding lesions to the number of inoculation sites; a lesion with a diameter > 2 mm was defined as an expanding lesion) of tested *B. cinerea* strains, represented in means with standard errors from three experiments. Statistics was performed using a one-way ANOVA test in GraphPad Prism, of which the significant differences are indicated by different letters. **(C)** Expanding lesion sizes at 3 dpi, represented as a bar chart with means and standard errors. The horizontal dashed line indicates the cutoff for distinguishing expanding from non-expanding lesions. The number of expanding lesions caused by each strain out of ~120 inoculations from three experiments is shown above the corresponding bar. Due to the low number of expanding lesions of *Δbot2#1* and *Δbot2Δboa6#6*, statistical analysis was only performed to compare the lesion sizes between WT B05.10 and *Δboa6#1* using a t-test, which resulted in no significant difference (not indicated in the chart).

BOT and BOA play minor roles in fungal virulence on tomato, *N. benthamiana* and cowpea

After determining the contribution of BOT and BOA to the virulence of *B. cinerea* on Arabidopsis, we set out to assess the role of these two phytotoxins in virulence on different host plants. Virulence assays were performed on leaves of tomato cv. Moneymaker using the WT strain B05.10, the single mutants *Δbot2#1* and *Δboa6#1,* and the double mutant *Δbot2Δboa6#6*. Unlike in *A. thaliana*, *Δbot2#1, Δboa6#1* and *Δbot2Δboa6#6* were always able to induce expanding lesions on tomato leaves, resulting in lesion sizes that were about 7%, 4% and 14% smaller as compared to lesions of the WT strain B05.10, respectively (Figure 2). The delicate difference in lesion size between the *Δboa6#1* mutant and B05.10 could not be observed by the naked eye (Figure 2A), although the difference was statistically significant (Figure 2B). The reductions in virulence of *Δbot2#1* and *Δbot2Δboa6#6* was observed visually and statistically. These data suggest that BOT is slightly more important than BOA for the virulence of *B. cinerea* on tomato, even though both metabolites play only minor roles in the virulence on this specific host. In addition, the disability to produce both BOT and BOA led to an additive but not synergistic effect on the reduction of fungal virulence.

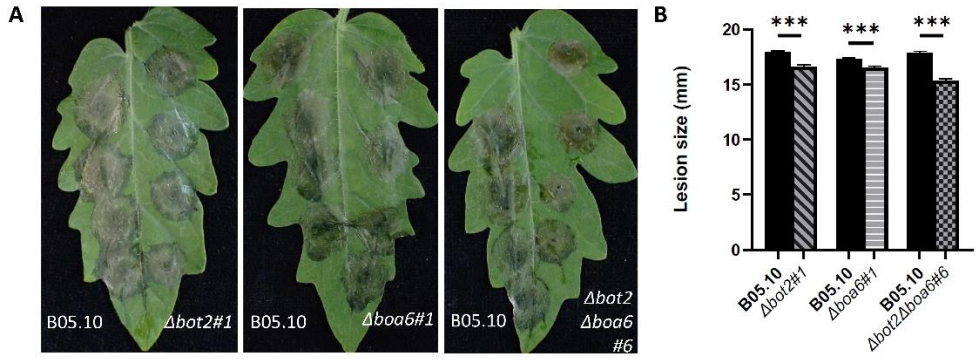

Figure 2. Virulence of *Δbot2#1, Δboa6#1* and *Δbot2Δboa6#6* compared with WT B05.10 on tomato leaves. **(A)** The symptoms on tomato leaves infected by each mutant strain (on the right of the central vein) compared with B05.10 (on the left of the central vein), photographed at 3 dpi. **(B)** Lesion sizes measured at 3 dpi are presented as means with standard errors from 96 datapoints, collected from three independent experiments. Asterisks indicate the significant differences (***p<0.001) by t-test.

In addition to tomato, the virulence of the double mutant *Δbot2Δboa6#6* was further assessed on leaves of *N. benthamiana*, *P. vulgaris* (French bean) and *Vigna unguiculata* (cowpea). The mutant *Δbot2Δboa6#6* displayed ~22% decreased virulence compared with B05.10 on *N. benthamiana* (Figure 3A). However, there was no significant difference or only a subtle difference (~6%) in virulence between *Δbot2Δboa6#6* and B05.10 on French bean

(Figure 3B) and on cowpea (Figure 3C), respectively. Collectively, the contribution of BOT and BOA to the virulence of *B. cinerea* is more pronounced on tomato and *N. benthamiana* than on French bean and cowpea.

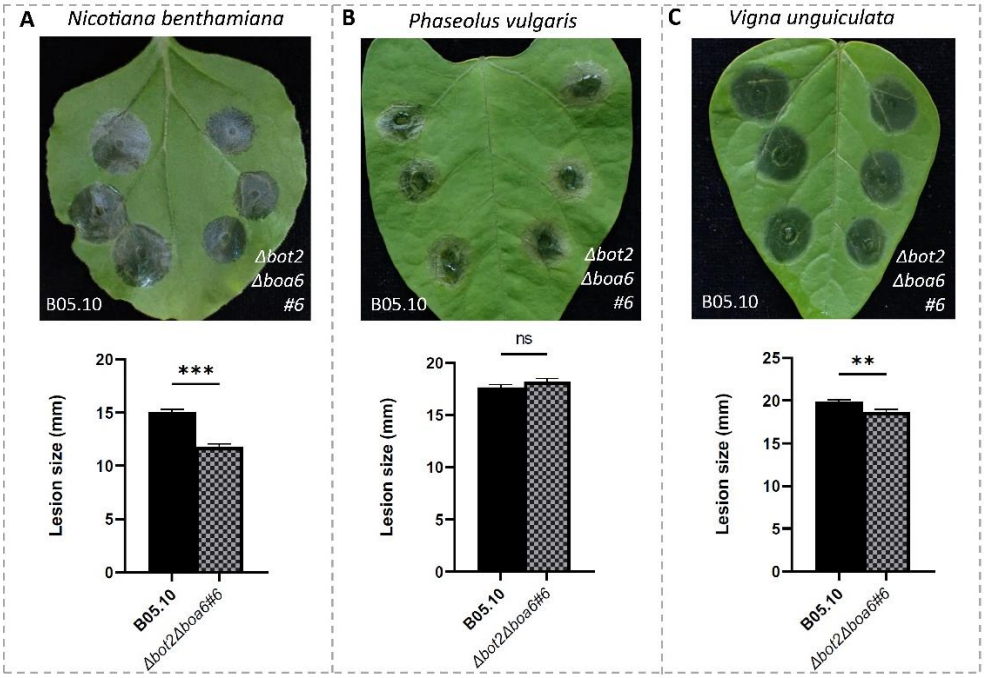

Figure 3. Virulence of *Δbot2Δboa6#6* as compared with WT B05.10 on **(A)** *N. benthamiana*, **(B)** French bean and **(C)** cowpea, shown by photographed symptoms (top) and mean lesion sizes with standard errors in bar charts (bottom) at 3dpi. The results are obtained from 134, 146 and 144 inoculations in three experiments on *N. benthamiana,* French bean and cowpea, respectively. Asterisks indicate the significant differences (***p<0.0001; **p<0.01) and ns stands for no significant difference, resulted from statistics performed by t-test.

BOT can induce cell death in leaves of different dicots

Previous studies have reported the toxicity of BOT on only a limited number of plant species, including *A. thaliana*, *N. tabacum* and French bean. Although BOT is considered to be non-selective, it has not been experimentally validated that this phytotoxin can indeed induce cell death in many different plants that are potential hosts for *B. cinerea*. Therefore, we tested the cell death inducing activity of pure BOT on the five dicotyledonous plant species which were used for the infection assays of the BOT-deficient *B. cinerea* strain(s) in this study (Figures 1 - 3). After surface application of droplets of 100 µM BOT dissolved in 40 % acetone, all leaves of *A. thaliana*, tomato, *N. benthamiana*, French bean and cowpea showed necrotic symptoms, while control applications with 40 % acetone alone did not

trigger any plant response (Figure 4), indicating that BOT has a phytotoxic effect on these five plant species. The symptoms were restricted to the areas where the droplets containing BOT was applied. However, the necrotic symptoms induced by BOT on leaves of the tested plants differed in appearance. Chlorosis (yellowing) was observed on *A. thaliana* (Figure 4A) and *N. benthamiana* leaves (Figure 4C) upon application of droplets containing BOT, while scattered brownish spots were seen on leaves of tomato, French bean and cowpea (Figure 4B, D & E). Besides visual inspection, we examined the red light emission in leaves treated with BOT in the ChemiDoc MP Imaging System (Landeo Villanueva et al., 2021), which is more sensitive than visual evaluation (Figure 4). Neither with the naked eye, nor by red light emission any response upon the 40 % acetone control treatment could be observed, whereas on all plants the plants BOT application yielded a fluorescent signal, indicating chlorophyll degradation and a plant cell death response.

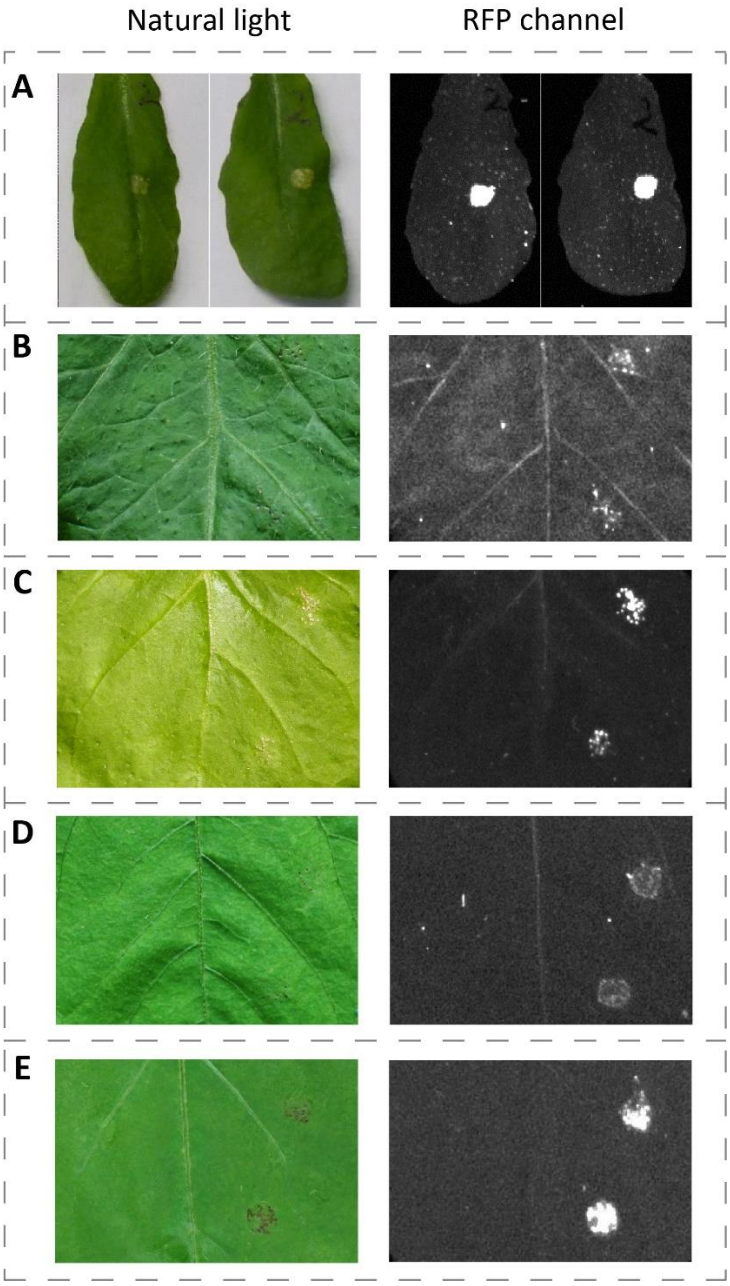

Figure 4. Response to BOT on leaves of **(A)** *A. thaliana*, **(B)** tomato. **(C)** *N. benthamiana*, **(D)** French bean and **(E)** cowpea. BOT was applied in 5 µl droplets of 100 µM BOT dissolved in 40% acetone on the adaxial surface of the leaves on the right side of the central vein. The control treatment was performed using 5 µl droplets of 40% acetone on the left side of the central vein. The symptoms were photographed by digital camera under natural light (left) and by red light imaging (right) on the 5th day after the treatment.

BOT is toxic to monocotyledonous plants

Genome sequence analysis revealed that *B. elliptica*, *B. aclada* and *B. squamosa* contain a functional gene cluster for the biosynthesis of BOT (Valero-Jiménez et al., 2020). To test whether BOT is able to induce cell death in monocotyledonous hosts of *Botrytis* spp. that can produce this phytotoxin, we treated leaves of *Lilium* (lily) with 100 µM and 500 µM BOT, and *Allium cepa* (onion) leaves with 100 µM BOT. Interestingly, the tested cultivars of lily and onion were both sensitive to BOT. The application of 500 µM BOT on lily leaves and 100 µM BOT on onion leaves resulted in clear cell death responses, as indicated by intense signals at the application spots detected by red light imaging (Figure 5A & B). Lily leaves treated with 100 µM BOT displayed much weaker responses as compared to the higher concentration of toxin, although these signals were still detectable by the red light imaging. In addition to lily and onion, we tested the toxicity of BOT on a few other monocotyledonous species that are not natural hosts of *Botrytis* species. *Zea mays* (maize), *Triticum aestivum* (wheat) and two grass species of the *Digitaria* genus (*D. ischaemum* and *D. sanguinalis*) were tested with 100 µM BOT, and they all turned out to be sensitive to this toxin (Figure 5 C-E). The 40%-acetone-treated controls did not show a different signal as compared to the non-treated areas (Figure 5).

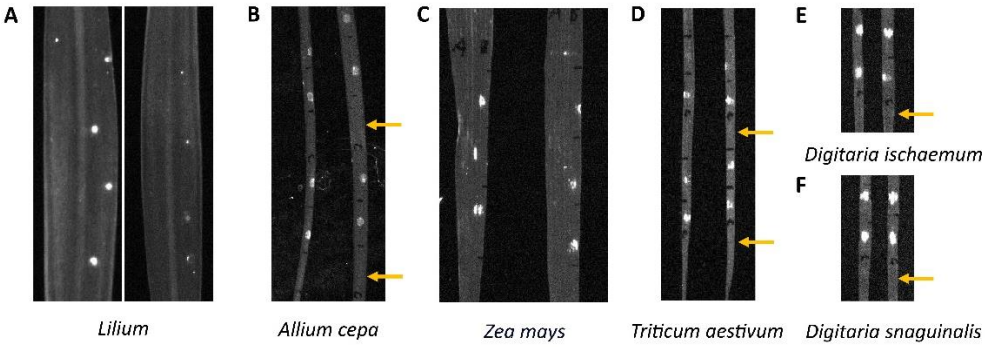

Figure 5. Necrotic symptoms triggered by application of BOT on leaves of **(A)** lily, **(B)** onion, **(C)** maize, **(D)** wheat and **(E-F)** two *Digitaria* species, detected by red light imaging on the 5th day after BOT treatment. Five µl droplets of BOT dissolved in 40% acetone were applied on the right side of the central vein on **(A)** lily (500 µM BOT for the leaf shown on the left and 100 µM BOT for the leaf shown on the right) and **(C)** maize (100 µM BOT) and droplets of 40% acetone were applied as control on the left side. **(B, D-F)** Alternating application of two droplets of 100 µM BOT and one droplet of 40% acetone (indicated by yellow arrows) on the leaf surfaces of onion, wheat and *Digitaria* grasses, after every two droplets of 100 µM BOT.

Discussion

The contribution of BOT and BOA to the virulence of *B. cinerea* differs between host species tested in this study. On *A. thaliana*, the production of BOT was essential for the fungus to successfully infect the plant under the inoculation conditions that were chosen, while BOA did not play a detectable role (Figure 1). The double mutant which produces neither BOT nor BOA showed slightly reduced virulence on the tested Solanaceous plants tomato (Figure 2) and *N. benthamiana* (Figure 3A), while it displayed similar virulence as the WT *B. cinerea* on two plant species belonging to the Fabaceae (Figure 3B&C). The importance of BOT and BOA for fungal virulence might thus not only be host species-dependent, but even host family-dependent. To test this hypothesis, it would be required to analyze the virulence of the mutant strains used in this study on additional plant species from the Brassicaceae, Solanaceae and Fabaceae. Moreover, testing a single genotype for each plant species may not sufficiently reflect the susceptibility of the whole species. Therefore, it is worth to perform virulence assays on different accessions of the same species as well. The results of these two proposed approaches will provide more detailed insights into the function of BOT and BOA in the virulence of *B. cinerea* on different hosts at a higher taxonomic level (family-wide) or lower taxonomic level (genotype-specific), respectively.

In addition to the different plant species that were tested in this study, the inoculation methods and conditions can also affect the outcome of the virulence assays and may influence the interpretation of the functions of these phytotoxins. For instance, the inoculation medium PDB (Potato Dextrose Broth) used in this chapter allowed the *Δbot2Δboa6#6* mutant to successfully infect tomato leaves, resulting in only ~14% reduction in lesion size. Based on this observation, we could conclude that BOT and BOA contribute only to minor extent to the virulence of *B. cinerea* on tomato. However, with the same spore density and droplet size (1000 conidia/µl and 2 µl/droplet) but in a different inoculation medium as described in Chapter 6, the *Δbot2Δboa6#6* double mutant was unable to infect tomato. Therefore, using this alternative inoculation medium the production of BOT and BOA would be considered indispensable for fungal pathogenicity. The difference in the results from the virulence assays between this chapter and Chapter 6 could be largely explained by the different nutrients which may affect the germination and growth of *B. cinerea* (Blakeman, 1975; Doehlemann et al., 2006; L. Zhang & van Kan, 2013), likely by activating or suppressing certain catabolic pathways and modulating gene expression. Except for the two inoculation conditions described in this thesis, two previous studies have reported infection assays with the WT B05.10 and the *Δbot2Δboa6#6* mutant using yet different inoculation methods, respectively. Dalmais et al. (2011) performed the

assays by suspending the conidia in sucrose phosphate buffer (10 mM sucrose, 10 mM KH_2PO_4) to a final density of 100 conidia/µl and applying 10 µl droplets of inoculum on French bean and tomato. This method resulted in an approx. 50% reduction in the lesion sizes of four independent *Δbot2Δboa6* transformants as compared with the WT B05.10. It is worth mentioning that the four *Δbot2Δboa6* transformants tested by Dalmais et al. (2011) also showed a growth retardation *in vitro*. The *Δbot2Δboa6#6* mutant that was used in this thesis and was originally generated by Leisen et al. (2020), showed no significant difference in growth rate *in vitro* compared to the WT fungus. Leisen et al. (2020) used the same inoculation medium as described in Chapter 6 of this thesis, however, they applied 20 µl droplets containing 100 conidia/µl on tomato leaves. The difference in droplet size may affect the exposure to oxygen for the conidia and the nutrient sources distributed to individual conidia, which could partially explain the different outcomes of virulence assays performed by Leisen et al. (2020) and our experiments reported in Chapter 6. To summarize, according to all these observations from different studies, media, spore density and droplet size can all have an impact on the outcome of the virulence assays, sometimes leading to different conclusions.

BOT has been reported to be toxic to dicots, and the pure compound was tested on Arabidopsis leaves by Rossi et al. (2011) at active concentrations of 161 µM and higher. Although a minimal active concentration of 1 ppm (~ 3.2 µM) was described both on *N. tabacum* by Rebordinos et al. (1996) and on French bean by Colmenares et al. (2002), 1 ppm of BOT could only cause necrotic symptoms on ~30% of tested leaf discs with < 5% of the treated area affected. To induce visible lesion on all treated leaf discs, Rebordinos et al. (1996) and Colmenares et al. (2002) had to apply at least 125 ppm (400 µM) BOT on *N. tabacum* and 50 ppm (160 µM) BOT on French bean, respectively. Deighton et al. (2001) reported that *B. cinerea* produces BOT during infection, and the highest concentration of BOT detected from the infected leaf tissue was 140 nmol/g (~140 µM). Due to the limitation of the technology, the concentration of BOT detected in the study of Deighton et al. (2001) was an averaged number of the accumulated toxin in the whole rotten tissue sampled at 6 dpi, instead of a real-time concentration at the interface between the fungal hyphae and the host plant cells. Therefore, it is conceivable that the actual concentration of BOT at the interaction zone should be much higher than the detected concentration. Besides, BOT has an unstable chemical structure and can be effectively converted into a less active derivative, dihydrobotrydial (I. G. Collado et al., 2007). The surface application of droplets containing BOT solutions inevitably led to reduced concentration of BOT that could eventually penetrate the leaf surface, due to the instability of BOT and the physical barriers of the leaf surfaces. In this chapter, we performed the pure BOT treatments with 100 µM and 500 µM

of the toxin, which are within a range of concentrations that could be produced locally by *Botrytis* hyphae in plant tissues. *A. thaliana* seemed to respond most intensively to 100 µM BOT as compared to the other plants which were tested in this study (Figure 4). This observation correlates with the strict requirement of BOT for the fungus to infect *A. thaliana* but not for infecting the other tested plants.

This study is the first to examine the toxicity of BOT to monocotyledon plants, and we showed that BOT can actually induce cell death in monocotyledonous plants. Testing whether the monocotyledonous species that are hosts of some specialist *Botrytis* spp. are sensitive to BOT, is the first step to elucidate the potential role of the toxin for these *Botrytis* spp. in infecting their respective hosts. To further validate whether BOT production is important for virulence of these species on their respective hosts, it is required to generate *Δbot2* deletion mutants in the *Botrytis* spp. that contain a functional gene cluster for BOT synthesis, followed by assessment of their virulence. Generation of mutants of *B. cinerea* has become relatively effective using the CRISPR/Cas9-mediated transformation protocol, and also transformants of other *Botrytis* spp. have been obtained with small adaptations to the protocol that was originally developed for *B. cinerea* (Leisen et al., 2020b; Steentjes et al., 2022). This approach is adopted in Chapter 5, which describes the contribution of BOT to the virulence of *B. elliptica* on different lily cultivars.

To protect crops against necrotrophic pathogens, scientists have worked on exploration of natural sources of resistance against pathogens using effectors as screening tools (Vleeshouwers & Oliver, 2014). Deployment of plant receptor genes that recognize avirulence gene from pathogens is an effective strategy for protecting plants against biotrophs or hemibiotrophs (Kanja & Hammond-Kosack, 2020). However, the programmed cell death induced by the recognition of effector proteins by their matching receptor proteins might facilitate the fungal invasion of necrotrophs, instead of restricting their growth. In this case, the genes encoding plant components that participate in the cell death response to the molecules derived from the necrotrophic pathogen should be considered as a susceptibility gene. Loss of susceptibility is emerging to be a breeding strategy for durable resistance (Pavan et al., 2010). Screening different accessions of a crop species for their sensitivity to cell death inducing molecules derived from a pathogen can be a suitable strategy for identifying the genetic locus (loci) (QTL) containing plant susceptibility factors against a necrotrophic pathogen. A recent study evaluated the sensitivity of different onion genotypes to the cytotoxic NEP1 protein produced by the onion pathogen *B. squamosa*, and identified a QTL for BsNep1 insensitivity that partially overlaps with a QTL for *B. squamosa* resistance in onion (Steentjes et al., 2022). To identify resistance loci against *B. cinerea*, BOT can be applied on different accessions of a single plant species and the variation in BOT

sensitivity can be quantified among the population, followed by QTL mapping. As will be described in Chapter 7 of this thesis, this strategy was pursued using a large HapMap population and published genomes of individual accessions of the model plant species *A. thaliana* (Alonso-Blanco et al., 2016; Weigel & Mott, 2009).

Materials and Methods

Fungal strains and growth conditions

B. cinerea strains used in this study were WT B05.10 (van Kan et al., 2017), the *Δbot2#1* mutant (Leisen et al., 2020b), the *Δboa6#1* mutant (Dalmais et al., 2011), and the *Δbot2Δboa6#6* double mutant (Leisen et al., 2020b). Fungal strains were grown and conidia harvested as described by Zhang & van Kan (2013).

Plant materials and growth conditions

A. thaliana Col-0, tomato (cv. Moneymaker), *N. benthamiana*, French bean (cv. Caruso) plants were grown as described in Chapter 2 (Qin et al., 2023). The cowpea (cv. Blackeye) was grown in the same condition as French bean plants, and two-week-old plants were used for the virulence assay or BOT treatment. Onion (cv. Bruce) and lily (cv. Longiforum - Asiatic 1) plants were grown as described by Steentjes et al. (2022) and Malvestiti et al. (2022). Plants of wheat, maize and two grass species (*Digitaria ischaemum* accession DIG1294 and *D. snaguinalis* accession DIG121) were grown at 20 °C with 70% relative humidity and a photoperiod of 10 hours in a climate chamber for 2-3 weeks until use for the BOT treatment.

Virulence assays

Inoculum was prepared by suspending conidia of *B. cinerea* in PDB (12 g/l) to a final density of 1000 conidia/µl. Two µl of the inoculum was applied on the adaxial leaf surface on different plants. Leaves of whole plants of *A. thaliana*, *N. benthamiana*, French bean and cowpea, or detached leaves from tomato were used for virulence assays. The whole plants or detached tomato leaves that were inserted into blocks of floral foam, were put in plastic trays with wet filter paper at the bottom. One droplet was applied on each *A. thaliana* leaf, and different *B. cinerea* strains were inoculated on the same plant. For tomato, *N. benthamiana*, French bean and cowpea, each mutant strain was inoculated on the same leaf(let) on the right side of the central vein together with the WT B05.10 on the left side to obtain pair-wise comparison. After inoculating *B. cinerea* on the leaf surface, the trays were covered with a transparent lid sprayed with water to keep ~100% relative humidity. The

trays were incubated in lab condition (22 °C with natural day-night rhythms), lesion sizes on infected leaves were measured with a digital caliper at 3 dpi.

Production, purification and purity determination of BOT

The production and purification of BOT and analysis of its purity was performed as described by Pinedo et al. (2008) with minor modifications. Liquid cultures of the mutant *Δboa6* mutant in modified Czapek-Dox medium (50 g glucose, 1g yeast extract, 5 g KH_2PO_4, 2 g $NaNO_3$, 0.5 g $MgSO_4 \cdot 7H2O$ and 0.01 g $FeSO_4 \cdot 7H2O$ for 1 l medium, pH adjusted to 6.5 ~ 7.0) were incubated at 25 °C under constant light for seven days to obtain high accumulation of BOT. Metabolites including BOT were extracted by pure ethyl-acetate from the culture filtrate with 1:1 ratio for three times. The ethyl-acetate extract was condensed using a rotary evaporator. To purify BOT, column chromatography (CC) was performed by loading the condensed extract in the column (Aluminum TLC Silicagel 60 F_{254}) with the first mobile phase of 4 ethyl-acetate : 6 Hexane and the second of 8 ethyl-acetate : 2 Hexane. The fractions collected by the eluent of CC were checked by thin-layer chromatography (TLC) using a Silica gel 60 F_{254} (Aluminum TLC plate, silica gel coated with fluorescent indicator F254) and a mobile phase of ethyl-acetate: Hexane (4:6), in order to confirm the fractions containing almost only BOT. These fractions were combined and the solvent was evaporated to determine the dry weight of the sample. The purity of BOT in the sample was analyzed by ^{1}H NMR at 400MHz.

BOT application on plants and visualization of the symptoms

To treat *A. thaliana*, tomato, *N. benthamiana*, French bean, cowpea and lily leaves, 5 µl droplets of a defined concentration of BOT dissolved in 40% acetone were applied on the adaxial surface of the leaves on the right side of the central vein. Five µl droplets of 40% acetone were applied as negative control on the left side of the central vein. For onion that has a narrow leaf surface, four droplets of 100 µM BOT were applied on each leaf, with two droplets of 40% acetone in between as control. *A. thaliana*, tomato, *N. benthamiana* and onion plants were treated with 100 µM BOT, and French bean, cowpea and lily were treated with 500 µM BOT. The symptoms on treated leaves were recorded by photos taken with a digital camera under natural light as well as images taken with the RFP channel of the ChemiDoc imaging system (Landeo Villanueva et al., 2021) on the 5th day (for dicots) or on the 3rd day after BOT treatment (for monocots).

Chapter 5

The phytotoxic fungal secondary metabolite botrydial causes cell death and contributes to *Botrytis elliptica* virulence in lily

Si Qin[1*], Michele C. Malvestiti[1*], Henriek G. Beenen[1] and Jan A. L. van Kan[1]

[1]Laboratory of Phytopathology, Wageningen University, Netherlands

[*] These authors equally contributed to this work

Abstract

Botrydial is a phytotoxic secondary metabolite of the fungal genus *Botrytis*. The compound can cause cell death in dicot plants and is therefore considered as a virulence factor in *Botrytis cinerea*. However, the phytotoxicity of botrydial has not been investigated in monocots. Chemically, botrydial represents a bicyclic sesquiterpene which is synthetized by a cluster of six biosynthetic genes. The functional botrydial biosynthetic gene cluster is present in the generalist *B. cinerea* and in the lily specialist *B. elliptica*. In this study we tested the cell death inducing activity of botrydial in lily by applying pure botrydial on leaves and tepals. Variation in cell death responses was observed between the different tissues and among the different lily cultivars tested. We detected botrydial production in *B. elliptica in vitro* cultures and *in planta* transcriptional activity of *Bebot2,* the key botrydial biosynthetic gene, during infection in lily. Finally *B. elliptica Bebot2* deletion mutants were generated via CRISPR/Cas9- mediated transformation to assess the contribution of botrydial to fungal virulence in lily. In all lily cultivars tested a statistically significant reduction in lesion size was observed upon inoculation with the *B. elliptica Bebot2* deletion mutants as compared to the wild type fungus. Taken together, these results provide evidence that under the tested conditions, botrydial contributes to fungal virulence in the *B. elliptica*-lily interaction.

Introduction

Lily (*Lilium* spp., Liliaceae) is one of the most important ornamental plants worldwide and its production is threatened by several pests and diseases. Among them, the most destructive is fire blight, a fungal disease caused by the Ascomycetes *Botrytis elliptica* and *B. cinerea* (Sclerotiniaceae). Both fungi initially form small brownish necrotic spots on leaves and flowers of the infected lily. Under favorable environmental conditions rapid outgrowth of necrotic spots leads to death of the entire plant. While the generalist *B. cinerea* occurs mainly at post-harvest stage on damaged and senescing plant tissue, *B. elliptica* is host-specific in lily and can inflict serious economic losses since it is able to cause disease also on healthy, vigorous plants (Malvestiti et al., 2021 and 2022). *Botrytis* fungi are filamentous Ascomycetes with a necrotrophic life style. After an initial biotrophic interaction with the host plant, *Botrytis* fungi kill the host cells to acquire nutrients for growth and reproduction from the dead plant tissue (Veloso & van Kan, 2018). Host cell death is achieved by means of fungal secreted compounds which can force the plant cell to commit suicide by triggering apoptotic-like Programmed Cell Death (PCD) (van Baarlen et al., 2004; Veloso & van Kan, 2018). These compounds are referred to as necrotrophic effectors, which comprise PCD inducing proteins (Leisen et al., 2022; Malvestiti et al., 2022; Steentjes et al., 2022) and phytotoxic secondary metabolites (Collado et al., 2000 and 2007). The best studied phytotoxic secondary metabolite from *Botrytis* is the bicyclic sesquiterpene botrydial (BOT) (Colmenares et al., 2002; Deighton et al., 2001; Pinedo et al., 2008). This compound is produced by *B. cinerea* during plant infection where it induces host immune responses such as accumulation of reactive oxygen species and the upregulation of expression of genes encoding pathogenesis related proteins (Deighton et al., 2001; Rossi et al., 2011). In addition, BOT was shown to be capable of causing cell death when exogenously applied on leaf and fruit tissue of phylogenetically unrelated dicot species such as *Nicotiana tabacum, Capsicum annuum*, *Phaseolus vulgaris* and *Arabidopsis thaliana* (Rebordinos et al., 1996; Deighton et al., 2001; Rossi et al., 2011). Since absence of BOT production in certain *B. cinerea* isolates was shown to correlate to reduced fungal virulence in different host plants, BOT is considered to be a virulence factor in the *B. cinerea*-host interaction (Pinedo et al., 2008; Siewers et al., 2005). Within the *B. cinerea* genome the genes involved in the biosynthesis of BOT are clustered in a specific locus. The BOT gene cluster consists of six genes encoding biosynthetic enzymes and one gene encoding a putative $Zn(II)_2Cys_6$ transcription factor (Porquier et al., 2016). *Bcbot2* encodes a sesquiterpene cyclase which represents the key-enzyme for the biosynthesis of the sesquiterpene backbone of the toxin, since it converts farnesyl pyrophosphate (FPP) into presilphiperfolan-8-beta-ol (Pinedo et al., 2008). *Bcbot1*, *Bcbot3* and *Bcbot4* encode cytochrome P450 proteins, and *Bcbot5* and *Bcbot7* respectively

encode an acetyl transferase and a dehydrogenase and involved in the biosynthesis of the final form of the secondary metabolite (Porquier et al., 2016). The transcriptional activation of the gene cluster is regulated by BcBOT6 which is a $Zn(II)_2Cys_6$ transcription factor (Porquier et al., 2016). Although all studies on BOT biosynthesis and phytotoxicity have been conducted in *B. cinerea* and dicot plant species, functional BOT biosynthetic gene clusters are also present in other members of the genus *Botrytis* that are host-specific in monocot plant taxa such as *B. elliptica* in lily (Valero-Jiménez et al., 2020). The BOT clusters in both *B. cinerea* and *B. elliptica* are located in different genomic regions, are both flanked by a gypsy/copia repeat on one side, and the *B. cinerea* BOT cluster contains an additional internal transposon (Valero-Jiménez et al., 2020). This study focusses on the role of BOT in the *B. elliptica*-lily pathosystem. This was investigated first by assessing the BOT production in *B. elliptica* during fungal solid and liquid cultures. Secondly we tested whether BOT displays phytotoxic activity in lily by exogenously applying purified BOT onto lily leaves and tepals. Finally we determined the contribution of BOT to *B. elliptica* virulence by generating *Bebot2* deletion mutants and by comparing the disease development on lily of the mutants to the wild type fungus.

Results

B. elliptica can produce BOT and deletion of *Bebot2* gene abolishes the production of BOT

B. cinerea wild type (WT) B05.10 is known to be capable of producing BOT, and deletion of the *Bcbot2* gene in B05.10 abolished BOT biosynthesis (Pinedo et al., 2008). To verify whether the ortholog of *Bcbot2* in *B. elliptica* (*Bebot2*) functions as the sesquiterpene cyclase for BOT synthesis in *B. elliptica*, CRISPR/Cas-mediated transformation was performed to knock out *Bebot2* in the *B. elliptica* isolate 254-8. Two independent deletion mutants were obtained. PCR analyses identified *ΔBebot2#2* and *ΔBebot2#3* as homokaryotic deletion mutants (Supplementary Figure S1A). Both *Bebot2* deletion mutants were genotyped to be homokaryotic knockout transformants free of the wild type Bebot2 gene, and displayed sclerotia formation as the recipient isolate 254-8 (Supplementary Figure S1A, B). However, *ΔBebot2#2* and *ΔBebot2#3* showed slightly slower radial growth rate than the WT 254-8 on the Malt-extract agar (Supplementary Figure S1C).

BOT production in *B. elliptica* WT 254-8, *ΔBebot2#2* and *ΔBebot2#3*, was investigated by running ethyl acetate (EtOAc) extracts of solid *in vitro* fungal cultures on a thin-layer chromatogram (TLC). The pure BOT sample, as well as extracts from *in vitro* cultures of the *B. cinerea* WT B05.10 and the *ΔBcbot2#1* mutant were run on the same TLC as controls. A pink band migrating at the position of pure BOT was observed in *B. cinerea* WT B05.10 extract but not in *ΔBcbot2#1* extract (Figure 1A). For *B. elliptica* isolates, WT 254-8 was able to produce BOT, while *ΔBebot2#2* and *ΔBebot2#3* mutants were not (Figure 1A).

We observed that all genes of the BOT cluster were highly expressed in *B. elliptica* 9401 and 9612 during infection in lily, according to the RNA sequencing dataset described in Malvestiti et al. (2022). Since the expression profile of BOT genes in *B. elliptica* isolate 254-8 was unknown, reverse RT-qPCR was performed to examine the *Bebot2* transcript levels in *B. elliptica* WT isolate 254-8, *ΔBebot2#2* and *ΔBebot2#3* during infection in leaves of two lily cultivars, Asiatic (A) and Longiflorum-Asiatic 2 (LA2). The mRNA of *Bebot2* in *B. elliptica* 254-8 WT on both cultivar A and cultivar LA2 was detected at 16 hours post inoculation (hpi), increased at 24 hpi, and then it slightly decreased at 40 hpi (Figure 1B). No significant difference in the *Bebot2* expression level was found in WT 254-8 between its infection on cultivar A and cultivar LA2 at each timepoint (Figure 1B). *Bebot2* transcript was not detected in *ΔBebot2#2* and *ΔBebot2#3* mutants during infection on lily leaves (Figure 1B).

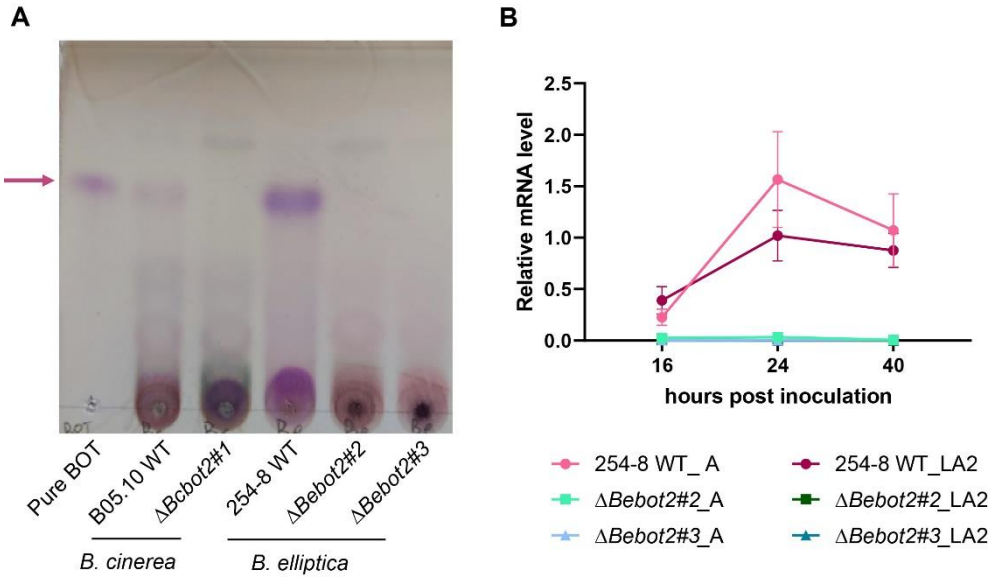

Figure 1. TLC analysis of EtOAc extracts from *in vitro* solid cultures of *B. cinerea* wild type (WT) isolate B05.10*, ΔBcbot2#1* mutant*, B. elliptica* WT isolate 254-8 *, ΔBebot2#2* and *ΔBebot2#3* mutants using a mobile phase of 40% EtOAc – 60 % hexane **(A)**. The pink band on the TLC shows the presence and migration of BOT in the sample (Rf = 0.7), indicated by a pink arrow on the left. The transcript level of *Bebot2* in *B. elliptica* WT 254-8, *ΔBebot2#2* and *ΔBebot2#3* during infection on lilies (cultivars A and LA2) **(B)**.

BOT induces cell death in lily leaves and tepals in different cultivars, with variation between cultivars

After confirming that *B. elliptica* WT 254-8 was able to produce BOT during lily infection, we tested whether BOT can induce cell death in lily leaves and tepals by applying pure BOT on leaves and tepals of four lily cultivars (cultivars A, LA1, LA2 and L). BOT sensitivity was quantified as the signal intensity of red light emission (Landeo Villanueva et al., 2021) at 3 days and 2 days after BOT treatment, respectively. We observed that both leaves and tepals of all four tested lily cultivars were BOT sensitive (Figure 2 and 3). Moreover, the signal intensity varied among the different lilies. In BOT treated leaves, cultivar LA1 and LA2 were the most sensitive, while cultivar A was the least sensitive (Figure 2B). Leaves of cultivar L showed significantly lower sensitivity than cultivar LA1, slightly lower sensitivity than cultivar LA2 but with no statistically significant difference, and significantly higher sensitivity than cultivar A. (Figure 2B). Analogously, tepals of lily cultivar A showed the lowest BOT sensitivity, whereas tepals of cultivar LA2 and L were the most sensitive, and cultivar LA1 was intermediate (Figure 3B). A control treatment with 40% acetone (on the left side of the treated leaves or tepals) triggered no response at all.

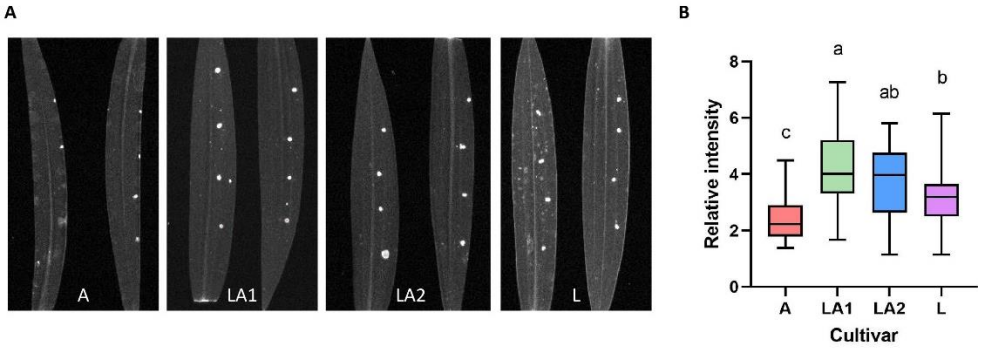

Figure 2. BOT sensitivity in leaves of lilies cultivars A, LA1, LA2 and L, visualized with the RFP channel of the ChemiDoc MP imaging system **(A)**. Boxplot showing signal intensities detected at 3 days after BOT treatment **(B)**. Red light signal intensity detected upon BOT treatment in lily leaves is shown in the boxplot with the mean value (horizontal line) and the data from min to max (error bar) for each box. Each box contains 40 datapoints from two independent experiments, and the statistical analysis was performed by one-way ANOVA with Tukey's honestly significant difference (HSD) test.

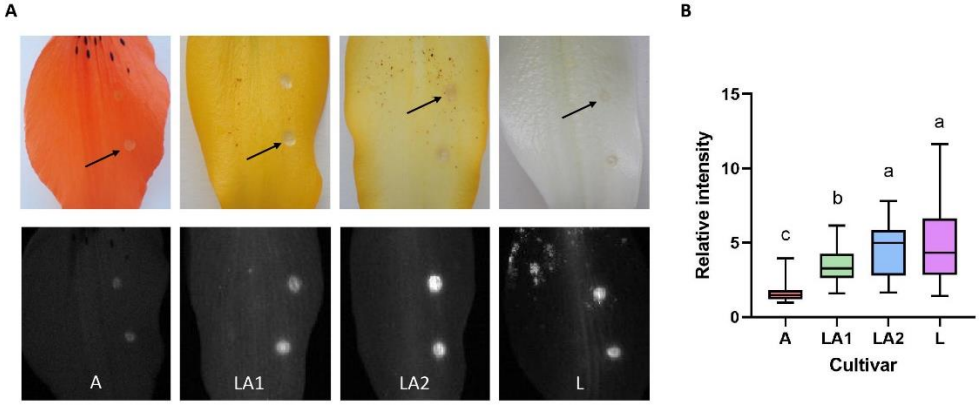

Figure 3. BOT sensitivity in tepals of lilies cultivars A, LA1, LA2 and L, visualized with normal light (upper panel) and with the RFP channel of the ChemiDoc MP imaging system (bottom panel) **(A)**. Necrotic spots observed upon BOT treatment are indicated with a black arrow. Boxplot showing signal intensities detected at 2 days after BOT treatment **(B)**. Red light signal intensity detected upon BOT treatment lily tepals is shown in the boxplot with the mean value (horizontal line) and the data from min to max (error bar) for each box. Each box contains 40 datapoints from two independent experiments, and the statistical analysis was performed by one-way ANOVA with Tukey's honestly significant difference (HSD) test.

BOT contributes to *B. elliptica* virulence in lily leaves and tepals

The contribution of BOT to virulence of *B. elliptica* in lily was evaluated by comparing lesion development in leaves and flowers upon inoculation of the *ΔBebot2#2* and *ΔBebot2#3* mutants and the *B. elliptica* WT 254-8. The four tested lily cultivars displayed differences in

lesion sizes upon inoculation of *B. elliptica* WT isolate 254-8, on both leaves and tepals (Figure 4A, B and 5A, B). Among the four tested lilies, cultivar A developed the largest lesions on leaves ranging between 12 and 22 mm whereas leaves of cultivar L showed the smallest lesions leaves which ranged between 5 and 12 mm (Figure 4A, B). Leaves of the cultivars LA1 and LA2 developed lesions of similar size whereby the majority ranged between 10 and 15 mm (Figure 4A, B). Analogously to leaves, the largest lesions were found on tepals of cultivars A and LA2 (ranging between 6 and 16 mm) whereas the smallest lesions were observed on cultivar L (ranging between 4 and 8 mm) (Figure 5A, B). When the lilies were inoculated with the mutants *ΔBebot2#2* and *ΔBebot2#3* a reduction in lesion size was observed on both leaves and tepals of all the tested lilies except from tepals of cultivar L (Figure 4A, C and Figure 5A, C). When comparing the sizes of lesions developing upon inoculation with *B. elliptica* WT and the two *ΔBebot2* mutants, the most pronounced reduction in lesion size was found on leaves of cultivars A and LA1 (Figure 4C). Upon leaf inoculation with the two *ΔBebot2* mutants the lesion size observed on cultivar A ranged between 2 and 22 mm (for *B. elliptica* WT lesions ranged between 12 and 22 mm) while the lesion sizes observed on cultivar LA1 ranged between 1 and 9 mm (for *B. elliptica* WT lesions ranged between 3 and 17 mm). By contrast, when comparing tepal inoculation with the two *ΔBebot2* mutants to tepal inoculation with *B. elliptica* WT, differences in lesions size were less pronounced than in leaves. Except from cultivar L, the lesion sizes of the *ΔBebot2* mutants on tepals were significantly smaller than those of the recipient (Figure 5C).

In parallel, the contribution of BOT to virulence of *B. cinerea* in lily leaves and tepals was assessed by comparing lesion size development upon inoculation of *B. cinerea* WT B05.10 and *ΔBcbot2#1* of the same four cultivars. No expanding lesion was observed when leaves were inoculated with any of the *B. cinerea* isolates (Supplementary Figure S2). Small expanding lesions were observed on tepals inoculated with *B. cinerea* WT and *ΔBcbot2#1*, and a slight reduction in lesion size was observed for the *ΔBcbot2#1* mutant only on cultivar A (Supplementary Figure S3).

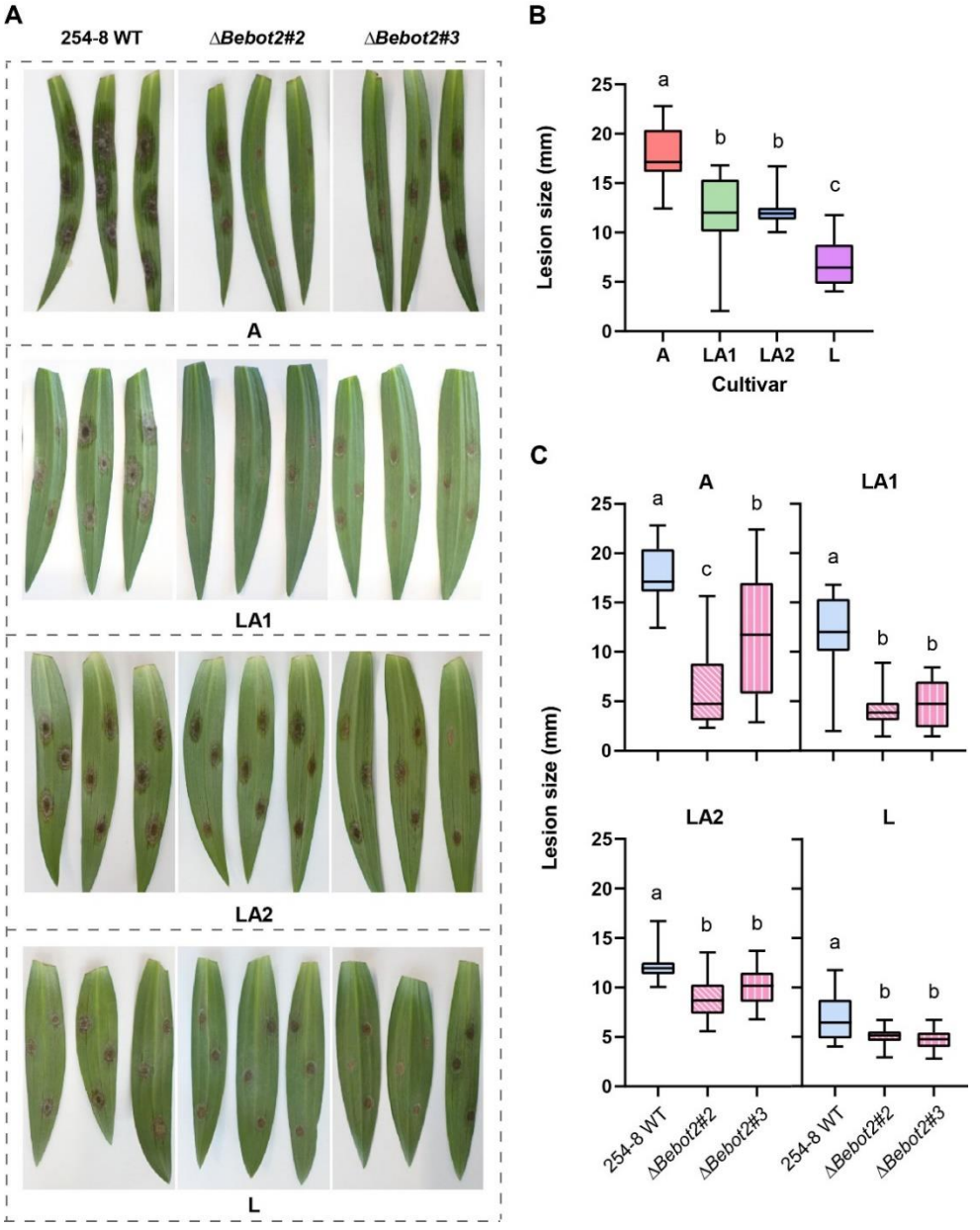

Figure 4. Lesions observed at 4 dpi upon inoculation with *B. elliptica* WT 254-8, *ΔBebot2#2* and *ΔBebot2#3* on leaves of lily cultivar A, LA1, LA2 and L, shown by **(A)** photos with normal light, **(B)** a boxplot showing only lesion sizes measured upon inoculation with *B. elliptica* WT 254-8 on all tested cultivars, and **(C)** boxplots showing lesion sizes measured upon inoculation with both *ΔBebot2* mutants compared to *B. elliptica* WT on each cultivar. Each box in plot **(B)** and **(C)** contains 24 datapoints from two independent experiments, and the statistical test was performed by one-way ANOVA with Tukey's HSD.

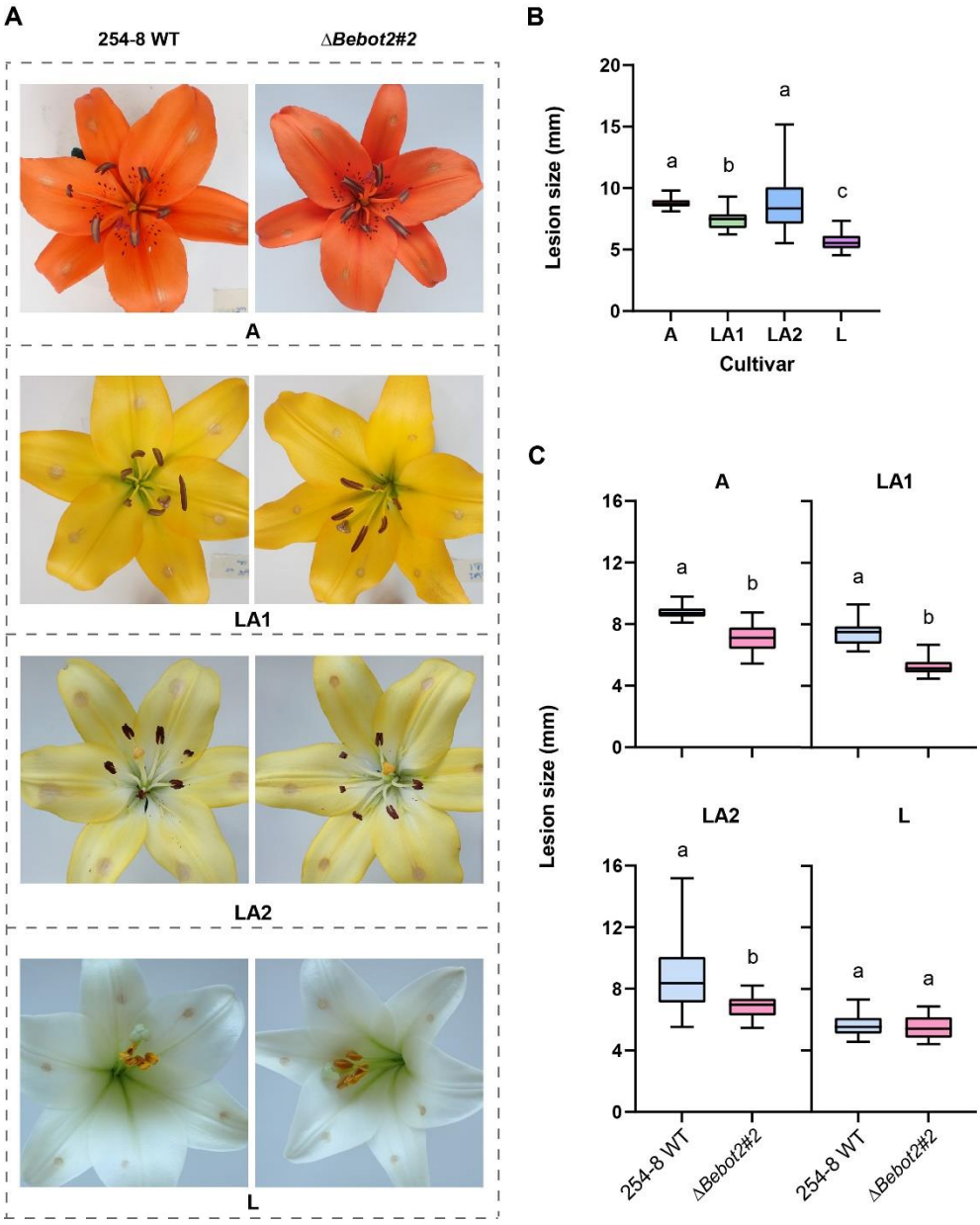

Figure 5. Lesions observed at 2 dpi upon inoculation with *B. elliptica* WT 254-8, *ΔBebot2#2* and *ΔBebot2#3* on tepals of lily cultivars A, LA1, LA2 and L, shown by **(A)** photos with normal light, **(B)** a boxplot showing only lesion sizes measured upon inoculation with *B. elliptica* WT 254-8 on all tested cultivars, and **(C)** boxplots showing lesion sizes measured upon inoculation with *ΔBebot2#2* compared to *B. elliptica* WT on each cultivar. Each box contains 24 datapoints from two independent experiments, and the statistical test was performed by one-way ANOVA with Tukey's HSD **(B)** and t-test **(C)**.

Discussion

In this study we investigated the role of BOT in the *B. elliptica* – lily interaction. Given the presence of the complete BOT biosynthetic gene cluster in *B. elliptica* (Valero-Jiménez et al., 2020) BOT production was assessed during *in vitro* grown fungal culture and during lily infection. In agreement with RNAseq analysis of *B. elliptica* isolates 9401 and 9612 (Malvestiti et al., 2022), the gene encoding the key enzyme for BOT biosynthesis (*Bebot2*) showed increasing transcript levels in the course of the first 24 h after lily leaves inoculation with the *B. elliptica* isolate used in this study (*B. elliptica* 254-8). In addition, BOT could be extracted and detected from *in vitro* grown *B. elliptica* cultures. These findings confirm the presence of the functional BOT biosynthetic gene cluster in *B. elliptica* and provide strong indications that BOT belongs to the arsenal of the cell death inducing compounds used by *B. elliptica* to infect lily. This hypothesis is further supported by the observation that exogenous BOT application on leaves and tepals of different lily cultivars caused a cell death response. Even if no necrotic spots (recognizable as brownish, dry and collapsed tissue) were visible with the naked eye on leaves upon BOT treatment, emission of red light was detected. This light signal derives from chlorophyl autofluorescence as a result of the abortion of photochemical activity in dying photosynthesizing plant tissue and is therefore considered as a sign of the occurrence of PCD (Landeo Villanueva et al., 2021). Necrotic symptoms were observed on BOT-treated tepals, both by the naked eye and by the red-light imaging (Landeo Villanueva et al., 2021). After measuring the red light signal intensity upon BOT application, differences in intensities were observed among the different lily tissues and cultivars tested. By correlating the red light signal intensity to plant tissue sensitivity to BOT, it was noticed that the lily cultivars differed in BOT sensitivity (Figures 2 and 3). The variation in red light signal intensity detected on BOT-treated leaves was influenced by the difference in the size of areas showing red light signal (Figure 2A) despite that the same volume of BOT solution was applied to all cultivars. This could be affected by differences in leaf surface architecture, composition and thickness of the epicuticular layers between the tested lilies. These factors collectively may have influenced the diffusion of the droplet and the penetration of BOT, and thus may have had an impact on the response of the plant to the compound. Differently from leaves, the areas on tepals treated with BOT were not noticeably different among the tested cultivars (Figure 3A). This indicates that the red light signal intensities detected on tepals may reflect more accurately the plant sensitivity to BOT.

Next to the differences in BOT sensitivity among the tested cultivars, we found that the lesions caused by *ΔBebot2* mutants were significantly smaller than the lesions caused by *B.*

elliptica WT (Figure 4 and 5) except for lesions on tepals of cultivar L. One would expect that if a given lily cultivar shows lower sensitivity to BOT than another lilies, the absence of BOT during infection (as in case of the *ΔBebot2*) would affect the fungal virulence to a lower extent, in comparison to a more BOT-sensitive lily. However, the tested lily cultivars in this study did not show such correlation. For instance, cultivar A had the lowest red light signal intensity in response to BOT treatment (both in leaves and tepals, Figure 2 and 3) but showed the greatest reduction in lesion size when comparing symptoms caused by the *ΔBebot2* mutants to symptoms caused by *B. elliptica* WT (Figure 4 and 5). It is possible that the BOT treatment alone does not provide the complete biological context for the role of BOT produced by *B. elliptica* during infection on lilies. Other virulence factors might require BOT to function in a synergistic manner during the fungal colonization in cultivar A but not in the other tested cultivars. Therefore, when BOT is not produced in the *ΔBebot2* mutants, the activity of such additional virulence factors might also be reduced, leading to a more pronounced reduction in lesion size on cultivar A than on other tested lilies. The observed reduction in lesion size upon *ΔBebot2* mutants inoculation might be specific for this particular Asiatic cultivar. Asiatic lily hybrids are derived from crosses of *Lilium* species which belong to the phylogenetic section *Sinomartagon.* This section is characterized by large genetic diversity because of its polyphyletic origin (J. Huang et al., 2018; H. T. Kim et al., 2019; J. S. Kim & Kim, 2018) and significant variation in *B. elliptica* susceptibility was found among Asiatic cultivars obtained from crosses of different *Lilium* spp. belonging to the section *Sinomartagon* (Malvestiti et al., 2021). It would be interesting to examine some additional cultivars from the Asiatic group, and check whether they also display low sensitivity to BOT and a remarkable reduction in lesion size upon inoculation with *ΔBebot2* mutants in comparison to the *B. elliptica* WT. Opposite to cultivar A, no reduced virulence of *ΔBebot2#2* compared to the WT *B. elliptica* 254-8 was observed on tepals of the cultivar L (Figure 5), which however is one of the most sensitive cultivars to BOT (Figure 3). This could be explained by considering the fact that tepals of cultivar L might be highly sensitive to many other cell death-inducing molecules except for BOT produced by the *B. elliptica* isolate. Accordingly, the secretion of these molecules by *ΔBebot2#2* could compensate the absence of BOT and still trigger strong cell death in the plant tissue, resulting in similar aggressiveness of *ΔBebot2#2* to the WT fungus.

It was surprising to observe that the colony diameters of *ΔBebot2* mutants were slightly smaller than the *B. elliptica* WT when the fungi were grown in solid cultures (Supplementary Figure S1), although the magnitude of reduction in lesion size of *ΔBebot2* mutants *in planta* was generally larger than the reduction in colony diameter *in vitro*. Thus, BOT is still considered to play a role in the virulence of *B. elliptica* on these lily cultivars. It is difficult to

understand how the lack of BOT production would result in the altered growth of *B. elliptica*, because the *ΔBcbot2#1* mutant in *B. cinerea* was reported to show a similar growth rate as WT (Leisen et al., 2020b). It should be noted that the *ΔBebot2* mutants were generated in a single experiment. To verify whether this phenotype is caused by a pleiotropic unknown mutation, it will be important to obtain additional mutants and to complement them in order to restore BOT production.

This study revealed two major findings. First, we presented that BOT can induce cell death responses in lilies and different cultivars of lily showed variation in the response to BOT. This work offers more details as compared to the observations in Chapter 4, which was the first report of BOT phytotoxicity in monocots. The monocots tested in Chapter 4 included not only lily, but also onion (*Allium cepa*, Amaryllidaceae) which can be infected by the leaf-specific pathogen *B. squamosa,* which also harbors a BOT biosynthetic gene cluster (Valero-Jiménez et al., 2020) that is expressed during early stages of onion leaf infection (Malvestiti et al., 2022). Whether the molecular mechanisms required for plant cell death induction upon BOT perception are conserved between monocot and dicot taxa awaits further investigation. In Chapter 7, we explored the plant genes that are involved in the response to BOT in the dicotyledonous model plant *Arabidopsis thaliana*. Secondly, we showed that BOT can be considered as a virulence factor in the *B. elliptica*-lily pathosystem. The next steps would be to quantify how much BOT contributes to fungal virulence and investigate whether BOT acts in combination with other factors. We have successfully generated *ΔBebot2* mutants using the CRISPR/Cas9-mediated transformation developed for *B. cinerea* (Leisen et al., 2020b), which offers the possibility to generate mutants in multiple virulence factors.

Materials and Methods

Plant material and growth conditions

Bulbs of *Lilium* spp. cultivar "Asiatic" (A), "Longiflorum" (L) and "Longiflorum-Asiatic" (LA1 and LA2) were planted in plastic crates containing potting soil and grown in greenhouse under natural day light regime at a minimum night temperature between 12 and 16 °C and maximum day temperature between 25 and 30 °C. Mature leaves as described by Bar and Ori (2014) were harvested and used for disease assays. Lilies carrying flower buds at initiation of bud color were harvested as cut flowers and transported to the laboratory to be inoculated or treated with BOT. Conidia inoculations and exogenous BOT application in lily flowers were conducted within 2 days after bud opening.

Growth conditions of fungal isolates

B. elliptica and *B. cinerea* isolates used in this research (Table 1) were stored as conidia suspensions in 20% glycerol at -80 °C. Fungi were grown on Malt Extract Agar (50 g/L, Oxoid) at 20 °C and sporulation was induced by illumination with UV-A lamps. After harvesting, conidia were collected and washed in demineralized water, counted with the Bürker-Türk counting chamber, adjusted to a concentration of 10^6 conidia/mL (*B. elliptica*) or 10^7 conidia/mL (*B. cinerea*) and stored until use in darkness at 4 °C.

Table 1. Fungal isolates used in this study

Fungal species	Isolate name	Source/Reference
B. elliptica	254-8	Malvestiti et al., 2021
B. elliptica	*ΔBebot2#2*	this study
B. elliptica	*ΔBebot2#3*	this study
B. cinerea	B05.10	van Kan et al., 2017
B. cinerea	*ΔBcbot2#1*	Leisen et al., 2020

BOT detection in fungal cultures

B. elliptica and *B. cinerea* isolates were grown on modified Czapek-Dox agar plates (50 g glucose, 1g yeast extract, 5 g KH_2PO_4, 2 g $NaNO_3$, 0.5 g $MgSO_4 \cdot 7H2O$, 0.01 g $FeSO_4 \cdot 7H2O$ and

15 g technical agar for 1 l medium, pH adjusted to 6.5 ~ 7.0) were incubated at 20 °C under constant light for seven days. The agar containing fungal mycelia and conidia were excised into small pieces (~0.8 cm x 0.8 cm) and transferred into Erlenmeyer flasks. Pure ethylacetate (EtOAc) was poured into the flasks until the agar pieces were covered, followed by extraction via ultra-sonication for 15 min. The EtOAc extract was collected through a filter paper, and the extraction was repeated once using the same agar pieces. The EtOAc extract was dried by nitrogen flow and subsequently re-dissolved in ca 300 µL pure acetone. The presence of BOT was analyzed on thin-layer chromatography (TLC). Samples were spotted on a Silica gel 60 F_{254} (Aluminum TLC plate, silica gel coated with fluorescent indicator F254), and a mobile phase of EtOAc : hexane (4:6, v/v) was used.

BOT production and purification

The production and purification of BOT and analysis of its purity were performed as described in Chapter 4.

Quantification cell death intensity upon BOT application on leaves and flowers

Droplets of 5 µL BOT (500 µM) dissolved in 40% acetone were applied on the right side of the abaxial surface of lily leaves or adaxial surface of flower tepals 5 µL droplets of 40% acetone were applied as negative control on the left side. Four droplets of BOT were applied to each leaf and two to three droplets were applied to each petal. The response was evaluated by exposing BOT treated leaves and tepals for one sec under the RFP channel of the ChemiDoc MP imaging system (Bio-Rad) (Landeo Villanueva et al., 2021). Response evaluation in tepals and leaves was done respectively at 2 and 3 days after BOT treatment. The mean red light emission intensity in the BOT-treated area was quantified by the circle volume tool in the ImageLab software (Bio-Rad), and the signal in the area treated by 40% acetone (no symptom) was quantified in the same way to be used as a background. The intensity of cell death response triggered by BOT was shown as the ratio of the mean intensity (BOT-treated area) to the mean intensity (negative control area).

Generation of *ΔBebot2* mutants by CRISPR/Cas9-mediated *B. elliptica* transformation

All oligonucleotides used in this study are listed in Supplementary Table S1. Donor DNA containing the hygromycin resistance cassette (hph) as selection marker was amplified from purified telomeric vector pTEL-Hyg (Leisen et al., 2020) isolated from *E.coli* liquid culture grown with 50µg/mL kanamycin overnight in the shaker incubator (28 °C; 200rpm). To achieve homologous recombination, the hph cassette was amplified via overhang PCR with 60 bp long flanks which were homologous to the 60 nucleotides at the 5' and 3' end of *Bebot2* (BELL_060g00490; Valero-Jimenéz et al., 2020). SgRNAs were designed for targeted

Cas9-mediated double strand break in exon 1 and exon 2 of *Bebot2*. SgRNAs were generated as described in Leisen et al. (2020) and purified using the RNA isolation Kit following the manufacturer's instructions (Zymo Research Orange, CA, USA). Cas9-Stu^{x2} protein used for fungal transformation was obtained from *E. coli* culture carrying pET24a_Cas9-Stu^{x2}-NLS-His as described in Leisen et al. (2020). *B. elliptica* isolate 254-8 transformation was carried out as described in Leisen et al. (2020) with some modifications. Fungal liquid cultures were grown for 36h at 20 °C in the shaker incubator (150rpm). No ice chilling was performed after protoplast collection and all incubation steps were conducted at room temperature. Ribonucleotide-Protein (RNP) complex assembly was performed as described in Leisen et al. (2020) adding 2 µg of each sgRNAs to 6 µg of Cas9-Stu^{x2} protein in cleavage buffer (20mM HEPES, pH 7.5, 100 mM KCl, 5% glycerol, 1 mM dithiothreitol, 0.5 mM EDTA, pH 8.0, 2 mM MgCl2). After RNP treatment, protoplasts were plated in SH medium containing 17,5 µg/mL hygromycin B. Protoplasts were allowed to regenerate in darkness at 20 °C. Four days after protoplast regeneration, appearing fungal colonies were transferred into MEA plates containing 80 µg/mL hygromycin B and screened via PCR. Homokaryotic *BeΔbot2* mutants were characterized with Phire Plant Direct PCR Kit (ThermoFisher Scientific, Bremen, Germany) using primers within the *Bebot2* gene and outside the 60bp flanks used for homologous recombination (Supplementary Figure S1C). The development of *BeΔbot2* mutants was checked by comparing colony growth and sclerotia formation in comparison to *B. elliptica* isolate 254-8 WT (Supplementary Figure S1A, B).

Infection assays of *B. elliptica* and *B. cinerea* in lily leaves and flowers

From each lily cultivar, 20 mature leaves were detached from 6 different plants and transported to the laboratory for inoculation. Per cultivar, three random detached leaves were placed in plastic boxes on petri-dish lids lying on wet filter paper. The leaves were inoculated with each *B. elliptica* and *B. cinerea* isolate as described in Malvestiti et al. (2021). After 4 days of incubation at constant temperature (19–21 °C) and under ambient day/night light regime, inoculated leaves were photographed and lesion diameter measurements were taken with a caliper as described in Malvestiti et al. (2021). Disease assays on flowers were carried out with two just opened flowers that were harvested from the inflorescence of lilies and fixed into wet floral foam, which were placed into plastic boxes containing tap water. Tepal inoculation with each *B. elliptica* and *B. cinerea* isolate was conducted as described in Malvestiti et al. (2021). Three separate rounds of inoculation for leaves and tepals were conducted for each fungal isolate-lily cultivar combination.

Gene expression analysis

Leaves of cultivar A and LA2 were inoculated with each *B. elliptica* as described in Malvestiti et al. (2021). Each *B. elliptica* -inoculated area was excised by a scalpel into ~5 mm x 5 mm squares from the infected leaf at either 16, 24 or 40 hours post inoculation (hpi). Three biological replicates were acquired. Harvested leaf samples were freeze-dried and used for RNA extraction with the Maxwell® 16 LEV Plant RNA Kit (Promega). Synthesis of cDNA was performed using 1 µg RNA as input and the M-MLV reverse transcriptase (Promega). Reverse transcription quantitative real-time PCR (RT-qPCR) was performed using the SensiMix SYBR Hi-ROX Kit (Bioline).

Supplementary materials

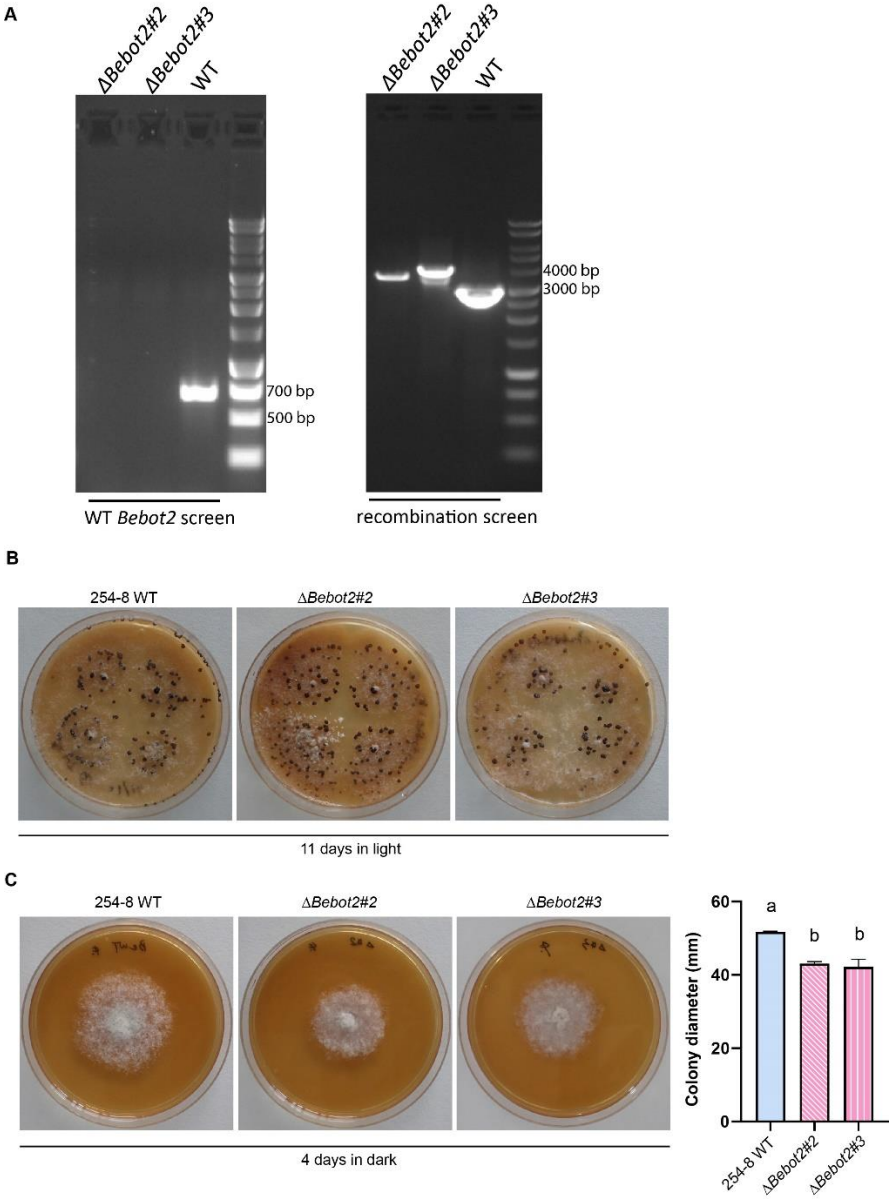

Supplementary Figure S1. Molecular characterization of *ΔBebot2#2* and *ΔBebot2#3* (**A**), sclerotia formation on 11-day-old MEA plates under constant light (**B**), and radial growth rate of *ΔBebot2#2* and *ΔBebot2#3* compared to WT 254-8 on 4-day-old MEA plates in dark (**C**). The radial growth rate was represented by the colony diameter (mm) measured from two dimensions of each colony, which is shown in the bar chart with the mean and standard error resulted from four separate plates (**C**). The statistical test was performed by one-way ANOVA with Tukey's HSD.

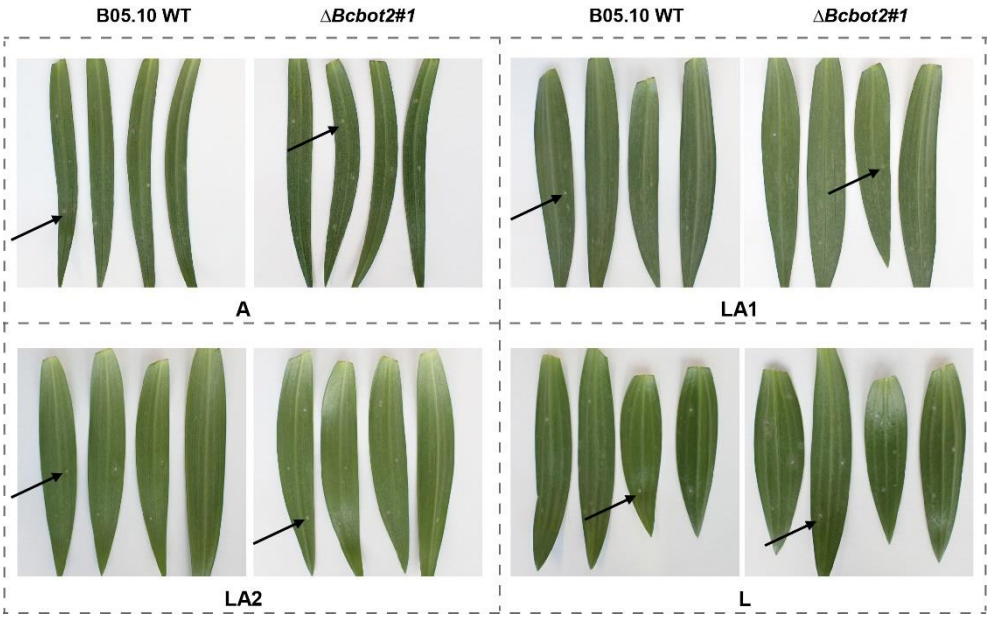

Supplementary Figure S2. Non-expanding lesions (indicated by black arrows) were observed at 4 dpi upon inoculation with *B. cinerea* WT B05.10 and *ΔBcbot2#1* on leaves of lily cultivars A, LA1, LA2 and L.

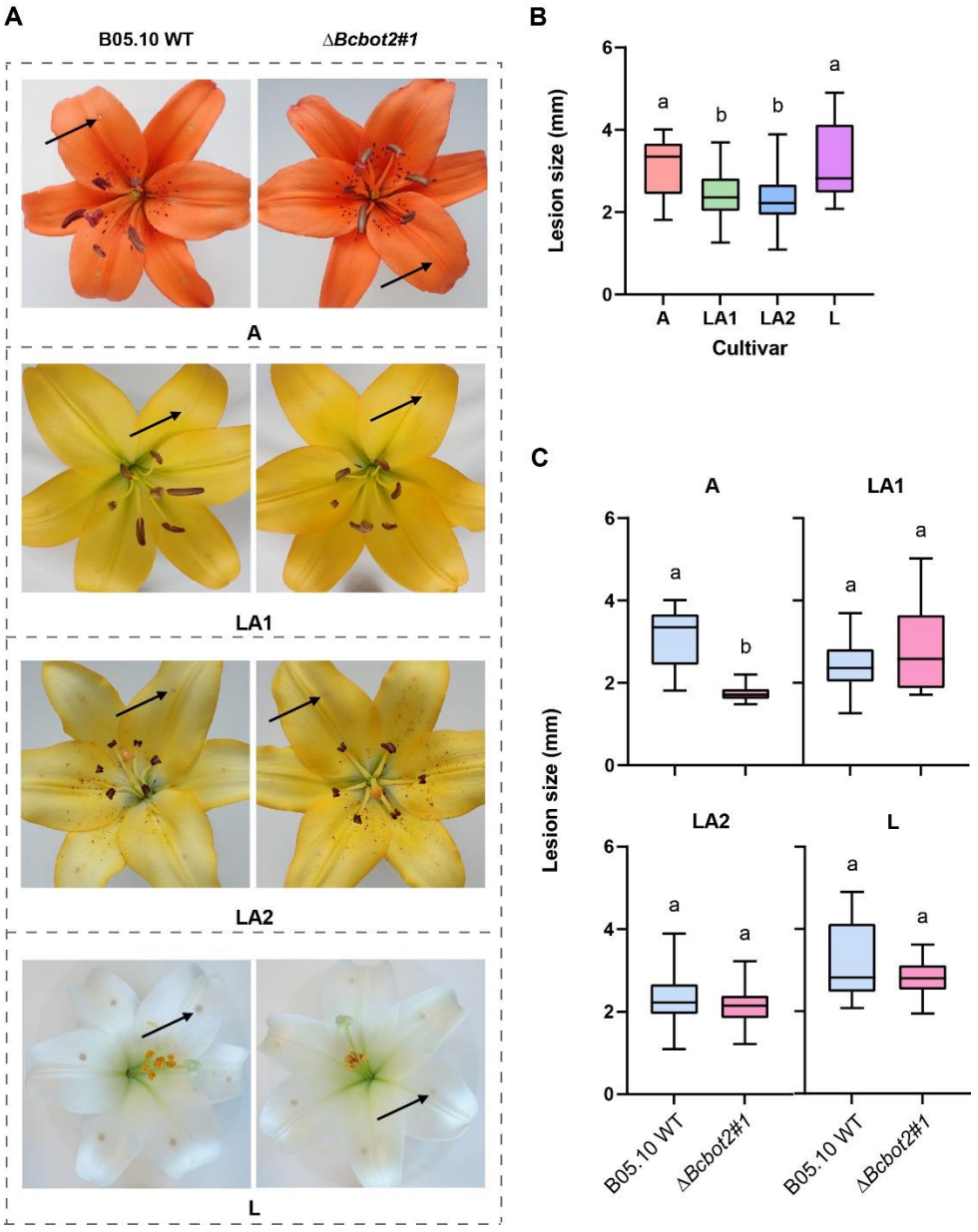

Supplementary Figure S3. Differences in lesion size observed at 2dpi upon inoculation with *B. cinerea* WT B05.10 and *ΔBcbot2#1* on tepals of lily cultivars A, LA1, LA2 and L. (**A**) Photos taken under normal light condition, in which lesions are indicated by black arrows. (**B**) A boxplot showing only lesion sizes measured upon inoculation with *B. cinerea* WT B05.10 on all tested cultivars. (**C**) Boxplots showing lesion sizes measured upon inoculation with *ΔBcbot2#1* compared to *B. cinerea* WT on each cultivar. The mean value (horizontal line) and the data from min to max (error bar) are displayed for each box in the boxplots. Each box contains 24 datapoints from two independent experiments, and the statistical test was performed by one-way ANOVA with Tukey's HSD (**B**) and t-test (**C**).

Supplementary Table S1. Primers used in this study

Primer name	Sequence	Application
Bebot2 sgRNA1	AAGCTAATACGACTCACTATAGGATGATAGAACCAAA GAGGTCGTTTTAGAGCTAGAAATAGCAAG	Generation of sgRNAs for *Botrytis* transformation
Bebot2 sgRNA2	AAGCTAATACGACTCACTATAGCGATGAATTTCAACAA GGCCGGTTTTAGAGCTAGAAATAGCAAG	
Bebot2 donor DNA generation F	ATGGCGATACCAGCACTTGAATCTCAGCTACACGACG CCGACACGGCCTCCAGCGATATGTGCTGGCCTTTTGCTCACATG CATG	Generation of donor DNA for *Botrytis* transformation
Bebot2 donor DNA generation R	TCATGCCACGAGCACGTCTTTAGCGGGCGGCAGG TACATGATACCTGTTTCATGGACATATCGCCGGAAAGGACCCGC AAATG	
Bebot2 check outside 5’	GCACTTGCACTAGATTTCGACGTC	*Bebot2* transformation check outside recombination flanks
Bebot2 check outside 3’	GGAAGACGCAGCAGGAGAGTAATG	
Bebot2 check inside 5’	CAGCGATATGAGCAGCAACAGCAC	*Bebot2* transformation check inside gDNA
Bebot2 check inside 3’	CGTTGTCACCCATGATGGCAATGGTC	
Bebot2 RT-qPCR 5’	ACGAATGCTATAGGCGGTGG	*BeBot2* and *BeActA* gene expression quantification
Bebot2 RT-qPCR 3’	CTCAGGACCCAGGTAACGAC	
BeactA RT-qPCR 5’	GAGCGGTGGTATCCACGTTACT	
BeactA RT-qPCR 3’	CAATGATCTTGACCTTCATCGAT	

Chapter 6

Unraveling mechanisms leading to incompatible and compatible interactions of tomato with *Botrytis cinerea* mutants defective in phytotoxin production by transcriptome analysis

Si Qin[1*], Xiaoqian Shi-Kunne[1*], Jie Chen[1,2], Henriek Beenen[1], Yaohua You[1] and Jan A. L. van Kan[1]

[1]Laboratory of Phytopathology, Wageningen University, Netherlands

[2]College of Forestry, Northeast Forestry University, China

[*] These authors equally contributed to this work

Abstract

Botrydial, botcinic acid and their derivatives are the major phytotoxic metabolites produced by the necrotrophic fungal pathogen *Botrytis cinerea*. These phytotoxins are able to induce programmed cell death in the host and thereby promote plant susceptibility to *B. cinerea.* We observed that a *Δbot2Δboa6* double mutant strain, which synthesizes neither botrydial nor botcinic acid, was almost avirulent on tomato leaves when the disease assay was performed using Gamborg B5 medium. However, the virulence of this mutant was restored when the inoculation medium was supplemented with yeast extract. Further virulence assays which compared the double mutant with other multiple knockout mutants using both inoculation media, revealed a prominent contribution of botrydial and botcinic acid to the full virulence of *B. cinerea*. Therefore, we performed an RNA-sequencing experiment to identify *B. cinerea* genes that contribute to the phenotypic switch from an "incompatible" to a "compatible" interaction between tomato and this *Δbot2Δboa6* double mutant. Four genes encoding cell death-inducing effector proteins were upregulated in *B. cinerea* by the addition of yeast extract, and their transcript profiles grouped within a co-expression module that was positively correlated with the compatible interaction. Functional analyses of these effector genes were performed by overexpressing them individually in the *Δbot2Δboa6* background, followed by disease assays with the Gamborg B5 medium without yeast extract.

Introduction

The grey mould fungus *Botrytis cinerea* is a plant pathogen that can infect more than 1000 host species (Elad et al., 2016). As a necrotrophic pathogen, *B. cinerea* has to kill its host cells to feed on the dead tissues after penetrating the plant surface. To achieve host cell death induction, *B. cinerea* secretes a cocktail of cell death-inducing molecules (CDIMs), such as phytotoxic secondary metabolites (SMs) and cell death-inducing proteins (CDIPs) (van Kan, 2006; Veloso & van Kan, 2018). The most abundantly phytotoxic SMs produced by *B. cinerea* are the bicyclic sesquiterpene botrydial (BOT) and the polyketide botcinic acid (BOA) (Collado et al., 2007; Collado & Viaud, 2015; Reino et al., 2006). The CDIPs secreted by *B. cinerea* and their modes of action are more extensively studied, as compared to phytotoxic SMs. The number of *B. cinerea* secreted proteins, which were experimentally proved to induce cell death in at least one plant species, has so far reached at least 19 (Bi et al., 2021; Denton-Giles et al., 2020; Leisen et al., 2022; Zhang et al., 2021; Zhu, et al., 2017). However, the number of proteinaceous effectors of this fungus was predicted to be more than 180 (Sperschneider et al., 2016), which indicates that *B. cinerea* may secrete more protein effectors functioning in cell death induction than the currently validated number of 19. Phytotoxic SMs and CDIPs were reported to contribute together to the fungal virulence with a high functional complementarity (Leisen et al., 2022), but the quantitative contribution of each individual CDIM remains to be clarified.

The BOT gene cluster in *B. cinerea* consists of seven genes (*Bcbot1*-*Bcbot7*), among which the gene *Bcbot2* encodes a key enzyme, sesquiterpene cyclase, that converts the precursor farnesyl diphosphate (FPP) to presilphiperfolan-8β-ol (Pinedo et al., 2008; Porquier et al., 2016). The BOA gene cluster contains 13 genes (*Bcboα1*-*Bcboα13*) (Porquier et al., 2019; van Kan et al., 2017), of which *Bcboα6* and *Bcboα9* encode polyketide synthases which are the key enzymes for BOA biosynthesis (Dalmais et al., 2011). The study by Dalmais et al. (2011) was the first to functionally analyze the roles of BOT and BOA in virulence, either separate or in combination, by testing knockout mutants in the key biosynthetic genes. Single mutants that were defective in the production of either BOT or BOA displayed similar virulence as the wild type (WT) *B. cinerea* while double mutants that produced neither BOT nor BOA formed ~50% smaller lesions on French bean (Dalmais et al., 2011). However, a recent study by Leisen et al. (2020) described no difference in virulence on tomato leaves between a *Δbot2Δboα6* double mutant generated by CRISPR/Cas-mediated transformation and the WT *B. cinerea*. In Chapter 4 of this thesis, we described that the deletion of either BOT or BOA biosynthetic genes, or both, had variable impact on the virulence of the mutants in a host-dependent manner. While deletion of *Bcbot2* caused a severe reduction in

virulence on *A. thaliana*, the impact on virulence was small in tomato, *N. benthamiana* and cowpea (*Vigna unguiculata*) and negligible in French bean (*Phaseolus vulgaris*). The effects of deletion of *Bcboa6* were on all hosts very small or negligible, even when combined with the deletion of the *Bcbot2* gene (Chapter 4). The different results between studies suggests that the role of BOT and BOA in virulence of *B. cinerea* requires further investigation. Commonly, the contribution of (single or multiple) genes to fungal virulence is tested by disease assays in which the lesion sizes of the wild type recipient fungus are compared with mutant strains lacking the gene(s) encoding putative virulence factors. Such disease assays can be performed under different conditions, with variations being applied by different labs either in the inoculation medium, fungal tissue (mycelial plugs or conidia), the plant growth conditions or the incubation after inoculation. Although Dalmais et al. (2011), Leisen et al. (2020) and Chapter 4 of this thesis all described disease assays using conidia suspensions to inoculate tomato leaves, there were differences between the studies regarding the inoculation media, spore density, the volume of droplets, and in growth conditions for tomato plants. In this chapter, we aimed to obtain a better understanding of the molecular basis for the fact that different inoculation conditions with the same set of mutant strains yields such different results on the virulence of the fungus.

RNA sequencing (RNA-seq) technology is an established and widely used method to study molecular processes during plant-pathogen interactions. From RNA-seq data, differentially expressed genes (DEGs) can be identified in the pathogen and the host between distinct conditions or time points during the interaction. In addition, applying clustering analysis can categorize groups of genes which display similar expression patterns to provide an overview of the transcriptome dynamics among all sampled conditions and time points. The clustered groups of genes can further be correlated with a certain phenotype or biological process of interest. An elegant RNA-seq study was performed by Lanver et al. (2018) on fungal gene expression in the *Ustilago maydis* – maize interaction from the pre-penetration phase to the penetrating appressoria, the biotrophic invasive phase all the way to tumor development. In this study, 14 modules of co-expressed genes were described with distinct profiles, some of which reflected fungal developmental stages, either on the plant surface or during penetration, while others correlated with the establishment and maintenance of biotrophy or the onset of tumor induction. Gene Ontology (GO) enrichment analysis revealed insight into the fungal genes and biological processes that contribute to these different infection stages (Lanver et al., 2018). Zhang et al. (2019) chose a different approach and performed a co-transcriptome analysis of fungal and plant genes using 96 distinct *B. cinerea* isolates inoculated on leaves of three *Arabidopsis* genotypes. In this analysis, the authors focused on *B. cinerea* genes of which transcript levels at 16 hpi were

correlated to the necrotic lesion area at 72 hpi. The list of 100 *B. cinerea* genes with the strongest correlation between these two parameters comprised all seven genes involved in BOT biosynthesis, as well as a large number of genes encoding plant cell wall degrading enzymes and peptidases (Zhang et al., 2019). These two studies illustrate of the biological insights that can be obtained about fungal infection processes from transcriptome studies.

In this chapter, we describe that inoculation of the *Δbot2Δboa6* double mutant in a minimal medium can result in the restriction of the fungus to necrotic spots at the inoculation site ("incompatible interaction"), whereas supplementation of the inoculation medium with yeast extract can restore the development of expanding lesions ("compatible interaction"). In order to obtain insights into the mechanisms that regulate such an unexpected binary outcome of an inoculation, we performed an RNA-seq study. We inoculated the *Δbot2Δboa6* double mutant on tomato leaves in two distinct inoculation media resulting in either compatible or incompatible interactions. As a control, the WT B05.10 isolate was inoculated in the same two media, which in both cases resulted in a compatible interaction on tomato leaves. Inoculated leaves were sampled at three time points for RNA extraction and sequencing. The resulting RNA-seq data were analyzed in several ways to investigate which functional differences in transcript profiles may underlie the distinction between compatible and incompatible interactions.

Results

The importance of BOT and BOA for fungal virulence depends on the inoculation medium

We first performed an infection assay by inoculating tomato leaves with the *Δbot2#1* mutant that cannot produce BOT, the *Δboa6#1* mutant that cannot produce BOA, and the *Δbot2Δboa6#6* double mutant that produces neither BOT nor BOA. Mutants were inoculated on the right half of leaflets, while the WT *B. cinerea* strain B05.10 was inoculated on the left half. For the infection assay we used Gamborg B5 medium supplemented with 25 mM glucose and 10 mM potassium phosphate (pH 6.0), as in the study of Leisen et al. (2020) and other studies describing *B. cinerea* infection assays. More than 80 % of the spots inoculated with WT B05.10 produced expanding lesions (Figure 1A, C). The *Δboa6* single knockout mutant displayed similar disease incidence and expanding lesion sizes as the WT B05.10 (Figure 1A, C), suggesting that BOA alone does not make a detectable contribution to fungal virulence on tomato. By contrast, disease incidence was significantly lower when the *Δbot2#1* was inoculated on tomato leaves: ~70% of the primary lesions formed by the mutant did not expand beyond the inoculation spot, while ~97% of primary lesions formed by WT B05.10 did. The few expanding lesions that the *Bcbot2* mutant could develop were ~25% reduced in size as compared to B05.10 (Figure 1A, C). This observation suggested that production of BOT contributes strongly to the ability to expand beyond the inoculation spot, and also to some extent to the expansion rate of the lesions. Expanding lesions were barely observed on the leaf half inoculated with the *Δbot2Δboa6#6* double mutant (average disease incidence of ~6%) (Figure 1A, C), and the few lesions that were able to expand were similar in size to the WT B05.10, mainly due to the small sample number which hampered proper statistical analysis. These observations indicate that the production of either BOT or BOA is pivotal for the capacity of the fungus to cause expanding lesions under these inoculation conditions. Moreover, the results suggested that BOT and BOA are functionally complementary to each other, but BOT plays a more important role than BOA in the virulence of *B. cinerea*.

When the infection assay was performed using the same fungal strains but with addition of 0.1% yeast extract (+y) in the inoculation medium, the capacity of *Δbot2#1* and *Δbot2Δboa6#6* mutants to cause expanding lesions was largely restored and comparable to the WT. Under this modified condition (+y), disease incidence of WT B05.10 increased to 100% and the lesion size increased by approx. 5 mm compared to the former condition (-y) (Figure 1B, D). The *Δboa6* single knockout mutant displayed similar disease incidence and lesion sizes as the WT B05.10 (Figure 1B, D). Interestingly, almost all inoculations with *Δbot2#1* and *Δbot2Δboa6#6* mutants showed expanding lesions, and the lesion sizes of

these mutants were slightly, but significantly smaller than those of the WT B05.10 (Figure 1B, D).

BOT and BOA have a larger impact on the virulence of *B. cinerea* than CDIPs

A recently published study by Leisen et al. (2022) and a presentation by Hahn (2022) reported that the contribution of *B. cinerea* CDIMs to the fungal virulence displays a high level of functional complementarity, as demonstrated by the virulence phenotype of 12xbb, 12xpg and 18x mutants (in which, respectively, 12, 12 and 18 *B. cinerea* genes are knocked out; Table 2). We performed infection assays to compare the virulence of the 12xbb, 12xpg and 18x mutants to WT B05.10 under inoculation conditions as described above. The *Δbot2Δboa6#6* strain was assessed along with these mutants in the same experiments. When no yeast extract was added into the inoculation medium, even fewer spots inoculated with the 12xbb mutant showed expanding lesions as compared to *Δbot2Δboa6#6,* and the 18x mutant was unable to cause even a single expanding lesion on the tomato leaves (Figure 1). The 12xpg mutant caused expanding lesions at most of the inoculation spots, although the lesion sizes were significantly smaller than for the WT B05.10 (Figure 1). These observations collectively suggested that the deletion of BOT and BOA caused a major reduction in virulence of the fungus, while the 12 genes missing in the 12xpg played a less pronounced role, as compared to BOT and BOA when tested under this condition (-y). After adding 0.1% yeast extract into the inoculation medium, disease incidences for *Δbot2Δboa6#6*, 12xbb and 18x mutants all increased to above 80% and were no longer significantly different from the WT B05.10 (Figure 1), but there were notable differences in the sizes of the expanding lesions. With this inoculation medium (+y), the reduction in lesion sizes of the 12xpg mutant was similar to the *Δbot2Δboa6#6* double mutant, but less pronounced than the reduction in lesion sizes of the 12xbb and 18x mutants (Figure 1). This observation suggests that the contribution of BOT and BOA to fungal virulence was quantitatively comparable to the contribution of the 12 CDIP-encoding genes which were knocked-out in the 12xpg mutant. The 18x mutant showed the most pronounced reduction in lesion size among the four tested knockout strains (Figure 1), indicating an additive effect of the deletion of *Bcssp2, Bccfem1, Bccdi1* and *Bccrh1* (genes knocked out in the 18x mutant but not in the other mutant strains) on the virulence of *B. cinerea*. Moreover, based on the reduction in lesion sizes, the 10 extra genes deleted in 12xbb, as compared with *Δbot2Δboa6#6*, seemed to contribute to the virulence to a similar extent as the six extra genes deleted in 18x, as compared with the 12xbb mutant (Figure 1).

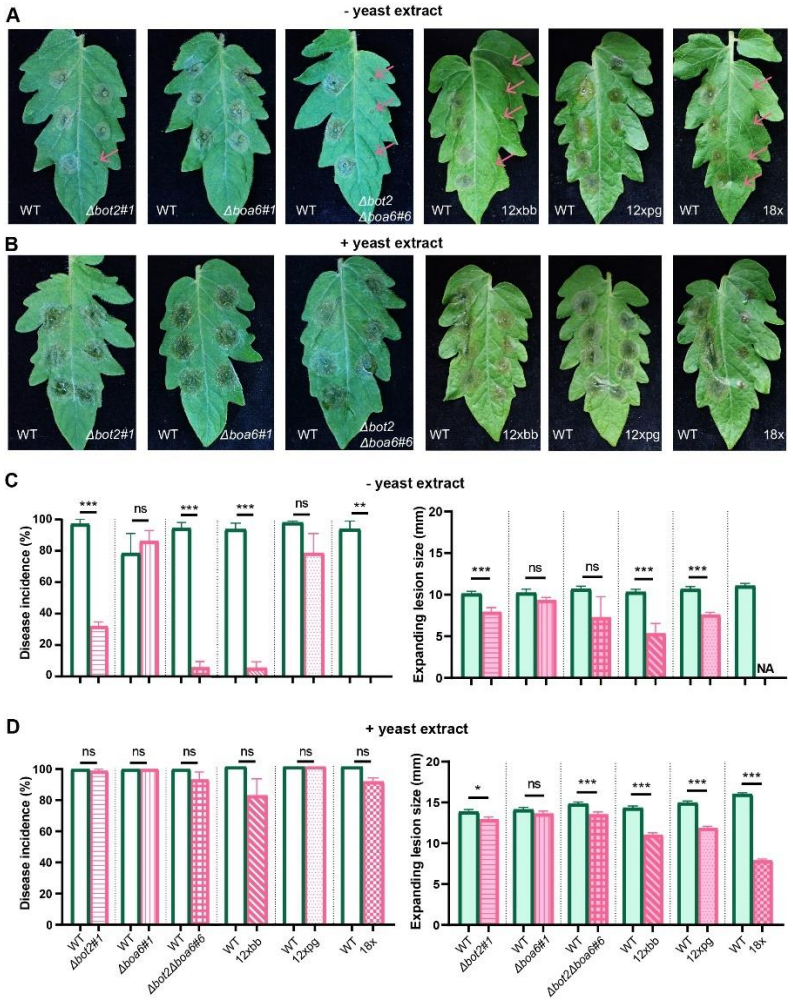

Figure 1. Infection assays to compare the virulence of *Δbot2#1, Δboa6* and *Δbot2Δboa6#6* and 12xbb, 12xpg and 18x mutants with WT B05.10 on tomato leaves using two inoculation media. The assays were performed using a Gamborg B5 medium without yeast extract **(A, C)** or with 0.1% yeast extract **(B, D)**. Symptoms of tomato leaflets inoculated with each mutant strain (on the right of the central vein) compared with B05.10 (on the left of the central vein) were photographed at 3 days post inoculation (dpi) **(A, B)**. Pink arrows in **(A)** indicate non-expanding lesions. Bar charts of disease incidences (left) and lesion sizes measured by a digital caliper (right) at 3 dpi, present the means with standard errors from 72 (for *Δbot2#1, Δboa6* and *Δbot2Δboa6#6* compared to WT fungus) or 96 inoculations (for 12xbb, 12xpg and 18x mutants compared to WT fungus) collected from three independent experiments **(C, D)**. The virulence assays for *Δbot2#1, Δboa6* and *Δbot2Δboa6#6* were performed separately from the experiments for 12xbb, 12xpg and 18x mutants. Disease incidence was calculated as the ratio of the number of expanding lesions to the total number of inoculated spots. Lesions showing a diameter no larger than 2 mm were considered as non-expanding lesions, which are indicated by the bars below the horizontal dashed line at 2 mm in bar charts. Statistical analyses were performed by t-test, and the results are shown by either asterisks indicating the significant differences (*p<0.05, **p<0.01, ***p<0.001) or ns indicating no significance.

RNA sequencing of compatible and incompatible interactions

It was remarkable that the incompatible interaction between the *Δbot2Δboa6#6* mutant and tomato leaves could be converted into a compatible interaction simply by supplementation of yeast extract to the inoculation medium. We hypothesized that the modification of inoculation medium altered the transcriptome of the *Δbot2Δboa6#6* mutant, leading to suppression of the expression of genes that result in restricting the fungus in the primary necrotic lesion, or to promoting the expression of genes that overrule plant resistance mechanisms that lead to fungal restriction. We performed an RNA-seq experiment to study differences in the fungal transcriptome of the *Δbot2Δboa6#6* mutant between the incompatible and compatible interaction. Conidia of the *Δbot2Δboa6#6* mutant and WT B05.10 were suspended in either of the Gamborg B5 media without or with yeast extract (indicated by "-y" or "+y", respectively) and inoculated on tomato leaves, which were sampled at 0, 12, 16 and 24 hpi. Mock-inoculated tomato leaves as well as *in vitro* cultures (both -y and +y media) of *Δbot2Δboa6#6* mutant and WT B05.10 at the same time points were included as controls. RNA extracted from these samples was used for constructing strand-specific libraries followed by paired-end sequencing (Supplementary Table S1).

In total 13,754 transcripts of *B. cinerea* were analyzed. Principal Component Analyses (PCA) showed that all samples clustered as expected (Supplementary Figure S1). Specifically, the biological replicates clustered within time points and all *in vitro* samples and all *in planta* samples clustered together, respectively. Since we were mainly interested in providing an explanation for the yeast extract-induced transition from an incompatible to a compatible interaction with the host plant, we focused our initial analysis on the *in planta* conditions.

Table 1. Number of Differentially Expressed Genes (DEGs) in different comparisons

Group	*In planta*		*In vitro*	
	Up-regulated	**Down-regulated**	**Up-regulated**	**Down-regulated**
WT[1]+y[3] (vs) WT-y[4]_0h[5]	0	0	0	0
WT +y (vs) WT-y_12h[5]	176	226	34	11
WT +y (vs) WT-y_16h[5]	116	63	640	259
WT +y (vs) WT-y_24h[5]	1231	1329	314	79
△△[2]+y (vs) △△-y_0h	3	3	3	3
△△ +y (vs) △△-y_12h	213	445	117	45
△△ +y (vs) △△-y_16h	299	166	129	49
△△ +y (vs) △△-y_24h	1695	1553	300	37

[1] Wild type; [2] *Δbot2Δboa6#6* double knockout mutant; [3] With yeast extract; [4] Without yeast extract ;[5] 0, 12, 16, or 24 hours post inoculation *in planta* or hours post incubation *in vitro*

To examine the influence of adding yeast extract on the fungal transcriptome, we compared the samples that were grown in media -y and +y across all time points. The highest number of DEGs was observed at 24 hpi, reflecting that a large number of genes were affected by yeast extract at the late time points, in both wild type (WT) and mutant samples (Table 1). A large number of the DEGs at 24 hpi (1491) overlaps between WT and mutant (Figure 2), which indicates that the fungal strains were similarly affected by the yeast extract. The up-regulated genes are mostly enriched in GO terms ($p < 0.05$) related to gene transcription and protein synthesis (Supplementary Figure S2). Although there were no significantly enriched GO terms detected in the set of down-regulated genes, several genes in this list are involved in iron/copper homeostasis. For example, *Bcin15g03090* and *Bcctr2/Bcin01g05510* were annotated as copper transporter and copper homeostasis protein, respectively. Moreover, *Bcatg13, Bcatg2* (Liu et al., 2022) and *Bcatg9* that are

involved in autophagy (ATG) were also down-regulated. ATG includes a set of programmed cell developmental changes that occur during cellular remodeling and serves as an adaptive response during nutrient starvation (Yorimitsu & Klionsky, 2005). In severe stress conditions, ATG may activate a programmed cell death cascade. The upregulation of transcripts of ATG genes in the mutant upon inoculation without yeast extract at 24 hpi coincides with the restriction of lesion outgrowth. There are also 1170 and 571 DEGs that were exclusively differentially expressed in the mutant or wild type fungus at 24 hpi, respectively. Interestingly, these two lists of DEGs contain distinct genes, however they share enriched GO terms, related to rRNA processing, protein translation, gene expression, oxidation-reduction and transmembrane transport (Supplementary Figure S3).

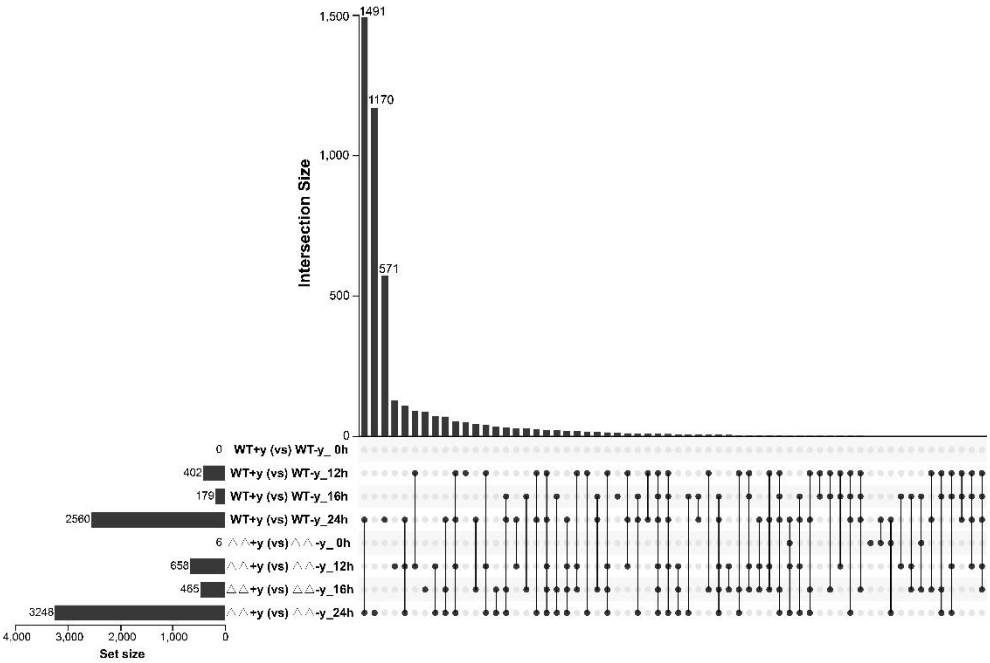

Figure 2. UpSet plot summarizing differentially expressed genes (DEGs) of either wild type or double mutant between samples with and without yeast, at different time points. The vertical bar plot reports the intersection size, the dot plot reports the set participation in the intersection. Links between different samples show overlapped DEGs between or among compared samples. The bottom left horizontal bar graph shows the total number of DEGs per compared group (set size).

Co-expression network analysis reveals gene clusters positively correlated with compatible interaction

In order to determine which genes show similar expression patterns and are co-regulated across all conditions, a co-expression network was created using Weighted correlation

network analysis (WGCNA). A total of 25 modules of co-expressed genes was obtained, of which the "Grey" module was the residual module, containing all genes that did not show significant correlation in expression profile with genes other modules (Supplementary Figure S4). Evaluation of the interconnection between all 25 modules revealed that each module correlated with its own the best, as may be expected (Supplementary Figure S5).

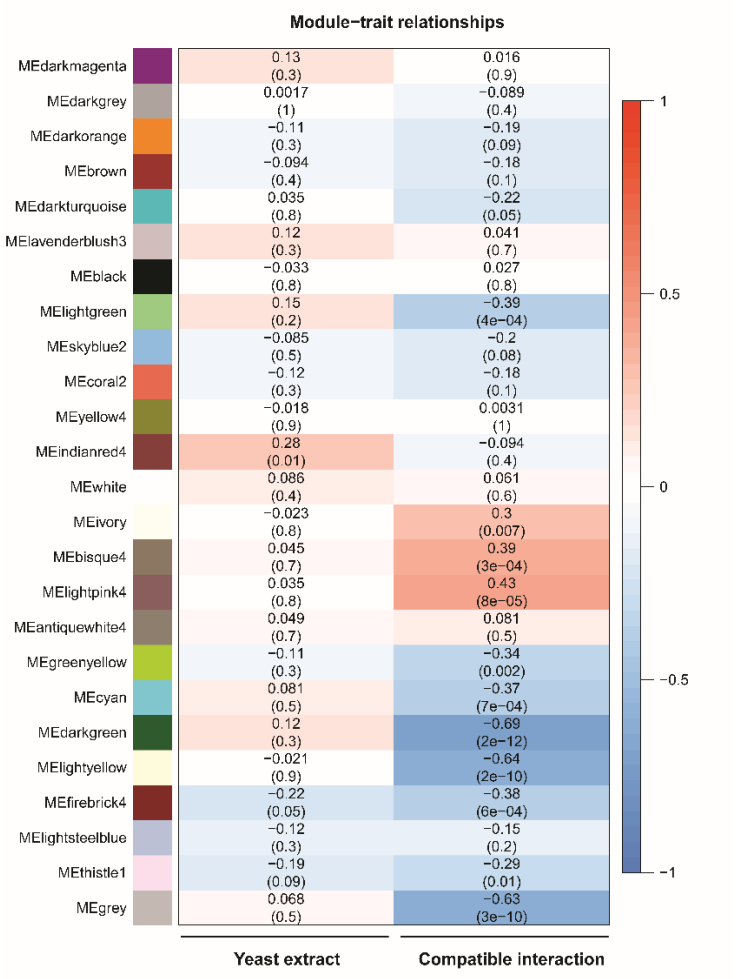

Figure 3. Heatmap showing the correlations of co-expression modules with experimental variables, the presence of yeast extract in the inoculation medium, or in the outcome of the interaction between *B. cinerea* and tomato. On the Y-axis are the merged co-expression modules, with both the names and colors assigned by the WGCNA algorithm. In the heatmap, Pearson correlation with the experimental conditions (the presence of yeast extract and outcome of the infection) are shown, respectively, left and right. Dark red colors indicate a high positive correlation, and dark blue colors indicate a high negative correlation with a condition. Lighter values indicate lower (positive or negative) correlation. For each module, the top line provides the correlation coefficient r, while the lower line (in a bracket) provides the p-value for significance.

To analyze which modules might be functionally involved either in the response to the presence of yeast extract in the inoculation medium, or in the outcome of the interaction between *B. cinerea* and tomato, we correlated genes of each module with their experimental variables. Both a positive and negative correlation can suggest involvement in either response and we chose thresholds of [r] > 0.30 and p < 0.01 as being significant. There was no significant correlation between any module and the presence of yeast extract (Figure 3). By contrast, nine modules show significant (positive or negative) correlations with the outcome of the infection, i.e. either with a compatible interaction or an incompatible interaction, respectively.

Three modules are positively correlated to the compatible interaction (conditions in which the lesions expanded), and their expression peaks were more pronounced *in planta* than *in vitro* (Figure 4). The “bisque4” and “light pink4” modules contain genes with transient peaks in transcript levels at 12 hpi and 16 hpi, respectively, whereas genes in the "ivory” cluster showed steady transcript levels at 12 and 16 hpi, followed by a strong increase at 24 hpi, especially in the compatible interactions. Interestingly, all three modules are enriched in proteins with a signal peptide for secretion (p < 0.01). It should be noted that two modules include genes encoding CDIPs. Module “bisque4” contains the *Bcnep1, Bcxyg1,* and *Bcplp1* genes, while “ivory” contains the genes *Bcnep2, Bcxyn11A, Bcpg1* and *Bcssp2* (Supplementary Data S1). Surprisingly, the module “lightyellow” that showed negative correlation to the compatible interaction contains even more of such CDIP-encoding genes, specifically *Bcspl1, Bchip1, Bcxyl1, Bcgs1, Bcbot2* and *Bccrh1.*

We examined in more detail the three modules that are positively correlated with the compatible interaction, with emphasis on their expression profiles, gene content and the ontology enrichment. Despite each showing a positive correlation to the compatible interaction, these three modules were quite distinct in their enriched GO terms (Supplementary Figure S6). The “bisque4” module contains 245 genes that showed a transient peak in expression *in planta* at 12 hpi, followed by a slight decline, while the *in vitro* transcript levels of genes in this cluster remained fairly constant (Figure 4). “Bisque4” is enriched in genes involved in mitochondrial activity (ATP synthesis, cytochrome c oxidase activity, electron transport) and gene transcription (splicing). The “lightpink4” module contains 85 genes that showed a transient peak in expression *in planta* at 16 hpi for the +y samples, while there was a steady increase in transcript levels for the -y samples (Figure 4). “Lightpink4” contains a number or CAZyme-encoding genes, including the pectin methylesterase genes *Bcpme*1 and *Bcpme*2, as well as a few cytochrome P450-encoding genes, including several genes from the BOA gene cluster. The genes in the "ivory” cluster (118 genes) showed a continuous increase in transcript levels over three infection time

points, though the increase was more pronounced in the +y samples as compared to the -y samples. The only GO term that was significantly enriched in the “ivory” cluster was associated with peptidase activity.

We also examined the modules that were correlated with the incompatible interaction, displaying expression profiles associated with a failure to cause expanding lesions (Figure 3). The “darkgreen” module (1604 transcripts) is typified by generally stable *in planta* transcript levels that markedly increase at 24 hpi exclusively in the incompatible interaction. The genes in this module are enriched in GO terms related to gene expression, chromatin organization, splicing, mitotic cell cycle, cell division and DNA repair. The “darkturquoise” module (1811 transcripts) is typified by a high *in planta* transcript level in the absence of yeast extract, especially at 0 hpi and 24 hpi, with a steep decline at 12 hpi and 16 hpi, while the expression in the presence of yeast extract is stable at all time points. The module contains six genes encoding light-dependent transcription factors (TFs), several light sensors, proteins from the Velvet complex, both phospholipase C proteins, as well as five polyketide synthases. The “lightyellow” module (2504 transcripts) is typified by increased *in planta* transcript levels in the absence of yeast extract at 24 hpi, and it is markedly higher in the mutant than in the wild type. The only significantly enriched GO terms for this module are related to protein translation. The “lightgreen” module (372 transcripts) is typified by a steady decline of *in planta* transcript levels over time in the three compatible interactions, while the expression slightly increases at 24 hpi in the incompatible interaction. The module contains several RNA polymerase I transcription initiation factors, two HHK histidine kinases and other signaling proteins, as well as two bicarbonate transporters and other H+ antiporters. The “cyan” module (867 transcripts) is typified by a peak of expression at 12 hpi, which drops at 16 hpi. Only in the inoculation medium with yeast extract, the transcript level continues to decrease at 24 hpi. The module contains proteins of the proteasome complex, ATPase complex, as well proteins involved in cytoskeleton binding, glycosylation and Golgi vesicle transport. The “firebrick4” module (37 transcripts) is typified by stable *in planta* transcript levels that markedly increase at 24 hpi exclusively in the *Δbot2Δboa6#6* mutant without yeast extract, leading to an incompatible interaction. The module contains 5 of the 6 copper transporter genes in the *B. cinerea* genome as well as a copper-binding protein and a copper metallochaperone, suggesting that the fungus experiences a depletion of copper from the environment.

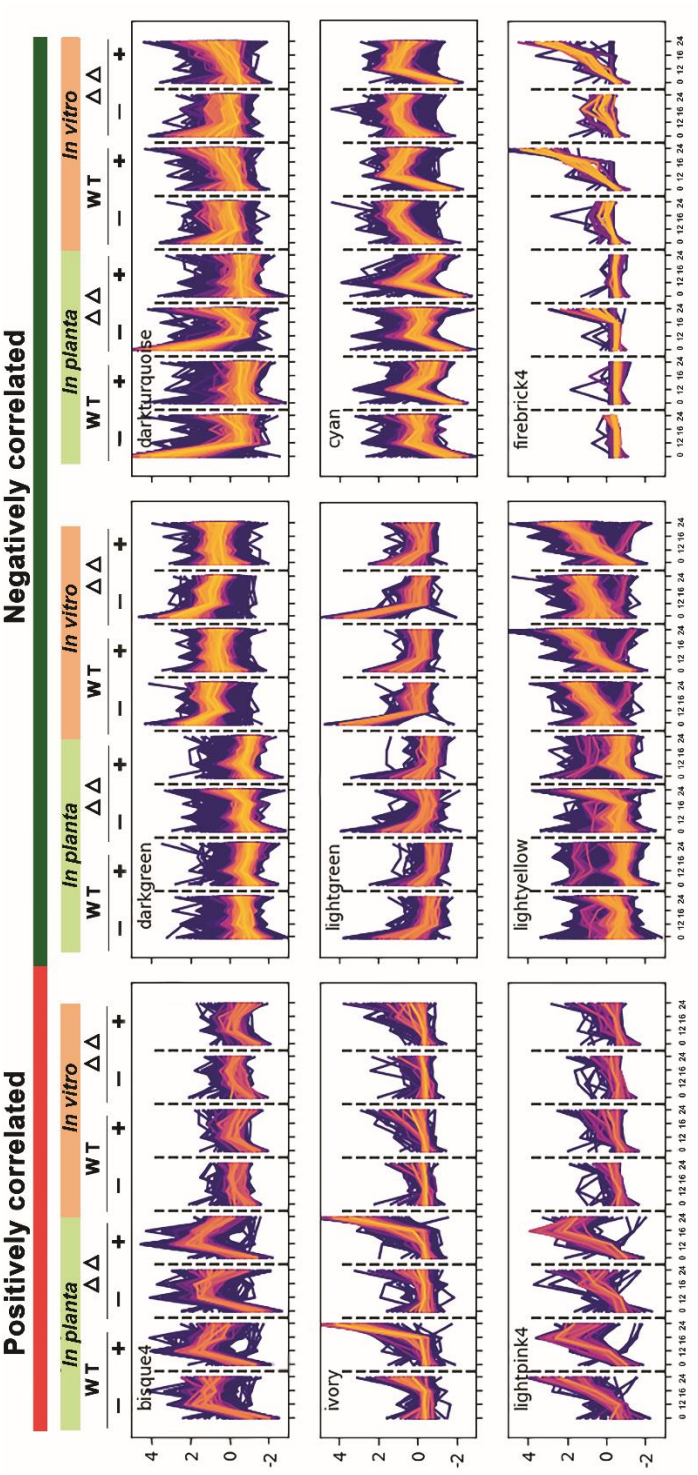

Figure 4. Expression profiles of co-expression modules that show significant (positive or negative) correlations to the compatible interaction between *B. cinerea* and tomato. Each sub-plot contains the full profile of all genes in a module, across all eight conditions. From left to right on the X-axis contains *in planta* and *in vitro* conditions (with the time points 0, 12, 16 and 24 hpi): wild type without yeast extract, wild type with yeast extract, double mutant without yeast extract, double mutant with yeast extract. On the Y-axis, the standardized gene expression is shown. Each profile is colored according to the assigned module membership value, defines as the correlation with the first principal component of the module profiles (module Eigengene). Lighter colors indicate greater module membership values.

Overexpressing single CDIPs cannot restore the pathogenicity of Δbot2Δboa6

Based on the phenotypic observations of the various mutants in Figure 1, and the fact that several CDIPs were present in co-expression modules that show a positive correlation with a compatible interaction (successful lesion expansion from the primary inoculation spot), we examined in closer detail the expression profiles in the RNAseq dataset of the 18 *B. cinerea* CDIP-encoding genes that are deleted in the 18x mutant. A heatmap was generated of the expression levels in WT B05.10 and in the *Δbot2Δboa6#6* mutant, both *in vitro* and during leaf infection, and in the absence or presence of yeast extract (Figure 5).

This heatmap illustrates that the genes *Bcssp2*, *Bcnep2*, *Bcxyn11A* and *Bcpg1*, which are members of the "ivory" module shared a similar transcript profile, that was specifically characterized by their upregulation during infection on tomato leaves and only upon addition of yeast extract into the inoculation medium. The *Bcssp2* gene was of specific interest, because it is one of the four genes only deleted in the 18x mutant but not in 12xbb or 12xpg mutants, while *Bcnep2*, *Bcxyn11A* and *Bcpg1* were deleted in the 12xpg mutant (Figure 5). As the 12xpg mutant was more virulent than *Δbot2Δboa6#6* in the absence of yeast extract and displayed similar virulence as *Δbot2Δboa6#6* in the presence of yeast extract (Figure 1), we hypothesized that the *Bcssp2* gene may play a more important role in fungal virulence under these conditions than *Bcnep2*, *Bcxyn11A* and *Bcpg1*. Among the four extra genes deleted only in the 18x mutant, *Bcssp2* was the only gene that was significantly upregulated by the addition of yeast extract; the transcript level of the *Bccfem1* gene was similar with and without yeast extract, while the *Bccdi1* and *Bccrh1* transcripts were downregulated when yeast extract was added. For this reason, the *Bccfem1, Bccdi1* and *Bccrh1* did not cluster in the co-expression analysis into a module that is correlated with the compatible interaction.

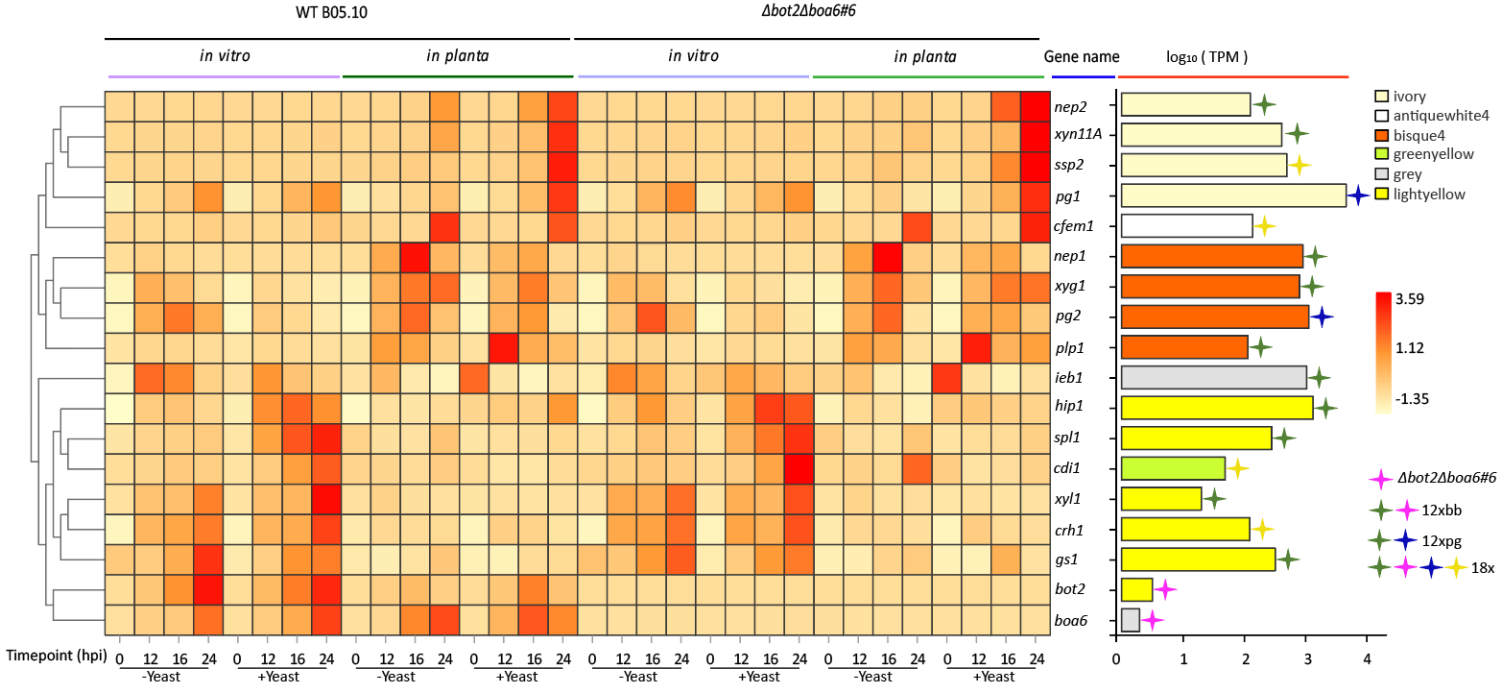

Figure 5. Transcript levels of 18 genes in the WT B05.10 and *Δbot2Δboa6#6*, represented by a heatmap generated by Z-score calculation (left) and the mean $\log_{10}$ (TPM) of the gene across all timepoints (right) both during *in vitro* growth and during infection. The genes knocked-out in *Δbot2Δboa6#6*, 12xbb, 12xpg and 18x mutants were marked by stars with corresponding colors, for which the legend is at the right bottom corner of the figure. The bar in the mean $\log_{10}$ (TPM) panel is filled with a color representing the module in which the gene grouped according to the WGCNA analysis.

In order to test the hypothesis that the *Bcssp2* gene product plays a more important role in fungal virulence than the other 15 CDIPs of which genes were deleted in the 18x mutant, we tested whether overexpression of the *Bcssp2* gene in the *Δbot2Δboa6#6* mutant could restore virulence without addition of yeast extract, by compensating for the absence of BOT and BOA production. Fungal transformants were generated in order to overexpress *Bcssp2*, under control of a strong constitutive promoter, in the genetic background of the *Δbot2Δboa6#6*mutant. The virulence of the *Δbot2Δboa6-OEssp2* (*ΔΔ-OEssp2*) mutants was compared with that of the *Δbot2Δboa6#6* recipient using inoculation medium without yeast extract. Even though the potential contribution of *Bcnep2*, *Bcxyn11A* and *Bcpg1* to the virulence of *B. cinerea* was expected to be less significant than *Bcssp2*, these genes grouped in the same module based on their expression profile. Considering this result, we also generated transformants that overexpressed, separately, either *Bcnep2*, *Bcxyn11A* or *Bcpg1* in the *Δbot2Δboa6#6* recipient, which were named *ΔΔ-OEnep2, ΔΔ-OExyn11A* and *ΔΔ-OEpg1* mutants. At least two independent transformants were obtained for each overexpression line (Supplementary Figure S7). Unexpectedly, all obtained independent *ΔΔ-OExyn11A* transformants showed growth retardation during *in vitro* growth and were thus eliminated from infection assays. Two transformants of *ΔΔ-OEssp2*, one transformant of *ΔΔ-Oepg1*, and one for *ΔΔ-Oenep2* were inoculated on tomato leaves in medium lacking yeast extract to compare their virulence with the recipient strain *Δbot2Δboa6#6*. Figure 6 shows that none of the overexpression transformants (*ΔΔ-OEssp2#10/#55*, *ΔΔ-OEpg1#22* and *ΔΔ-OEnep2#4*) caused a significantly higher proportion of expanding lesions than *Δbot2Δboa6#6* when using the inoculation medium without yeast extract. The result indicated that overexpressing *Bcssp2, Bcnep2* or *Bcpg1* individually cannot compensate for the defect of the *Δbot2Δboa6#6* mutant in virulence.

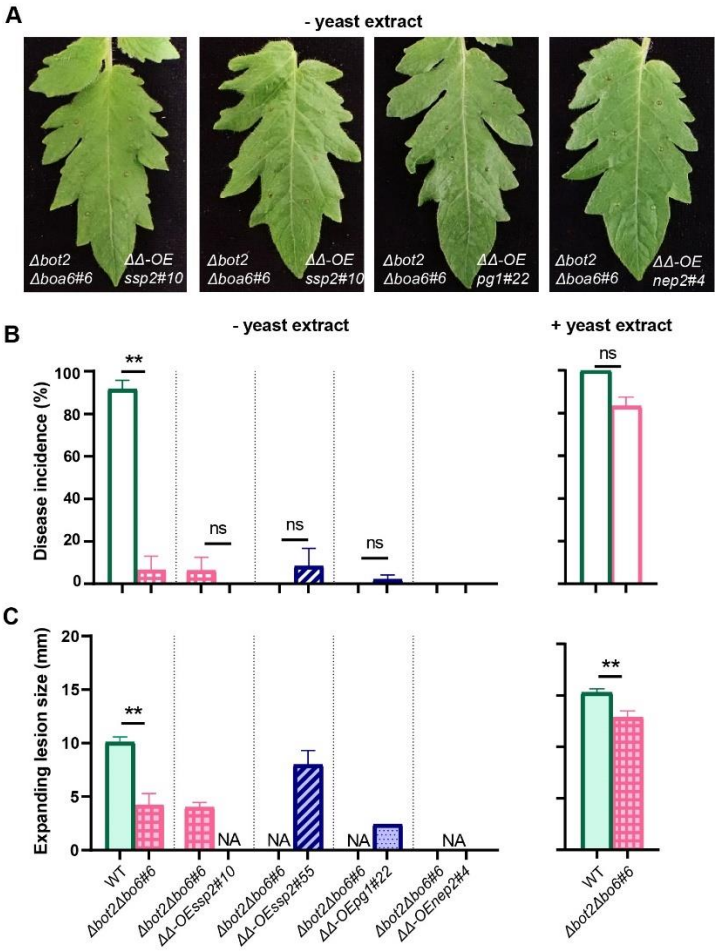

Figure 6. Infection assays to compare the virulence of overexpression mutants to the recipient strain *Δbot2Δboa6#6* on tomato leaves using a Gamborg B5 medium without yeast extract. The comparisons between WT B05.10 and *Δbot2Δboa6#6* were also inoculated using both medium without and with yeast extract in the same experiments, showing similar results as shown in Figure 1. **(A)** Symptoms of tomato leaflets infected by each overexpression mutant strain (on the right of the central vein) compared with *Δbot2Δboa6#6* (on the left of the central vein) were photographed at 3 days post inoculation (dpi). **(B)** Bar charts of disease incidences of inoculations performed using the medium without yeast extract (left) and the disease incidences of WT B05.10 and *Δbot2Δboa6#6* inoculated with the medium with yeast extract in the same experiments (right), which are represented as means with standard errors from 48 datapoints collected from two independent experiments. **(C)** Bar charts representing expanding lesion sizes upon inoculations using the medium without yeast extract (left) and with yeast extract (right), measured by a digital caliper at 3 dpi. The total number of expanding lesions caused by each of the mutant strains, which were inoculated with the medium without yeast extract, was no more than 5 from these two experiments. The inoculations of mutant strains causing no expanding lesion are indicated as "NA" in the chart on the left. Statistical analyses were performed by t-test, showing no significance (ns) or significant difference (**p<0.01) in disease incidence and expanding lesion size between the mutant and the recipient strain (*Δbot2Δboa6#6* for overexpression mutants or WT B05.10 for the *Δbot2Δboa6#6* mutant).

Discussion

The occurrence of an incompatible interaction between a necrotrophic fungus and its host

Most pathologists will by definition consider a gene to encode a virulence factor if a knock-out mutant strain of the gene produces lesions with significantly smaller lesion sizes as compared to the wild type fungus. This definition of a virulence factor is, however, generally neglecting the contribution of the inoculation medium to the eventual disease development. The infection assays performed in this study illustrate the significant impact of the composition of inoculation medium on the disease incidence resulting from inoculation of *B. cinerea* mutants, but not the wild type fungus. Using inoculation medium without yeast extract, the *Δbot2#1* mutant showed significant reduction in disease incidence and the *Δbot2Δboa6#6* mutant was almost non-pathogenic on tomato leaves. The mutants retained their capacity to cause primary necrotic lesions, but these primary lesions did not expand beyond the inoculation site, resulting in restriction of fungal outgrowth that reflects an "incompatible interaction". The terms "compatible" and "incompatible" interaction are commonly used for interactions of plants with biotrophic microbial pathogens (Keen, 1990a). In that case the outcome of an interaction is often determined by gene-for-gene interactions of pathogen effectors, acting as avirulence factors, with cognate receptors in the host plant that recognize the effector and trigger a hypersensitive cell death and resistance (Giraldo & Valent, 2013; Jones & Dangl, 2006). We are aware that it appears unusual to use the term (in)compatible for the infection of a necrotrophic fungus, and especially in the context of a fungal mutant in combination with the composition of the inoculation medium. We recently used the same terminology to describe the interaction between *B. cinerea* WT strain B05.10 and the wild tomato relative *Solanum habrochaites* (You et al., 2023). In that case, the ability of the fungus to produce expanding lesions on *S. habrochaites* leaves depended on the sucrose concentration in the inoculum. In Gamborg B5 medium with 10 mM sucrose, *B. cinerea* induced primary necrotic lesions, but the proportion of primary lesions that expanded (disease incidence) was <20%. When the sucrose concentration was increased to 50 mM, disease incidence increased to >90% (You et al., 2023). One of the possible explanations for this observation was that the sucrose concentration may affect gene expression in the fungus in such a way that high sucrose levels induce the expression of (unknown) fungal genes that suppress an effective resistance response by the wild tomato. Alternatively, the high sucrose level might repress the expression of genes that would otherwise trigger a resistance response in *S. habrochaites* (You et al., 2023).

In our experiments with *Δbot2#1* and *Δbot2Δboa6#6* mutants, as well as the 12xbb and 18x mutants, the addition of yeast extract to the medium restored the disease incidence to the level of the WT B05.10 ("compatible interaction") although lesion sizes caused by the mutants at 3 dpi were smaller as compared to WT B05.10. The results from virulence assays using both media indicated a more pronounced contribution of BOT and BOA to the virulence of *B. cinerea* than previously reported by Dalmais et al. (2011) and Leisen et al. (2020). Leisen et al. (2020) reported that the lesion size caused by the *Δbot2Δboa6#6* mutant was similar to that of WT B05.10, using the same Gamborg B5 medium as in this study (without yeast extract) but using a lower spore density combined with a larger droplet size for the infection assay (the total number of conidia in each droplet was similar between both studies). In addition, we described in Chapter 4 that the *Δbot2Δboa6#6* mutant caused expanding lesions on tomato leaves using Potato Dextrose Broth as the inoculation medium, which differs in the type and concentration of nutrients from the Gamborg B5 media (-y/+y) used in this chapter. We are not aware of any previous study on *B. cinerea* or any other fungus where such seemingly small variation in experimental procedures leads to opposite outcomes of disease development (incompatible versus compatible interaction). Hopefully, these observations will encourage the research community to more thoroughly consider the methodology used for testing the virulence of knockout mutants in *B. cinerea* and possibly other fungi.

The obtained results inspired us to implement an RNA-seq strategy to acquire insights into the "compatible" or "incompatible" interaction of the *Δbot2Δboa6#6* mutant (but not WT B05.10) with tomato leaves and into the effect of adding yeast extract to the inoculum. We considered that restoration of compatibility for the *Δbot2Δboa6#6* mutant by the addition of yeast extract could be mediated by influences on the transcript levels of fungal genes that govern crucial stages of the infection process, either the primary lesion induction or the subsequent lesion expansion. In order to study these processes with as few experimental variables as possible, we performed an RNA-seq experiment using two Gamborg B5 media (-/+ yeast extract) as the only difference in the inoculation condition to investigate the molecular mechanisms mediating the transition from an incompatible interaction between *Δbot2Δboa6#6* and tomato to a compatible interaction. We cannot neglect the possible effect of yeast extract in the inoculum on gene expression in the host plant, specifically of genes involved in immune responses and plant cell death. However, the analysis of the tomato transcriptome remains to be performed. The focus of our analysis was on the *B. cinerea* gene expression in three (early) phases of the infection: penetration of the host surface (12 hpi), initiation of primary cell death (16 hpi) and onset of lesion expansion (24 hpi).

The role of yeast extract

So what could be the physiological impact of yeast extract on a fungus that is in the process of infecting a host plant? Yeast extract is a concentrate of the water-soluble portion of autolyzed *Saccharomyces cerevisiae* cells and provides water-soluble vitamins, amino acids and small peptides to the medium formulation. The Gamborg B5 medium itself consists of minerals, vitamins, and it contains both nitrate and ammonium as nitrogen sources but no carbon source. We supplemented the medium with 25 mM glucose as the carbon source. The Gamborg B5 medium with glucose suffices to allow *B. cinerea* germination and it enables the WT strain B05.10 to achieve primary lesion induction and subsequent expansion of the lesion ("compatible interaction") in the absence of supplemented yeast extract. However, yeast extract provides amino acids that enable the fungus to accelerate protein biosynthesis, as it sidesteps the requirement to first synthesize an entire set of amino acids from primary nitrogen and carbon sources in the medium. The immediate availability of (a small amount of) amino acids would give *B. cinerea* a head start that can accelerate the production of proteins and metabolites by a few hours, which stimulates host penetration and the subsequent induction of a primary lesion. Although the WT B05.10 did not require yeast extract to achieve a high disease incidence, the addition of yeast extract to the inoculum resulted in larger lesion sizes at 3 dpi (Figure 1), which was presumably facilitated by faster, or more effective, activation of pathogenicity-related mechanisms and thereby enabled the fungus to proceed to the lesion expansion phase at an earlier timepoint. When WT B05.10 was inoculated in Gamborg B5 medium lacking yeast extract, the development of primary lesions was commonly observed from 16 hpi onwards but expansion of primary lesions occurred only beyond 24 hpi. The addition of yeast extract accelerated the onset of expansion, as the lesions were clearly larger than the inoculation droplet at 24 hpi.

Primary lesion induction and lesion expansion are distinct processes

We propose that a successful infection by *B. cinerea* involves two aspects, which may be governed by distinct fungal virulence factors, and which require that the fungus achieves certain milestones at specific time points. It is not merely sufficient to trigger plant cell death by producing a cocktail of CDIMs, but these must be produced and operate timely to prevent the host plant from mounting defense responses that otherwise restrict fungal outgrowth. In this context it is important to note that the primary lesions that were produced in the incompatible interaction by the *Δbot2Δboa6#6* mutant remained unable to expand once the restriction of lesion outgrowth was observed, regardless how long the incubation was continued. Apparently, the plant response that restricted the expansion provided an effective, absolute host resistance response which was achieved around the 24

hpi benchmark. We thus hypothesize that the lack of BOT and BOA production caused such significant delay in the capacity of the fungus to induce host (programmed) cell death in a timely manner, that it allowed the plant to mount an effective resistance. This highlights the importance of time in the interaction.

Support for our hypothesis that the primary lesion induction and the lesion expansion are distinct processes in the infection by *B. cinerea* is provided by several observations. Firstly, all the multiple gene mutants that were deficient in BOT and BOA production (including the 12xbb and the 18x mutants), remained able to produce a primary necrotic lesion, but they could only expand when yeast extract was provided in the inoculum. With all tested mutants, some (tiny) spots of necrotic plant tissue were observed. Secondly, *B. cinerea* expresses different genes at the stages of primary lesion development and lesion expansion. One example is provided by the family of cell death-inducing NEP1-Like proteins that contains two members, BcNEP1 and BcNEP2. *Bcnep1* is expressed in very early phases of the interaction, from 8 hpi onwards and reaches a peak at 12-16 hpi, coinciding with the appearance of primary lesions (Cuesta Arenas et al., 2010). The *Bcnep1* transcript levels then decline sharply at 24 hpi and there is a simultaneous strong increase in *Bcnep2* transcript levels that will remain high while the lesion continues to expand (Cuesta Arenas et al., 2010). The cell death-inducing capacity of BcNEP1 protein, on a molar basis, is ~30 times stronger than of BcNEP2 and also the cell death response triggered by BcNEP1 is notably faster (usually 4-8 h after protein infiltration) than for BcNEP2 (~24 hpi) (Schouten et al., 2008). These results support the hypothesis that primary lesion induction and lesion expansion are distinct processes, involving distinct fungal proteins. Thirdly, You (2022) reported that during infection on tomato, *B. cinerea* expresses the *BcTom*1 gene encoding a ß-xylosidase that hydrolyses the glycoalkaloid α-tomatine and thereby inactivates its antifungal activity. The expression of *BcTom*1 is low in the absence of α-tomatine and is rapidly induced as soon as the fungus comes into contact with α-tomatine. As α-tomatine is located inside the vacuoles of tomato cells, contact of *B. cinerea* with α-tomatine can only occur when host cells are damaged by cell death induction. The expression of the *BcTom*1 gene can thus serve as a marker for the timing of host cell death in the *B. cinerea*-tomato interaction (You, 2022). The expression profile of the *BcTom*1 gene revealed a different timing of α-tomatine responses between the wild type and *Δbot2Δboa6#6* mutant and between inoculation media. In the absence of yeast extract, both wild type and *Δbot2Δboa6#6* mutant at 12 hpi showed similar *BcTom*1 transcript levels that were equal to the 0 hpi level, indicating that the fungus did not yet respond to α-tomatine. In the samples where yeast extract was added, the expression already increased at 12 hpi by 4-fold and 7-fold in the *Δbot2Δboa6#6* mutant and wild type, respectively. This observation

suggests that host cell death was induced and primary lesion development was likely in progress. The expression of the *BcTom*1 gene continued to increase in the subsequent time points. The transcript level in the inoculation without yeast extract at 16 hpi was similar to the level of the inoculation with yeast extract at 12 hpi, both for the *Δbot2Δboa6#6* mutant and wild type, suggesting that the addition of yeast extract accelerated the host cell death induction by approximately 4h. At 24 hpi, the transcript profiles under the two inoculation conditions diverged notably. The *BcTom*1 transcript level for the inoculation of the *Δbot2Δboa6#6* mutant without yeast extract was similar between 16 hpi and 24 hpi, while it doubled for the wild type under the same conditions. By contrast, the transcript levels for the inoculation of the *Δbot2Δboa6#6* mutant and the wild type inoculated with yeast extract were similar at 24 hpi. We propose that the transcriptional response of *B. cinerea* to α-tomatine, released from damaged tomato cells, could serves as a marker for estimating the timing and the extent of tomato cell death during interaction with *B. cinerea*.

Differential expression of other SM biosynthetic genes

Except for the impact of yeast extract on the *B. cinerea* transcriptome, many DEGs that were identified in the *Δbot2Δboa6#6* mutant strain were different from those in the WT fungus. One of the reasons that could partially explain these differences is the removal of the two major phytotoxic SMs in the mutant. More than 40 gene clusters for the biosynthesis of polyketides, terpenes, nonribosomal peptides and alkaloids were identified in the *B. cinerea* genome (Collado & Viaud, 2015). It is unknown whether transcriptional upregulation of alternative SM biosynthetic genes in the mutant (or the downregulation in the WT) is mediated by the changes in intracellular levels of farnesyl pyrophosphate and acetyl-CoA, that serve as substrates for the BOT2 and BOA6 enzymes, respectively. Nevertheless, more SM biosynthetic genes (except for BOT and BOA) showed upregulation in *Δbot2Δboa6#6* than in WT B05.10 in the presence of yeast extract. For example, two sesquiterpene cyclase genes (*Bcstc4* and *Bcstc7*) and two polyketide synthase genes (*Bcpks7* and *Bcpks11*) were upregulated in the mutant by addition of yeast extract at 16 hpi, while only the *Bcpks7* gene was also upregulated in the WT fungus at the same time point. Besides, the *Bcpks14* gene was up-regulated in the mutant by adding yeast extract at 24 hpi, while the same gene was downregulated in the WT at 24 hpi. These findings indicate that the production of BOT and/or BOA may suppress (or delay) the biosynthesis of other SMs. However, the chemical structures and biological functions of the products of these clusters remain to be identified, and it is also uncertain whether the enzymes encoded by these genes catalyze the rate-limiting step in the biosynthetic pathway.

Attempts to restore compatible interaction in absence of yeast extract by overexpression of CDIPs

The WGCNA analysis identified three modules ("lightpink4", "bisque4" and "ivory") that were computationally associated with the compatible interaction (Figure 3), and contained several genes encoding previously identified *B. cinerea* CDIPs. Especially the expression levels of the CDIP-encoding genes in module "ivory" were increased by addition of yeast extract in both WT B05.10 and *Δbot2Δboa6#6*. Based on this finding, we considered that the gain of virulence of *Δbot2Δboa6#6* by addition of yeast extract to the inoculum was possibly facilitated by the higher production levels of CDIPs that might compensate for the absence of the cell death-inducing activities from BOT and BOA. The virulence assays that assessed the virulence of *Δbot2Δboa6#6*, 12xbb, 12xpg and 18x (Figure 1), not only showed that BOT and BOA play a prominent role in fungal virulence among the 18 CDIMs, but also provided additional information to select candidate genes for such a compensatory mechanism. We speculated that BcSSP2 may have a stronger impact on fungal virulence than the other 15 CDIPs as it was the only gene that was deleted in the 18x mutant but functional in the 12xbb and 12xpg mutants, while at the same time being induced by yeast extract in the inoculation medium. For this reason, we generated *ΔΔ-OEssp2* transformants and as controls we also generated mutants *ΔΔ-OEnep2, ΔΔ-OExyn11A* and *ΔΔ-OEpg1* to overexpress other members of the ivory module. Neither of these genes could, individually, restore the virulence of *Δbot2Δboa6#6* in the absence of yeast extract, which can be explained by three hypotheses. Firstly, additional single (as yet unknown) CDIMs from the ivory module are involved in stimulating primary lesion expansion and thereby overcome the lack of BOT and BOA production. Secondly, multiple previously described CDIPs might be jointly involved in restoring pathogenicity of the *Δbot2Δboa6#6* mutant via synergistic action. To validate this hypothesis, it may be useful to generate overexpression mutants in which multiple genes are overexpressed, either by using strong constitutive promoters or by identifying a TF that specifically governs the expression of genes in the ivory module and generating a transformant expression a constitutively active form of such a TF. At present, it is unclear which TF(s) regulate the yeast inducible expression of CDIPs, but a recent paper by Olivares-Yañez et al. (2021) may help to identify TFs that control the expression of virulence factors. Lastly, considering that the successful infection of a host by *B. cinerea* requires certain milestones to be achieved by the fungus at specific time points, *B. cinerea* should induce host programmed cell death (PCD) at a proper intensity and timing. As proposed by Veloso and van Kan (2018), the early phase of the *B. cinerea* – host interaction resembles a "biotrophic infection" (8-16 hpi), during which the fungus needs to avoid PCD without triggering plant defense responses in order to permit the biotrophic colonization of

the fungus. Therefore, we hypothesize that only certain modes of action for inducing PCD at a certain time period could help *Δbot2Δboa6#6* to break through the critical point and further cause expanding lesions. When overexpressing a gene with a strong promoter (e.g., the oliC promoter used in this study), the gene would be expressed at high level from the moment of germination of the conidia on the host surface. This would lead to CDIP accumulation during the "biotrophic stage" of the fungus, which would prematurely induce host PCD and thereby restrict the invasion of *B. cinerea*. In order to test this hypothesis, we could overexpress such gene(s) encoding PCD-inducing molecules in the WT B05.10 background and check whether these transformants trigger host resistance and the invasion of the fungus would be prohibited.

Summary and future perspectives

Transcriptomic analysis supported by RNA-seq technology and versatile bioinformatic tools has become a popular tool to study plant-microbe interactions. However, the massive amount of information may obscure interpretation of the data and prevent researchers from grasping all relevant biological aspects of the story. In this study, we largely focused on the relationship between different CDIMs in *B. cinerea* and their roles in fungal virulence, especially when selecting genes for experimental validation after examining the output of computational analyses. This dataset contains immense number of DEGs and interesting co-expressed gene modules in the fungus that could not all be discussed in this chapter. Further in depth analyses may reveal genes that will be useful for exploring their contribution to fungal virulence and their role in the transition from incompatibility to compatibility. Moreover, we should also analyze in depth the host response to the *Δbot2Δboa6#6* mutant and the WT fungus (inoculated without yeast extract), as well as its response to the *Δbot2Δboa6#6* mutant (inoculated without and with yeast extract). Insights in the pathways and mechanisms that tomato activates to achieve complete restriction of primary lesion outgrowth may on the long run assist in rational strategies to improve tomato resistance to *B. cinerea*.

Materials and Methods

Plant and fungal materials and their growth conditions

B. cinerea strains used and generated in this study are listed in Table 2. All *B. cinerea* strains were grown and conidia were harvested as described in Qin et al. (2023) (Chapter 2). *S. lycopersicum* cv. Moneymaker plants were grown and compound leaves were excised as described in Chapter 2.

Inoculation assays and in vitro cultures of *B. cinerea* for RNA sequencing

The media used were Gamborg B5 + vitamins (Duchefa, Haarlem, NL) and yeast extract (Oxoid, UK). *B. cinerea* conidia were diluted in two types of modified Gamborg B5 media (- yeast extract = Gamborg B5, 25 mM glucose, 10 mM potassium phosphate, pH 6.0; and + yeast extract = Gamborg B5, 25 mM glucose, 10 mM potassium phosphate, 0.1 % yeast extract, pH 6.0) to a final density of 1000 conidia/µl. The conidial suspension was pre-incubated on a rolling bench for one hour before being used for inoculation on plants or *in vitro* cultures. For disease assays, each leaf half of the adaxial surface of *S. lycopersicum* detached leaves was inoculated with 3-4 droplets containing 2 µl of the inoculum per droplet. The inoculated detached leaves were incubated in a plastic tray with a transparent lid (20x40x10 cm) in the lab and disease symptoms were scored at 3 days post inoculation (dpi). The number of expanding lesions (lesion diameter > 2mm) and non-expanding lesions (lesion diameter ≤ 2mm) were counted for calculating disease incidence (= the number of expanding lesions/the total number of inoculations). The diameters of expanding lesions were measured by a digital caliper and leaves were photographed by a digital camera. Statistical analyses were performed and bar charts generated using GraphPad Prism software. Details for the statistics and charts are described in figure legends.

In order to sample tomato leaves for RNA-seq, the adaxial surface of *S. lycopersicum* detached leaves was inoculated in six to eight circular areas, and each area included five droplets containing 2 µl of the inoculum per droplet. Four leaflets of one compound leaf were inoculated, and one leaflet was sampled at each time point (t = 0, 12, 16 and 24 hours post inoculation (hpi)). Tomato leaves were mock-inoculated with the -yeast extract medium and collected at 0, 12, 16 and 24 hpi. Eight ml of *B. cinerea* conidia suspensions in two different media (- / + yeast extract) were pipetted on glass petri-dishes (diameter = 90 mm) and incubated in a plastic tray with a transparent lid (20x40x10 cm) in the lab, and fungal tissue was sampled at 0, 12, 16 and 24 hpi for *in vitro* samples. Three biological replicates were collected for all infected and mock-inoculated tomato leaf samples (Supplementary Table S1). Two biological replicates were collected for *B. cinerea in vitro*

culture samples (Supplementary Table S1). All biological samples were freeze-dried and mRNA was extracted using the Maxwell® 16 LEV Plant RNA Kit (Promega).

Table 2. *B. cinerea* strains used in this study.

***B. cinerea* strain**	**Recipient**	**Description**	**Origin/Reference**
B05.10	-	wildtype *B. cinerea* isolate	van Kan et al. (2017)
Δbot2#1	B05.10	*Bcbot2* knockout mutant	Leisen et al. (2020)
Δboa6#1	B05.10	*Bcboa6* knockout mutant	Dalmais et al. (2011)
Δbot2Δboa6#6 (ΔΔ)	B05.10	*Bcbot2* and *Bcboa6* double knockout mutant	Leisen et al. (2020)
12xbb	B05.10	*Bcbot2, Bcboa6, Bcspl1, Bcnep1, Bcnep2, Bcxyn11A, Bchip1, Bcxyg1, Bcplp1, Bcieb1, Bcxyl1* and *Bcgs1* were knocked-out	Leisen et al. (2022)
12xpg	B05.10	*Bcpg1, Bcpg2, Bcspl1, Bcnep1, Bcnep2, Bcxyn11A, Bchip1, Bcxyg1, Bcplp1, Bcieb1, Bcxyl1* and *Bcgs1* were knocked-out	Leisen et al. (2022)
18x	B05.10	*Bcbot2, Bcboa6, Bcpg1, Bcpg2, Bcspl1, Bcnep1, Bcnep2, Bcxyn11A, Bchip1, Bcxyg1, Bcplp1, Bcieb1, Bcxyl1, Bcgs1, Bcssp2, Bccfem1, Bccdi1* and *Bccrh1* genes were knocked-out	Hahn (2022), 31st Fungal Genetics Conference
ΔΔ-OEssp2#10/ #55	*Δbot2Δboa6#6*	*Bcssp2* was overexpressed with an oliC promoter, independent transformants *#10* and *#55* were tested for virulence	this study
ΔΔ-OEpg1#18 /#22	*Δbot2Δboa6#6*	*Bcpg1* was overexpressed with an oliC promoter, transformant *#22* was tested for virulence	this study
ΔΔ-OEnep2#2/#4	*Δbot2Δboa6#6*	*Bcnep2* was overexpressed with an oliC promoter, transformant *#4* was tested for virulence	this study
ΔΔ-OExyn11A#10/#22	*Δbot2Δboa6#6*	*Bcxyn11A* was overexpressed with an oliC promoter, both transformants showed growth retardation *in vitro* and thus were not tested for virulence	This study

RNA sequencing and identification of differentially expressed genes (DEGs)

Strand-specific libraries of the RNA samples were constructed, followed by paired-end sequencing with a DNBseq platform (BGI Tech Solutions, Hongkong), with a read depth of 20-50 Million as described in Supplementary Table S1. Mapping and quantifying gene transcripts from sequenced RNA-seq reads of all samples were performed using Kallisto (v0.44.0) (Bray et al., 2016), with a 100 bootstrap value. The principal component analysis (PCA) was conducted as transcriptome samples clustered by the ggplot2 package in R. The R package Sleuth (v0.30.0) was used for differential expression analysis (Pimentel et al., 2017). DEG analysis was done with default settings, removing all genes that do not have at least 5 estimated read counts in at least 47% of all the samples. Genes were considered differentially expressed if they displayed between two samples a fold change ≥ 2 with an adjusted p-value ≤ 0.05 (Benchamini–Hochberg method). UpSet plots were generated using the R packages UpSetR (Conway et al., 2017).

Network construction and co-expression analysis

A total of 80 samples were used for constructing co-expression analysis using the R package WGCNA (v1.69) (Langfelder & Horvath, 2008). The normalized gene expression matrix was imported into WGCNA to construct co-expression modules. The gene expression matrix was searched for a suitable soft threshold to build gene networks using a scale-free topology model (N. Wang et al., 2018). The scale-free network obtained by power processing at β = 13, resulted in an adequate fit with r^2 = 0.85 with average connectivity approaching 0. Therefore, β = 13 was used to construct a scale-free network. The adjacency matrix was transformed into a topological overlap matrix (TOM) to evaluate the correlation between expression profiles of the genes (N. Wang et al., 2018). The dissimilar topological matrix (dissTOM= 1-TOM) was used to carry out the matrix clustering and module partitioning by the dynamic shearing algorithm. The minimum number of elements in a module was 30 (minModule Size=30), and the threshold for merging of a similar module was 0.25 (CutHeight = 0.25) (Supplementary Figure S4). Module eigengenes (MEs) were used to calculate the correlation coefficients to the traits to identify the biologically significant modules. The Pearson correlation coefficient of the corPvalueStudent () function was used to calculate the correlations between the infection and yeast extract matrix and the module feature gene matrix to obtain the p-values.

Functional analysis of module genes

Gene Ontology (Ashburner et al., 2000) (GO) enrichment analysis provides all GO terms that are significantly enriched in a module, as compared to the genome background, and filters the module genes that correspond to biological processes or molecular functions. All genes

in a module were mapped to GO terms in the Gene Ontology database (http://www.geneontology.org/), gene numbers were calculated for every term, and significantly enriched GO terms in modules were defined by hypergeometric distribution algorithm. The FDR was set to ≤ 0.05 as a threshold. GO terms meeting this condition were defined as significantly enriched GO terms in modules. The GO enrichment was visualized using ggplot2 (R package) (Wickham et al., 2016).

***B. cinerea* transformation by CRISPR/Cas9-mediated approach**

B. cinerea mutant strains used in this study were generated by CRISPR/Cas9-mediated transformation with minor modification from (Leisen et al., 2020a). The primers for synthesis of sgRNAs and for amplification of donor templates are provided in Supplementary Table S2. The donor templates were amplified from reconstructed pNDH-OGG vector harboring *Bcssp2*, or pNAN-OGG vector harboring *Bcpg1* or *Bcnep2*. The original pNDH-OGG and pNAN-OGG plasmids were obtained from Schumacher (2012). *Bcssp2, Bcpg1* and *Bcnep2* were amplified from WT B05.10 genomic DNA by PCR using Phusion Hot Start II DNA Polymerase (Thermo Scientific™) and then cloned into pNDH-OGG or pNAN-OGG by replacing the GFP cassette using the ClonExpress MultiS One Step Cloning Kit (Vazyme). *Bcssp2* gene was overexpressed by replacing the *BcniaD* gene in the *Δbot2Δboa6#6* recipient strain via homologous recombination upon cleavage of Cas9 at *BcniaD* to obtain *ΔΔ-OEssp2* transformants, while *Bcpg1* or *Bcnep2* was overexpressed by replacing *BcniiA* gene to obtain *ΔΔ-OEpg1* or *ΔΔ-OEnep2* mutants. Molecular characterization of the transformants was performed as described in Qin et al. (2023) using primers shown in Supplementary Table S2.

Supplementary materials

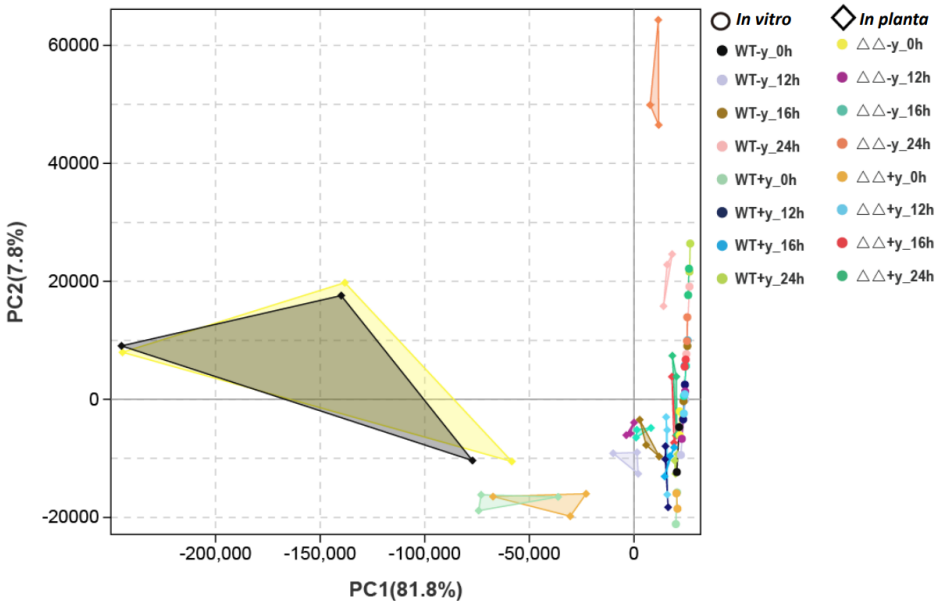

Supplementary Figure S1. The PCA plot of the RNA-seq dataset shows the differences (distances) between all samples generated in this study, according to gene expression levels. Each circular dot indicates an *in vitro* sample, and each squared dot indicates an *in planta* sample. Different colors represent different fungal strains (WT B05.10 and *Δbot2Δboa6#6* (WT and ΔΔ)), different media (- and +y), and different timepoints (0, 12, 16 or 24 hpi).

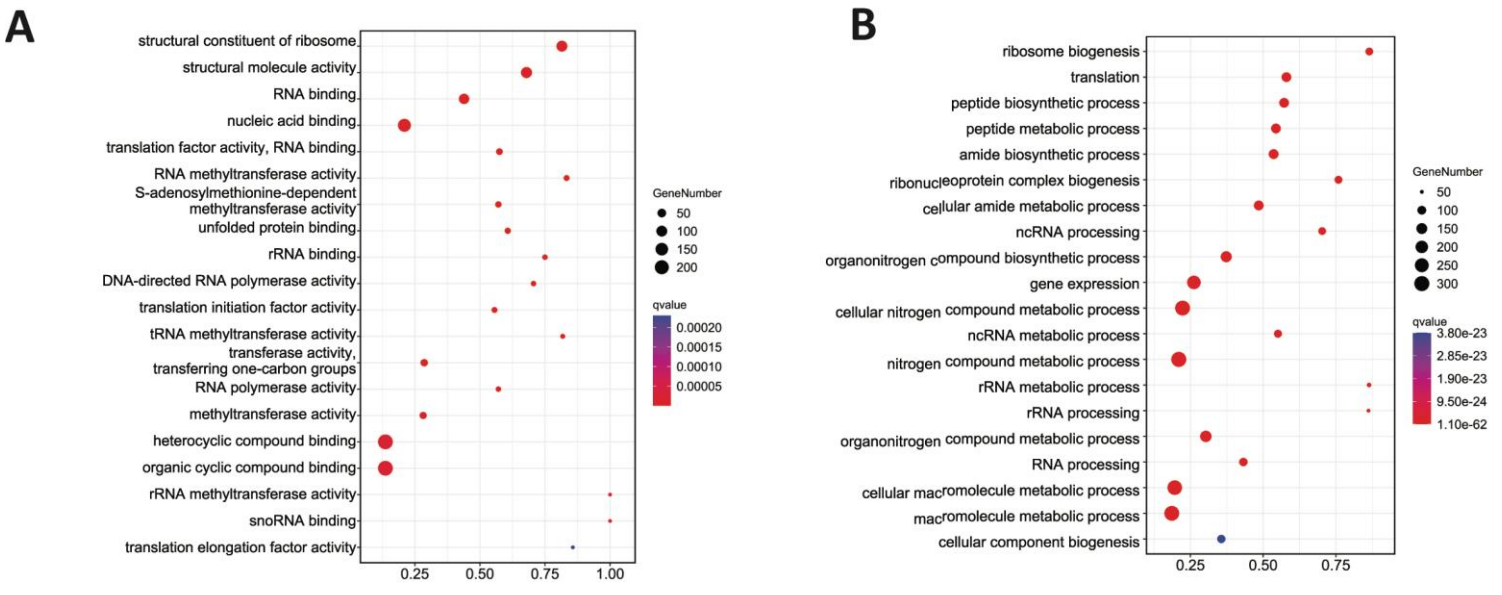

Supplementary Figure S2. GO enrichment analysis for genes that are up-regulated (+yeast vs -yeast) both in WT and mutant at 24 hpi. **(A)** Molecular function. **(B)** Biological process.

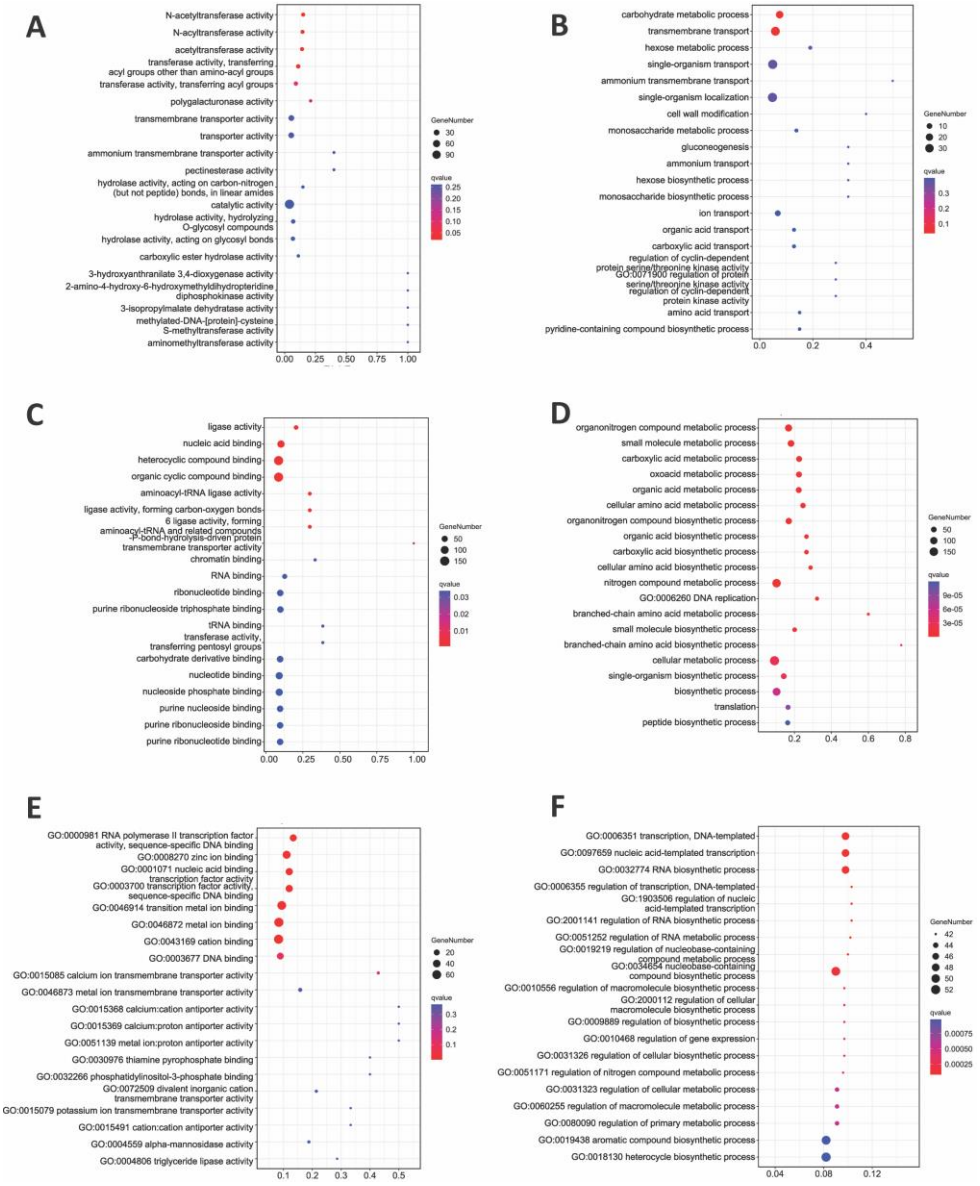

Supplementary Figure S3. GO enrichment analysis for DEGs (+yeast vs -yeast) that are unique in WT **(A, B)** and mutant **(C, F)** at 24 hpi. WT only contains enriched GO terms in up-regulated DEGs **(A, B)**, whereas both up- **(C, D)** and down- **(E, F)** regulated genes of mutant contain enriched GO terms. **(A, C, E)** Molecular function. **(B, D, F)** Biological process.

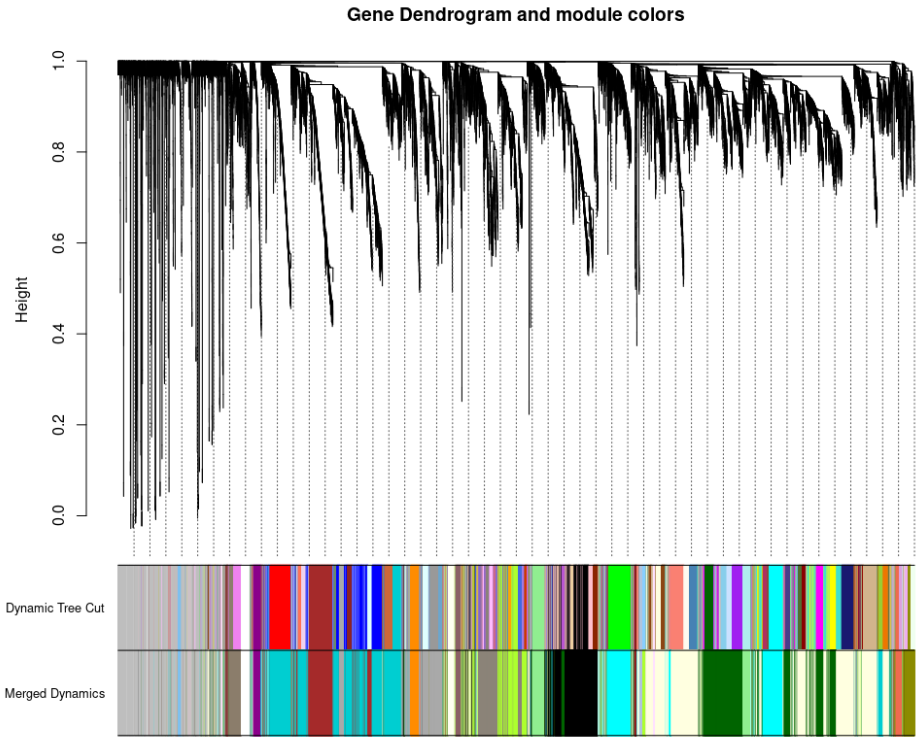

Supplementary Figure S4. Dendrogram of gene co-expression network. In the top part of the figure, a dendrogram of the filtered set of genes is shown, constructed using the topological overlap between genes. Below the dendrogram, the top colored bar indicates the co-expression modules produced by the dynamic tree cutting algorithm, and the bottom colored bar indicates the merged co-expression modules.

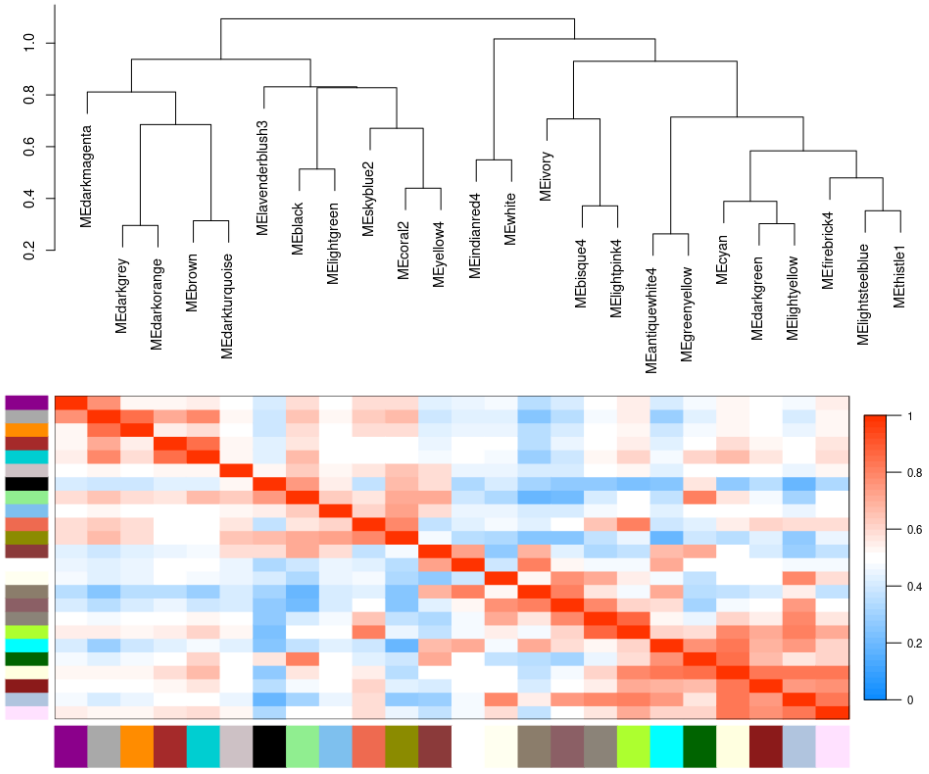

Supplementary Figure S5. Module significance correlation based on the Pearson correlation.

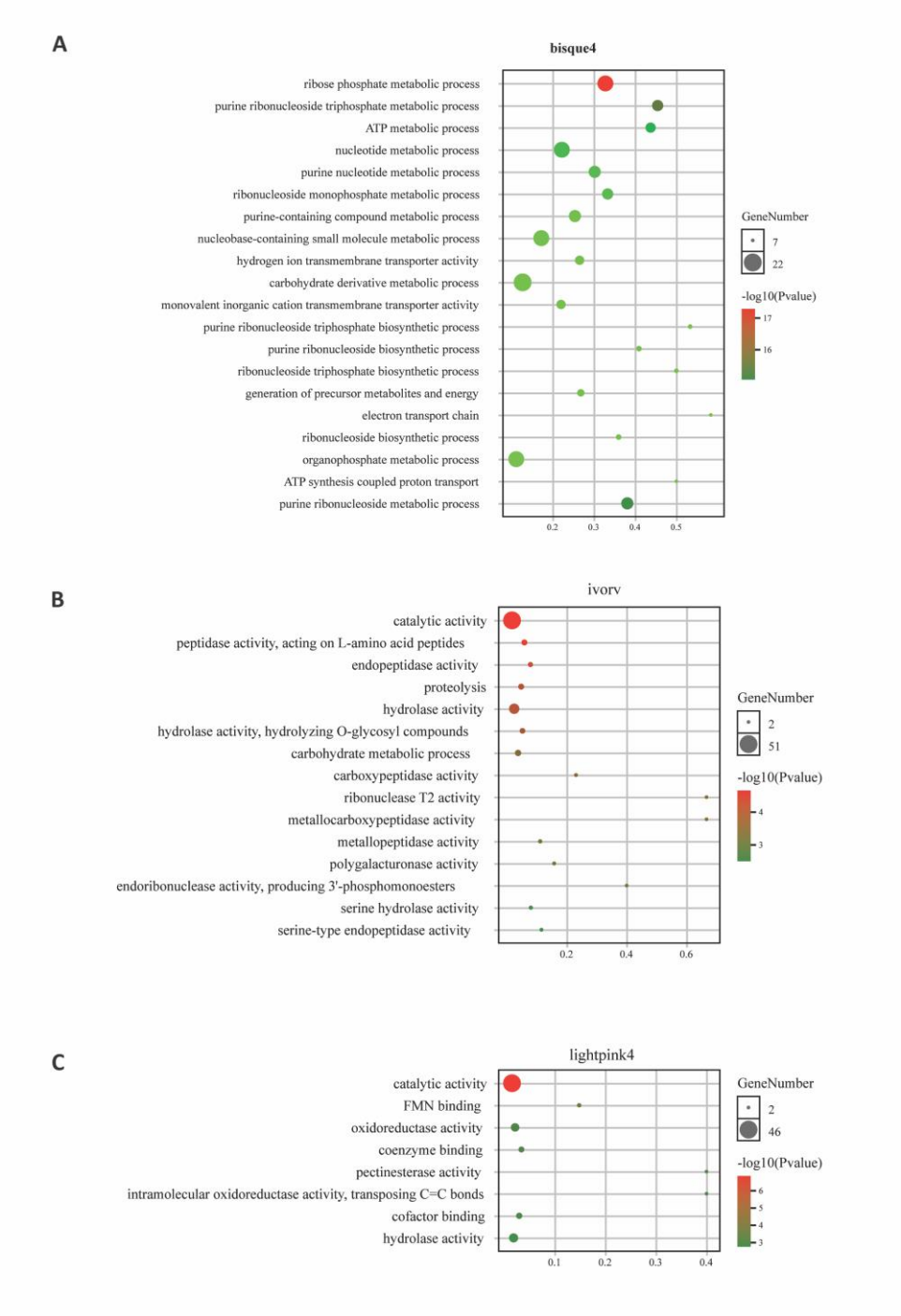

Supplementary Figure S6. GO enrichment analysis of three gene modules that are positively corrected to compatible interaction between *B. cinerea* and tomato.

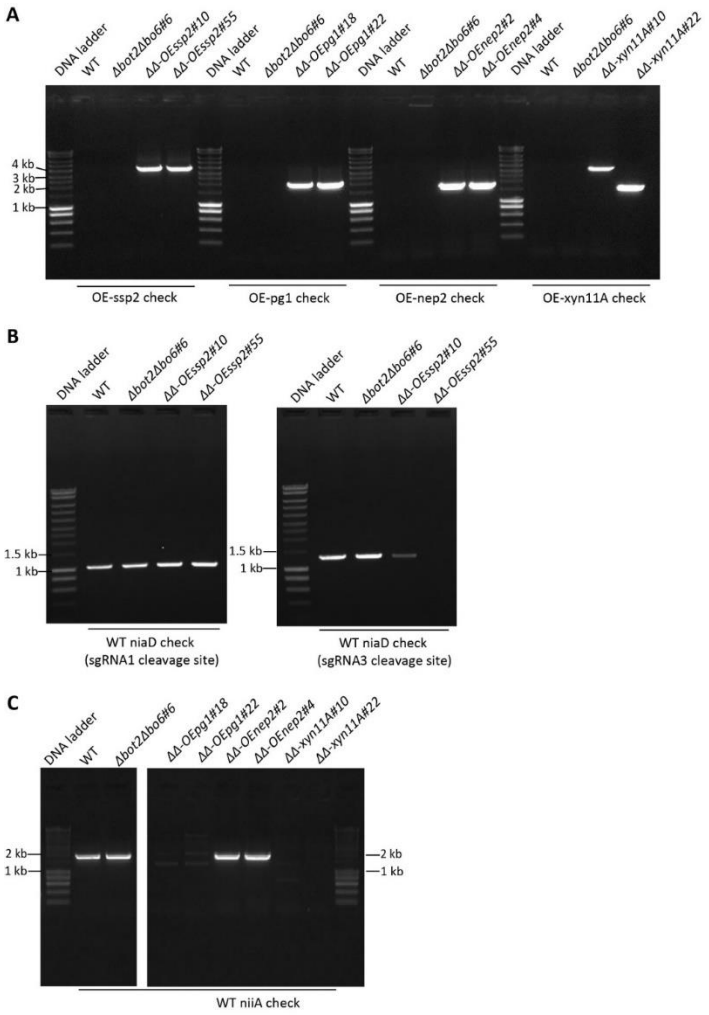

Supplementary Figure S7. Molecular characterization of overexpression mutants *ΔΔ-OEssp2#10, ΔΔ-OEssp2#55*, *ΔΔ-OEpg1#18*, *ΔΔ-OEpg1#22, ΔΔ-OEnep2#2, ΔΔ-OEnep2#4, ΔΔ-OExyn11A#10* and *ΔΔ-OExyn11A#22*. WT B05.10 and *Δbot2Δboa6#6* double mutant were used as controls. **(A)** PCR results confirmed that the overexpression of *ssp2*, *pg1*, *nep2* and *xyn11A* were successful, and two independent transformants for each contrast were obtained. The OE*ssp2*-donor-template was inserted ectopically inside of the *niaD* gene via non-homologous end joining (NHEJ), instead of replacing the whole *niaD* gene via homologous recombination. Similar situation happened to the *ΔΔ-OExyn11A#10* transformant. The other transformants were obtained via replacing the *niiA* gene by corresponding overexpression-donor-template. **(B)** The insertion of OE*ssp2*-donor-template by NHEJ was confirmed to be located at the sgRNA3 cleavage site for *ΔΔ-OEssp2#55* which was a homokaryotic transformant. *ΔΔ-OEssp2#10* was either a heterokaryon or the ectopic insertion location cannot be confirmed by these PCR. (C) *ΔΔ-OEpg1#18*, *ΔΔ-OEpg1#22, ΔΔ-OExyn11A#10* and *ΔΔ-OExyn11A#22* were confirmed to be homozygous transformants, while *ΔΔ-OEnep2#2* and *ΔΔ-OEnep2#4* were heterokaryons. Names of the *B. cinerea* strains are indicated above each DNA gel picture, and the aims for the primer combinations are indicated below the gel.

Supplementary Table S1. Overview of all samples in this study

Sample name	**Strain**	**Inoculation medium**	***In planta*** (# of replications)				***In vitro*** (# of replications)			
			0 h	12 h	16 h	24 h	0 h	12 h	16 h	24 h
WT-y	B05.10	- y[1]	3	3	3	3	2	2	2	2
WT+y	B05.10	+ y[2]	3	3	3	3	2	2	2	2
ΔΔ-y	*Δbot2Δboa6#6*	- y	3	3	3	3	2	2	2	2
ΔΔ+y	*Δbot2Δboa6#6*	+ y	3	3	3	3	2	2	2	2

[1] Gamborg B5, 25 mM glucose, 10 mM potassium phosphate, pH 6.0; [2]Gamborg B5, 25 mM glucose, 10 mM potassium phosphate, 0.1 % yeast extract, pH 6.0

Supplementary Table S2. Primers used in this study

Primer name	sequence (5'-3')	Description
BcNiaDsgRNA1	AAGCTAATACGACTCACTATAGGAGGAAAACGATATTCGACGAGTTTTAGAGCTAGAAATAGCAAG	To synthesize sgRNAs targeting at BcniaD gene, both sgRNA1&3 were used for generating transformants to overexpress Bcssp2 at BcniaD locus
BcNiaDsgRNA3	AAGCTAATACGACTCACTATAGGATGGATGGCCATGAATTCGTGTTTTAGAGCTAGAAATAGCAAG	
sgRNA_BcNiiA1	AAGCTAATACGACTCACTATAGGATCTGCCATCTCGATCCCAGGTTTTAGAGCTAGAAATAGCAAG	To synthesize sgRNAs targeting at BcniiA gene, both sgRNA1&2 were used for generating transformants to overexpress Bcssp2 at BcniaD locus
sgRNA_BcNiiA2	AAGCTAATACGACTCACTATAGGTAAAAATCTACCGATCAGGGGTTTTAGAGCTAGAAATAGCAAG	
Bcssp2_NcoI_F	TCACAATCGATCCAAccATGGTCCGCATCTCCTCCATCGTC	To amplify the Bcssp2 gene with overhangs that can be cloned into pNDH-OGG vector through NcoI (ccATGG) - NotI (gcggccgc) sites.
Bcssp2_NotI_R	ATCTACATACGCTAagcggccgcTTACTGCTTGTAACATGGGGTACGAT	
Nep2_NcoI_F	TCACAATCGATCCAAccATGGTTGCCTTCTCAAAATCATTACAGCT	To amplify Bcnep2 gene with overhangs that can be cloned into pNAN-OGG vector through NcoI (ccATGG) - NotI (gcggccgc) sites.
Nep2_NotI_R	ATCTACATACGCTAagcggccgcCTAGAAAGTAGCCTTCGCAAGATTGTCTG	
Bcpg1_NcoI_F	TCACAATCGATCCAAccATGGTTCAACTTCTCTCAATGGCCTC	To amplify Bcpg1 with overhangs that can be cloned into pNAN-OGG vector through NcoI (ccATGG) - NotI (gcggccgc) sites; Bcpg1_NotI_R was also used together with primer pNDH-PoliC-Fw to check whether the cloning of Bcpg1 gene into pNAN-OGG vector is successful
Bcpg1_NotI_R	ATCTACATACGCTAagcggccgcTTAACACTTGACACCAGATGGGAGACC	
Xyn11A_NcoI_F	TCACAATCGATCCAAccATGGTTTCTGCATCTTCCCTCCTC	To amplify Bcxyn11A gene with overhangs that can be cloned into pNAN-OGG vector through NcoI (ccATGG) - NotI (gcggccgc) sites.
Xyn11A_NotI_R	ATCTACATACGCTAagcggccgcTTAAGAAACAGTGATGGAAGCGGAACCA	

pNDH-PoliC-Fw	GCTGTGGAGCCGCATTCCCG	Primer in oliC promoter, use it together with other primers to check whether the cloning of target gene into pNDH-OGG/pNAN-OGG vector is successful
pNDH-ssp2-Rv	AGCTGTGAAAGCACTCGCGC	Use it together with primer pNDH-PoliC-Fw to check whether the cloning of Bcssp2 gene into pNDH-OGG vector is successful
Nep2_RT_rev	GGCTCGTCCTTTGGCATGTAC	Use it together with primer pNDH-PoliC-Fw to check whether the cloning of Bcnep2 gene into pNAN-OGG vector is successful
BcXyn11A_rv	CGTACGCTTGCTAGTACGGAC	Use it together with primer pNDH-PoliC-Fw to check whether the cloning of Bcxyn11A gene into pNAN-OGG vector is successful
OE-dt-pNDH-3'NiaD	GCAGTTCAATGGCAAAAACTACAAC	To amplify the donor template for overexpressing Bcssp2 from the re-constructed pNDH-OGG plasmid containing Bcssp2
OE-dt--pNDH-5'NiaD	CATATCAATTGTGTCTCGAGATCGGAAA	
pNAN_bcniiA-5'_FW	TCATTGAGGCTCTGGTGAACAGTTCA	To amplify the donor template for overexpressing Bcnep2/Bcxyn11A/Bcpg1 from the re-constructed pNAN-OGG plasmid containing Bcnep2/Bcxyn11A/Bcpg1
pNAN_bcniiA-3'_RV	CGCTAGTATCAATGAGATCATAGAGCTAATGC	
pNDH-ssp2-Rv	AGCTGTGAAAGCACTCGCGC	To screen the integration of donor template at NiaD site in ΔΔ-OEssp2 transformants, the primer pNDH-ssp2-Rv is in the donor template, and NiaD_3'_screenRv is outside of the flanks of the donor template.
NiaD_3'_screenRv	GATACTATATTCAAACATCCTCTCTCCC	
BcniaD_WT_sgRNA1 site	ACCTTCGTCGAATATCGTTTTCCTCT	To check if ΔΔ-OEssp2 transformants are homokaryons, and if the OEssp2 donor template is inserted at the cleavage site of sgRNA1
BcniaD_midRv	GCTAGGAGCTGCGGTAACAA	

BcniaD_midFw	CGGAAACCGCCGTAAAGAAC	To check if ΔΔ-OEssp2 transformants are homokaryons, and if the OEssp2 donor template is inserted at the cleavage site of sgRNA3
BcniaD_WT_sgRNA3 site	GATGGCCATGAATTCGTCGGTG	
Bcniia_screenFw	CTGCTAGACAGATTGTGGCTGGT	To screen the integration of donor template at NiiA site in the ΔΔ-OEpg1/nep2/xyn11A transformants, the primer Bcpg1/Nep2/Xyn11A_NcoI_F is inside of the corresponding donor template, and Bcniia_screenFw is outside of the flanks of the donor template.
Bcpg1_NcoI_F	TCACAATCGATCCAAccATGGTTCAACTTCTCTCAATGGCCTC	
Nep2_NcoI_F	TCACAATCGATCCAAccATGGTTGCCTTCTCAAAATCATTACAGCT	
Xyn11A_NcoI_F	TCACAATCGATCCAAccATGGTTTCTGCATCTTCCCTCCTC	
Bcniia_WT-Fw	GGAATTAAATGCGCTGAACGCG	To check if ΔΔ-Bcnep2/Bcxyn11A/Bcpg1 transformants are homokaryons in which the WT BcniiA is no longer present, primers are inside of the flanks of the donor template
Bcniia_WT-Rv	GTCGAAGAAACTCCCCACTAGCTC	

The following Supplementary Data is available to be downloaded from the "Supplementary materials_PhD thesis_Qin(2023).zip" file, and thus only the legend is shown below.

Supplementary Data S1. Genes encoding secreted proteins in three modules are positively correlated to the compatible interaction. Sheet 1 (named "Summary") contains an overview of the total number of genes encoding secreted proteins in each module resulted from the GGCNA analysis. Sheet 2-4 contains the gene list for module "lightpink4", "bisque4", and "ivory", respectively.

Chapter 7

Identification of Arabidopsis genes involved in the response to the *Botrytis cinerea* phytotoxic metabolite botrydial

Si Qin[1], Sabine de Graauw[1], Sanna Henriquez[1], Xiaoqian Shi-Kunne[1], Haris Spyridis[1], Henriek Beenen[1], Inmaculada Izquierdo-Bueno[2], Isidro González Collado[2], Joost Keurentjes[3] and Jan A. L. van Kan[1]

[1]Laboratory of Phytopathology, Wageningen University, Netherlands

[2]Departamento de Química Orgánica, Facultad de Ciencias, Universidad de Cádiz, Spain

[3]Laboratory of Genetics, Wageningen University, Netherlands

Abstract

Plants naturally possess genetic resources conferring resistance and susceptibility to pathogens. To cope with the notorious necrotrophic pathogen *Botrytis cinerea,* which is the causal agent of the grey mold disease, introducing resistance (*R*) genes and abandoning susceptibility (*S*) genes in host plants open up a dual path for breeding against the pathogen. It has been studied in the previous chapters that the phytotoxic secondary metabolite botrydial (BOT) produced by *B. cinerea*, which can trigger host programmed cell death, has a significant contribution to the fungal virulence, especially on Arabidopsis. It is presumed that a host gene conferring sensitivity to BOT would also function as an *S* gene to the fungus. In this study, we used BOT as a tool to explore natural variation in resistance against *B. cinerea* by unraveling BOT-(in)sensitivity genes or genetic loci in Arabidopsis, with the application of two different forward genetic approaches in parallel. Interestingly, from 36 candidate genes selected from a genome-wide association study (GWAS), we identified four genes encoding three positive and one negative player in BOT-sensitivity. Functions of these genes were demonstrated by altered cell death intensity responding to BOT treatment in mutant lines of each individual gene. The Arabidopsis mutant of a *serine/threonine kinase* (*STK*) gene that functions as a suppressor in the BOT-triggered cell death also showed increased host susceptibility to *B. cinerea*, indicating that *STK* is an *R* gene against the fungus. Inversely, the genes that positively participate in the cell death response to BOT would likely function as *S* genes to *B. cinerea*. Our work provides a deeper understanding of the molecular mechanisms underlying BOT-induced programmed cell death in host plants. Moreover, the characterized novel candidate genes in this study can (potentially) function as *R/S* genes to *B. cinerea*, which offers prospects in crop protection against grey mold disease.

Introduction

Botrytis cinerea has been ranked as the second most important plant pathogenic fungus from an economic and scientific perspective (Dean et al., 2012). This fungus can infect more than a thousand plant species and causes gray mould disease both in the pre- and post-harvest period, leading to an annually worldwide economic loss of more than $1 billion (Dean et al., 2012). Therefore, effective control of *B. cinerea* is necessary for optimization of crop production and storage. A sustainable way to control this fungal disease is to breed for resistant plants, either by introducing resistance (*R*) genes or by abandoning susceptibility (*S*) genes in the host plants. Forward genetics has been exploited to excavate genes or quantitative trait loci (QTL) associated with host resistance to *B. cinerea* (Anuradha et al., 2011; Coolen et al., 2019; Davis et al., 2009; Denby et al., 2004; Rowe & Kliebenstein, 2008), although none of the identified genes or QTL functions as a major *R* gene against this disease. In recent years, genes or QTL conferring increased host susceptibility to *B. cinerea* have also been identified (Audenaert et al., 2002; Bessire et al., 2007; Davis et al., 2009; Fiil & Petersen, 2011; Sun et al., 2017). Notably, the *Botrytis*-resistant 1 (*bre1*) mutant of *Arabidopsis thaliana* (Arabidopsis) showed a complete arrest of invasion by *B. cinerea*. *A. thaliana* BRE1 encodes a long-chain acyl-CoA synthetase2 (LACS2) that is essential for the biosynthesis of cutin (Bessire et al., 2007). This finding encouragingly suggests that deletion of particular *S* genes could provide a more complete resistance to *B. cinerea* than utilizing individual *R* genes. In order to discover *S* genes, a promising strategy is to identify plant targets for virulence factors of *B. cinere*a, as the presence of plant targets can facilitate the infection of the pathogen. Conversely, plant components that act antagonistically in the plant response to the fungal virulence factors may confer resistance to *B. cinerea*.

The necrotrophic pathogen *B. cinerea* employs several virulence factors to kill plant cells in order to consume nutrients from the host. Three groups of virulence factors play important roles in killing host cells: phytotoxic metabolites, phytotoxic proteins and reactive oxygen species (ROS) (Choquer et al., 2007b). One of the most well-studied phytotoxic metabolite of *B. cinerea* is the sesquiterpene botrydial (BOT), which plays a role in the full virulence of *B. cinerea* on different host species, especially on *A. thaliana* (Chapter 3). A *B. cinerea* mutant unable to produce BOT was almost non-virulent on leaves of *A. thaliana* (Chapter 3). Rossi et al. (2011) reported that application of BOT on *A. thaliana* could induce the expression of the *HYPERSENSITIVITY-RELATED 3* (*HSR3*) gene, callose deposition and the accumulation of ROS and phenolic compounds. Arabidopsis mutant lines which accumulate very little salicylic acid (SA) also showed lower sensitivity to BOT, while the jasmonic acid (JA)-insensitive mutant was more sensitive to BOT (Rossi et al., 2011). These observations

indicate that BOT can initiate programmed cell death (PCD) in the host and that the host response to BOT is mediated through SA/JA signaling pathways. However, the molecular basis of the PCD triggered by BOT in the host has not been revealed yet.

Evidence suggests that phytotoxic metabolites produced by plant pathogens can interact with plant targets to induce host cell death. A well-known example is the fungal cyclic peptide victorin and its corresponding sensitivity locus in oat and Arabidopsis. Victorin is a host-selective toxin (HST) secreted by the fungus *Cochliobolus victoriae*, the causal agent of oat victoria blight disease. The dominant allele at the *Vb* locus confers victorin sensitivity and Victoria blight disease susceptibility in oats (Wolpert et al., 2002). In *A. thaliana*, the *LOV1* locus, encoding an intracellular coiled-coil nucleotide-binding site-leucine rich repeat (CC-NBS-LRR) receptor, confers sensitivity to victorin and susceptibility to *C. victoriae* (Lorang et al., 2007). Moreover, victorin physically interacts with thioredoxin h5 (TRXh5), which regulates the activity of NPR1 (a receptor of SA and the central regulator of systemic acquired resistance (SAR)) and is probably guarded by the LOV1 receptor, creating a victorin-TRXh5-LOV1 complex triggering host PCD (Gilbert & Wolpert, 2013; Wolpert & Lorang, 2016). Other modes of action for phytotoxic secondary metabolites from fungal pathogens have also been reported. For instance, the HC-toxin produced by *C. carbonum* inhibits host histone-deacetylases and leads to H3 and H4 histone-hyperacetylation so that transcript levels of many genes are disturbed, which eventually results in host cell death, as demonstrated in maize (Broschla et al., 1995). Furthermore, T-toxin and PM-toxin secreted by *C. heterostrophus* (also known as *Bipolaris maydis*) and *Mycosphaerella zeae-maydis*, respectively, can directly bind to the mitochondrial protein URF13, leading to aberrant mitochondrial activity (Rhoads et al., 1995; Yun et al., 1998). Finally, the perylenequinone toxins cercosporin from *Cercospora spp*. and elsinochromes from *Elsinoë spp*. are able to react with oxygen to produce ROS in a light-dependent manner, inducing the peroxidation of plant membrane lipids (Daub & Briggs, 1983; Daub & Ehrenshaft, 2000; Daub et al., 2005).

The hypersensitive response (HR) induced upon binding of ligands by receptors can effectively restrict the invasion of biotrophic phytopathogens, whereas the cell death response would be advantageous to necrotrophs for taking up nutrients from their hosts, leading to host susceptibility (Govrin & Levine, 2000). Therefore, identification of the plant targets and signaling components, which participate in the PCD triggered by necrotrophic factors, is an obvious step in the exploration of *S* genes in the host. We hypothesize that plant components involved in the PCD signaling pathway activated by BOT, may lead to host sensitivity to BOT and susceptibility to *B. cinerea*. Mining the molecular mechanisms involved in BOT-induced PCD (or BOT-sensitivity) in the host plant thus might reveal novel *S* genes. In order to realize the goal, forward genetic screens that have been extensively

exploited in studies on plant-pathogen interactions can be applied to our study as well. For example, the previously mentioned *LOV1* gene was characterized by an initial screen with 433 ecotypes of *A. thaliana* which identified six accessions sensitive to victorin (Lorang et al., 2004), and a subsequent fine mapping with the F_2 population of a cross between a sensitive and an insensitive accession (Lorang et al., 2007). Similarly, the plant receptor for *B. cinerea* endopolygalacturonases, which induces cell death in a subset of *A. thaliana* accessions, was identified via a map-based cloning from an F2 progeny (Zhang et al., 2014). By analogy, it is anticipated that loci conferring BOT-sensitivity can be pinpointed by screening an *A. thaliana* population for their responses to BOT.

Here we report that BOT triggers a series of plant defense responses and activates PCD in the model plant species *A. thaliana*. We further explored natural variation in BOT-(in)sensitivity in *A. thaliana* by adopting two different forward genetic approaches in parallel. We performed a genome-wide association study (GWAS) on a population of 333 accessions, as well as a bulk segregant analysis (BSA) in an F_2 population of an experimental cross between two accessions which differed substantially in the BOT-sensitivity. Our work provides a number of candidate genes (and genomic regions) that are associated with the (in)sensitivity to BOT, which may function as potential *S* or *R* genes against *B. cinerea*.

Results

BOT induces immune responses and a SA mediated apoptotic-like PCD in *A. thaliana*

The toxicity of BOT to *A. thaliana* was assessed by applying droplets containing 30-1000 µM BOT (dissolved in 40% acetone) or control solution (40% acetone) on leaves of Col-0 plants. Necrotic lesions were observed on leaves with all concentrations of BOT at the site of application. Additionally, the intensity of chlorotic symptoms as well as the area displaying necrotic symptoms were dose-dependent (Figure 1A). In this study, the concentration of BOT that still exerted toxic effects on *A. thaliana* (30 µM) was much lower than a previously reported effective concentration range of 322-3220 µM (Rossi et al., 2011).

As BOT is considered to be an effector as discussed in Chapter 1, it is likely that it can induce a number of plant defense responses that resemble typical effector-triggered immunity (ETI). Plant defense responses associated with ETI not only include PCD but also earlier responses such as ROS burst and mitogen-activated protein kinase (MAPK) activation (Tsuda & Katagiri, 2010). ROS burst and MAPK activity assays with Col-0 leaves upon BOT treatment at sublethal concentrations triggered ROS burst in Col-0 at all tested BOT concentrations (1.5, 5 and 15 µM). Moreover, higher BOT concentration levels resulted in a more rapid and narrower temporal peak in the ROS-burst curve, albeit with similar magnitude (Figure 1B). Likewise, the MAPKs in *A. thaliana* (MPK6 and MPK3) were transiently activated to a high level 15 min after BOT treatment and the MAPK phosphorylation level decreased after 30 min (Figure 1C).

The BOT-triggered PCD is most likely mediated by SA/JA signaling, as BOT-induced necrotic symptom is reduced in SA-accumulation deficient mutants and enhanced in JA-insensitive mutants of *A. thaliana* (Rossi et al., 2011). Here we further evaluated the correlation between the BOT-induced PCD response and the SA signaling/SAR pathway by examining the BOT-sensitivity in an *A. thaliana* mutant that is deficient in the *NPR1* (*nonexpressor of PR genes 1*) gene. NPR1 is known to act as a receptor of SA and plays a master role in the activation of SA-dependent defense genes and SAR (Wu et al., 2012). NPR1 mutant plants (Table 1) displayed significantly lower sensitivity to BOT than wild type (WT) Col-0 plants (Figure 1D), in line with previously reported findings (Rossi et al., 2011).

Furthermore, we hypothesized that BOT may induce apoptotic-like PCD, which can be important for the initiation of necrotic lesions at the onset of *B. cinerea* infection (Veloso & van Kan, 2018). Plant apoptotic PCD is mediated by metacaspases (MCs) and the *A. thaliana* genome contains nine *MC* genes, including three Type-I *MC*s (*MC1-3*) and six Type-II *MC*s (*MC4-9*) (Tsiatsiani et al., 2011). Five *A. thaliana* lines, which have mutations in different *MC*

genes (*mc1#1, mc2#1, mc4#1, mc7#1* and *mc8#1*, respectively), were compared to the WT Col-0 accession for sensitivity to BOT. One of these matacaspase mutants (*mc1#1*) exhibited significant reduction in BOT-sensitivity compared to the WT Col-0 background (Figure 1E), in contrast to all other tested *MC* mutants (Table 1, Supplementary Figure S1A & Table S1).

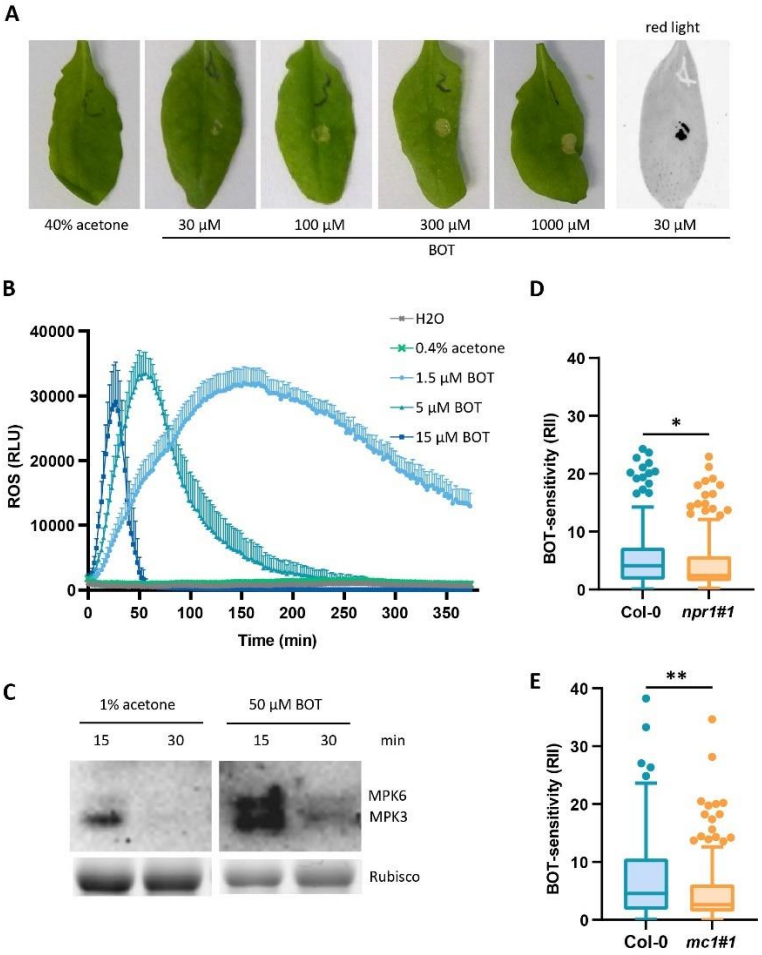

Figure 1. BOT triggers ROS burst and MAPK activation, and induces cell death in an NPR1- and MC1-dependent manner. (**A**) Necrotic symptom on Arabidopsis leaves, photographed on the 5th day after applying 4 µl droplets containing different concentrations of BOT (dissolved in 40% acetone) or control solution (40% acetone) using a digital camera under natural light. In addition, an image of red light emission that shows necrotic symptoms upon 30 µM BOT treatment is provided on the right side of the panel. (**B**) ROS burst over a 6 h period following application of different concentrations of BOT or controls (0.4% acetone and water) to leaf discs, quantified by relative luminescence units (RLU). The line chart shows mean RLU values with standard errors from 8 leaf discs at each time point in the measurement. The ROS burst assay was performed four times, with similar results. (**C**) Phosphorylation status of MPK6 and MPK3 at 15 and 30 min after infiltration of 50 µM BOT (dissolved in 1% acetone) or 1% acetone (as control), as detected in a western blot. The MAPK activation was repeated twice, with similar results. (**D**, **E**) Cell death quantification by red light emission in (**D**) *npr1#1* and (**E**) *mc1#1* mutant plants compared to WT Col-0 plants, represented by a Tukey box plot of data from ~ 160 BOT-treated leaves (40 plants) in two independent experiments. Each leaf was infiltrated with 50 µM BOT and the left side was infiltrated with 1% acetone, and the treated leaves were examined 5 days after BOT treatment. Relative integral intensity (RII) was quantified based on red light images and statistical analysis was performed by t-tests, resulting in significant differences that are indicated by asterisks (* $p < 0.05$ and ** $p < 0.01$).

Table 1. *A. thaliana* mutant lines used in this study, together with their corresponding candidate genes selected from the GWAS result or from literature.

Origin	Gene ID	Protein description**	Gene name	Mutant line #1***	Mutant line #2***
Literature & hypothesis	At1g64280	Impaired salicylic acid signaling	*NPR1*	*npr1* (Cao et al., 1997)	Salk_117100
	At1g02170	Metacaspase 1	*MC1*	Salk_132275C	-
	At1g16420	Metacaspase 8	*MC8*	Salk_047489C	-
GWAS	**AT1G69580***	**Myb transcription factor**	***PHL8***	**Salk_208737C**	Gabi_272G02
	AT3G11010	Receptor-like protein 34	*RLP34*	Salk_023381C	Salk_127176C
	AT3G11080	Receptor-like protein 35	*RLP35*	Salk_057434C	Salk_096171
	AT3G46160	Protein kinase	*PK*	Salk_208779C	-
	AT4G11390	Cysteine/Histidine-rich C1 domain family protein	*CHC1A*	Salk_067928C	Salk_087757C
	AT4G11490	**Cysteine-rich receptor-like kinase 33**	*CRK33*	**Salk_148136C**	Salk_119041C
	AT4G11830*	**Phospholipase D gamma 2**	*PLDγ2*	**Salk_078226C**	Salk_014510C
	AT4G11845*	**Serine/threonine kinase**	*STK*	**Salk_209109C**	Salk_076790C2
	AT4G38700	Dirigent protein 15/ Disease resistance-response protein	*DIR15*	Salk_023786C	Salk_102871C
	AT5G39471	Cysteine/Histidine-rich C1 domain family protein	*CHC1B*	Salk_208188C	Salk_131544
	AT5G39560*	Galactose oxidase/kelch repeat protein	*GO*	Salk_148581C	Salk_066527C
	AT5G51640	Yellow-leaf-specific gene 7	*YLS7*	Salk_044425C	Salk_029464

The table includes gene ID, description, gene abbreviation and the corresponding mutant accession(s).

*These mutant lines showed significantly different BOT-sensitivity compared to WT Col-0, and the genes highlighted in bold were checked for expression levels in Col-0 upon BOT treatment by RT-qPCR.

**Information of the descriptions of proteins was from Uniprot (https://www.uniprot.org) and the Arabidopsis Information Resource (TAIR: https://www.arabidopsis.org/index.jsp).

***All of the mutant lines #1 were tested first for one experiment (including 80 leaves from 20 plants infiltrated by BOT) and showed a difference in sensitivity to botrydial compared to the WT Col-0. Subsequently, the mutant line #1 was tested for a second experiment and the mutant line #2 were tested in parallel to confirm the function of the target gene. The T-DNA insertion lines generated by SALK institute which are named with a "C" in the end were indicated to be homozygous lines by NASC institute for (one of) the target gene. Nevertheless, accessions ordered from NASC in this study were still genotyped by PCR regardless whether the line was claimed to be homozygous or heterozygous by NASC.

Natural variation in sensitivity to BOT among accessions of *A. thaliana*

To assess natural variation in the sensitivity to BOT in the global population of *A. thaliana*, a HapMap panel of 359 accessions (https://naturalvariation.org/hapmap/) was examined. Ten leaves from five individual plants of each accession were treated by surface application of droplets containing 50 µM BOT and control solution on different leaf-halves. Five days after the treatment, the cell death intensity triggered by the application of BOT or control solution was quantified using red light emission imaging (Landeo Villanueva et al., 2021). The BOT-sensitivity of a tested leaf was represented by the relative intensity (RI), of which the quantification method is described in detail in Materials and Method. The RI value of each ecotype was later normalized to the RI of Col-0 (the reference RI_{Col-0}=1) followed by a logarithm transformation (logRI) before being used as the input data for the GWAS analysis (Supplementary Data S1). Out of the 359 *A. thaliana* accessions, 333 are incorporated in the fully imputed single-nucleotide polymorphism (SNP) dataset, a union of 1386 accessions with a 250k SNPs matrix (Horton et al., 2012) and 1135 accessions from the 1001 genomes project with a 10M SNPs matrix (Alonso-Blanco et al., 2016) employed by the online GWAS tool GWA-Portal (https://gwas.gmi.oeaw.ac.at/) (Seren et al., 2012).

A wide range of variation in BOT-sensitivity was observed among the 333 ecotypes (Figure 2A). The estimated narrow sense heritability (pseudo heritability) of BOT-sensitivity in the examined population was 0.35, indicating substantial heritable genetic variation. However, the BOT-sensitivity in the tested *A. thaliana* accessions exhibited no correlation with the geographical location of the site of origin (Supplementary Figure S2).

The reference accession Col-0 was one of the relatively sensitive genotypes ($log(RI_{Col-0})$= -0.62), as 258 out of the 333 tested accessions were less sensitive than Col-0 (Figure 2 and Supplementary Data S1). The moderate red light intensity as well as the size of affected areas observed in Col-0 reflected the medium BOT-sensitivity (Figure 2B). The BOT-treated areas on leaves of the least sensitive accessions Uk-1 and Li-5:2 (with respective logRI of -4.07 and -4.22) exhibited the faintest red light signal and sometimes scattered spots of detectable signal (Figure 2B). Leaf areas of the most sensitive accessions Pa-1 and Ra-0 (with respective logRI of 0.77 and 1.16) displayed the most intense red light signal upon treatment with BOT, covering (almost) the whole area (Figure 2B). These observations validate the relationship between the calculation of RI (and logRI) and the severity of necrotic symptoms detected by the red light imaging system.

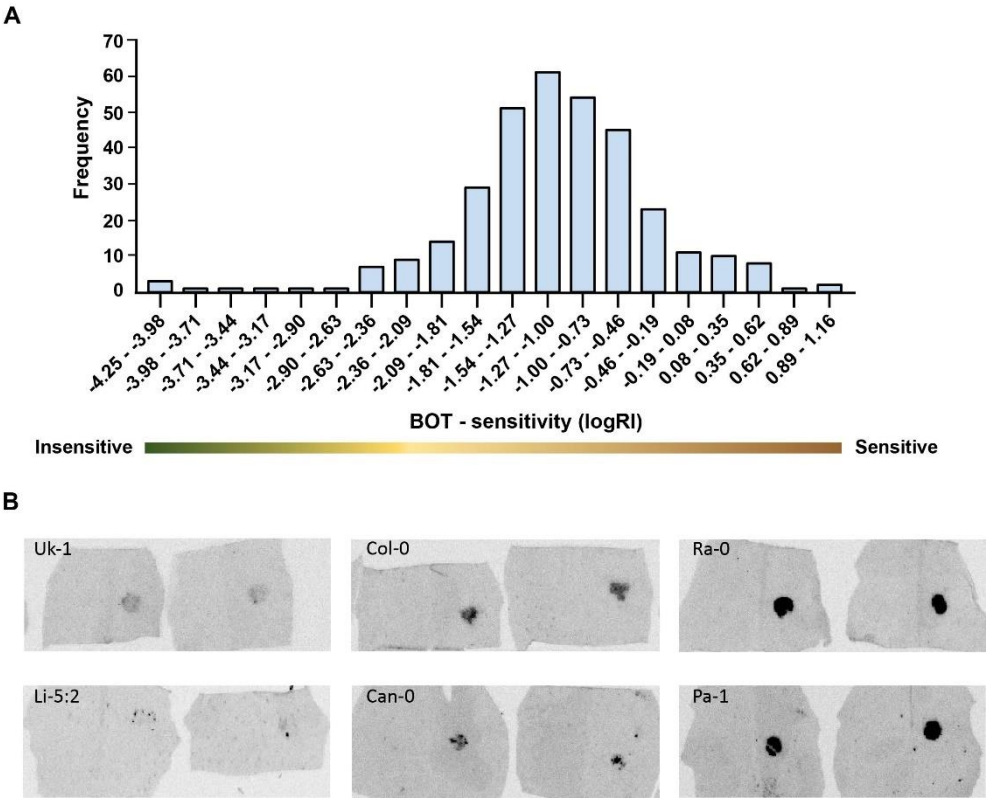

Figure 2. Variation in the sensitivity to BOT among 333 ecotypes of *A. thaliana*. **(A)** Frequency histogram of the number of accessions corresponding to sub-classes of sensitivity to BOT. **(B)** Symptoms of representative insensitive (Uk-1 and Li-5:2), medium sensitive (Col-0 and Can-0), and most sensitive (Pa-1 and Ra-0) accessions at spots treated with BOT at the right side of the central vein of leaves, revealed by red light emission.

GWAS reveals genetic loci associated with BOT-sensitivity

To map genetic factors explaining the observed variation in the BOT-sensitivity levels (logRI values) of the 333 ecotypes, a GWA approach using a standard linear regression model (LM) was performed in GWA-Portal (Seren et al., 2012). Although a number of loci clearly reflected statistical associations escaping the neutral background of the bulk of SNPs only very few of the representing SNPs passed the stringent thresholds commonly used for multiple testing statistics (Figure 3). The GWA-Portal, for instance, calculates a Benjamini-Hochberg-Yekutieli multiple testing cut-off of log(P-value) = ~7.0 (Seren et al., 2012). Other studies used similar false discovery rate (FDR) or permutation-based thresholds (Z. Chen et al., 2021). Nonetheless, valuable results have also been obtained applying less stringent thresholds. Notably, SNP association with host susceptibility to *B. cinerea* under different

biotic and abiotic stresses in *A. thaliana* was previously investigated with a very loose threshold of -log(P-value) = 4.0 (Coolen et al., 2019). Here, we set an arbitrary threshold of -log(P-value) = 6.0, which was stringent enough to exclude the majority of false positives (type I error) and relaxed enough to avoid false negatives (Type II error). Applying this threshold resulted in 22 loci containing multiple significant SNPs located in close physical proximity and 21 SNP singletons (i.e. loci represented by a single significant SNP).

From these 43 genomic regions, a list of candidate genes that might be involved in BOT-sensitivity was selected according to the following criteria or steps: i) ~240 genes located in a window of 20 kb surrounding the significant SNP (10 kb up- and down-stream), (Supplementary Data S2); ii) genes that are expressed in leaves (https://www.arabidopsis.org/index.jsp); iii) genes with sequence polymorphisms between a sub-group of the sensitive and insensitive ecotypes (http://signal.salk.edu/atg1001/3.0/gebrowser.php); iv) genes manually selected for annotation of protein domains. Finally, a set of 36 candidate genes, meeting all criteria, were selected for further validation, including genes encoding 12 receptor(-like) proteins or kinases, 7 cysteine- or cysteine/histidine-rich proteins, 4 kinases, 4 proteins related to biotic/abiotic stress responses, and 4 transcription factors (Supplementary Data S2).

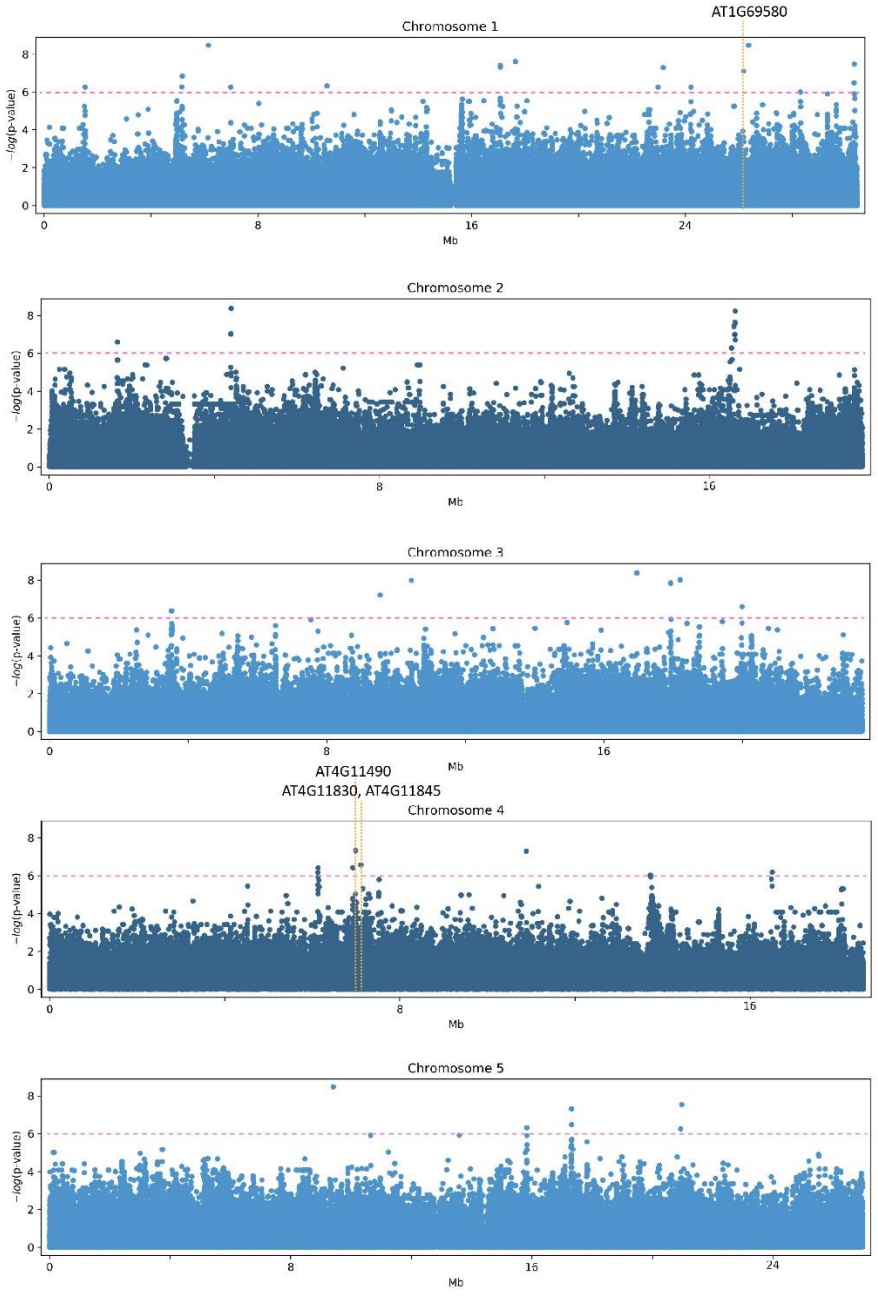

Figure 3: Manhattan plots of the five chromosomes of Arabidopsis after GWA mapping of sensitivity to BOT in 333 accessions. The horizontal pink dashed line indicates the logarithm of odds (LOD) significance threshold of 6.0 (− log(p-value) = 6.0), and the vertical yellow dashed lines indicate the coordinates of four candidate genes that were subjected to further analysis.

Functional validation of candidate genes by testing BOT-sensitivity of mutant plants

In order to validate the role in sensitivity to BOT of the candidate genes selected from the GWAS, we analyzed for each of the candidate genes at least one *A. thaliana* mutant line in a Col-0 background (or two lines, if available from NASC), in which the coding sequence was mutated by T-DNA insertion or EMS mutagenesis (Table 1 and Supplementary Table S1). The acquired knock-out (KO) lines were genotyped in order to assess whether the mutation was homozygous or heterozygous. Homozygous mutants were obtained for 14 of the 36 candidate genes. These homozygous mutant plants were propagated and examined for their sensitivity to BOT alongside the WT Col-0. In total, 15 mutant lines for 12 candidate genes (two separate mutant lines were available for three of the 12 genes) were tested for sensitivity to BOT in two independent experiments (Table 1). Mutant lines for two other genes were not included in the second experiment (BOT-sensitivity data not shown) because they showed similar BOT-sensitivity as WT Col-0 in the first experiment (Supplementary Table S1).

Interestingly, mutant plants for four candidate genes showed a significant difference in sensitivity to BOT, as compared with the WT Col-0 (Figure 4 A, B), while the sensitivity of the other 11 mutants (for 8 candidate genes) was similar to the WT Col-0 (Supplementary Figure S1). Specifically, mutant lines for the genes encoding the MYB family transcription factor PHL8 (*phl8#1*), the cysteine-rich receptor-like kinase 33 (*crk33#1*), and phospholipase D gamma 2 (*pldγ2#1*) displayed reduced sensitivity to BOT, while the mutant line for a serine/threonine kinase gene (*stk#1*) showed enhanced sensitivity to BOT as compared to the WT Col-0 (Figure 4 A, B). These observations suggest that PHL8, CRK33 and PLDγ2 positively participate in the PCD response triggered by BOT, whereas STK may function as a negative regulator. It is important to note that the *CRK33*, *PLDγ2* and *STK* genes are in close proximity in the *A. thaliana* genome (at chromosome 4), and that the *PLDγ2* and *STK* genes were both selected because of their location in close proximity of the same significant SNP (Figure 3).

We next assessed the gene expression levels of three candidate genes (*PHL8, PLDγ2* and *STK*) in WT Col-0 plants at different time points after BOT or mock treatment. The *STK* transcript level was shown to be down-regulated in BOT-treated leaves at 10 and 24 hours after the treatment, as compared to the control (Figure 4C). Transcript levels of *PHL8* and *PLDγ2* in BOT-treated leaves were similar to those in mock-treated leaves at all tested time points (Figure 4C).

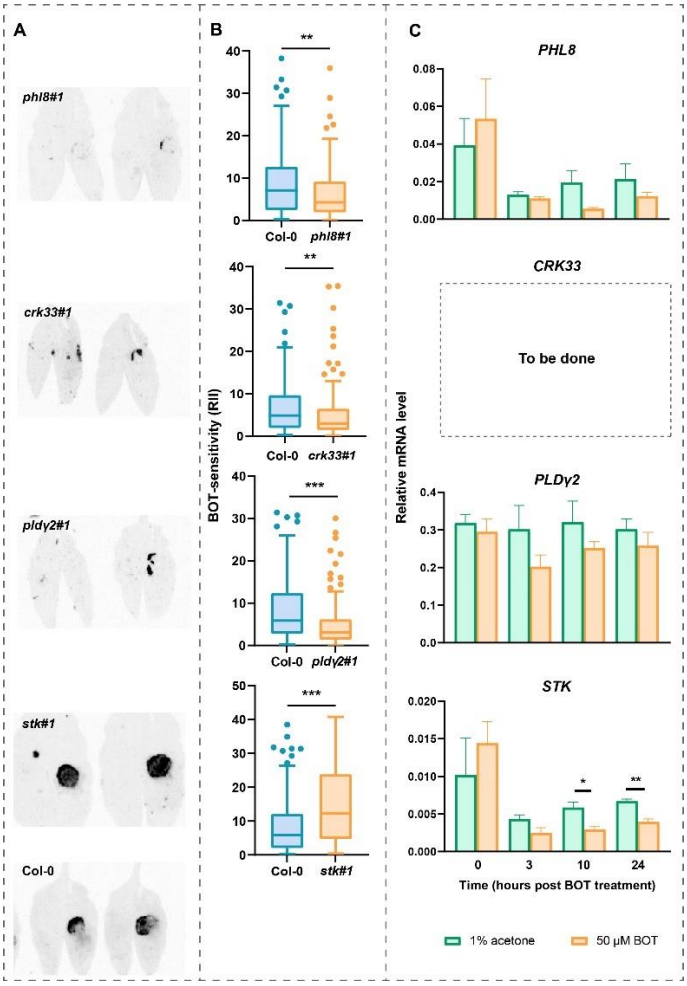

Figure 4. Characterization of candidate genes. **(A)** Necrotic symptoms of Col-0 and four mutant lines (*phl8#1, crk33#1*, *pldγ2#1* and *stk#1*), visualized by red-light emission on the 5th day after BOT treatment. The right side of each leaf was infiltrated by 50 µM BOT and the left side was infiltrated with 1% acetone at the same time. **(B)** Tukey box plots representing the difference in cell death intensity triggered by BOT between Col-0 and mutant lines. Each box plot includes 160 datapoints from two independent experiments (20 plants/experiment and 4 leaves/plant, and thus 80 leaves/experiment were treated by BOT). Asterisks indicate a significantly different BOT-sensitivity of a mutant line compared to the WT Col-0. Statistical analysis was performed by t-test (*p<0.05, **p<0.01 and ***p<0.001). **(C)** Relative expression levels of four candidate genes (*PHL8*, *PLDγ2* and *STK*) in Col-0 plants at 0, 3, 10 and 24 hours post infiltration of 50 µM BOT or control (1% acetone). The transcript levels were normalized to the reference gene *A. thaliana UBIQUITIN-10* at each examined time point, using the calculation of $2^{\wedge(-\Delta Ct)}$. Data are presented in bar charts (mean value and standard errors from 4 biological replicates), and statistical analysis was performed by a t-test to compare the mRNA level between leaf samples treated with BOT to the control at each time point. The significant differences are shown by asterisks (* p< 0.05, ** p< 0.01). The *CRK33* gene was not examined by RT-qPCR yet which remains to be done **(C)**, though the mutant line for this gene displayed a reduced BOT-sensitivity **(A, B)**.

STK plays a role in resistance to *B. cinerea* in *A. thaliana*

Six *A. thaliana* mutant lines were tested for their susceptibility to *B. cinerea* WT strain B05.10 and a *Δbot2* mutant strain. The *B. cinerea Δbot2#1* mutant caused expanding lesions at a low frequency on leaves of WT Col-0, while expanding lesions were observed in ~ 97 % of the WT B05.10-inoculated Col-0 leaves (Figure 5A, B). These observations are in line with the findings in Chapter 4. Five out of the six tested *A. thaliana* mutant lines did not show a significant difference in susceptibility to *B. cinerea* compared with the WT Col-0 (Supplementary Figure S3), and these mutants were also not significantly different in BOT-sensitivity compared to the WT plant (Supplementary Figure S1B). Interestingly, the *stk#1* mutant, which showed a significantly higher BOT-sensitivity compared to the WT Col-0 (Figure 4), exhibited enhanced susceptibility to both WT B05.10 and *Δbot2#1* mutant (Figure 5A, C). This indicates that STK may contribute to host resistance against *B. cinerea*.

Despite that the disease incidences of WT B05.10 and the *Δbot2#1* mutant were not significantly higher in the *stk#1* mutant than in WT Col-0 (Figure 5B), the difference in virulence between *Δbot2#1* and WT B05.10 was slightly larger in the *stk#1* mutant than in WT Col-0 (Figure 5C). The expanding lesion size of *Δbot2#1* was not significantly different from the WT B05.10 on leaves of WT Col-0, while the lesion size of *Δbot2#1* was significantly smaller than the WT fungus on the *stk#1* mutant (Figure 5C). Since the difference in virulence of *Δbot2#1* compared to the WT B05.10 in a plant could suggest the importance of BOT for the fungus to infect the host, the higher reduction in virulence of the *Δbot2#1* mutant on the *stk#1* mutant plant reflects that BOT contributes to the virulence of *B. cinerea* to a larger extent during the fungal infection on *stk#1* mutant than WT Col-0. This again illustrates that STK might function as a negative regulator in the response to BOT.

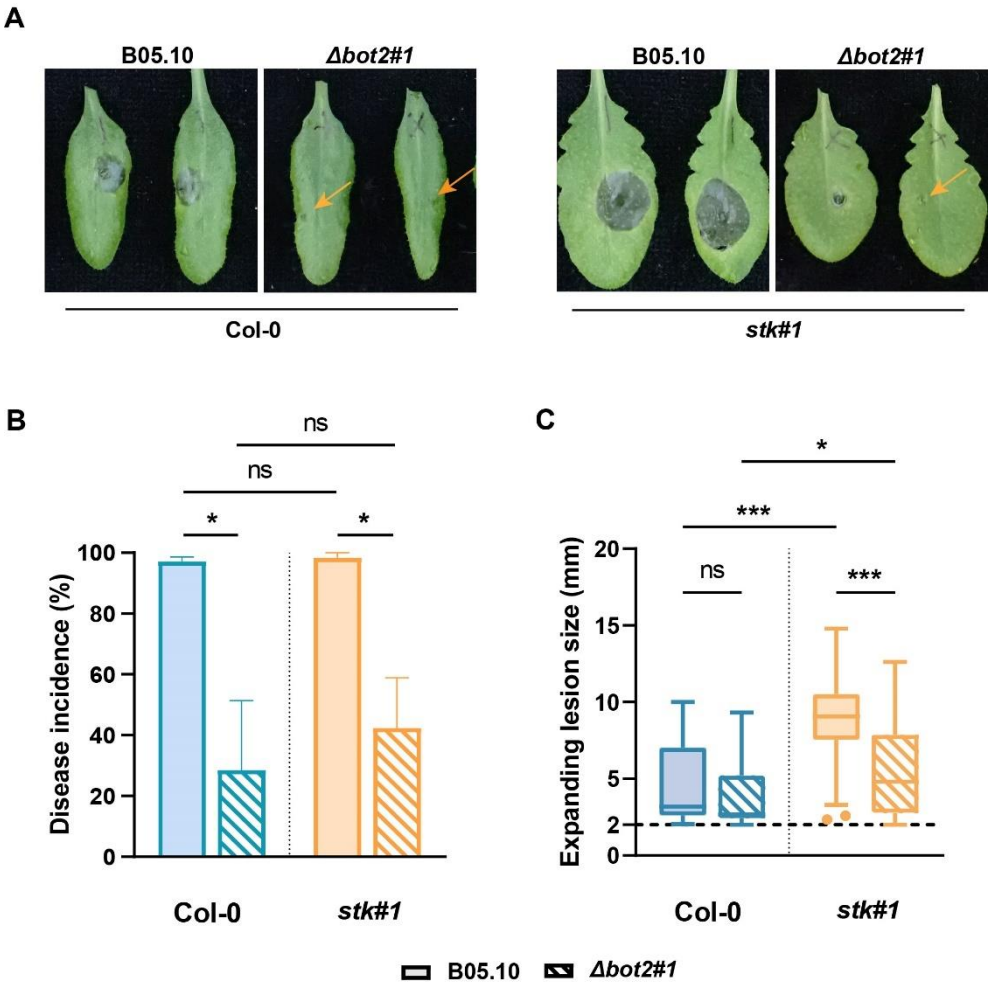

Figure 5. Susceptibility of the *A. thaliana* mutant line *stk#1* to the WT *B. cinerea* strain B05.10 and the *Δbot2#1* mutant, compared to WT Col-0. **(A)** Necrotic lesions on leaves of Col-0 and *stk#1* upon infection, photographed at 3 days post inoculation (dpi). Orange arrows indicate the non-expanding lesions caused by inoculation of *Δbot2#1* mutant on Col-0 and *stk#1* leaves. **(B)** Disease incidence (the ratio of the number of expanding lesions to the number of total inoculations) of WT B05.10 and *Δbot2#1* on leaves of Col-0 and *stk#1*. The bar chart shows the mean disease incidence and standard errors from three independent experiments. The statistical analysis was performed using a t-test for each pair-wise comparison. Significant differences are shown by an asterisk (*p<0.05) and nonsignificant differences as "ns". **(C)** Tukey box plot depicting the lesion size (diameter in mm) caused by the infection of WT B05.10 and *Δbot2#1 B. cinerea* strains on leaves of Col-0 and *stk#1*. The non-expanding lesions are defined by lesion diameters below 2 mm. Statistical analysis was performed using Brown-Forsythe and Welch ANOVA tests (multiple comparisons) for plot **(C)**, and significant differences are indicated by asterisks (*p<0.05; *** p<0.001) and "ns" for nonsignificant difference. The filled bars/boxes represent infection results from WT B05.10, and hatched bars/boxes represent *Δbot2#1 B. cinerea* in **(B)** and **(C)**.

Bulk segregant analysis reveals genomic association with BOT-sensitivity

Broad variation in the sensitivity to BOT was observed between the 333 *A. thaliana* accessions, among which Uk-1 was one of the ecotypes displaying the lowest BOT-sensitivity (Figure 2). Col-0, on the other hand, grouped with the sensitive accessions. The genome of Col-0 is the best sequenced and assembled *A. thaliana* genome so far, and it is used as the reference genome for the GWAS. The observation that Col-0 and Uk-1 display a very pronounced difference in sensitivity to BOT (Figure 2), opens up the opportunity of a forward genetics approach by bulk-segregant analysis (BSA), in parallel with the GWAS to identify genetic loci associated with BOT-sensitivity. Uk-1 and Col-0 were crossed (reciprocally) and the BOT-sensitivity of the two parental lines and F_1 plants were subsequently examined. The sensitivity of Col-0 to BOT was significantly higher than that of Uk-1 and F_1 plants, while there was no significant difference in sensitivity between Uk-1 and F_1 (Figure 6A). In the next generation, a BOT-sensitivity test was performed on 217 F_2 plants grown from seeds collected from a single F_1 plant. A large quantitative variation in sensitivity levels was observed among the 217 F2 plants, ranging from values that resembled the insensitive and sensitive Uk-1 and Col-0 parents, respectively. However, many F_2 plants displayed intermediate levels of sensitivity to BOT and also strong transgression in both directions occurred (Figure 6B).

To perform a BSA with the aim to identify genetic loci associated with BOT-sensitivity, we applied a whole-genome sequencing (~220x coverage) to two DNA pools. Each of these pools contained DNA samples from the 20 F_2 individual plants that displayed the lowest and the highest sensitivity to BOT, respectively. The two DNA pools were designated as ATI (*A. thaliana* insensitive) and ATS (*A. thaliana* sensitive). The sequencing data were analyzed for SNP frequency based on the reference (parental) genome Col-0 using SHOREmap (Schneeberger et al., 2009). The frequencies of all SNPs in all five chromosomes in ATI and ATS were then plotted and analyzed for distortions of the expected 1-to-1 segregation ratio (Figure 7). As the sensitive parental line Col-0 provided the reference alleles, the genetic loci associated with insensitivity to BOT were expected to be overrepresented by SNPs descending from the insensitive parent Uk-1. Genomic regions, containing a relatively high frequency of SNPs (0.8-1.0) in the ATI pool but a medium to low frequency ($\leq$ 0.5) in the ATS pool, were predominantly found in chromosomes 1, 3 and 5. These regions might represent genetic variation explaining the insensitivity to BOT (Figure 7). A region at the end of chromosome 4 showed a contrasting pattern, as the frequency of SNPs was high in the ATS pool but low in ATI (Figure 7). This region might contain genetically variable loci explaining higher sensitivity to BOT.

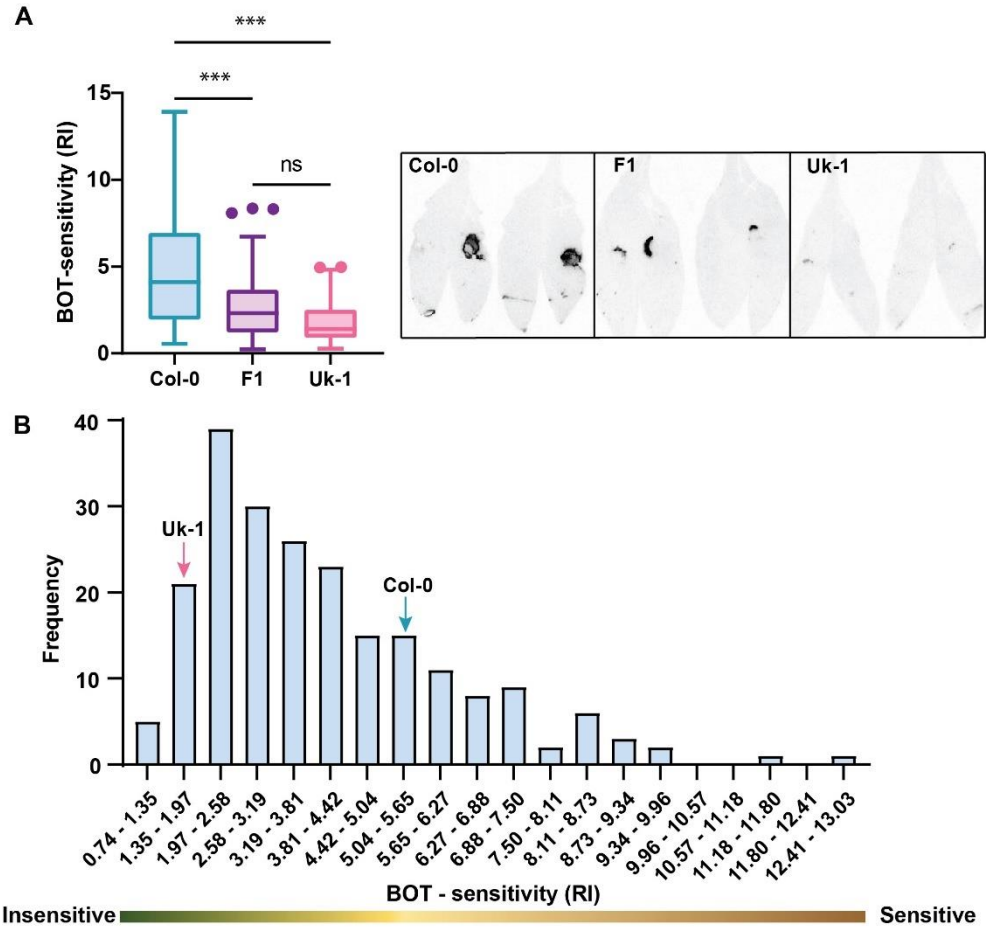

Figure 6. BOT-sensitivity of Col-0, Uk-1, F1 and F2 plants. **(A)** The Tukey box plot on the left shows the difference in BOT-sensitivity between Col-0 (16 individual plants), Uk-1 (16 plants) and F1 plants (20 plants). The statistical analysis was performed using a one-way ANOVA test, and the significant differences are shown in asterisks (*** $p<0.001$) and the non-significance is shown as "ns". On the right of panel **(A)**, images show the red light emission by representative leaves of Col-0, Uk-1 and F1 which were infiltrated with 50 µM BOT on the 5th day after treatment. **(B)** Histogram representing the quantitative variation in BOT-sensitivity (RI) among 217 F_2 plants. The BOT-sensitivity levels (mean RI) of Col-0 and Uk-1 are indicated in this histogram by the blue and pink arrows, respectively.

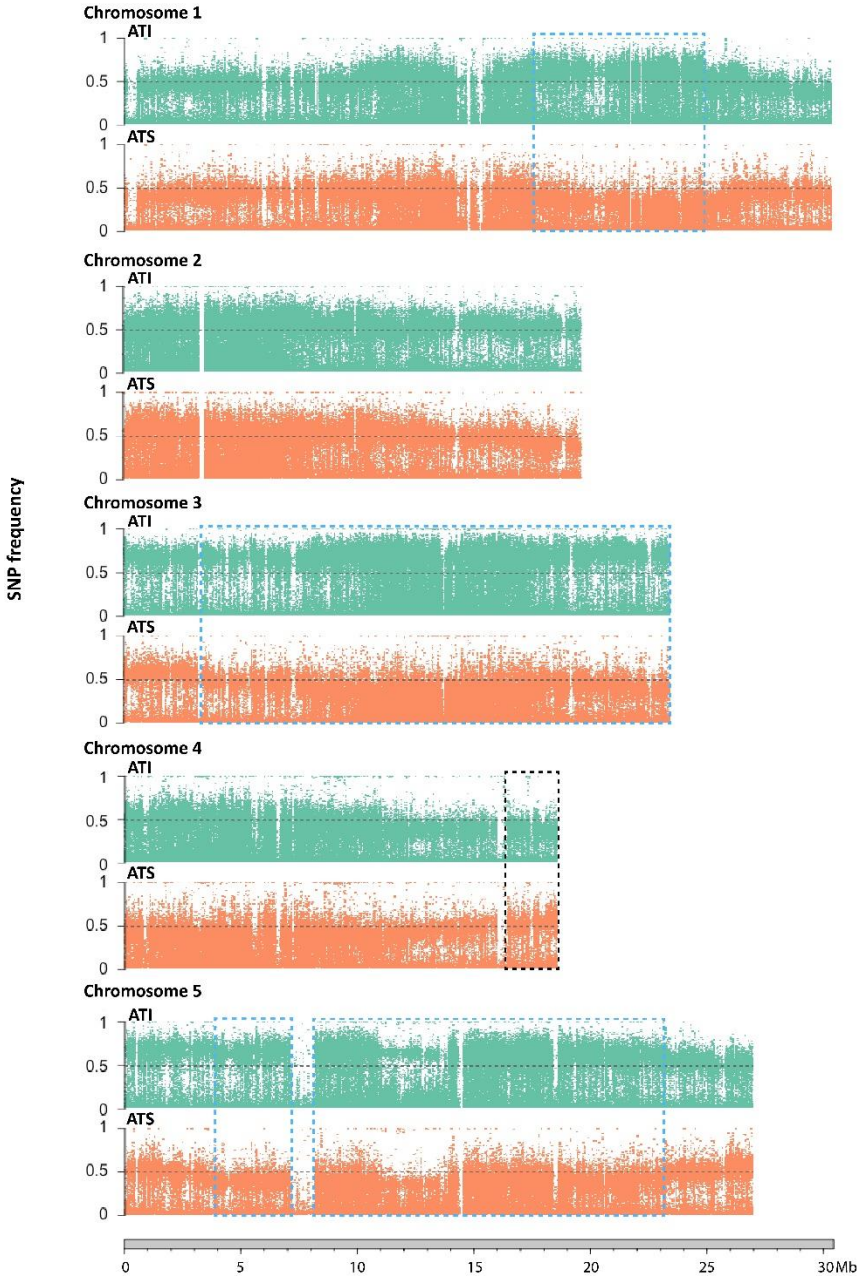

Figure 7. SNP frequency in BSA pools of ATI and ATS in each of the five chromosomes of *A. thaliana* Col-0, represented by dot plots. The x-axis shows the position of the SNPs and the y-axis shows the frequency of each SNP. A scale is shown at the bottom of this figure, which is applied to all five chromosomes. The SNP-frequency of 0.5 is indicated by grey dashed lines. Regions marked by both blue and black dashed frames indicate contrasting landscapes of the two pools. The blue frames indicate regions with higher SNP frequency in ATI than ATS, and the black frame indicates a region where higher SNP frequencies were found in ATS than ATI.

Discussion

This study demonstrates that BOT can induce a cell death response in *A. thaliana* in a dose-dependent manner, as well as other plant responses (ROS burst and MAPK activation) that resemble common outputs of ETI (Figure 1). BOT makes an important contribution to the virulence of *B. cinerea* on *A. thaliana* (Chapter 4 and Figure 5). Therefore, this non-proteinaceous effector acts as a virulence factor which might be useful as an appropriate tool to explore Susceptibility or Resistance genes in *A. thaliana.* This can be implemented by identifying plant genes involved in the PCD response induced by the toxin. The *A. thaliana npr1#1* mutant displayed a reduced sensitivity to BOT (Figure 1D), which further confirms that SA signaling plays a positive role in the BOT-induced PCD response, as previously proposed by Rossi et al. (2011). Secondly, BOT may induce a specific type of plant PCD referred to as apoptosis ('self-killing'), considering the following aspects. 1) The PCD balance between apoptosis and autophagy was suggested to be key to disease progression in the early phases of *B. cinerea* infection (Veloso & van Kan, 2018); 2) BOT triggers plant responses that are commonly thought to be associated with HR (Rossi et al., 2011); the *Bcbot2* gene is the key gene in the BOT-gene cluster and displays a transient expression peak at 12-16 hpi (the initiation and completion of forming the primary necrotic lesion) while its expression decreases at 24 hpi (the onset of lesion expansion) as shown in Chapter 6.

Plant apoptotic PCD is mediated by metacaspases (MCs), which are homologs of caspases that are classified in the clan CD of cysteine proteases and were initially identified in animals (Tsiatsiani et al., 2011; Vercammen et al., 2007). Two *A. thaliana* type I MCs, MC1 and MC2, have been reported to antagonistically regulate PCD. MC1 positively regulates cell death while MC2 counteracts the promoted cell death effect of MC1 (Coll et al., 2010). We observed that the BOT-induced necrotic symptoms were less severe in leaves of *mc1#1* mutant than the WT Col-0 (Figure 1E), suggesting that the PCD induced by BOT is (at least partly) activated through the function of MC1. However, we did not detect obviously increased cell death intensity upon BOT treatment in the *mc2#1* mutant (data not shown). In addition, some of the six other *A. thaliana* type II MCs have been annotated. For instance, MC4 (alternatively named MC2d) positively regulates cell death induction upon biotic or abiotic stress, demonstrated by the phenotypes of *MC4*-knockout, -overexpression, or -inactivation mutants (Watanabe & Lam, 2011). Furthermore, the *MC8*-knockout and -overexpression mutants display reduced and increased PCD triggered by UV light and H_2O_2, respectively (He et al., 2008). It requires further investigation to validate whether (and

which) members of the metacaspase family can also suppress the PCD response triggered by BOT in *A. thaliana*.

After applying a reverse genetics approach to validate the roles of NPR1 and MC1 in the plant response to BOT, two forward genetic approaches (GWAS and BSA) were adopted in parallel to identify more genes (or loci) associated with the sensitivity to BOT. These forward genetic approaches are considered to be (almost) non-biased, as they may reveal genes that have never before been reported to be correlated either with sensitivity to phytotoxins, susceptibility to *B. cinerea* or PCD signaling. By comparing the results of our GWAS study with that from Coolen et al. (2019), which reported a GWAS performed for traits regarding *Botrytis* susceptibility in combination with additional biotic or abiotic stresses, we found that the loci associated with BOT-sensitivity in this study (mostly) do not overlap with the loci correlated to the resistance to *B. cinerea* revealed by Coolen et al. (2019) (Supplementary Figure S4). This is not surprising since the plant susceptibility to *B. cinerea* involves many more variables besides the response to BOT. Using the fungus to screen the same HapMap population could have identified loci associated with plant responses to multiple *B. cinerea* virulence factors, but also with the level of camalexin, or with the structure or composition of the cuticle. In contrast, we only used the toxin in the screening, which restricted the range of plant components involved in the response to this single virulence factor. The GWAS in our study identified a serine/threonine kinase-encoding gene (*STK*, At4g11845) as a candidate, and the *A. thaliana stk#1* T-DNA insertion mutant indeed showed increased sensitivity to BOT, as well as enhanced susceptibility to the fungus (Figure 4 and 5). These observations suggest that STK not only acts as a suppressor of the cell death response to BOT, but also confers partial resistance to *B. cinerea*. The STK protein is annotated as positive regulator of brassinosteroid (BR) signaling downstream of the receptor kinase BRI1 (the receptor for brassinolide) and is predicted to be located at the cell membrane, based on annotation in Uniprot (UniRule - UR001627761). BRI1 is able to form heterodimeric complexes with another LRR-RLK, BRI1-associated receptor kinase 1 (BAK1), and thereby modulate BR signaling (J. Li et al., 2002). We speculate that STK binds to BRI1 which can subsequently associate with BAK1, thereby preventing BAK1 from interacting with other receptor proteins, which would lead to the induction of PCD. This could explain the increased susceptibility of *stk1#1* mutants, and future research should include experiments to test whether the *bri1* mutant also shows higher sensitivity to BOT and increased susceptibility to *B. cinerea*.

In contrast to the phenotype of the *stk#1* mutant, the *phl8#1*, *crk33#1*, and *pldγ2#1* plants were less sensitive to BOT compared with WT Col-0 (Figure 4). The susceptibility of these three mutants to *B. cinerea* will be further tested in the near future. It is anticipated that

these mutants confer increased resistance to *B. cinerea,* and thus that *PHL8*, *CRK33* and *PLDγ2* function as *S* genes in *A thaliana*. PHL8 belongs to the Myb transcription factor (TF) family, which in *A. thaliana* contains ~200 members that participate in a broad spectrum of processes, including responses to biotic stresses and HR induction (de Vos et al., 2006; Repetti & Staskawicz, 2002). Transient overexpression of *CaPHL8* in pepper (*Capsicum annuum*) induces an HR, increased ROS production and up-regulation of immunity-associated marker genes (Noman et al., 2019). Although CaPHL8 in pepper is phylogenetically relatively distant from AtPHL8 in *A. thaliana*, it is likely that the PHL8 Myb TFs play a positive role in plant PCD in both plant species.

The family of cysteine-rich receptor-like kinases (CRKs) in *A. thaliana* contains 44 members, which have been suggested to play roles in mediating defense responses and PCD (Wrzaczek et al., 2010). An earlier study examined the transcription profiles of the 44 *CRKs*, revealing that the expression levels of a subset of *CRKs* were upregulated (e.g., CRK11, 36, 37 and 45) or downregulated (e.g., CRK4 and 21) during *B. cinerea* infection, while *CRK33* was not transcriptionally regulated in either direction (Wrzaczek et al., 2010). Other studies reported similar findings of different CRKs having opposite functions in defense against pathogens. For instance, CRK45 contributes to resistance against *Pseudomonas syringae* (X. Zhang et al., 2013), while CRK20 contributes to susceptibility to *P. syringae* (Ederli et al., 2011). In addition, our study suggests CRK33 as a participant in the PCD response induced by a fungal phytotoxin.

PLD is responsible for the production of phosphatidic acid (PA) through hydrolyzing membrane phospholipids. Both PLD and its product PA exert influence on signal transduction cascades. The plant PLD family is large and diverse PLD isoforms participate in responses to various stresses (Bargmann & Munnik, 2006; J. Li & Wang, 2019). A recent study reported that an *A. thaliana* mutant in *PLDγ1* displayed increased resistance against *B. cinerea* (Schlöffel et al., 2019). By contrast, *B. cinerea* inoculation on *pldγ2* and *pldγ3* mutant plants results in lesions with similar sizes but elevated fungal biomass (indicated by DNA content), as compared to the WT Col-0 plant (Schlöffel et al., 2019). The increased *B. cinerea* biomass in the *pldγ2* mutant supports our hypothesis that *PLDγ2* may contribute to the susceptibility of *A. thaliana* to *B. cinerea.*

The identification of host genes that contribute to susceptibility offers perspectives for engineering resistance (van Schie & Takken, 2014). The *S* genes participating in the sensitivity to BOT may serve as a starting point for identifying orthologs in crop species and for testing whether mutants in these orthologs indeed display increased resistance to *B. cinerea.* Alternatively, it may be feasible to test germplasm of crop species with BOT and

perform GWAS to find associations to the sensitivity to BOT, as well as susceptibility to the fungus. As described in Chapter 6, BOT plays an important role in promoting disease incidence of *B. cinerea* on tomato leaves, since inoculation with the *B. cinerea Δbot2#1* mutant caused significantly lower symptom development than the WT fungus on this host. Hence, altering plant genes that contribute to BOT-sensitivity offers perspectives for obtaining (partial) resistance to *B. cinerea* in tomato. Molecular markers of >770 tomato accessions are available, and GWA studies using these tomato accessions have already been performed (Zhang et al., 2015; Zhao et al., 2019). Based on these technical advances, it seems resourceful to perform GWAS to find genetic variants explaining the variation in sensitivity to BOT in tomato.

This study identified novel genes involved in the PCD signaling cascade triggered by BOT, which demonstrates that mining the molecular mechanisms underlying the mode of action of a virulence factor of a necrotrophic pathogen can contribute to increasing host resistance. Nevertheless, a number of additional experiments need to be performed to corroborate our findings or to answer emerging questions derived from our observations. Firstly, since only a single mutant line was tested for each of the genes (*STK*, *PHL8*, *CRK33* and PLDγ2) in this study, it would strengthen our conclusions to perform BOT-sensitivity and *B. cinerea* virulence assays with additional mutant lines or with a complemented transformant line to verify the functions of these genes. Secondly, apart from studying the role of individual genes in the plant response to BOT, the simultaneous effect of two genes can be evaluated by investigating the BOT-sensitivity of double-mutant plants, generated from crossing two single mutant lines. Notably, the list of 36 candidate genes selected by GWAS contains six members from the family of cysteine/histidine-rich C1 domain (*CHC1*) genes. Mutants for two of them (*CHC1a* and *CHC1b*) do not express a significant difference in BOT-sensitivity as compared to the WT plant, but that does not necessarily imply that these CHC1 proteins do not participate in the response to BOT. Instead, it is possible that CHC1 proteins function redundantly and could compensate for each other's loss of function in single mutants. Therefore, generating double mutants or even multi-mutants may offer a chance to elucidate the roles of multiple functionally redundant genes. Thirdly, the genetic approaches taken in this study have explored genes associated with BOT-sensitivity at the DNA level (by SNPs between sensitive and insensitive accessions), but the differential expression of genes involved in the response to BOT has not been taken into account yet. Figure 4C confirms that BOT treatment suppresses the expression level of *STK*, which acts as a negative regulator in the PCD response to the toxin. In contrast, genes that are commonly considered to be markers of HR, JA (or SAR) and JA signaling were reported to be upregulated at different time points in Col-0 leaves after application of BOT (Rossi et al.,

2011). Moreover, more than 600 *A. thaliana* genes are induced by *B. cinerea* infection, and *A. thaliana* mutants of two *Botrytis*-induced genes show increased susceptibility to the fungus (AbuQamar et al., 2006). Therefore, performing an RNA-sequencing experiment using Col-0 together with the most insensitive and sensitive accessions may offer novel insight about genes that affect BOT-(in)sensitivity via dynamics in their transcript levels. Finally, the BSA approach in the F2 population (Uk-1 x Col-0) lacked resolution because BOT sensitivity was associated with genomic regions that covered around a quarter to two thirds of chromosomes 1, 3 and 5. This finding can be explained by the small population (and pool) sizes and the limited recombination frequency in the F2 population. For these reasons, linkage disequilibrium (LD) can be high, leading to a genetic hitchhiking effect. It can be seen that SNP frequencies within the marked regions in Figure 7 between the two pools were not remarkably distant (ΔSNP-frequency was around 0.3). This might be the consequence of stochastic distortions which could mask or confound with causal associations. The genomic region in chromosome 4, displaying an inverse landscape in ATI/ATS - SNP frequency from the three regions in chromosome 1, 3 and 5, appeared to be positively correlated with sensitivity to BOT (Figure 7). This explains that Uk-1 is not completely insensitive to BOT (Figure 2B and 6A) and that it still possesses alleles that increase the cell death response induced by BOT. Finally, in order to narrow down the genomic regions harboring associations with BOT-sensitivity, it is worthwhile performing the BSA with additional F_2 individuals that are recombinant in those candidate regions and then a fine mapping using the BSA approach with an inbred F6 or F8 population (Uk-1 x Col-0). Collectively, our study provides better understanding of molecular mechanisms underlying the host response to the *B. cinerea* virulence factor BOT. We unraveled a considerable amount of candidate genes associated with BOT-sensitivity, of which four have been validated in this study and more remain to be further verified as potential S/R genes to *B. cinerea*.

Materials and Methods

Plant materials and growth conditions

A. thaliana plants were grown as described in Chapter 2 (Qin et al., 2023). The core set of 360 accessions from the HapMap population was kindly provided by the Laboratory of Genetics from Wageningen University. The detailed mapping information of these accessions is available at https://naturalvariation.org/hapmap/. Seeds of T-DNA mutant lines used in this study, summarized in Table 1 and Supplementary Table S1, were ordered from the Nottingham Arabidopsis Stock Centre (NASC). Genotyping of the mutant lines was performed by PCR using primer combinations shown in Supplementary Table S2.

B. cinerea strains and growth conditions

B. cinerea WT strain B05.10 (van Kan et al., 2017), *Δbot2#1* (Leisen et al., 2020b), and *Δboa6#1* (Dalmais et al., 2011) were used in this study. The fungal strains were grown and conidia were harvested as described in Chapter 2 (Qin et al., 2023). Conidia suspensions were stored in darkness at 4 °C until use.

Extraction and purification of BOT

BOT was extracted and purified as described in Chapter 4 of this thesis.

BOT application on Arabidopsis plants and quantification of cell death intensity

For the BOT toxicity test using different concentrations of BOT and the screening of 359 *A. thaliana* accessions, droplets of four µl containing a defined concentration of BOT (dissolved in 40% acetone) were applied to the adaxial surface of *A. thaliana* leaves in living plants. To achieve a higher reproducibility and more distinct variation between plants with different BOT-sensitivities, the mutant plants used for functional validation of candidate genes and F1/F2 plants (Col-0 x Uk-1) together with their parental lines were treated by infiltration of 50 µM BOT (dissolved in 1% acetone) on the right side of the central vein of each leaf. The left side of each BOT-treated leaf was infiltrated by 1% acetone as control. The treated plants were incubated in closed boxes with transparent lids in a climate chamber at 21 °C for day and 19 °C for night under a 12-hour day/night cycle. BOT-treated leaves were detached from the living plants on the 5th day after the treatment, and photographed using the red fluorescent protein (RFP) channel in the ChemiDoc^{MP} machine (model Universal Hood III, Bio-Rad) (Landeo Villanueva et al., 2021) with 1 sec exposure time. The BOT-triggered cell death intensity was quantified by two different approaches depending on the method of BOT treatment. 1) The leaves treated by applying BOT droplets on the adaxial surface were scored using a relative red light intensity (RI) approach. The mean red light

emission intensity in the BOT-treated area was quantified by a circle with a fixed size, drawing by the circle volume tool in the ImageLab software (Bio-Rad). The signal in the area treated by 40% acetone (no necrotic symptom) was quantified in the same way to be used as a background. The intensity of cell death response triggered by BOT (RI) was shown as the ratio of the mean intensity (BOT-treated area) to the mean intensity (negative control area). 2) The leaves treated by infiltrating the leaves with BOT solution were scored using a relative integral intensity (RII) approach. The images generated by the ChemiDoc^{MP} machine were first converted from .scn to .tiff format using the software Fiji/ImageJ (Supplementary Data S3). To measure the intensity of each treatment per leaf from the images, a python script was used (Supplementary Data S3). The results were then processed and adapted by an R studio script (Supplementary Data S3 and Supplementary Figure S5). However, the quantification of BOT-sensitivity in the F2 population (Uk-1 x Col-0) was performed using the RI approach, since the RII method had not been developed when the F2 plants were scored. The quantification results using the RII method to compare BOT-sensitivity between mutant plants and WT Col-0 were plotted as Tukey box plots and tested for statistical significance by t-test, following the guidelines of the GraphPad Prism software.

***B. cinerea* infection assay**

The *B. cinerea* infection assay was performed as described in Chapter 2 (Qin et al., 2023). The measured lesion sizes were plotted in Tukey box plot and the statistical analysis was performed using an ANOVA test following the recommended approach in GraphPad Prism.

Assays for plant immune responses

Mature rosette leaves in 5-week-old *A. thaliana* plants were used for both the ROS burst and MAPK activation assays. The ROS burst was performed as described in Huang et al. (2021), and the applied concentrations of BOT are shown in the legend of Figure 1. The MAPK activation in *A. thaliana* leaves that were infiltrated with 50 µM BOT or 1% acetone (control solution) was assessed by performing a western blotting experiment using an α-phospho-p44/42 MAPK antibody, mainly as described in Wan et al. (2019). The sampling time points after BOT/control treatment for the MAPK assay are shown in the legend of Figure 1.

Quantification of gene expression level by RT-qPCR

A. thaliana leaves were fully infiltrated by 50 µM BOT or 1% acetone (control) were excised from living plants at defined time points (t=0, 3, 10 and 24 hours post infiltration). The leaf samples were further processed for RNA extraction, cDNA synthesis and RT-qPCR using 30

ng cDNA, mainly as described in Chapter 2 (Qin et al., 2023). The reference gene and the calculation of relative expression are described in the legend of Figure 4.

GWAS analysis

The logRI values of the 333 tested accessions were used as the input phenotype, the GWAS was performed using a standard linear regression model (LM) in GWA-Portal as described by Seren et al. (2012). The GWAS result can be viewed as a Manhattan plot in an interactive way, which exhibited the negative log P values for the SNP association and positions of the SNPs in all five chromosomes of *A. thaliana*. The minor allele count was set to be no lower than two (MAC ≥ 2) and an arbitrary threshold of -log(P-value) = 6.0, resulting in the Manhattan plot shown in Figure 7.

BSA analysis

The most insensitive and sensitive 20 individuals from the F2 (Uk-1 x Col-0) population were chosen to be combined, which resulted in two pools named ATI and ATS, respectively. DNA extraction was performed using one mature leaf of each plant by a CTAB-based chloroform-isoamylalcohol method. DNA concentrations from the 20 plants of the ATI (or ATS) pool were measured by a Qubit fluorometer and then confirmed by a 0.8% agarose gel. DNA samples from the 20 plants of each pool were mixed by adding equal amount of DNA from each plant, resulting in two DNA samples named ATI and ATS. These two DNA samples were constructed for two separate DNBseq Normal DNA libraries, followed by whole genome sequencing with a DNBSEQ platform (paired-end sequencing with 150 bp-reads and an output of 150 Million read depth per sample) which was executed by BGI TECH SOLUTIONS (HONGKONG) CO., LIMITED. The sequenced short reads were processed for mapping and SNP calling using the pipeline of SHOREmap with default settings (Schneeberger et al., 2009). The SNP frequencies ATI and ATS on each chromosome were plotted using R packages karyoploteR (Gel & Serra, 2017) and Sushi (Phanstiel et al., 2015). Scripts are provided by Supplementary Data S4.

Supplementary materials

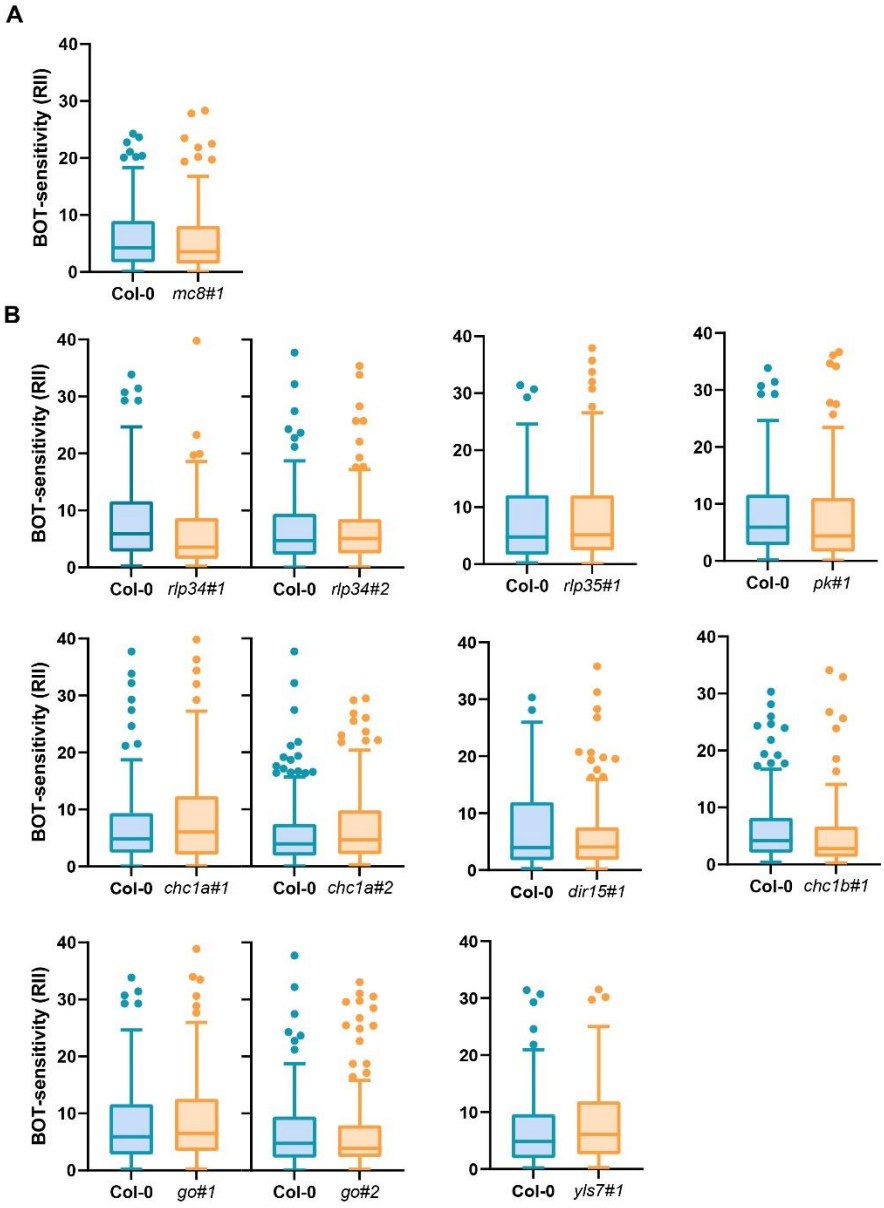

Supplementary Figure S1. Cell death response to BOT quantified by red light emission in various mutant plants compared to WT Col-0 plants. These mutant lines displayed no significant difference in BOT-sensitivity (measured by RII) compared to the WT Col-0, depicted by Tukey box plots. Each box plot includes ~ 160 datapoints collected from two independent experiments (20 plants/experiment and 4 leaves/plant, and thus 80 leaves/experiment were treated by BOT). (**A**) The *mc8#1* mutant was selected based on the hypothesis that BOT might induce apoptotic-like PCD, and (**B**) the mutants were selected from the GWAS to identify candidate genes associated with BOT-sensitivity.

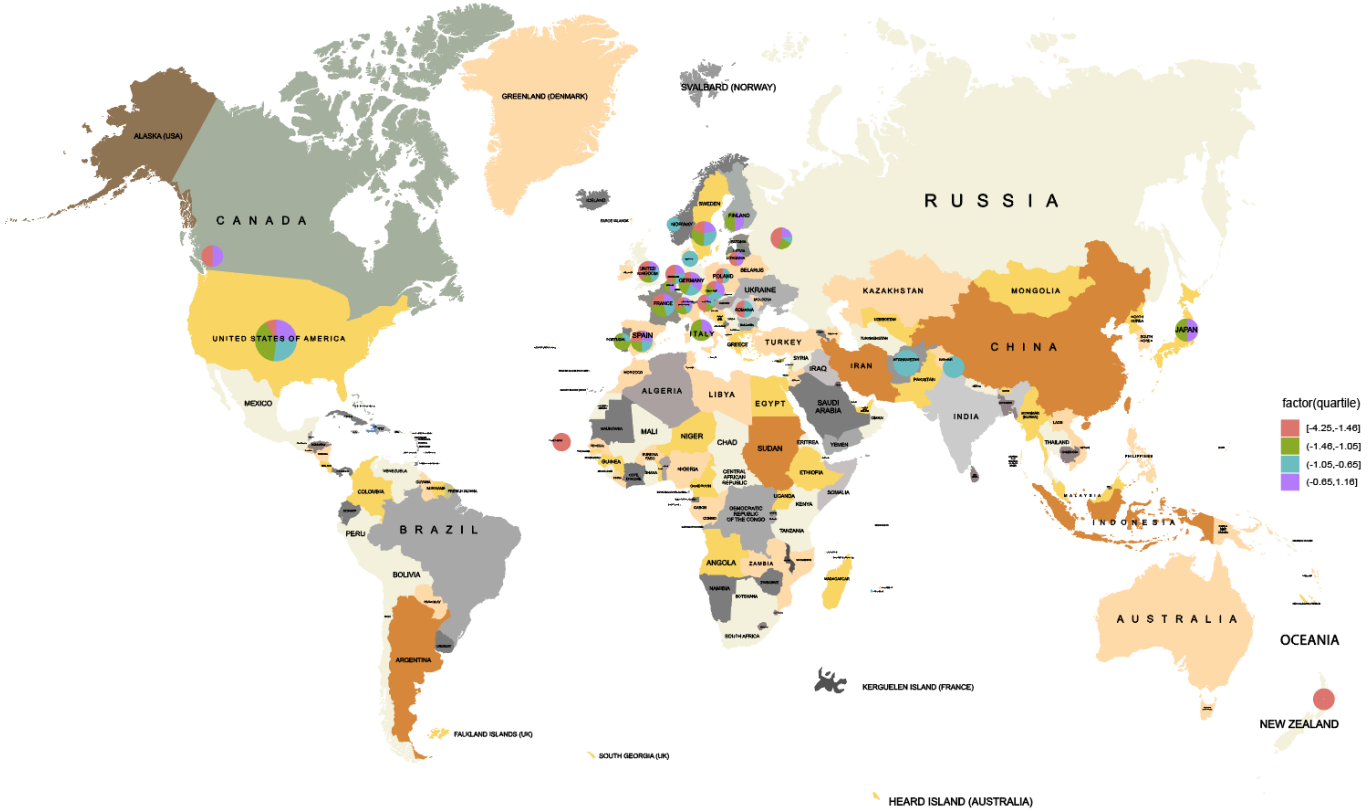

Supplementary Figure S2. Natural variation for BOT-sensitivity in the global population of *A. thaliana*. The BOT-sensitivity (logRI) of accessions is classified in four quartiles and their site of origin assigned to local geographical regions.

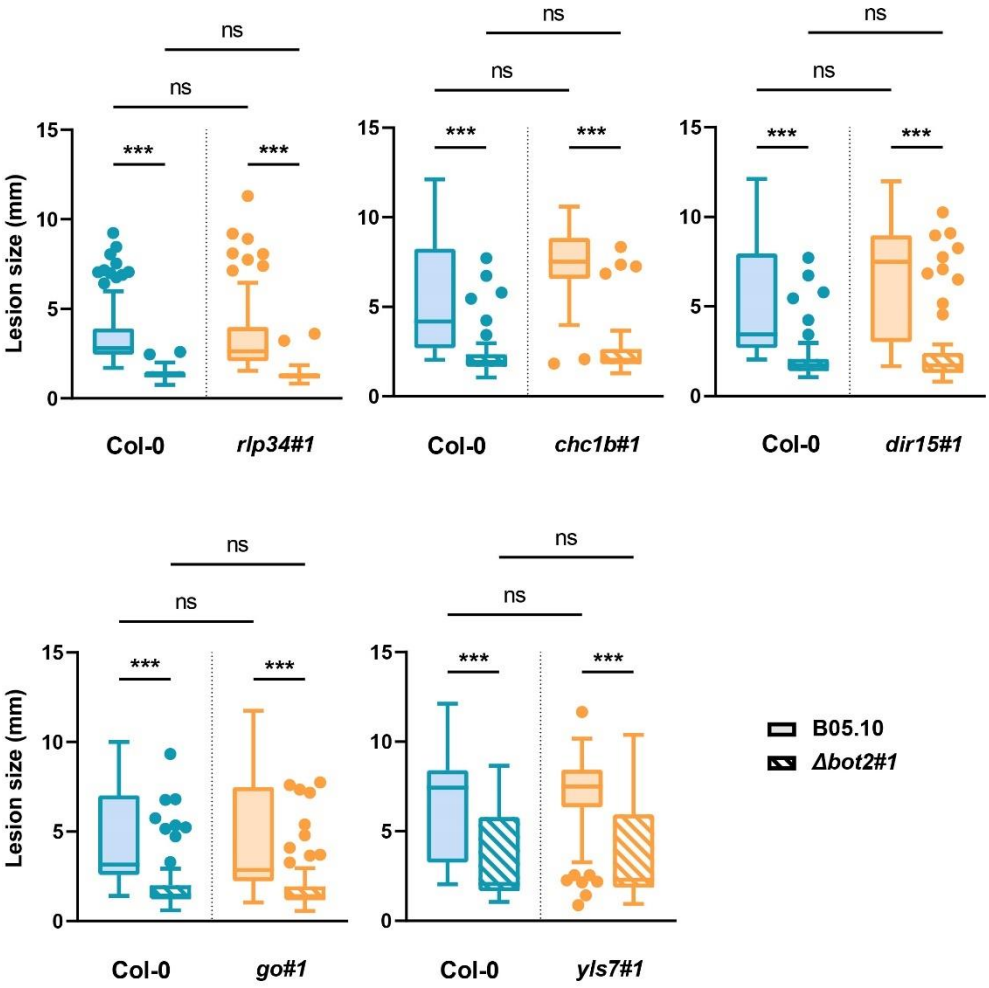

Supplementary Figure S3. Susceptibility to WT *B. cinerea* and a *Δbot2#1* mutant in five *A. thaliana* mutant lines, compared to WT Col-0. The Tukey box plots depict the lesion size caused by the infection of WT and *Δbot2#1 B. cinerea* strains on leaves of Col-0 and mutant plants, and the lesion size is indicated by diameter (mm) measured at 3 dpi. Each box plot includes around 60 total inoculations collected from 2 independent experiments. Statistical analysis was performed using Brown-Forsythe and Welch ANOVA tests (multiple comparisons), significant differences are indicated by asterisks (*** p<0.001) and "ns" for nonsignificant difference.

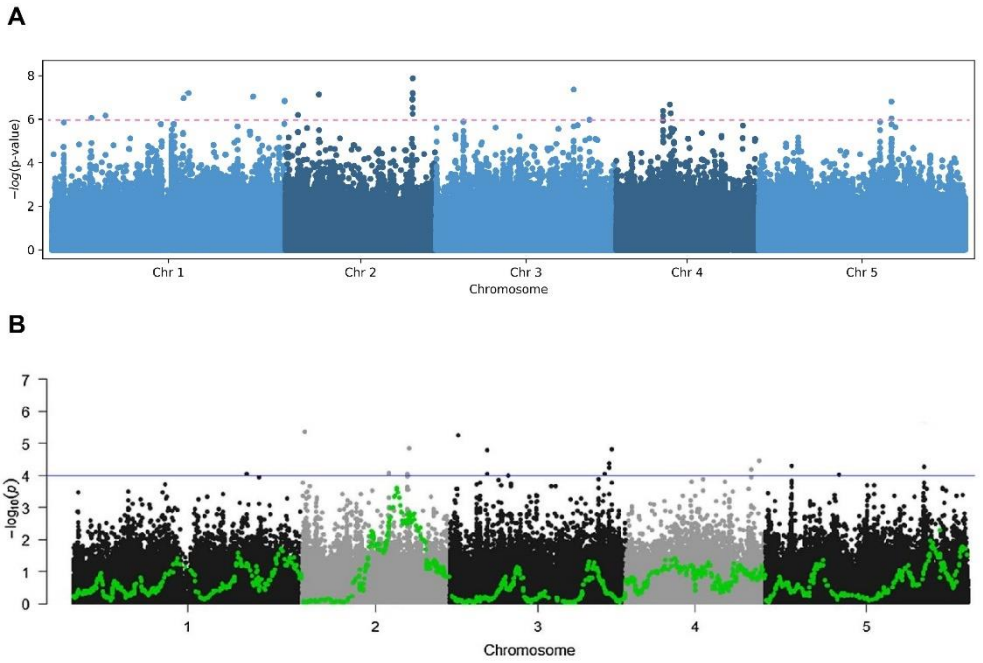

Supplementary Figure S4 Comparison of GWA studies involving *B. cinerea* resistance. **(A)** Genomic SNP association with sensitivity to BOT (this study). **(B)** Genomic SNP association with the level of *B. cinerea* resistance and QTL mapping in the MAGIC population (in green) (Coolen et al., 2019). Significance of SNPs is indicated on the y-axis (− log10(p-values), SNP positions on the five chromosomes are depicted in alternating colours. Horizontal lines indicate significance threshold levels.

A Leaf treated by a droplet of BOT on the surface

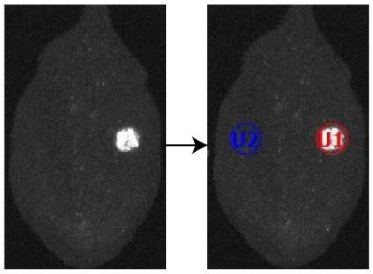

Intensity measured by the volume tool in ImageLab

No.	Label	Mean Value (Int)	Std. Dev.	Area (mm2)
1	U1	1,372.5	823.4	6.7
2	U2	322.0	43.5	6.7

$$\text{Relative Intensity (RI)} = \frac{\text{Mean Value (Intensity) BOT-treated area}}{\text{Mean Value (Intensity) control-treated area}}$$

B Leaf treated by infiltration of BOT

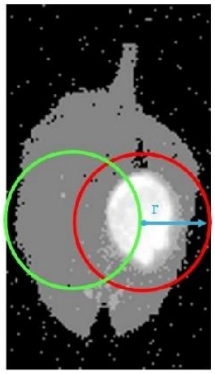

Intensity measured by the python script and data processed in R

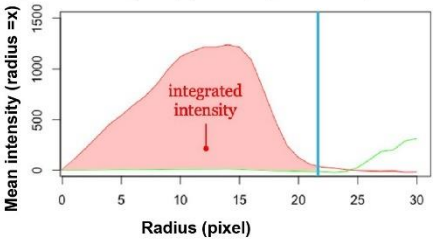

$$\text{Relative Integral Intensity (RII)} = \frac{\text{Integrated intensity BOT-treated area}}{\text{Integrated intensity control-treated area}}$$

Supplementary Figure S5. The BOT-sensitivity of a tested leaf was quantified by either **(A)** the relative intensity (RI) approach or **(B)** the relative integral intensity (RII) approach, depending on whether the leaf was treated by a droplet containing BOT or infiltrated by BOT solution, respectively.

Supplementary Table S1. *A. thaliana* T-DNA mutant lines used in this studies, shown together with their corresponding candidate genes selected from the GWAS result or literature.

Origin	Gene ID	Protein description*	Gene name	Mutant line #1**	Mutant line #2**
Literature & hypothesis	At3g06490	Redox stress sensitivity	*BOS1*	Mengiste et al. (2003)	Salk_076395C
	At5g03280	Impaired ethylene responses	*EIN2*	Alonso et al. (1999)	Salk_086500C
	At3g20770	Impaired ethylene responses	*EIN3*	Chao et al. (1997)	-
	At2g46370	Impaired jasmonic acid signaling	*JAR1*	Staswick et al. (1992)	Salk_059774C
	At1g79340	Metacaspase 4	*MC4*	Salk_097134	-
	At1g79310	Metacaspase 7	*MC7*	Salk_054230	Salk_148148C
	At4g25110	Metacaspase 2	*MC2*	Salk_009045	-
GWAS	AT5G51630	Disease resistance protein (TIR-NBS-LRR class) family	*TNL*	Salk_014431C	Salk_124803C
	AT4G11470	Cysteine-rich receptor-like protein kinase 31	*CRK 31*	Salk_106993C	Salk_113269C

*Information of the descriptions of proteins encoded by these genes was supported by the publicly available sources of Uniprot (https://www.uniprot.org) and the Arabidopsis Information Resource (TAIR: https://www.arabidopsis.org/index.jsp).

** All of the mutant lines #1 were tested first for one experiment and did not show a significant difference in sensitivity to botrydial compared to the WT Col-0, and thus the mutant line was not repeated to be assessed for the BOT-sensitivity and mutant line #2 was not further tested.

Supplementary Table S2. Primers used in this study.

Primer name	sequence (5'-3')	Description
Fw_AT5G39560_qPCR	TAGTTATGTGGCGTCCGGTG	qPCR primers for the Arabidopsis gene GO (AT5G39560)
Rv_AT5G39560_qPCR	CACACAACTTGGGGACCGTA	
Fw_AT1G69580_qPCR	CTCGGAAGTGATGAAGGGGA	qPCR primers for the Arabidopsis gene PHL8 (AT1G69580)
Rv_AT1G69580_qPCR	TTCGTACACGCCTCCATGTC	
AT4G11845_qPCR_fw	TTTTGGAACCGTTTTGCTCGAT	qPCR primers for the Arabidopsis gene STK (AT4G11845)
AT4G11845_qPCR_Rv	AGATTCCTGCATCTGGGTTGT	
Fw_AT4g11830_qPCR	TTGGGGACAGTATGCAGCAG	qPCR primers for the Arabidopsis gene PLDγ2 (AT1G69580)
Rv_AT4g11830_qPCR	TCCTATGATCTTGCCACCGA	
Fw_UB_ori_shifted	CCCTGATGAATAAGTGTTCTACTATGTTTCCG	qPCR primers for the Arabidopsis reference gene UBQUITIN10 (AT4G05320)
Rv_UB_ori_shifted	AACGAAGCGATGATAAAGAAGAAGTTCG	
Salk_LBa1	TGGTTCACGTAGTGGGCCATCG	universal primer for screening SALK T-DNA lines; use it together with specific primers of each mutant line for genotyping
pAC161_o2588	CGCCAGGGTTTTCCCAGTCACGACG	universal primer for screening GABI T-DNA lines; use it together with specific primers of each mutant line for genotyping
SALK_023381C_LP	ACAAGTCGTCCAATTTGGTTG	genotyping mutant line *rlp34#1*
SALK_023381C_RP	TCCAATTGAAGACGGAAACTG	
Salk_127176C_Fw	ACAAGTCGTCCAATTTGGTTG	genotyping mutant line *rlp34#2*
Salk_127176C_Rev	GCCAAAAGAAGATGGGATTTC	
SALK_148581C_LP	AAAAACGTTGCGTTTTGAATG	genotyping mutant line *go#1*
SALK_148581C_RP	ATAGTACCGGTACCGGTGAGG	

Salk_066527C_Fw	AAAAACGTTGCGTTTTGAATG	genotyping mutant line *go#2*
Salk_066527C_Rev	ATAGTACCGGTACCGGTGAGG	
SALK_067928C_LP	ACGACAACTTCCAAACGTTTG	genotyping mutant line *chc1a#1*
SALK_067928C_RP	ATTTTGCAGGGTGTGTGAGTC	
Salk_087757C_Fw	GGAGTCTGATGATGACGATCG	genotyping mutant line *chc1a#2*
Salk_087757C_Rev	TTTCTAGGAGATTCAGCGCAG	
GABI_272G02_Fw	TCCGAGTTGATCTCCATCAAC	genotyping mutant line *phl8#1*
GABI_272G02_Rev	TCATCGAAGCCGTTAATCAAC	
SALK_057434C_LP	ATCAGTTTTCGGGTCAAATCC	genotyping mutant line *rlp35#1*
SALK_057434C_RP	TCATAGATGGTTTCCGGACAG	
SALK_148136C_LP	ACCGGAGTTGTCATCTCTGTG	genotyping mutant line *crk33#1*
SALK_148136C_RP	TTCTTGCCATTCCAAAATCTG	
Salk_119041C_Fw	TATAATCCGAGGATGCGTCAG	genotyping mutant line *crk33#2*
Salk_119041C_Rev	ATTGTACCATGGAAGCGTCTG	
Salk_102871C_Fw	CTGAGGGTGAACAGGCTGTAG	genotyping mutant line *dir15#1*
Salk_102871C_Rev	TGTTTACAGGAAAAAGATTTTCTCC	
Salk_014510C_Fw	GAAACCCTAGATGTTCTGCCC	genotyping mutant line *pldy2#1*
Salk_014510C_Rev	TGGGATTCAAACAAGGACTTG	
SALK_208188C_LP	TATTGGTCAAATGGCTTGTGC	genotyping mutant line *chc1b#1*
SALK_208188C_RP	TGATTCATGCGCTAATCTTCC	

The following Supplementary materials are available to be downloaded from the "Supplementary materials_PhD thesis_Qin(2023).zip" file, and thus only legends are shown below.

Supplementary Data S1. The RI value and logRI of each ecotype (sheet 1) as well as their origins (country, longitude and latitude, in sheet 2) that were used as the input data for the GWAS analysis.

Supplementary Data S2. Sheet 1 contains all ~240 genes located in a window of 20 kb surrounding the significant SNP (10 kb up- and down-stream), (Supplementary Data S2); Sheet 2 contains a final set of 36 candidate genes.

Supplementary Data S3. Contains scripts (a python script and an R studio script) used for the quantification of integrated red light intensity upon BOT treatment and control treatment.

Chapter 8

General discussion

The necrotrophic plant pathogen *Botrytis cinerea* secretes an array of effectors during infection on host plants. In this thesis, the term effector is defined as any secreted molecule from a pathogen that can suppress or induce plant defense responses and modulate plant physiology (Chapter 1). Effector molecules can be classified into four groups: 1. secreted proteins that are usually cysteine-rich and small; 2. small RNAs (sRNAs) that can be translocated into host cells and interfere with the expression of genes involved in plant immunity; 3. secondary metabolites (SMs) that modulate host immunity and physiology; and 4. plant hormones produced by a pathogen. Experimental results of this thesis especially encompassed the contribution of *B. cinerea* sRNAs (Chapter 2) and two major phytotoxic SMs (Chapter 4 and 6) to the virulence of the fungus on different plant species. Besides, we examined the role of one phytotoxin, botrydial (BOT), in triggering cell death in lilies and in the virulence of the lily specialist *B. elliptica* (Chapter 5). To investigate the plant – *B. cinerea* interaction from an inverse angle, we studied the effect of a plant sRNA that was predicted to target an effector protein of *B. cinerea* (Chapter 3) and attempted to identify plant genes that participate in the response of *Arabidopsis thaliana* to BOT (Chapter 7).

The effectiveness of the natural occurrence of cross-kingdom RNA interference is disputable

The phenomenon that sRNAs derived from *B. cinerea* (Bc-sRNAs) can be naturally transferred into plant cells and subsequently down-regulate the transcript level of matching host genes by RNA interference (RNAi) was first reported by Weiberg et al. (2013). As some of the targeted plant genes participate in immune responses, the silencing mediated by fungal sRNAs may favor the invasion of the pathogen (Weiberg et al., 2013). For this reason, fungal sRNAs which play a role in regulating host immunity via the natural occurrence of cross-kingdom RNA interference **(**ckRNAi) can be considered as effectors. These Bc-sRNAs are initially generated through the cleavage of non-coding single-stranded RNAs with hairpin structures and double-stranded RNAs (dsRNAs) by DCL proteins in the fungus, before being translocated into host cells (Weiberg et al., 2013). Complexes composed of fungal sRNAs, plant AGOs and auxiliary proteins execute silencing of target transcripts in the host plant (Weiberg et al., 2013). The contribution of Bc-sRNAs to fungal virulence was tested by Weiberg et al. (2013) and later by our study in Chapter 2 (Qin et al., 2023), via the generation of *B. cinerea* double mutants that were defective in the only two *Dicer-like* genes *Bcdcl1* and *Bcdcl2*. The virulence of the mutant obtained by Weiberg et al. (2013) was strongly impaired, but this *ΔBcdcl1/ΔBcdcl2* mutant displayed pleiotropic phenotypes *in vitro* (namely retardation in growth rate and aberrant sporulation).By contrast, three

independent *ΔBcdcl1/ΔBcdcl2* transformants that we generated showed neither reduction in virulence on four distinct host species, nor any detectable growth defects as reported by Weiberg et al. (2013). The divergent observations for the virulence of *ΔBcdcl1/ΔBcdcl2* mutants from Weiberg et al. (2013) and Chapter 2 of this thesis triggered a debate on whether Bc-sRNAs truly play a role in the virulence of *B. cinerea*.

Except for *B. cinerea*, the occurrence of ckRNAi has been reported in other plant-associated microbes. The obligate biotrophic oomycete *Hyaloperonospora arabidopsidis* (*Hpa*) was reported to deliver sRNAs to silence *Arabidopsis thaliana* (Arabidopsis) defense genes and these Hpa-sRNAs contribute to the virulence of the pathogen (Dunker et al., 2020). The conclusions were supported by the enhanced resistance to *H. arabidopsidis* in Arabidopsis *ago1* mutants and also by transgenic Arabidopsis plants expressing a short-tandem-target-mimic RNA to block three specific Hpa-sRNAs (Dunker et al., 2020). Besides, it has been recently reported that a microRNA from the ectomycorrhizal fungus *Pisolithus microcarpus* can enter root cells of its host plant and regulate host transcript levels to stabilize the mutualistic interaction (Wong-Bajracharya et al., 2022). The application of synthetic sRNAs that inhibit the endogenous fungal microRNA led to reduced capacity of the fungus to colonize root tips (Wong-Bajracharya et al., 2022). It is worthwhile to further investigate whether the sRNAs produced by *H. arabidopsidis* and *P. microcarpus* are indeed important for the colonization on their respective host plants, via more direct approaches such as generating mutants of the microbes lacking their respective *dcl* genes. Furthermore, it seems plausible that the sRNAs derived from the biotrophic pathogen *H. arabidopsidis* and the mycorrhizal *P. microcarpus* could contribute more effectively to the colonization of the host via ckRNAi than is the case of a versatile killer like *B. cinerea*. We have extensively discussed in Chapter 2 the possible explanations why, in my opinion, the Bc-sRNAs may not significantly contribute to virulence of *B. cinerea,* especially the highly aggressive strain B05.10 which was used in both studies of Weiberg et al. (2013) and Qin et al. (2023). Considering that the decisive processes for determining a successful or failed infection by *B. cinerea* in the host occur roughly at 16 hours post inoculation (hpi), the ckRNAi would have an impact on the fungal colonization only if essential plant immunity genes could be suppressed by Bc-sRNAs at even earlier phases. However, the amount of fungal biomass is extremely low as compared to plant biomass at the early interaction stage, reflected by ~1% fungal sRNAs (or mRNAs) in the total pool of sRNA (or mRNAs) in the whole dataset (Chapter 2). Therefore, it is highly unlikely that the sRNAs produced by *B. cinerea* at this phase would achieve a vigorous silencing effect on plant transcripts. Although it may happen that the primary silencing of a target gene in the plant cell(s) would result in the production of larger amounts of secondary sRNAs, this procedure would take some time and may not be

sufficiently rapid to interfere with the fungal invasion processes mediated by cell-wall degrading enzymes and phytotoxic molecules (proteins and SMs). Once lesion expansion has been initiated, triggering plant defense responses, such as reactive oxidative species (ROS) production and host programmed cell death, would actually facilitate the expansion and consumption of dead tissues by *B. cinerea* instead of restricting the fungal invasion. Unlike necrotrophs that feed on dead host tissues, the compatible colonization of biotrophic and symbiotic microbes that grow in between living plant cells requires continuous suppression of host immune responses and ultimately prevention of HR. In such cases, the interaction would last sufficiently long for microbial biomass to accumulate, and the power of ckRNAi mediated by sRNAs derived from these microbes might be effective in attenuating host immunity during the interaction.

When turning to the inverse side of the plant-microbe interaction, plant sRNAs have also been reported to regulate transcript levels in microbial pathogens through naturally occurring ckRNAi. It has been demonstrated that a host plant can secrete exosome-like vesicles containing sRNAs which can subsequently be taken up by *B. cinerea* hyphae at the infection site (Cai et al., 2018). In Chapter 3 of this thesis, we studied the effect of a single tomato sRNA on silencing its sole predicted Bc-mRNA target. Although we could not observe any impact of sRNA1187 on the transcript level of *Bcspl*1, we discussed why it is still possible for plant sRNAs to have an impact on the expression of *B. cinerea* genes that are involved in fungal development or virulence. To directly prove the effect of plant sRNAs in naturally occurring ckRNAi, however, it remains challenging to design feasible experiments without disturbing the plant genes that may be important for the endogenous RNAi machinery or for plant fitness.

The role of BOT is not confined to the induction of host (programmed) cell death

As one of the two major phytotoxic SMs produced by *B. cinerea*, BOT has been studied more extensively than other phytotoxins of this fungus. Purified BOT can induce chlorotic symptoms and tissue collapse on leaves and fruits of several dicotyledonous plant species (Colmenares et al., 2002; Rebordinos et al., 1996; Rossi et al., 2011). The phytotoxic activity of BOT was further studied in Chapters 4, 5 and 7, resulting in several novel findings. First, BOT-triggered necrotic symptoms were observed on leaves of dicots, some of which have not been tested before (Chapter 4). In addition, we report for the first time that BOT can also induce cell death in monocots, including lily, onion, wheat, maize and two model grass species from the *Digitaria* genus (Chapters 4 and 5). In Chapter 7, we present evidence that BOT-triggered plant responses resembling the common outputs of effector-triggered immunity in Arabidopsis, and the BOT-induced programmed cell death (PCD) was likely

activated through the signaling cascade for apoptosis (Figure 1A). Despite that all tested plant species and cultivars responded to BOT treatment in this thesis, we observed notably different BOT-sensitivity levels and necrotic symptoms. For instance, we observed a large variation in BOT-sensitivity among 333 tested Arabidopsis ecotypes, which was used as input for a genome-wide association study (GWAS) in order to identify plant genes that are involved in the response to BOT. Since the BOT-deficient *ΔBcbot2* mutant was almost avirulent on Arabidopsis (Col-0) (Chapter 4), we hypothesized that Arabidopsis genes contributing to BOT-sensitivity should also confer some degree of susceptibility to *B. cinerea*. In line with this hypothesis, the Arabidopsis mutant in a serine/threonine kinase gene (*STK,* AT4G11845) identified by the GWAS showed enhanced cell death response to BOT as well as increased susceptibility to *B. cinerea*.

However, this correlation could not be simply applied to other pathosystems which were studied in this thesis. When investigating the role of BOT in the *B. elliptica* – lily interaction in four lily cultivars (Chapter 5), we did not observe a complete correlation between the BOT sensitivity and the relative virulence of the *B. elliptica ΔBebot2* mutants as compared to the wild type (WT) fungus. Specifically, there was one Asiatic cultivar showing low BOT-sensitivity, while exhibiting the most significant difference in the susceptibility to *ΔBebot2* mutants compared to the WT *B. elliptica.* To explain this observation, we propose a synergistic action of BOT with other virulence factors of *B. elliptica* only in this lily genotype but not in three other genotypes (Chapter 5). Furthermore, Chapter 6 illustrates that deleting BOT (and botcinic acid, BOA) had a drastic impact on the capability for *B. cinerea* to produce expanding lesions and on the lesion expansion rate when inoculated in a medium without yeast extract. We observed that BOT (and BOA) have a quantitative contribution in fungal virulence that is at least as important as that of 12 cell death-inducing proteins (CDIPs), although some of these *CDIP* genes had higher expression levels during the first 24 h after inoculation. It is possible that BOT either induces cell death more rapidly or more effectively, or that the type of PCD triggered by BOT is unique, and more favorable for the pathogenicity of *B. cinerea* than the cell death inflicted by CDIPs. Nonetheless, we could not exclude that the simultaneous production of BOT and other virulence factors may act synergistically to manipulate the host physiology and/or the induction of PCD (Figure 1B), which was eventually manifested by a dramatic reduction in virulence of the *ΔBcbot2* (and *ΔBcbot2ΔBcboa6*).

In addition to the aforementioned effects on physiological process in the host plant, BOT has been reported to have an antagonistic effect on other microbes. Vignatti et al. (2020) demonstrated that the *in vitro* growth of several bacteria, collected from the rhizosphere or phyllosphere of horticultural crops, was inhibited when incubated with either pure BOT

or with BOT-producing *B. cinerea* strains, alongside BOT-deficient strains serving as controls. Vignatti et al., 2020 proposed to include the tolerance to BOT as one of the biological criteria for selecting biocontrol agents against *B. cinerea*. Furthermore, studies by Malmierca et al. (2015 & 2016) showed that BOT can participate in a chemical dialogue between fungi when confronted with one another. On the one hand, BOT as a pure chemical strongly reduced the transcript levels of *Trichoderma arundinaceum* genes involved in biosynthesis of the antimicrobial sesquiterpene, Harzianum A (HA). Conversely, HA as a pure chemical strongly enhanced the expression of the BOT biosynthetic gene cluster in *B. cinerea.* When *T. arundinaceum* was co-cultured with *B. cinerea* the amount of HA production was reduced as compared to the *T. arundinaceum* single culture, but when *T. arundinaceum* was co-cultured with a *B. cinerea* mutant strain lacking BOT production, the HA production increased to levels even higher than in the *T. arundinaceum* single culture. These results indicate that fungi may communicate by means of SMs during microbial interaction and one should consider that BOT may play such a role in *B. cinerea* besides its activity as a phytotoxin.

Since *B. cinerea* is an airborne pathogen that infects all above-ground host tissues, it will be most relevant to study the potential of BOT for manipulating the phyllosphere and endosphere microbiome rather than the rhizosphere microbiome (Figure 1C). On the one hand, BOT might inhibit plant-associated beneficial microbes that enhance host immunity or physiological development. On the other hand, *B. cinerea* may inhibit the growth of other (competing) pathogenic microbes by secreting BOT to favor the niche adaptation of the fungus in the host.

To study the effect of botrydial on the phyllosphere microbial community *in vitro* and *in vivo*, I have performed some pilot experiments (data not shown in this thesis). To obtain a first overview of whether bacteria or fungi from the tomato leaf phyllosphere could tolerate or thrive in the presence of BOT, healthy tomato leaves were ground and incubated with botrydial in MS medium. After two days the samples were plated on solid media upon serial dilution. Bacterial and fungal colonies with different appearances were observed between BOT treatments and the acetone control, and also between different media. This observation encouraged me to perform 16S sequencing with DNA samples extracted from tomato leaf tissues infected by *B. cinerea* WT and the *ΔBcbot2* mutant. The results were inconclusive due to the high abundance of plant DNA which yielded mainly 16s rDNA sequence from plant chloroplasts with the primer sets that the sequencing company used for 16S sequencing. This issue can technically be solved by using specific blockers for chloroplast rDNA and more specific primers to amplify the microbial 16S rDNA before sequencing the PCR amplicons. Once those technical issues can be solved, one could obtain

a comprehensive view of the distribution of bacteria and fungi in the samples containing WT *B. cinerea* or the BOT-deficient mutant. Besides such experiments, it is recommended to compare the virulence of WT *B. cinerea* and the *ΔBcbot2* mutant on plants, grown under sterile conditions from sterilized seeds, with that on plants grown under normal greenhouse conditions. If an effect of BOT on the host microbiome indeed contributes to the infection of *B. cinerea*, one might expect a stronger reduction in virulence of *ΔBcbot2* on non-sterile plants than on sterile plants. However, though the sterile plants are supposed to be free of acquired phyllospheric and rhizospheric microbes, the endophytic microbes in seeds could still be present in such plants and may still participate in host immunity against *B. cinerea*.

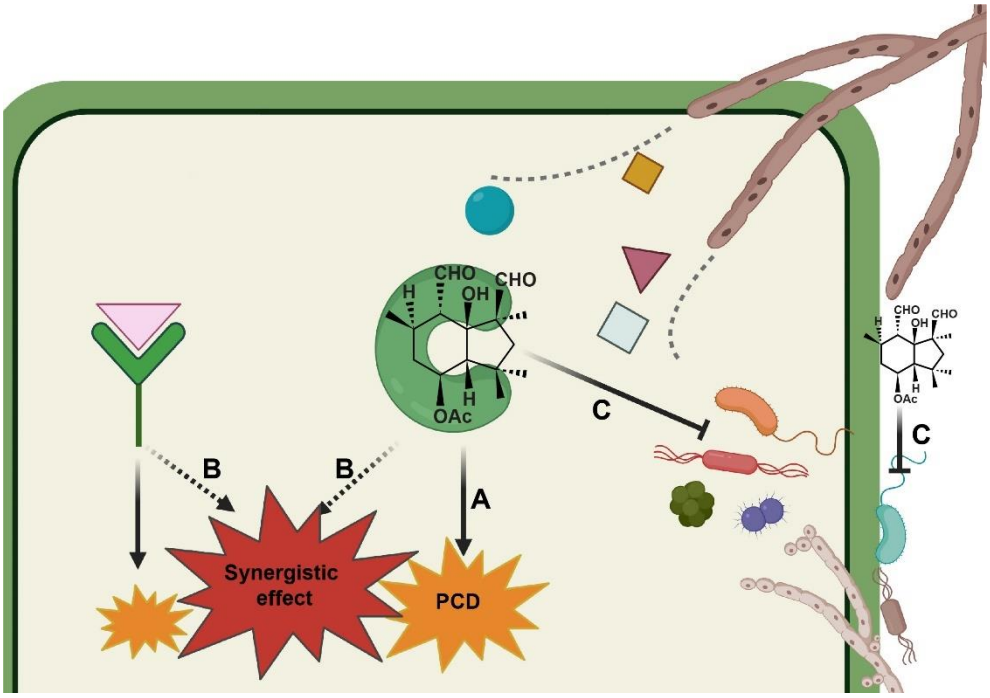

Figure 1. The (proposed) multi-functional roles of the phytotoxin botrydial (BOT) produced by *Botrytis* during fungal infection. **(A)** The phytotoxic activity that directly induces PCD in the host; **(B)** The hypothetical synergistic effect of BOT together with other virulence factors of *Botrytis*; and **(C)** The potential manipulation of the host microbiome which favors the niche adaptation of the pathogen. The figure is created with BioRender.com and the chemical structure is drawn using PubChem Sketcher V2 (https://pubchem.ncbi.nlm.nih.gov//edit3/index. html).

In contrast to the functions of BOT as a virulence factor of *Botrytis* species for their necrotrophic infection, it is unlikely that BOT contributes to asymptomatic colonization. The BOT gene cluster is not only present in pathogenic *Botrytis* species, but also in *B. deweyae* (Valero-Jiménez et al., 2020) colonizing *Hemerocallis* (daylily) in an asymptomatic manner

as an endophyte. This fungus can occasionally cause necrotic symptoms on the tips of young shoots referred to as “spring sickness” (Kan et al., 2014). Assuming that *Hemerocallis* is sensitive to BOT, it would be logical to assume that BOT is not produced the asymptomatic colonization phase. Also *B. cinerea* can under certain circumstances colonize plants in an asymptomatic manner on several plants including *Primula* hybrids, lettuce and Arabidopsis (Barnes & Shaw, 2002; Sowley et al., 2010; Shaw et al., 2016). Also in such interactions, one could propose that production of BOT by the fungus would disturb the delicate harmonious balance between the host and the endophytic fungus. A study on the gene expression in *B. cinerea* in asymptomatically colonized Arabidopsis plants indeed revealed that the expression of the BOT biosynthetic gene *Bcbot1* in such plants was undetectable (Emmanuel et al., 2018). This indicates that BOT is redundant for *B. cinerea* to colonize its hosts as an endophyte and the same might be true for the *B. deweyae* – daylily interaction.

Inoculation conditions dramatically affect *Botrytis* disease development during artificial infections

In studies on plant-pathogen interactions, it is common to illustrate the contribution of virulence factors to the aggressiveness of a pathogen based on the difference in lesion size or biomass of mutant strains lacking the corresponding gene(s) as compared to the recipient WT fungus, using artificial infection assays in the laboratory. These infection assays can be performed under different conditions, with variables in the inoculation medium, the fungal tissue (mycelial agar plugs or conidia), the plant growth conditions, and/or the incubation conditions after inoculation. In this thesis, all *B. cinerea* virulence assays were performed by inoculating small droplets of conidia suspensions on the surface of non-wounded plant tissues. When the same tomato genotype was inoculated with the same *ΔBcbot2ΔBcboa6* mutant using three different media in Chapter 4 and Chapter 6, we observed three different levels of reduction in the virulence of this mutant, ranging from non-virulent to slightly less virulent than the WT fungus. Thereby, the roles of BOT and BOA could have been interpreted to be from minor to essential in the virulence of *B. cinerea*.

In view of the high impact of inoculation conditions on the disease severity, it is worthwhile to assess the virulence of some *Botrytis* strains used in this thesis again by adjusting the inoculation method. For instance, the three *ΔBcdcl1/ΔBcdcl2* transformants generated in Chapter2 displayed similar virulence to the recipient strain on tomato, *Nicotiana benthamiana*, Arabidopsis and French bean plants. Since the WT fungus could not expand from the primary inoculation areas on Arabidopsis and French bean plants when the conidia were suspended in the Gamborg B5 medium, we performed all infection assays in Chapter 2 using PDB as the inoculation medium on all tested hosts. If the inoculum contains a less

nutrient-rich medium or/and a lower spore density, we might be able to witness a detectable reduction in virulence of the *ΔBcdcl1/ΔBcdcl2* mutants on tomato.

B. cinerea infection assays can also be performed by placing agar plugs of the fungus on plant tissues. Agar plugs of an aggressive *B. cinerea* isolate containing physiologically active mycelia grown on potato dextrose agar (PDA) were found to be more virulent than conidia suspended in the liquid PDB medium (Oirdi et al., 2009). In our research group, we always wash the freshly collected *B. cinerea* conidia with sterile water and store them in cold condition to prevent these conidia from (fast) germination before using them in infection assays. Thus, when inoculation is performed with conidia suspensions, the first few hours are required for conidia to reactivate their metabolism before they germinate. It can be imagined that mycelia from agar plugs penetrate the plant surface more rapidly than the germ tubes that emerge from conidia, and there are likely many genes that are differentially expressed in those active mycelia as compared to young germlings. Moreover, the inoculation with *B. cinerea* agar plugs will result in a specific infection structure, referred to as " infection cushions" which are multicellular appressoria, distinct from the unicellular appressoria commonly formed when using a conidial suspension as the inoculum (Choquer et al., 2007a). Choquer et al. (2021) reported that genes related to the production of SMs, cell death inducing proteins and cell wall-degrading enzymes, were up-regulated in infection cushions *in vitro* and *in planta.* A recent study reported that a *ΔBcLysM1* mutant displayed a lower disease incidence and retarded expansion of the secondary lesions only when the bean leaves were inoculated with mycelial plugs, while the same mutant was similarly virulent as the WT fungus when inoculated with conidia (Crumière et al., 2022). This study also showed up-regulation of the *BcLysM1* gene exclusively in infection cushions in the early phase of infection, and demonstrated an additional role for the BcLysM1 effector in adhesion to the host besides the chitin-binding feature that is commonly shared among fungal LysM effectors (Crumière et al., 2022). Additionally, the agar plugs containing fungal hyphae are likely to contain CDIPs and phytotoxic SMs that have been produced and accumulated in the pre-culture (where the agar plugs are excised from), which could boost the fungal infection from the very early phase of the interaction. Finally yet importantly, one should consider that the number of conidia in a droplet containing spore suspension can be quantified and standardized across different experiments, while the fungal biomass of mycelia in an agar plug cannot be strictly unified. Therefore, I would recommend to perform the disease assay using conidia inoculations in most cases when investigating the role of novel virulence factors, unless the gene of interest is known or anticipated to be exclusively expressed in infection cushions.

The utilization of effectors of filamentous pathogens as tools in mining host resistance resources

It is conceptually well accepted that using effectors as tools can simplify or accelerate the breeding process for resistance against the pathogens producing these effectors. Host receptor proteins that are responsible for the perception of effectors, which are secreted by (hemi)biotrophic pathogens and act as Avirulence (Avr) proteins, have been extensively studied and this perception was described to be based on gene-for-gene interactions (Flor, 1954; Keen, 1990b). The hypersensitive response (HR) triggered by such interactions allows the host receptor genes for the matching Avr genes to be used as resistance (*R*) genes in breeding practice (Giraldo & Valent, 2013). Conversely, host receptor genes for matching cell death-inducing proteinaceous effectors produced by necrotrophs serve as susceptibility (*S*) genes, and these interactions fit an inverse gene-for-gene model (Faris & Friesen, 2020). Well-developed and newly emerging experimental and bioinformatic methods have effectively contributed to the in-depth understanding of the interactions between protein effectors and their receptor proteins. For instance, yeast two-hybrid screening and co-immunoprecipitation (Co-IP) have been widely employed over the past three decades (Cristea et al., 2005; Fields & Song, 1989) to study the physical interactions between proteins. New techniques are recently emerging such as the proximity labelling based on systems like Biotinylation (BioID) (P. Li et al., 2017) and TurboID (Branon et al., 2018) which have enabled the detection of weak interactions and indirect binding between proteins. A recent exciting study has reported that the artificial fusion of an intracellular nucleotide-binding, leucine-rich repeat immune receptor (NLR) to a “nanobody”, which is a single-domain antibody generated against a given antigen, can confer plant resistance against pests (Kourelis et al., 2023). As a proof-of-concept, Kourelis et al. (2023) replaced the effector-binding domain of an NLR by a nanobody perceiving the green fluorescent protein (GFP) and transiently expressed this NLR-nanobody fusion protein in *N. benthamiana*, resulting in resistance against the recombinant GFP-labeled Potato Virus X. Although the study did not yet provide evidence for a NLR-nanobody that recognizes a real effector derived from a pathogen, such “pseudo-adaptive immunity” has the potential to create functional antibodies against effector proteins derived from plant parasites in the near future.

Compared to effector protein – plant receptor pairings, much less is known for the phytotoxic SM-plant target interactions that are more difficult to be experimentally validated. Within the category of phytotoxins that include host specific toxins (HSTs) and non-host-specific toxins (nHSTs), the plant targets for HSTs have been better studied as their

interactions usually fit the inverse gene-for-gene model. For example, The sensitivity to the HST victorin produced by the oat fungal pathogen *Cochliobolus victoriae* as well as susceptibility to this fungus are conferred by a single locus in oat for which the causal gene has not been characterized or by the *LOV1* gene in Arabidopsis (Wolpert & Lorang, 2016). For the wheat- *Bipolaris sorokiniana* (spot blotch fungus) pathosystem, all wheat accessions carrying the *Tsn1* allele were susceptible to *B. sorokiniana* isolates possessing the *ToxA* gene (Navathe et al., 2020). By contrast, a nHST might target some conserved plant components or activate conserved signaling cascades among different plant species. Therefore, we should aim for identifying plant components that are dispensable for the fitness of the host and (specifically) important for the response to the nHST of interest. As reported by Rossi et al. (2011) and described in Chapter 7 of this thesis, the salicylic acid (SA) signaling pathway is positively associated with the strong response to BOT. Nevertheless, it may not be a viable strategy to manipulate SA signaling in a crop to reduce the sensitivity to BOT and thereby increase resistance to *B. cinerea*, since the host may consequently become more susceptible to biotrophic pathogens (van Butselaar & Van den Ackerveken, 2020). It would be interesting to test the Arabidopsis mutant lines, which showed decreased BOT-sensitivity in Chapter 7, for their resistance to *B. cinerea* as well as other pathogens with different lifestyles (e.g., the biotroph *H. arabidopsidis* and hemibiotroph *Verticillium dahliae*).

Prior to using necrotrophic effectors as tools to accelerate the resistance breeding against the corresponding pathogens, one should select appropriate effector individuals by prudently setting certain criteria. In our opinion, the most important features should be that the effector is important for virulence or host-specificity, and/or the sensitivity to this effector is quantitatively correlated with the susceptibility to this necrotrophic pathogen among the tested accessions of certain host species (or closely related species). In this thesis, we observed that BOT plays an important role for *B. cinerea* in infecting Arabidopsis and tomato. Hence, it is rational to explore Arabidopsis genes that are involved in the response to BOT and these plant genes are predicted to function as *S* genes against the fungus. We also proposed in the discussion of Chapter 7 that a similar GWAS approach can be applied to tomato, in order to identify tomato *S* genes to *B. cinerea*. On the contrary, the BOT-sensitivity level of the four tested lily cultivars did not correlate to their susceptibility to *B. elliptica*. This suggests that screening lily cultivars for low sensitivity to BOT will probably not distinguish resistant from susceptible lilies. An interesting but puzzling example is the utilization of the cytotoxic protein NEP1 produced by the onion pathogen *B. squamosa* as a tool in screening onion accessions. Steentjes et al. (2022) detected by quantitative trait locus (QTL) mapping a genomic region that confers sensitivity to BsNEP1 in an interspecific *Allium* trihybrid population (*A. cepa* x (*A. roylei* × *A. fistulosum*)), and this region colocalized

with a QTL that had been previously identified for the host susceptibility to *B. squamosa* in *A. roylei*. However, the *ΔBsnep1* mutant was similarly virulent as the WT *B. squamosa* on seven tested onion cultivars, and the severity of the necrotic response to BcNEP1 was not correlated with the host susceptibility to *B. squamosa* within these seven onions (Steentjes et al., 2022). One logical hypothesis would be that the QTL characterized for the BsNEP1-sensitivity in onion may contain genes that participate in a downstream signaling pathway, which is convergent from the activation by multiple cytotoxic effectors derived from the pathogen. In this case, BsNEP1 on its own is not a virulence factor of *B. squamosa,* but a group of effectors including BsNEP1 could function as a virulence pool of the fungus. Then, using such pool of effectors to screen onion cultivars may result in an association between cell death response to the effector cocktail and the host resistance to *B. squamosa.*

Urgency for improving reference genome assemblies and annotation

Genomic, transcriptomic and sRNA-sequencing approaches have been exploited in the studies described in this thesis. A sRNA/mRNA-sequencing dataset and another independent mRNA-sequencing dataset of *B. cinerea*-tomato early-phase interactions were generated as described in Chapters 2 & 3, and in Chapter 6, respectively. Reads from these datasets were mapped and analyzed according to genome assemblies and annotations of *B. cinerea* (van Kan et al., 2017) and tomato (Sato et al., 2012). The gapless fungal genome allowed us to identify a much larger number of Bc-sRNAs in our dataset as compared to that in the *B. cinerea*-tomato sRNA pool earlier reported by Weiberg et al. (2013), which made use of a draft assembly of the *B. cinerea* genome (Amselem et al., 2011). In addition, we used a much higher read depth than Weiberg et al. (2013) for sequencing the *in planta* samples. However, we noticed during our data analyses that the latest annotation of the tomato genome (ITAG4.0) (Hosmani et al., 2019) had eliminated multiple gene models or altered the lengths of transcripts which were previously annotated in the earlier version ITAG3.2 (Sato et al., 2012). We performed the molecular quantification experiments for nine selected tomato mRNAs that were predicted targets of Bc-sRNAs in 2017, when ITAG3.2 was the latest version of annotation at that moment. Unexpectedly, only two out of the nine selected tomato transcripts remained unchanged in the “upgraded” ITAG4.0 annotation of tomato genes, and several of the seven ITAG3.2 transcripts were shortened or deleted from ITAG4.0, despite the fact that we detected their expression in RT-qPCR experiment. As a result, we decided to stay with the older version of the annotation (ITAG3.2) in Chapter 2. This experience raised serious questions regarding the quality of the tomato genome annotation, and it might be worthwhile for the tomato community to invest

in improving the genome annotation to a more satisfactory level for such an economically and scientifically important plant species in the future.

By virtue of the 1001 Genomes project for the model plant species *A. thaliana*, we performed GWAS (Chapter 7) with publicly available single nucleotide polymorphism (SNP) markers for more than a thousand accessions (Weigel & Mott, 2009). However, it is inevitable that there are some heterozygous regions in the genomes of accessions from the HapMap population. Raw reads from these heterozygous regions have been discarded and then became "invisible" in the genomes, and were not included in the SNP matrix. For instance, the accession Uk-1 was (almost) insensitive to BOT, and thus was chosen to be crossed with the sensitive accession Col-0 for a bulk segregant analysis (Chapter 7). One the one hand, when we redid the mapping using public raw sequence reads of this accession (1001 Genomes project), we found that Uk-1 contains up to 0.3 – 0.8 % heterozygous SNPs in some regions throughout all five chromosomes (data not shown in this thesis). The Uk-1 seed batch that was used for sequencing was apparently not homozygous, either because the stock center did not make an effort, or because homozygosity of some loci could be lethal and only plants with heterozygous alleles in these loci have survived. On the other hand, the SNP matrix only provides information for SNPs and indels in Uk-1 that are distinct from the reference Col-0 genome, as reads of Uk-1 were only mapped to the Col-0 genome instead of being assembled *de novo*. Therefore, regions or genes that are uniquely present in Uk-1 and absent in Col-0 are overlooked. It is conceivable that heterozygous alleles and unique genes in Uk-1 might be associated with the insensitivity to BOT, which is the trait that we investigated in Chapter 7. Therefore, the Uk-1 genome should preferably be re-sequenced in a higher read-depth using our own seed stock and assembled to obtain a reliable reference Uk-1 genome. This new assembly, including information about heterozygosity, should be shared with the Arabidopsis community.

The functional annotation, which refers to the assignment of functional roles to coding sequences (CDSs) in (predicted) gene models, is the key to the genomic and transcriptomic analyses for unraveling biological significance. Typically, the functional annotation process includes the identification of domains and motifs and ontology description (Dominguez et al., 2018). The combined data resulting from these three sources would finally present highly valuable gene definitions. Among the differentially expressed genes in the transcriptomic data or candidate genes identified from the GWAS in this thesis, we usually focused on *B. cinerea* genes that are related to virulence and development, and on plant genes that are involved in defense responses. One would assume that the gene functions in the model plant *A. thaliana* should have been reasonably well-annotated, especially in the dataset published on The Arabidopsis Information Resource (TAIR,

https://www.arabidopsis.org/index.jsp). However, we observed that the candidate gene AT4G11845 identified from our GWA mapping, is described as "Interleukin-1 receptor-associated kinase 4 protein" according to the latest Arabidopsis genome information (Araport11). This annotation cannot be meaningful, as Interleukin-1 receptors are involved in response to inflammations and are only present in vertebrates. Subsequently, we inspected the annotation of this gene in the UniProt database (https://www.uniprot.org/), which resulted in an automatic annotation of "serine/threonine kinase that acts as a positive regulator of brassinosteroid (BR) signaling downstream of the receptor kinase BRI1." However, there is no published information that provides even a hint that the *STK* gene product participates in BR signaling or interacts with BRI1. We speculate that this Serine/threonine kinase (*STK*) gene functions in the response to BOT in a pathway (likely) mediated by BRI1. In Chapter 6, we applied gene ontology (GO) enrichment analysis to the gene clusters that were correlated with successful infection, in order to obtain insights into the biological processes that operate in *B. cinerea* and participate in the eventual (in)compatible host-pathogen interaction. Despite the presence of multiple CDIPs in the co-expressed modules that were (positively or negatively) correlated with the compatible interaction, this was not reflected in the GO enrichment analysis, because there are no terms like "effector" or "cell death-inducing activity" defined in the molecular function or biological process domains of GO databases. Moreover, the GO terms or functional annotations for some *B. cinerea* genes do not necessarily make sense in the context of plant-microbe interactions. We are aware that a Plant-Associated Microbe Gene Ontology (PAMGO) consortium has collaborated with the GO Consortium and added more than 700 GO terms related to biological processes that are relevant in plant- and animal-associated microbes (Torto-Alalibo et al., 2009). However, the PAMGO terms have not been updated since 2009, while other prediction tools for functional protein annotations (such as SignalP, TargetP, EffectorP and so on) have been updated throughout the past 10 years. A re-union of the PAMGO consortium and resumption of the manual curation of plant-microbe interactions-specific GO terms would be of great benefit to our research community.

Collectively, the genome assemblies and annotations for both pathogens and plants deserve more effort in maintenance and improvement. I propose to improve the quality of assemblies and annotations for the organisms that have been already sequenced, especially for (model) organisms that were sequenced in the early days of the 'omics' era. This might have more added value than generating new sequencing data of fungal isolates or plant accessions that have not been previously examined. In the future, if we map the sequencing datasets generated by studies in this thesis to the newer genome assembly and analyze the

data with the improved annotations, we will probably be able to gain deeper understanding of the biological and molecular mechanisms behind the same subjects.

Summary and perspectives

From the research in this thesis, I have acquired novel insights on some *B. cinerea* non-proteinaceous effectors that had been studied before, and have unraveled novel mechanisms of the interaction between plants and the phytotoxic SM effector BOT. Nonetheless, I have experienced that several experimental details can be improved and the research questions that were addressed at the onset of these studies are not yet fully resolved.

In order to examine the function of individual effector molecules in *B. cinerea*, a methodology that was applied to studying the effector repertoire of the pathogenic bacterium *Pseudomonas syringae* might currently be feasible for implementation. The model strain *P. syringae* pv. tomato DC3000 possesses 28 effectors that are delivered into host cells by the type III secretion system, and Cunnac et al. (2011) managed to generate a DC3000D28E mutant in which all 28 effector genes were knocked out. Subsequently, small sets of effector genes were reintroduced into the "effector-free" DC2000D28E background, revealing that a minimal effector repertoire of five members was sufficient for the restoration of full virulence in a host plant (Cunnac et al., 2011). Since marker-free CRISPR/Cas9-mediated transformation has been well established in *B. cinerea* (Leisen et al., 2022) and a 18x mutant (lacking *Bcbot2*, *Bcboa6* and other 16 genes encoding CDIPs) has been successfully generated (Hahn, oral presentation in BotrySclero2022), the approach used for *P. syringae* becomes amenable for *B. cinerea*. In Chapter 6, we observed that the 18x *B. cinerea* mutant still showed a similar disease incidence as the WT fungus albeit with a ~50% reduced lesion size on tomato leaves when inoculated in Gamborg B5 medium with additional yeast extract. I presume that a *B. cinerea* mutant lacking dozens of effector genes (maybe about 30 genes, including *Bcbot2* and *Bcboa6*) might lose the ability to cause expanding lesions under this particular inoculation condition. Once such multiple mutant has been obtained, one can exploit it as a recipient strain to reintroduce individual (or combinations of) effector genes and study their contributions to the fungal virulence. Undoubtedly, the effector repertoire of *B. cinerea* is much more elaborate than that of *P. syringae*, as the number of predicted proteinaceous effectors in *B. cinerea* is over 180 (Sperschneider et al., 2016) and there would be a larger pool of effectors in this pathogen according to the broad definition provided in Chapter 1. For this reason, there are challenges accompanied with opportunities for us to unravel the functions of individual

effector molecules and the interaction (including additive or epistatic effects) between multiple effectors.

At the onset of this thesis project, I did not expect that the inoculation conditions would have such a remarkable impact on the virulence of *B. cinerea* until we tested different inoculation media for various purposes. There should have been more in-depth investigations on the molecular basis for the phenomenon that different inoculation methods with the same set of mutant strains can yield such different outcomes on the virulence of *B. cinerea* on the same host species. I am not aware of any other pathosystem where similar observations were reported. Analogously, the issues regarding genome assemblies and annotation only became apparent to us when we had already started bioinformatic analyses. It is conceivable that such obstacles would also hamper research into other plant-microbe interactions. It may be important for more plant scientists and microbiologists to be aware of this situation, and to improve our information resources collaboratively.

References

AbuQamar, S., Chen, X., Dhawan, R., Bluhm, B., Salmeron, J., Lam, S., Dietrich, R. A., & Mengiste, T. (2006). Expression profiling and mutant analysis reveals complex regulatory networks involved in Arabidopsis response to *Botrytis* infection. *The Plant Journal*, 48(1), 28–44.

Alonso-Blanco, C., Andrade, J., Becker, C., Bemm, F., Bergelson, J., Borgwardt, K. M. M., Cao, J., Chae, E., Dezwaan, T. M. M., Ding, W., Ecker, J. R. R., Exposito-Alonso, M., Farlow, A., Fitz, J., Gan, X., Grimm, D. G. G., Hancock, A. M. M., Henz, S. R. R., Holm, S., … Zhou, X. (2016). 1,135 Genomes reveal the global pattern of polymorphism in *Arabidopsis thaliana*. *Cell*, 166(2), 481–491.

Amselem, J., Cuomo, C. A., van Kan, J. A. L., Viaud, M., & Benito, E. P. (2011). Genomic analysis of the necrotrophic fungal pathogens *Sclerotinia sclerotiorum* and *Botrytis cinerea*. *PLoS Genetics*, 1(8), 1002230.

Anuradha, C., Gaur, P. M., Pande, S., Gali, K. K., Ganesh, M., Kumar, J., & Varshney, R. K. (2011). Mapping QTL for resistance to *Botrytis* grey mould in chickpea. *Euphytica*, 182, 1–9.

Ashburner, M., Ball, C.A., Blake, J.A., Botstein, D., Butler, H., Cherry, J.M., Davis, A.P., Dolinski, K., Dwight, S.S., Eppig, J.T. & Harris, M.A. (2000). Gene ontology: tool for the unification of biology. *Nature Genetics*, 25(1), 25-29.

Assante, G., Merlini, L., & Nasini, G. (1977). (+)-Abscisic acid, a metabolite of the fungus *Cercospora rosicola*. *Experientia*, 33(12), 1556–1557.

Audenaert, K., de Meyer, G. B., & Hö, M. M. (2002). Abscisic acid determines basal Susceptibility of tomato to *Botrytis cinerea* and suppresses salicylic acid-dependent signaling mechanisms. *Plant physiology,* 128(2), 491-501.

Bai, M., Yang, G.S., Chen, W.T., Mao, Z.C., Kang, H.X., Chen, G.H., Yang, Y.H. & Xie, B.Y. (2012). Genome-wide identification of Dicer-like, Argonaute and RNA-dependent RNA polymerase gene families and their expression analyses in response to viral infection and abiotic stresses in *Solanum lycopersicum*. *Gene*, 501(1), 52-62.

Bar, M., & Ori, N. (2014). Leaf development and morphogenesis. *Development*, 141, 4219–4230.

Bar, M., Sharfman, M., Ron, M., & Avni, A. (2010). BAK1 is required for the attenuation of ethylene-inducing xylanase (Eix)-induced defense responses by the decoy receptor LeEix1. *The Plant Journal*, 63(5), 791–800.

Bargmann, B. O., & Munnik, T. (2006). The role of phospholipase D in plant stress responses. *Current Opinion in Plant Biology*, 9(5), 515-522.

Baulcombe, D. (2004). RNA silencing in plants. *Nature*, 431, 356–363.

Baum, J. A., Bogaert, T., Clinton, W., Heck, G. R., Feldmann, P., Ilagan, O., Johnson, S., Plaetinck, G., Munyikwa, T., Pleau, M., Vaughn, T., & Roberts, J. (2007). Control of coleopteran insect pests through RNA interference. *Nature Biotechnology*, 25, 1322–1326.

Behr, M., Motyka, V., Weihmann, F., Malbeck, J., Deising, H. B., & Wirsel, S. G. R. (2012). Remodeling of cytokinin metabolism at infection sites of *Colletotrichum graminicola* on maize leaves. *Molecular Plant-Microbe Interactions*, 25(8), 1073–1082.

Berestetskiy, A. O. (2008). A review of fungal phytotoxins: From basic studies to practical use. *Applied Biochemistry and Microbiology,* 44(5), 453–465.

Bessire, M., Chassot, C., Jacquat, A. C., Humphry, M., Borel, S., Petétot, J. M. D. C., Métraux, J. P., & Nawrath, C. (2007). A permeable cuticle in Arabidopsis leads to a strong resistance to *Botrytis cinerea*. *EMBO Journal*, 26(8), 2158–2168.

Bi, K., Scalschi, L., Jaiswal, N., Mengiste, T., Fried, R., Sanz, A. B., Arroyo, J., Zhu, W., Masrati, G., & Sharon, A. (2021). The *Botrytis cinerea* Crh1 transglycosylase is a cytoplasmic effector triggering plant cell death and defense response. *Nature Communications*, 12(1), 1–15.

Blakeman, J. P. (1975). Germination of *Botrytis cinerea* conidia in vitro in relation to nutrient conditions on leaf surfaces. *Transactions of the British Mycological Society*, 65(2), 239–247.

Bleecker, A. B., & Kende, H. (2000). ETHYLENE: A Gaseous Signal Molecule in Plants. *Annual Review of Cell and Developmental Biology*, 16, 1–18.

Böhnert, H. U., Fudal, I., Dioh, W., Tharreau, D., Notteghem, J.-L., & Lebrun, M.-H. (2004). A putative polyketide synthase/peptide synthetase from *Magnaporthe grisea* signals pathogen attack to resistant rice. *The Plant Cell*, 16, 2499–2513.

Bouché, N., Lauressergues, D., Gasciolli, V., & Vaucheret, H. (2006). An antagonistic function for Arabidopsis DCL2 in development and a new function for DCL4 in generating viral siRNAs. *The EMBO journal*, 25(14), 3347-3356.

Branon, T. C., Bosch, J. A., Sanchez, A. D., Udeshi, N. D., Svinkina, T., Carr, S. A., Feldman, J. L., Perrimon, N., & Ting, A. Y. (2018). Efficient proximity labeling in living cells and organisms with TurboID. *Nature Biotechnology*, 36(9), 880–898.

Bray, N. L., Pimentel, H., Melsted, P., & Pachter, L. (2016). Near-optimal probabilistic RNA-seq quantification. *Nature Biotechnology*, 34(5), 525–527.

Brilli, M., Asquini, E., Moser, M., Bianchedi, P. L., Perazzolli, M., & Si-Ammour, A. (2018). A multi-omics study of the grapevine-downy mildew (*Plasmopara viticola*) pathosystem unveils a complex protein coding-and noncoding-based arms race during infection. *Scientific Reports*, 8(1), 1–12.

Broschla, G., Ransom, R., Lechnerla, T., Walton, J. D., & Loidlai', P. (1995). Inhibition of maize histone deacetylases by HC toxin, the host-selective toxin of *Cochliobolus carbonum*. *The Plant Cell*, *7*, 1941–1950.

Cai, Q., Qiao, L., Wang, M., He, B., Lin, F., Palmquist, J., & Jin, H. (2018). Plants send small RNAs in extracellular vesicles to fungal pathogen to silence virulence genes. *Science*, 360(6393), 1126-1129.

Cessna, S. G., Sears, V. E., Dickman, M. B., & Low, P. S. (2000). Oxalic acid, a pathogenicity factor for *Sclerotinia sclerotiorum*, suppresses the oxidative burst of the host plant. *The Plant Cell*, 12, 2191–2199.

Chanclud, E., Kisiala, A., Emery, N. R. J., Chalvon, V., Ducasse, A., Romiti-Michel, C., Gravot, A., Kroj, T., & Morel, J. B. (2016). Cytokinin production by the rice blast fungus Is a pivotal requirement for full virulence. *PLOS Pathogens*, 12(2), e1005457.

Chanclud, E., & Morel, J. B. (2016). Plant hormones: a fungal point of view. *Molecular plant pathology*, 17(8), 1289-1297.

Chaloner, T., van Kan, J. A. L., & Grant-Downton, R. T. (2016). RNA 'Information Warfare' in Pathogenic and Mutualistic Interactions. Trends in Plant Science, 21, 738–748.

Chang, S. S., Zhang, Z., & Liu, Y. (2012). RNA interference pathways in fungi: Mechanisms and functions. Annual Review of Microbiology, 66, 305–323.

Chen, S., Kim, C., Lee, J. M., Lee, H. A., Fei, Z., Wang, L., & Apel, K. (2015). Blocking the QB-binding site of photosystem II by tenuazonic acid, a non-host-specific toxin of Alternaria alternata, activates singlet oxygen-mediated and EXECUTER-dependent signalling in Arabidopsis. *Plant Cell and Environment*, 38(6), 1069–1080.

Chen, Z., Boehnke, M., Wen, X., & Mukherjee, B. (2021). Revisiting the genome-wide significance threshold for common variant GWAS. *G3*, 11(2), jkaa056.

Choquer, M., Fournier, E., Kunz, C., Levis, C., Pradier, J.-M., Simon, A., & Viaud, M. (2007). *Botrytis cinerea* virulence factors: new insights into a necrotrophic and polyphageous pathogen. *FEMS Microbiology Letters*, 277(1), 1–10.

Choquer, M., Rascle, C., Gonçalves, I. R., de Vallée, A., Ribot, C., Loisel, E., Smilevski, P., Ferria, J., Savadogo, M., Souibgui, E., Gagey, M. J., Dupuy, J. W., Rollins, J. A., Marcato, R., Noûs, C., Bruel, C., & Poussereau, N. (2021). The infection cushion of *Botrytis cinerea*: a fungal 'weapon' of plant-biomass destruction. *Environmental Microbiology*, 23(4), 2293–2314.

Choquer, M., Robin, G., Le Pêcheur, P., Giraud, C., Levis, C., & Viaud, M. (2008). Ku70 or Ku80 deficiencies in the fungus *Botrytis cinerea* facilitate targeting of genes that are hard to knock out in a wild-type context. *FEMS Microbiology Letters*, 289, 225–232.

Coll, N. S., Vercammen, D., Smidler, A., Clover, C., van Breusegem, F., Dangl, J. L., & Epple, P. (2010). Arabidopsis type I metacaspases control cell death. *Science*, 330(6009), 1393–1397.

Collado, I., Aleu, J., Hernandez-Galan, R., & Duran-Patron, R. (2000). *Botrytis* species: an intriguing source of metabolites with a wide range of biological activities. Structure, chemistry and bioactivity of metabolites isolated from *Botrytis* species. *Current Organic Chemistry*, 4(12), 1261–1286.

Collado, I. G., Sánchez, A. J. M., & Hanson, J. R. (2007). Fungal terpene metabolites: Biosynthetic relationships and the control of the phytopathogenic fungus *Botrytis cinerea*. *Natural Product Reports*, 24(4), 674–686.

Collado, I. G., & Viaud, M. (2015). Secondary metabolism in *Botrytis cinerea*: Combining genomic and metabolomic approaches. *Botrytis - The Fungus, the Pathogen and its Management in Agricultural Systems* (pp. 291–313). Springer International Publishing.

Collemare, J., Griffiths, S., Iida, Y., Karimi Jashni, M., Battaglia, E., Cox, R. J., & de Wit, P. J. G. M. (2014). Secondary metabolism and biotrophic lifestyle in the tomato pathogen *Cladosporium fulvum*. *PLOS ONE*, 9(1), e85877.

Colmenares, A. J., Aleu, J., Durán-Patrón, R., Collado, I. G., & Hernández-Galán, R. (2002). The putative role of botrydial and related metabolites in the infection mechanism of *Botrytis cinerea*. *Journal of Chemical Ecology*, 28(5), 997–1005.

Conway, J. R., Lex, A., & Gehlenborg, N. (2017). UpSetR: an R package for the visualization of intersecting sets and their properties. *Bioinformatics*, 33(18), 2938–2940.

Coolen, S., van Pelt, J. A., Saskia, ·, van Wees, C. M., Corné, ·, & Pieterse, M. J. (2019). Mining the natural genetic variation in *Arabidopsis thaliana* for adaptation to sequential abiotic and biotic stresses. *Planta*, 1, 1087–1105.

Cristea, I. M., Williams, R., Chait, B. T., & Rout, M. P. (2005). Fluorescent proteins as proteomic probes. *Molecular & Cellular Proteomics*, 4(12), 1933–1941.

Cristescu, S. M., de Martinis, D., te Lintel Hekkert, S., Parker, D. H., & Harren, F. J. M. (2002). Ethylene production by *Botrytis cinerea in vitro* and in tomatoes. *Applied and Environmental Microbiology*, *68*(11), 5342–5350.

Crocoll, C., Kettner, J., & Dörffling, K. (1991). Abscisic acid in saprophytic and parasitic species of fungi. *Phytochemistry*, 30(4), 1059–1060.

Crumière, M., De Vallée, A., Rascle, C., Nahar, S., van, J. AL, Bruel, C., Poussereau, N., & Choquer, M. (2022). A multifunctional LysM effector of *Botrytis cinerea* contributes to plant infection. *BioRixv*, 11.

Cuesta Arenas, Y., Kalkman, E. R. I. C., Schouten, A., Dieho, M., Vredenbregt, P., Uwumukiza, B., Osés Ruiz, M., & van Kan, J. A. L. (2010). Functional analysis and mode of action of phytotoxic Nep1-like proteins of *Botrytis cinerea*. *Physiological and Molecular Plant Pathology*, 74(5–6), 376–386.

Cunnac, S., Chakravarthy, S., Kvitko, B. H., Russell, A. B., Martin, G. B., & Collmer, A. (2011). Genetic disassembly and combinatorial reassembly identify a minimal functional repertoire of type III effectors in *Pseudomonas syringae*. *Proceedings of the National Academy of Sciences of the United States of America*, 108(7), 2975–2980.

Curtis, M. J., & Wolpert, T. J. (2004). The victorin-induced mitochondrial permeability transition precedes cell shrinkage and biochemical markers of cell death, and shrinkage occurs without loss of membrane integrity. *Plant Journal*, 38(2), 244–259.

Dai, X., & Zhao, P. X. (2011). psRNATarget: a plant small RNA target analysis server. *Nucleic acids research*, 39(suppl_2), W155-W159.

Dalmais, B., Schumacher, J., Moraga, J., le Pêcheur, P., Tudzynski, B., Collado, I. G., & Viaud, M. (2011). The *Botrytis cinerea* phytotoxin botcinic acid requires two polyketide synthases for production and has a redundant role in virulence with botrydial. *Molecular Plant Pathology*, 12(6), 564–579.

Daub, M. E., & Briggs, S. P. (1983). Changes in tobacco cell membrane composition and structure caused by cercosporin. *Plant Physiology*, 71(4), 763–766.

Daub, M. E., & Ehrenshaft, M. (2000). THE PHOTOACTIVATED CERCOSPORA TOXIN CERCOSPORIN: Contributions to Plant Disease and Fundamental Biology. *Annual Review of Phytopathology*, 38, 461–490.

Daub, M. E., Herrero, S., & Chung, K. R. (2005). Photoactivated perylenequinone toxins in fungal pathogenesis of plants. In *FEMS Microbiology Letters,* 252(2), 197-206.

Davis, J., Yu, D., Evans, W., Gokirmak, T., Chetelat, R. T., & Stotz, H. U. (2009). Mapping of loci from *Solanum lycopersicoides* conferring resistance or susceptibility to *Botrytis cinerea* in tomato. *Theoretical and applied genetics,* 119, 305–314.

de Vos, M., Denekamp, M., Dicke, M., & Vuylsteke, M. (2006). The *Arabidopsis thaliana* transcription factor AtMYB102 functions in defense against the insect herbivore *Pieris rapae*. *Plant Signaling & Behavior* , 1(6), 305–311.

Dean, R., van Kan, J. A. L., Pretorius, Z. A., Hammond-Kosack, K. E., di Pietro, A., Spanu, P. D., Rudd, J. J., Dickman, M., Kahmann, R., Ellis, J., & Foster, G. D. (2012). The Top 10 fungal pathogens in molecular plant pathology. *Molecular plant pathology*, 13(4), 414–430.

Deighton, N., Muckenschnabel, I., Colmenares, A. J., Collado, I. G., & Williamson, B. (2001). Botrydial is produced in plant tissues infected by *Botrytis cinerea*. *Phytochemistry*, 57(5), 689–692.

Denancé, N., Sánchez-Vallet, A., Goffner, D., Molina, A., & Munné-Bosch, S. (2013). *Disease resistance or growth: the role of plant hormones in balancing immune responses and fitness costs*. *Frontiers in Plant Science*, 4, 155

Denby, K. J., Kumar, P., & Kliebenstein, D. J. (2004). Identification of *Botrytis cinerea* susceptibility loci in *Arabidopsis thaliana*. *The Plant Journal*, 38, 473–486.

Denton-Giles, M., McCarthy, H., Sehrish, T., Dijkwel, Y., Mesarich, C. H., Bradshaw, R. E., Cox, M. P., & Dijkwel, P. P. (2020). Conservation and expansion of a necrosis-inducing small secreted protein family from host-variable phytopathogens of the Sclerotiniaceae. *Molecular Plant Pathology*, 21(4), 512–526.

Doehlemann, G., Berndt, P., & Hahn, M. (2006). Different signalling pathways involving a Gα protein, cAMP and a MAP kinase control germination of *Botrytis cinerea* conidia. *Molecular Microbiology*, 59(3), 821–835.

Dominguez, V., Angel, D., Hjerde, E., Sterck, L., Capella-Gutierrez, S., Notredame, C., Pettersson, O. V., Amselem, J., Bouri, L., Bocs, S., Klopp, C., Gibrat, J.-F., Vlasova, A., Leskosek, B. L., Soler, L., Binzer-Panchal, M., & Lantz, H. (2018). Ten steps to get started in Genome Assembly and Annotation. *F1000Research,* 7.

Dörffling, K., Petersen, W., Sprecher, E., Urbasch, I., & Hanssen, H. P. (1984). Abscisic acid in phytopathogenic fungi of the genera botrytis, ceratocystis, fusarium, and rhizoctonia. *Zeitschrift Fur Naturforschung - Section C Journal of Biosciences*, 39(6), 683–684.

Dubey, H., Kiran, K., Jaswal, R., Jain, P., Kayastha, A. M., Bhardwaj, S. C., Mondal, T. K., & Sharma, T. R. (2019). Discovery and profiling of small RNAs from Puccinia triticina by deep sequencing and identification of their potential targets in wheat. *Functional & Integrative Genomics*, 19, 391–407.

Dunker, F., Trutzenberg, A., Rothenpieler, J. S., Kuhn, S., Pröls, R., Schreiber, T., Tissier, A., Kemen, A., Kemen, E., Hückelhoven, R., & Weiberg, A. (2020). Oomycete small RNAs bind to the plant RNA-induced silencing complex for virulence. *ELife*, 9. e56096.

Ederli, L., Madeo, L., Calderini, O., Gehring, C., Moretti, C., Buonaurio, R., Paolocci, F., & Pasqualini, S. (2011). The *Arabidopsis thaliana* cysteine-rich receptor-like kinase CRK20 modulates host responses to Pseudomonas syringae pv. tomato DC3000 infection. *Journal of Plant Physiology*, 168(15), 1784–1794.

Elad, Y., Pertot, I., Cotes Prado, A. M., & Stewart, A. (2016). Plant hosts of *Botrytis* spp. *Botrytis - The Fungus, the Pathogen and its Management in Agricultural Systems* (pp. 413–486). Springer International Publishing.

El-Oirdi, M., El-Rahman, T. A., Rigano, L., El-Hadrami, A., Rodriguez, M. C., Daayf, F., Vojnov, A., & Bouarab, K. (2011). *Botrytis cinerea* manipulates the antagonistic effects between immune pathways to promote disease development in Tomato. *Plant Cell*, 23(6), 2405–2421.

Faris, J. D., & Friesen, T. L. (2020). Plant genes hijacked by necrotrophic fungal pathogens. *Current Opinion in Plant Biology*, 56, 74–80.

Favaron, F., Sella, L., & D'ovidio, R. (2004). Relationships Among Endo-Polygalacturonase, Oxalate, pH, and Plant Polygalacturonase-Inhibiting Protein (PGIP) in the Interaction Between Sclerotinia sclerotiorum and Soybean. *Molecular Plant-Microbe Interactions*, 17(12), 1402–1409.

Fields, S., & Song, O.-K. (1989). A novel genetic system to detect protein-protein interactions. *Nature*, 340(6230), 245–246.

Fiil, B. K., & Petersen, M. (2011). Plant Signaling & Behavior Constitutive expression of MKS1 confers susceptibility to *Botrytis cinerea* infection independent of PAD3 expression. *Plant Signaling & Behavior*, 6(10), 1425–1427.

Fillinger, S., & Elad, Y. (2016). Botrytis - The fungus, the pathogen and its management in agricultural systems. *Botrytis - The Fungus, the Pathogen and Its Management in Agricultural Systems*, 1–486.

Flor, H. H. (1954). *Identificati on of Races of FLAX RUST Rust-Conditioning Genes* (No. 1087). US Department of Agriculture.

Frías, M., González, C., & Brito, N. (2011). BcSpl1, a cerato-platanin family protein, contributes to *Botrytis cinerea* virulence and elicits the hypersensitive response in the host. *New Phytologist*, 192(2), 483–495.

Frías, M., González, M., González, C., & Brito, N. (2016). BcIEB1, a *Botrytis cinerea* secreted protein, elicits a defense response in plants. *Plant Science*, 250, 115–124.

Friesen, T. L., Meinhardt, S. W., & Faris, J. D. (2007). The *Stagonospora nodorum*-wheat pathosystem involves multiple proteinaceous host-selective toxins and corresponding host sensitivity genes that interact in an inverse gene-for-gene manner. *The Plant Journal*, 51(4), 681–692.

Fudal, I., Collemare, J., Böhnert, H. U., Melayah, D., & Lebrun, M. H. (2007). Expression of *Magnaporthe grisea* avirulence gene ACE1 is connected to the initiation of appressorium-mediated penetration. *Eukaryotic Cell*, 6(3), 546–554.

Gel, B., & Serra, E. (2017). karyoploteR: an R/Bioconductor package to plot customizable genomes displaying arbitrary data and 2 CIBERONC. *Bioinformatics*, 33(19), 3088–3090.

Ghildiyal, M., & Zamore, P. D. (2009). Small silencing RNAs: an expanding universe. *Nature Reviews Genetics*, 10(2), 94-108.

Gilbert, B. M., & Wolpert, T. J. (2013). Characterization of the LOV1-mediated, victorin-induced, cell-death response with virus-induced gene silencing. *Molecular Plant-Microbe Interactions*, 26(8), 903–917.

Gimenez-Ibanez, S., Solano, R., Rivas, S., & Reymond, P. (2013). Nuclear jasmonate and salicylate signaling and crosstalk in defense against pathogens. *Froniers in Plant Science*, 4, 72.

Giraldo, M. C., & Valent, B. (2013). Filamentous plant pathogen effectors in action. *Nature Reviews Microbiology*, 11(11), 800–814.

Giraud, T., Fortini, D., Levis, C., Lamarque, C., Leroux, P., LoBuglio, K., & Brygoo, Y. (1999). Two sibling species of the *Botrytis cinerea* complex, *transposa* and *vacuma*, are found in sympatry on numerous host plants. *Phytopathology*, 89, 967–973.

Govrin, E. M., & Levine, A. (2000). The hypersensitive response facilitates plant infection by the necrotrophic pathogen *Botrytis cinerea*. *Current Biology*, 10(13), 751–757.

Hahn, M. (2022) Multiple mutagenesis of *Botrytis cinerea* by an improved CRISPR/Cas9 protocol reveals high redundancy of phytotoxic proteins for necrotrophic infection. *Oral presentation at the 31st Fungal Genetics Conference*, California, USA.

He, B., Cai, Q., Qiao, L., Huang, C. Y., Wang, S., Miao, W., Ha, T., Wang, Y., & Jin, H. (2021). RNA-binding proteins contribute to small RNA loading in plant extracellular vesicles. *Nature Plants*, 7, 342.

He, R., Drury, G. E., Rotari, V. I., Gordon, A., Willer, M., Farzaneh, T., Woltering, E. J., & Gallois, P. (2008). Metacaspase-8 modulates programmed cell death induced by ultraviolet light and H_2O_2 in Arabidopsis. *Journal of Biological Chemistry*, 283(2), 774–783.

Hinsch, J., Vrabka, J., Oeser, B., Novák, O., Galuszka, P., & Tudzynski, P. (2015). De novo biosynthesis of cytokinins in the biotrophic fungus *Claviceps purpurea*. *Environmental Microbiology*, 17(8), 2935–2951.

Hogenhout, S. A., van der Hoorn, R. A. L., Terauchi, R., & Kamoun, S. (2009). Emerging concepts in effector biology of plant-associated organisms. *Molecular plant-microbe interactions,* 22(2), 115–122.

Horton, M. W., Hancock, A. M., Huang, Y. S., Toomajian, C., Atwell, S., Auton, A., Muliyati, W., Platt, A., Gianluca Sperone, F., Vilhjálmsson, B. J., Nordborg, M., Borevitz, J. O., & Bergelson, J. (2012). Genome-wide patterns of genetic variation in worldwide *Arabidopsis thaliana* accessions from the RegMap panel. *Nature genetics*, 44(2), 212-216.

Hosmani, P. S., Flores-Gonzalez, M., Geest, H. van de, Maumus, F., Bakker, L. V., Schijlen, E., Haarst, J. van, Cordewener, J., Sanchez-Perez, G., Peters, S., Fei, Z., Giovannoni, J. J., Mueller, L. A., & Saha, S.

(2019). An improved de novo assembly and annotation of the tomato reference genome using single-molecule sequencing, Hi-C proximity ligation and optical maps. *BioRxiv*, 767764.

Hou, Y., Zhai, Y., Feng, L., Karimi, H. Z., Rutter, B. D., Zeng, L., Choi, D. S., Zhang, B., Gu, W., Chen, X., Ye, W., Innes, R. W., Zhai, J., & Ma, W. (2019). A *Phytophthora* effector suppresses trans-kingdom RNAi to promote disease susceptibility. *Cell Host & Microbe*, 25, 153-165.

Huang, J., Yang, L.-Q., Yu, Y., Liu, Y.-M., Xie, D.-F., Li, J., He, X.-J., & Zhou, S.-D. (2018). Molecular phylogenetics and historical biogeography of the tribe Lilieae (Liliaceae): bi-directional dispersal between biodiversity hotspots in Eurasia. *Annals of Botany*, 122, 1245–1262.

Huang, W. R. H., Schol, C., Villanueva, S. L., Heidstra, R., & Joosten, M. H. A. J. (2021). Knocking out *SOBIR1* in *Nicotiana benthamiana* abolishes functionality of transgenic receptor-like protein Cf-4. *Plant Physiology*, 185, 290–294.

Iqbal, S., Fosu-Nyarko, J., & Jones, M. G. K. (2020). Attempt to silence genes of the RNAi pathways of the root-knot nematode, *Meloidogyne incognita* results in diverse responses including increase and no change in expression of some genes. *Frontiers in Plant Science*, 11, 328.

Jones, J. D. G., & Dangl, J. L. (2006). The plant immune system. *Nature 2006 444:7117*, *444*(7117), 323–329.

Joosten, M. H. A. J., Cozijnsen, T. J., & de Wit, P. J. G. M. (1994). Host resistance to a fungal tomato pathogen lost by a single base-pair change in an avirulence gene. *Nature*, 367, 384–386.

Kamthan, A., Chaudhuri, A., Kamthan, M., & Datta, A. (2015). Small RNAs in plants: recent development and application for crop improvement. *Frontiers in Plant Science*, 6, 208.

Kanja, C., & Hammond-Kosack, K. E. (2020). Proteinaceous effector discovery and characterization in filamentous plant pathogens. *Molecular Plant Pathology*, 21(10), 1353–1376.

Kanneganti, T.-D., Huitema, E., Cakir, C., & Kamoun, S. (2006). Synergistic interactions of the plant cell death pathways induced by *Phytophthora infestans* Nep1-like protein PiNPP1. 1 and INF1 elicitin. *Molecular Plant-Microbe Interactions*, 19(8), 854–863.

Kars, I., McCALMAN, M. E. L. Y. S. I. A., Wagemakers, L., & van Kan, J. A. (2005). Functional analysis of *Botrytis cinerea* pectin methylesterase genes by PCR-based targeted mutagenesis: *Bcpme1* and *Bcpme2* are dispensable for virulence of strain B05. 10. *Molecular Plant Pathology*, 6(6), 641-652.

Keen, N. T. (1990). Gene-for-gene complementarity in plant-pathogen interactions. *Annual Review of Genetics*, 24(1), 447-463.

Kelley, B. S., Lee, S. J., Damasceno, C. M. B., Chakravarthy, S., Kim, B. D., Martin, G. B., & Rose, J. K. C. (2010). A secreted effector protein (SNE1) from *Phytophthora infestans* is a broadly acting suppressor of programmed cell death. *Plant Journal*, 62(3), 357–366.

Kettles, G. J., Hofinger, B. J., Hu, P., Bayon, C., Rudd, J. J., Balmer, D., Courbot, M., Hammond-Kosack, K. E., Scalliet, G., & Kanyuka, K. (2019). SRNA profiling combined with gene function analysis reveals a lack of evidence for cross-kingdom RNAi in the wheat – *Zymoseptoria tritici* pathosystem. *Frontiers in Plant Science*, 10, 892.

Kim, H. T., Lim, K. B., & Kim, J. S. (2019). New insights on *Lilium* phylogeny based on a comparative phylogenomic study using complete plastome sequences. *Plants,* 8(12), 547.

Kim, J. S., & Kim, J. H. (2018). Updated molecular phylogenetic analysis, dating and biogeographical history of the lily family (Liliaceae: Liliales). *Botanical Journal of the Linnean Society*, 187(4), 579–593.

Kim, K. S., Min, J.-Y., & Dickman, M. B. (2008). Oxalic acid is an elicitor of plant programmed cell death during *Sclerotinia sclerotiorum* disease development. *Molecular Plant-Microbe Interactions*, 21(5), 605-612.

Kind, S., Hinsch, J., Vrabka, J., Hradilová, M., Majeská-Čudejková, M., Tudzynski, P., & Galuszka, P. (2018). Manipulation of cytokinin level in the ergot fungus Claviceps purpurea emphasizes its contribution to virulence. *Current Genetics*, 64, 1303–1319.

Kourelis, J., Marchal, C., Posbeyikian, A., Harant, A., & Kamoun, S. (2023). NLR immune receptor–nanobody fusions confer plant disease resistance. *Science*, 379(6635), 934–939.

Kravchik, M., Damodharan, S., Stav, R., & Arazi, T. (2014). Generation and characterization of a tomato DCL3-silencing mutant. *Plant Science*, 221, 81-89.

Kravchik, M., Sunkar, R., Damodharan, S., Stav, R., Zohar, M., Isaacson, T., & Arazi, T. (2014). Global and local perturbation of the tomato microRNA pathway by a *trans-activated DICER-LIKE 1* mutant. *Journal of experimental botany*, 65(2), 725-739.

Lai, Z., Schluttenhofer, C. M., Bhide, K., Shreve, J., Thimmapuram, J., Lee, S. Y., Yun, D. J., & Mengiste, T. (2014). ARTICLE MED18 interaction with distinct transcription factors regulates multiple plant functions. *Nature Communications*, 5(1), 3064.

Landeo Villanueva, S., Malvestiti, M. C., van Ieperen, W., Joosten, M. H. A. J., & van Kan, J. A. L. (2021). Red light imaging for programmed cell death visualization and quantification in plant–pathogen interactions. *Molecular Plant Pathology*, 22(3), 361–372.

Langfelder, P., & Horvath, S. (2008). WGCNA: An R package for weighted correlation network analysis. *BMC Bioinformatics*, 9(1), 1–13.

Lanver, D., Müller, A. N., Happel, P., Schweizer, G., Haas, F. B., Franitza, M., Pellegrin, C., Reissmann, S., Altmüller, J., Rensing, S. A., & Kahmann, R. (2018). The biotrophic development of *Ustilago maydis* studied by RNA-seq analysis. *The Plant Cell*, 30, 300–323.

Lax, C., Tahiri, G., Patiño-Medina, J. A., Cánovas-Márquez, J. T., Pérez-Ruiz, J. A., Osorio-Concepción, M., Navarro, E., & Calo, S. (2020). The Evolutionary Significance of RNAi in the Fungal Kingdom. *International Journal of Molecular Sciences*, 21(24), 9348.

Leisen, T., Bietz, F., Werner, J., Wegner, A., Schaffrath, U., Scheuring, D., Willmund, F., Mosbach, A., Scalliet, G., & Hahn, M. (2020). CRISPR/Cas with ribonucleoprotein complexes and transiently selected telomere vectors allows highly efficient marker-free and multiple genome editing in *Botrytis cinerea*. *PLOS Pathogens*, 16(8), e1008326.

Leisen, T., Werner, J., Pattar, P., Safari, N., Ymeri, E., Sommer, F., Schroda, M., Suárez, I., Collado, I. G., Scheuring, D., & Hahn, M. (2022). Multiple knockout mutants reveal a high redundancy of phytotoxic compounds contributing to necrotrophic pathogenesis of *Botrytis cinerea*. *PLoS Pathogens*, 18(3).

Lenarčič, T., Albert, I., Böhm, H., Hodnik, V., Pirc, K., Zavec, A. B., ... & Nürnberger, T. (2017). Eudicot plant-specific sphingolipids determine host selectivity of microbial NLP cytolysins. *Science*, 358(6369), 1431–1434.

Leroch, M., Kleber, A., Silva, E., Coenen, T., Koppenhöfer, D., Shmaryahu, A., Valenzuela, P. D. T., & Hahn, M. (2013). Transcriptome profiling of *Botrytis cinerea* conidial germination reveals upregulation of infection-related genes during the prepenetration stage. *Eukaryotic Cell*, 12, 614–626.

Li, J., & Wang, X. (2019). Phospholipase D and phosphatidic acid in plant immunity. *Plant Science*, 279, 45–50.

Li, J., Wen, J., Lease, K. A., Doke, J. T., Tax, F. E., & Walker, J. C. (2002). BAK1, an Arabidopsis LRR receptor-like protein kinase, interacts with BRI1 and modulates brassinosteroid signaling. *Cell*, 110(2), 213–222.

Li, P., Li, J., Wang, L., & Di, L.-J. (2017). Proximity labeling of interacting proteins: application of BioID as a discovery tool. *Proteomics*, 17, 1700002.

Liao, H. L., & Chung, K. R. (2008). Genetic dissection defines the roles of elsinochrome phytotoxin for fungal pathogenesis and conidiation of the citrus pathogen *Elsinoë fawcettii*. *Molecular Plant-Microbe Interactions*, 21(4), 469–479.

Liu, N., Lian, S., Li, B., & Ren, W. (2022). The autophagy protein BcAtg2 regulates growth, development and pathogenicity in the gray mold fungus *Botrytis cinerea*. *Phytopathology Research*, 4(1), 1-8.

lo Presti, L., Lanver, D., Schweizer, G., Tanaka, S., Liang, L., Tollot, M., Zuccaro, A., Reissmann, S., & Kahmann, R. (2015). Fungal effectors and plant susceptibility. *Annual Review of Plant Biology*, 66, 513–545.

Lorang, J. M., Carkaci-Salli, N., & Wolpert, T. J. (2004). Identification and Characterization of Victorin Sensitivity in *Arabidopsis thaliana*. *Molecular Plant-Microbe Interactions*, 17(6), 577-582.

Lorang, J. M., Sweat, T. A., Wolpert, T. J., & Briggs, S. P. (2007). Plant disease susceptibility conferred by a "'resistance'" gene. *Proceedings of the National Academy of Sciences*, 104(37), 14861–14866.

Malmierca, M. G., Izquierdo-Bueno, I., Mccormick, S. P., Cardoza, R. E., Alexander, N. J., Moraga, J., Gomes, E. V., Proctor, R. H., Collado, I. G., Monte, E., & Gutiérrez, S. (2016). Botrydial and botcinins produced by *Botrytis cinerea* regulate the expression of *Trichoderma arundinaceum* genes involved in trichothecene biosynthesis. *Molecular Plant Pathology*, 17(7), 1017–1031.

Malmierca, M. G., Mccormick, S. P., Cardoza, R. E., Alexander, N. J., Monte, E., & Gutiérrez, S. (2015). Production of trichodiene by *Trichoderma harzianum* alters the perception of this biocontrol strain by plants and antagonized fungi. *Environmental Microbiology*, 17(8), 2628–2646.

Malvestiti, M. C., Immink, R. G. H., Arens, P., Quiroz Monnens, T., & van Kan, J. A. L. (2021). Fire blight susceptibility in *Lilium* spp. correlates to sensitivity to *Botrytis elliptica* secreted cell death inducing compounds. *Frontiers in Plant Science*, 12, 660337.

Malvestiti, M. C., Steentjes, M. B. F., Beenen, H. G., Boeren, S., van Kan, J. A. L., & Shi-Kunne, X. (2022). Analysis of plant cell death-inducing proteins of the necrotrophic fungal pathogens Botrytis squamosa and Botrytis elliptica. *Frontiers in Plant Science*, 13, 3701.

Manteau, S., Abouna, S., Lambert, B., & Legendre, L. (2003). Differential regulation by ambient pH of putative virulence factor secretion by the phytopathogenic fungus *Botrytis cinerea*. *FEMS Microbiology Ecology*, 43, 359–366.

Marín, R. M., & Vaníček, J. (2011). Efficient use of accessibility in microRNA target prediction. *Nucleic acids research*, 39(1), 19-29.

Martinez, F., Blancard, D., Lecomte, P., Levis, C., Dubos, B., & Fermaud, M. (2003). Phenotypic differences between *vacuma* and *transposa* subpopulations of *Botrytis cinerea*. *European Journal of Plant Pathology*, 109(5), 479–488.

Marumo, S., Katayama, M., Komori, E., Ozaki, Y., Natsume, M., & Kondo, S. (1982). Microbial production of abscisic acid by *Botrytis cinerea*. *Agricultural and Biological Chemistry*, 46(7), 1967–1968.

Mauch-Mani, B., & Mauch, F. (2005). The role of abscisic acid in plant-pathogen interactions. *Current Opinion in Plant Biology*, 8(4), 409–414.

McLoughlin, A. G., Wytinck, N., Walker, P. L., Girard, I. J., Rashid, K. Y., De Kievit, T., Fernando, W. G. D., Whyard, S., & Belmonte, M. F. (2018). Identification and application of exogenous dsRNA confers plant protection against *Sclerotinia sclerotiorum* and *Botrytis cinerea*. *Scientific Reports*, 8(1), 1-14.

Mesarich, C. H., Griffiths, S. A., van der Burgt, A., Ökmen, B., Beenen, H. G., Etalo, D. W., Joosten, M. H. A. J., & de Wit, P. J. G. M. (2014). Transcriptome sequencing uncovers the Avr5 avirulence gene of the tomato leaf mold pathogen *Cladosporium fulvum*. *Molecular Plant-Microbe Interactions*, 27(8), 846-857.

Michaelson, L. V., Napier, J. A., Molino, D., & Faure, J. D. (2016). Plant sphingolipids: Their importance in cellular organization and adaption. *Biochimica et Biophysica Acta - Molecular and Cell Biology of Lipids*, 1861(9), 1329–1335.

Morrison, E. N., Emery, R. J. N., & Saville, B. J. (2017). Fungal derived cytokinins are necessary for normal *Ustilago maydis* infection of maize. *Plant Pathology*, 66(5), 726–742.

Nakajima, M., & Akutsu, K. (2014). Virulence factors of *Botrytis cinerea*. *Journal of General Plant Pathology*, 80(1), 15–23.

Navarre, D. A., & Wolpert, T. J. (1999). Victorin Induction of an Apoptotic/Senescence-like Response in Oats. *The Plant Cell*, 11, 237–249.

Navathe, S., Yadav, P. S., Chand, R., Mishra, V. K., Kumar Vasistha, N., Meher, P. K., Kumar Joshi, A., & Kumar Gupta, P. (2020). ToxA–Tsn1 interaction for spot blotch susceptibility in Indian wheat: an example of inverse gene-for-gene relationship. *Plant Disease*, 104, 71–81.

Nerva, L., Sandrini, M., Gambino, G., & Chitarra, W. (2020). Double-stranded rnas (dsRNAs) as a sustainable tool against gray mold (*Botrytis cinerea*) in grapevine: Effectiveness of different application methods in an open-air environment. *Biomolecules*, 10(2), 200.

Noda, J., Brito, N., & González, C. (2010). The *Botrytis cinerea* xylanase Xyn11A contributes to virulence with its necrotizing activity, not with its catalytic activity. *BMC Plant Biology*, 10(1), 1–15.

Noman, A., Hussain, A., Adnan, M., Khan, M. I., Ashraf, M. F., Zainab, M., Khan, K. A., Ghramh, H. A., & He, S. (2019). A novel MYB transcription factor CaPHL8 provide clues about evolution of pepper immunity against soil borne pathogen. *Microbial Pathogenesis*, 137, 103758.

Novina, C. D., & Sharp, P. A. (2004). The RNAi revolution. *Nature*, 430, 161–164.

Nowara, D., Schweizer, P., Gay, A., Lacomme, C., Shaw, J., Ridout, C., Douchkov, D., Hensel, G., & Kumlehn, J. (2010). HIGS: Host-induced gene silencing in the obligate biotrophic fungal pathogen *Blumeria graminis*. *Plant Cell*, 22, 3130–3141.

Oirdi, M. El, Trapani, A., & Bouarab, K. (2009). The nature of tobacco resistance against *Botrytis cinerea* depends on the infection structures of the pathogene mi_2063 239..253. *Environmental Microbiology*, 12(1), 239–253.

Olivares-Yañez, C., Sánchez, E., Pérez-Lara, G., Seguel, A., Camejo, P. Y., Larrondo, L. F., Vidal, E. A., & Canessa, P. (2021). A comprehensive transcription factor and DNA-binding motif resource for the construction of gene regulatory networks in *Botrytis cinerea* and *Trichoderma atroviride*. *Computational and Structural Biotechnology Journal*, 19, 6212–6228.

Pavan, S., Evert, A. E., Ae, J., Ae, R. G. F. V., & Bai, Y. (2010). Loss of susceptibility as a novel breeding strategy for durable and broad-spectrum resistance. *Molecular Breeding*, *25*, 1–12.

Pfaffl, M. W. (2006). Relative quantification. *Chapter 3 in real-time PCR*. (1st ed.) Ed. M. Dorak (London: Taylor & Francis).

Pimentel, H., Bray, N. L., Puente, S., Melsted, P., & Pachter, L. (2017). *Differential analysis of rna-seq incorporating quantification uncertainty*. 14, 687.

Pinedo, C., Wang, C., Pradier, J., Dalmais, B., Choquer, M., Pascal, L., Morgant, G., Collado, I. G., Cane, D. E., & Viaud, M. (2008). Sesquiterpene synthase from the botrydial biosynthetic gene cluster of the phytopathogen *Botrytis cinerea*. *ACS chemical biology*, *3*(12), 791–801.

Porquier, A., Moraga, J., Morgant, G., Dalmais, B., Simon, A., Sghyer, H., Collado, I. G., & Viaud, M. (2019). Botcinic acid biosynthesis in *Botrytis cinerea* relies on a subtelomeric gene cluster surrounded by relics of transposons and is regulated by the Zn2Cys6 transcription factor BcBoa13. *Current Genetics*, 65(4), 965–980.

Porquier, A., Morgant, G., Moraga, J., Dalmais, B., Luyten, I., Simon, A., Pradier, J. M., Amselem, J., Collado, I. G., & Viaud, M. (2016). The botrydial biosynthetic gene cluster of *Botrytis cinerea* displays a bipartite genomic structure and is positively regulated by the putative Zn(II)2Cys6 transcription factor BcBot6. *Fungal Genetics and Biology*, 96, 33–46.

Porquier, A., Tisserant, C., Salinas, F., Glassl, C., Wange, L., Enard, W., Hauser, A., Hahn, M., & Weiberg, A. (2021). Retrotransposons as pathogenicity factors of the plant pathogenic fungus *Botrytis cinerea*. *Genome Biology*, 22, 1-19.

Pringle, R. B., & Scheffer, R. P. (1964). HOST-SPECIFIC PLANT TOXINSl.2.3. *Annual Review of Phytopathology*, *2*(1), 133–156.

Qin, S., Veloso, J., Baak, M., Boogmans, B., Bosman, T., Puccetti, G., Shi-Kunne, X., Smit, S., Grant-Downton, R., Leisen, T., Hahn, M., & van Kan, J. A. (2023). Molecular characterization reveals no functional evidence for naturally occurring cross-kingdom RNA interference in the early stages of *Botrytis cinerea*-tomato interaction. *Molecular Plant Pathology,* 24(1), 3–15.

Raffaele, S., Farrer, R. A., Cano, L. M., Studholme, D. J., MacLean, D., Thines, M., Jiang, R. H. Y., Zody, M. C., Kunjeti, S. G., Donofrio, N. M., Meyers, B. C., Nusbaum, C., & Kamoun, S. (2010). Genome evolution following host jumps in the irish potato famine pathogen lineage. *Science*, 330(6010), 1540–1543.

Rebordinos, L., Cantoral, J. M., Prieto, M. V., Hanson, J. R., & Collado, I. G. (1996). The phytotoxic activity of some metabolites of *Botrytis cinerea*. *Phytochemistry*, 42(2), 383–387.

Reino, J. L., Durán-Patrón, R. M., Daoubi, M., Collado, I. G., & Hernández-Galán, R. (2006). Biosynthetic Studies on the Botcinolide Skeleton: New Hydroxylated Lactones from *Botrytis cinerea*. *The Journal of Organic Chemistry*, 71(2), 562-565.

Repetti, P. P., & Staskawicz, B. (2002). A R2R3-MYB gene, AtMYB30, acts as a positive regulator of the hypersensitive cell death program in plants in response to pathogen attack. *Proceedings of the National Academy of Sciences* , 99(15), 10179–10184.

Rhoads, D. M., Levings, C. S., & Siedow, J. N. (1995). URF13, a ligand-gated, pore-forming receptor for T-toxin in the inner membrane of *cms-T* mitochondria. *Journal of Bioenergetics and Biomembranes*, 27, 437-445.

Ron, M., & Avni, A. (2004). The Receptor for the Fungal Elicitor Ethylene-Inducing Xylanase Is a Member of a Resistance-Like Gene Family in Tomato. *The Plant Cell*, 16, 1604–1615.

Rooney, H. C. E., Van't Klooster, J. W., van der Hoorn, R. A. L., Joosten, M. H. A. J., Jones, J. D. G., & de Wit, P. J. G. M. (2005). *Cladosporium* Avr2 inhibits tomato Rcr3 protease required for Cf-2-dependent disease resistance. *Science*, 308(5729), 1783–1786.

Rossi, F. R., Gárriz, A., Marina, M., Romero, F. M., Gonzalez, M. E., Collado, I. G., & Pieckenstain, F. L. (2011). The sesquiterpene botrydial produced by *Botrytis cinerea* induces the hypersensitive response on

plant tissues and its action is modulated by salicylic acid and jasmonic acid signaling. *Molecular Plant-Microbe Interactions*, 24(8), 888–896.

Rowe, H. C., & Kliebenstein, D. J. (2008). Complex genetics control natural variation in *Arabidopsis thaliana* resistance to *Botrytis cinerea*. *Genetics*, 180(4), 2237–2250.

Rutter, B. D., & Innes, R. W. (2020). Growing pains: addressing the pitfalls of plant extracellular vesicle research. *New Phytologist*, 228, 1505–1510.

Samuel, S., Veloukas, T., Papavasileiou, A., & Karaoglanidis, G. S. (2012). Differences in frequency of transposable elements presence in *Botrytis cinerea* populations from several hosts in Greece. *Plant Disease*, 96, 1286–1290.

Sato, S., Tabata, S., Hirakawa, H., Asamizu, E., Shirasawa, K., Isobe, S., Kaneko, T., Nakamura, Y., Shibata, D., Aoki, K., Egholm, M., Knight, J., Bogden, R., Li, C., Shuang, Y., Xu, X., Pan, S., Cheng, S., Liu, X., … Gianese, G. (2012). The tomato genome sequence provides insights into fleshy fruit evolution. *Nature,* 485(7400), 635–641.

Schlöffel, M. A., Salzer, A., Wan, W. L., van Wijk, R., Šemanjski, M., Symeonidi, E., Slaby, P., Kilian, J., Maček, B., Munnik, T., & Gust, A. A. (2019). The BIR2/BIR3-interacting Phospholipase D gamma 1 negatively regulates immunity in Arabidopsis. *BioRxiv*, 815282.

Schneeberger, K., Ossowski, S., Lanz, C., Juul, T., Høgh Petersen, A., Lehmann Nielsen, K., Jørgensen, J.-E., Weigel, D., & Uggerhø Andersen, S. (2009). SHOREmap: simultaneous mapping and mutation identification by deep sequencing. *Nature methods,* 6(8), 550-551.

Schouten, A., Van Baarlen, P., & van Kan, J. A. L. (2008). Phytotoxic Nep1-like proteins from the necrotrophic fungus *Botrytis cinerea* associate with membranes and the nucleus of plant cells. *New Phytologist*, 177(2), 493–505.

Schumacher, J. (2012). Tools for *Botrytis cinerea*: New expression vectors make the gray mold fungus more accessible to cell biology approaches. *Fungal Genetics and Biology*, 49(6), 483–497.

Schumacher, J. (2016). DHN melanin biosynthesis in the plant pathogenic fungus *Botrytis cinerea* is based on two developmentally regulated key enzyme (PKS)-encoding genes. *Molecular Microbiology*, 99(4), 729-748.

Seren, Ü., Vilhjálmsson, B. J., Horton, M. W., Meng, D., Forai, P., Huang, Y. S., Long, Q., Segura, V., & Nordborg, M. (2012). GWAPP: A web application for genome-Wide association mapping in arabidopsis. *Plant Cell*, 24(12), 4793–4805.

Shahid, S., Kim, G., Johnson, N. R., Wafula, E., Wang, F., Coruh, C., Bernal-Galeano, V., Phifer, T., Depamphilis, C. W., Westwood, J. H., & Axtell, M. J. (2018). MicroRNAs from the parasitic plant *Cuscuta campestris* target host messenger RNAs. *Nature*, 553(7686), 82-85.

Siewers, V., Viaud, M., Jimenez-Teja, D., Collado, I. G., Gronover, C. S., Pradier, J.-M., Tudzynski, B., & Tudzynski, P. (2005). Functional analysis of the cytochrome P450 monooxygenase gene bcbot1 of *Botrytis cinerea* indicates that botrydial is a strain-specific virulence factor. *Molecular Plant-Microbe Interactions*, 18(6), 602–612.

Sijen, T., Vijn, I., Rebocho, A., Van Blokland, R., Roelofs, D., Mol, J. N. M., & Kooter, J. M. (2001). Transcriptional and posttranscriptional gene silencing are mechanistically related. *Current Biology*, 11(6), 436-440.

Silvestri, A., Fiorilli, V., Miozzi, L., Accotto, G. P., Turina, M., & Lanfranco, L. (2019). In silico analysis of fungal small RNA accumulation reveals putative plant mRNA targets in the symbiosis between an arbuscular mycorrhizal fungus and its host plant. *BMC Genomics*, 20(1), 1-18.

Snelders, N. C., Kettles, G. J., Rudd, J. J., & Thomma, B. P. H. J. (2018). Plant pathogen effector proteins as manipulators of host microbiomes? *Molecular Plant Pathology*, 19(2), 257–259.

Spada, M., Pugliesi, C., Fambrini, M., & Pecchia, S. (2021). Silencing of the Slt2-type MAP kinase *Bmp3* in *Botrytis cinerea* by application of exogenous dsRNA affects fungal growth and virulence on *Lactuca sativa*. *International Journal of Molecular Sciences*, 22(10), 5362.

Sperschneider, J., Gardiner, D. M., Dodds, P. N., Tini, F., Covarelli, L., Singh, K. B., Manners, J. M., & Taylor, J. M. (2016). EffectorP: Predicting fungal effector proteins from secretomes using machine learning. *New Phytologist*, 210(2), 743–761.

Spoel, S. H., Johnson, J. S., & Dong, X. (2007). Regulation of tradeoffs between plant defenses against pathogens with different lifestyles. *Proceedings of the National Academy of Sciences of the United States of America*, 104(47), 18842–18847.

Staats, M., van Baarlen, P., Schouten, A., van Kan, J. A. L., & Bakker, F. T. (2007). Positive selection in phytotoxic protein-encoding genes of *Botrytis* species. *Fungal Genetics and Biology*, 44(1), 52–63.

Steentjes, M. B. F., Herrera Valderrama, A. L., Fouillen, L., Bahammou, D., Leisen, T., Albert, I., Nürnberger, T., Hahn, M., Mongrand, S., Scholten, O. E., & van Kan, J. A. L. (2022). Cytotoxic activity of Nep1-like proteins on monocots. *New Phytologist*, 235(2), 690–700.

Sun, K., van Tuinen, A., van Kan, J. A. L., Wolters, A. M. A., Jacobsen, E., Visser, R. G. F., & Bai, Y. (2017). Silencing of DND1 in potato and tomato impedes conidial germination, attachment and hyphal growth of *Botrytis cinerea*. *BMC Plant Biology*, 17(1), 235.

ten Have, A., Tenberge, K. B., Benen, J. A. E., Tudzynski, P., Visser, J., & van Kan, J. A. L. (2002). The contribution of cell wall degrading enzymes to pathogenesis of fungal plant pathogens. *Agricultural Applications*, 341–358.

Torres-Martínez, S., & Ruiz-Vázquez, R. M. (2017). The RNAi universe in fungi: a varied landscape of small RNAs and biological functions. *Annual review of microbiology*, 71, 371-391.

Torres, M. A., Jones, J. D. G., & Dangl, J. L. (2006). Reactive oxygen species signaling in response to pathogens. *Plant Physiology*, 141(2), 373-378.

Torto-Alalibo, T., Collmer, C. W., & Gwinn-Giglio, M. (2009). The Plant-Associated Microbe Gene Ontology (PAMGO) Consortium: Community development of new Gene Ontology terms describing biological processes involved in microbe-host interactions. *BMC microbiology*, 9(1), 1-5.

Tsiatsiani, L., van Breusegem, F., Gallois, P., Zavialov, A., Lam, E., & Bozhkov, P. v. (2011). Metacaspases. *Cell Death and Differentiation*, 18(8), 1279–1288.

Tsuda, K., & Katagiri, F. (2010). Comparing signaling mechanisms engaged in pattern-triggered and effector-triggered immunity. *Current Opinion in Plant Biology*, 13(4), 459–465.

Valero-Jiménez, C. A., Steentjes, M. B. F., Slot, J. C., Shi-Kunne, X., Scholten, O. E., & Van Kan, J. A. L. (2020). Dynamics in secondary metabolite gene clusters in otherwise highly syntenic and stable genomes in the fungal genus *Botrytis*. *Genome Biology and Evolution*, 12(12), 2491–2507.

van Baarlen, P., Woltering, E. J., Staats, M., & van Kan, J. A. L. (2007). Histochemical and genetic analysis of host and non-host interactions of Arabidopsis with three *Botrytis* species: An important role for cell death control. *Molecular Plant Pathology*, 8(1), 41–54.

van Butselaar, T., & Van den Ackerveken, G. (2020). Salicylic acid steers the growth–immunity tradeoff. *Trends in Plant Science*, 25(6), 566–576.

van den Burg, H. A., Harrison, S. J., Joosten, M. H. A. J., Vervoort, J., & de Wit, P. J. G. M. (2006). *Cladosporium fulvum* Avr4 protects fungal cell walls against hydrolysis by plant chitinases accumulating during infection. *Molecular Plant-Microbe Interactions*, 19(12), 1420–1430.

van der Burgh, A. M., & Joosten, M. H. A. J. (2019). Plant immunity: thinking outside and inside the box. *Trends in Plant Science*, 24(7), 587-601.

van Kan, J. A. L. (2006). Licensed to kill: the lifestyle of a necrotrophic plant pathogen. *Trends in Plant Science*, 11(5), 247–253.

van Kan, J. A., Shaw, M. W., & Grant-Downton, R. T. (2014). *Botrytis* species: relentless necrotrophic thugs or endophytes gone rogue? *Molecular Plant Pathology*, 15(9), 957-961.

van Kan, J. A. L., Stassen, J. H. M., Mosbach, A., van Der Lee, T. A. J., Faino, L., Farmer, A. D., Papasotiriou, D. G., Zhou, S., Seidl, M. F., Cottam, E., Edel, D., Hahn, M., Schwartz, D. C., Dietrich, R. A., Widdison, S., & Scalliet, G. (2017). A gapless genome sequence of the fungus *Botrytis cinerea*. *Molecular Plant Pathology*, 18(1), 75–89.

van Kan, J. A. L., van den Ackerveken, G. F. J. M., & de Wit, P. J. G. M. (1991). Cloning and characterization of cDNA of avirulence gene avr9 of the fungal pathogen *Cladosporium fulvum*, causal agent of tomato leaf mold. *Mol. Plant-Microbe Interact*, 4, 52–59.

van Schie, C. C. N., & Takken, F. L. W. (2014). Susceptibility genes 101: how to be a good host. *Annual review of phytopathology*, 52, 551-581.

Veloso, J., & van Kan, J. A. L. (2018). Many shades of grey in *Botrytis*–host plant interactions. *Trends in Plant Science*, 23(7), 613–622.

Vercammen, D., Declercq, W., Vandenabeele, P., & van Breusegem, F. (2007). Are metacaspases caspases? *The Journal of Cell Biology*, 179(3), 375–380.

Viaud, M., Brunet-Simon, A., Brygoo, Y., Pradier, J. M., & Levis, C. (2003). Cyclophilin A and calcineurin functions investigated by gene inactivation, cyclosporin A inhibition and cDNA arrays approaches in the phytopathogenic fungus *Botrytis cinerea*. *Molecular Microbiology*, 50(5), 1451-1465.

Vignatti, P., Gonzalez, M. E., Jofré, E. C., Bolívar-Anillo, H. J., Moraga, J., Viaud, M., Collado, I. G., & Pieckenstain, F. L. (2020). Botrydial confers *Botrytis cinerea* the ability to antagonize soil and phyllospheric bacteria. *Fungal Biology*, 124(1), 54–64.

Vleeshouwers, V. G. A. A., & Oliver, R. P. (2014). Effectors as tools in disease resistance breeding against biotrophic, hemibiotrophic, and necrotrophic plant pathogens. *Molecular Plant-Microbe Interactions*, 27(3), 196–206.

Wan, W. L., Zhang, L., Pruitt, R., Zaidem, M., Brugman, R., Ma, X., Krol, E., Perraki, A., Kilian, J., Grossmann, G., Stahl, M., Shan, L., Zipfel, C., van Kan, J. A. L., Hedrich, R., Weigel, D., Gust, A. A., & Nürnberger, T. (2019). Comparing Arabidopsis receptor kinase and receptor protein-mediated immune signaling reveals BIK1-dependent differences. *New Phytologist*, 221(4), 2080–2095.

Wang, H., Li, J., Bostock, R. M., & Gilchrista, D. G. (1996). Apoptosis: a functional paradigm for programmed plant cell death induced by a host-selective phytotoxin and invoked during development. *The Plant Cell*, 8(3), 375-391.

Wang, M., Weiberg, A., Dellota, E., Yamane, D., & Jin, H. (2017). *Botrytis* small RNA Bc-siR37 suppresses plant defense genes by cross-kingdom RNAi. *RNA Biology*, 14(4), 421–428.

Wang, M., Weiberg, A., Lin, F. M., Thomma, B. P. H. J., Huang, H. Da, & Jin, H. (2016). Bidirectional cross-kingdom RNAi and fungal uptake of external RNAs confer plant protection. *Nature Plants*, 2(10) , 1-10.

Wang, N., Wang, R., Wang, R., & Chen, S. (2018). Transcriptomics analysis revealing candidate networks and genes for the body size sexual dimorphism of Chinese tongue sole (*Cynoglossus semilaevis*). *Functional & Integrative Genomics*, 18, 327–339.

Wang, T., Deng, Z., Zhang, X., Wang, H., Wang, Y., Liu, X., Liu, S., Xu, F., Li, T., Fu, D. & Zhu, B. (2018). Tomato DCL2b is required for the biosynthesis of 22-nt small RNAs, the resulting secondary siRNAs, and the host defense against ToMV. *Horticulture research*, 5.

Watanabe, N., & Lam, E. (2011). Arabidopsis metacaspase 2d is a positive mediator of cell death induced during biotic and abiotic stresses. *Plant Journal*, 66(6), 969–982.

Weiberg, A., & Jin, H. (2015). Small RNAs-the secret agents in the plant-pathogen interactions. *Current Opinion in Plant Biology*, 26, 87–94.

Weiberg, A., Wang, M., Bellinger, M., & Jin, H. (2014). Small RNAs: A new paradigm in plant-microbe interactions. *Annual Review of Phytopathology*, 52, 495–516.

Weiberg, A., Wang, M., Lin, F. M., Zhao, H., Zhang, Z., Kaloshian, I., Huang, H. da, & Jin, H. (2013). Fungal small RNAs suppress plant immunity by hijacking host RNA interference pathways. *Science*, 342(6154), 118–123.

Weigel, D., & Mott, R. (2009). The 1001 genomes project for *Arabidopsis thaliana*. *Genome Biology*, *10*(5), 107.

Westerink, N., Brandwagt, B. F., de Wit, P. J. G. M., & Joosten, M. H. A. J. (2004). *Cladosporium fulvum* circumvents the second functional resistance gene homologue at the Cf-4 locus (Hcr9-4E) by secretion of a stable avr4E isoform. *Molecular Microbiology*, 54(2), 533–545.

Wickham, H., Chang, W., & Wickham, M. H. (2016). *Package 'ggplot2'. Create elegant data visualisations using the grammar of graphics*. *Version,* 2(1), 1-189.

Wolpert, T. J., Dunkle, L. D., & Ciuffetti, L. M. (2002). Host-selective toxins and avirulence determinants: What's in a name? In *Annual Review of Phytopathology,* 40(1), 251-285.

Wolpert, T. J., Duroy, ', Navarre, A., Moore, D. L., & Macko, V. (1994). Identification of the 100-kD victorin binding protein from oats. *The Plant Cell*, 6(8), 1145-1155.

Wolpert, T. J., & Lorang, J. M. (2016). Victoria Blight, defense turned upside down. *Physiological and Molecular Plant Pathology*, 95, 8–13.

Wolpert, T. J., & Macko, V. (1989). Specific binding of victorin to a 100-kDa protein from oats. *Proceedings of the National Academy of Sciences,* 86(11), 4092-4096.

Wong-Bajracharya, J., Singan, V. R., Monti, R., Plett, K. L., Ng, V., Grigoriev, I. v., Martin, F. M., Anderson, I. C., & Plett, J. M. (2022). The ectomycorrhizal fungus *Pisolithus microcarpus* encodes a microRNA involved in cross-kingdom gene silencing during symbiosis. *Proceedings of the National Academy of Sciences,* 119(3), e2103527119.

Wrzaczek, M., Brosché, M., Salojärvi, J., Kangasjärvi, S., Idänheimo, N., Mersmann, S., Robatzek, S., Karpiński, S., Karpińska, B., & Kangasjärvi, J. (2010). Transcriptional regulation of the CRK/DUF26 group of Receptor-like protein kinases by ozone and plant hormones in Arabidopsis. *BMC Plant Biology*, 10, 95.

Wu, Y., Zhang, D., Chu, J. Y., Boyle, P., Wang, Y., Brindle, I. D., de Luca, V., & Després, C. (2012). The Arabidopsis NPR1 protein is a receptor for the plant defense hormone salicylic acid. *Cell Reports*, 1(6), 639–647.

Xiong, F., Liu, M., Zhuo, F., Yin, H., Deng, K., Feng, S., Liu, Y., Luo, X., Feng, L., Zhang, S. & Li, Z. (2019). Host-induced gene silencing of BcTOR in *Botrytis cinerea* enhances plant resistance to grey mould. *Molecular Plant Pathology*, 20(12), 1722-1739.

Xue, C., Park, G., Choi, W., Zheng, L., Dean, R. A., & Xu, J. R. (2002). Two novel fungal virulence genes specifically expressed in appressoria of the rice blast fungus. *The Plant Cell*, 14(9), 2107-2119.

Yang, P., Chen, Y., Wu, H., Fang, W., Liang, Q., Zheng, Y., Olsson, S., Zhang, D., Zhou, J., Wang, Z. & Zheng, W. (2018). The 5-oxoprolinase is required for conidiation, sexual reproduction, virulence and deoxynivalenol production of *Fusarium graminearum*. *Current genetics*, 64, 285-301.

Yang, Y., Yang, X., Dong, Y., & Qiu, D. (2018). The *Botrytis cinerea* xylanase BcXyl1 modulates plant immunity. *Frontiers in Microbiology*, 9, 2535.

Yao, N., Tada, Y., Park, P., Nakayashiki, H., Tosa, Y., & Mayama, S. (2001). Novel evidence for apoptotic cell response and differential signals in chromatin condensation and DNA cleavage in victorin-treated oats. *Plant Journal*, 28(1), 13–26.

Yifhar, T., Pekker, I., Peled, D., Friedlander, G., Pistunov, A., Sabban, M., Wachsman, G., Alvarez, J.P., Amsellem, Z. & Eshed, Y. (2012). Failure of the tomato trans-acting short interfering RNA program to regulate AUXIN RESPONSE FACTOR3 and ARF4 underlies the wiry leaf syndrome. *The Plant Cell*, 24(9), 3575-3589.

Yorimitsu, T., & Klionsky, D. J. (2005). Autophagy: Molecular machinery for self-eating. *Cell Death & Differentiation*, 12(2), 1542-1552.

You, Y. (2022). *Host resistance mechanisms and fungal infection strategies in the Botrytis cinerea-tomato interaction* (Doctoral dissertation, Wageningen University).

Yun, S. H., Turgeon, B. G., & Yoder, O. C. (1998). REMI-induced mutants of *Mycosphaerella zeae-maydis* lacking the polyketide PM-toxin are deficient in pathogenesis to corn. *Physiological and Molecular Plant Pathology*, 52(1), 53–66.

Zhang, J., Zhao, J., Xu, Y., Liang, J., Chang, P., Yan, F., Li, M., Liang, Y., & Zou, Z. (2015). Genome-wide association mapping for tomato volatiles positively contributing to tomato flavor. *Frontiers in Plant Science*, 6, 1–13.

Zhang, L., Hua, C., Pruitt, R. N., Qin, S., Wang, L., Albert, I., Albert, M., van Kan, J. A. L., & Nürnberger, T. (2021). Distinct immune sensor systems for fungal endopolygalacturonases in closely related Brassicaceae. *Nature Plants*, *7*(9), 1254–1263.

Zhang, L., Kars, I., Essenstam, B., Liebrand, T. W. H., Wagemakers, L., Elberse, J., Tagkalaki, P., Tjoitang, D., Van Den Ackerveken, G., & Van Kan, J. A. L. (2014). Fungal endopolygalacturonases are recognized as microbe-associated molecular patterns by the Arabidopsis receptor-like protein RESPONSIVENESS TO BOTRYTIS POLYGALACTURONASES1. *Plant physiology*, 164(1), 352-364.

Zhang, L., & van Kan, J. A. L. (2013). *Botrytis cinerea* mutants deficient in d-galacturonic acid catabolism have a perturbed virulence on *Nicotiana benthamiana* and Arabidopsis, but not on tomato. *Molecular Plant Pathology*, 14(1), 19–29.

Zhang, T., Zhao, Y.L., Zhao, J.H., Wang, S., Jin, Y., Chen, Z.Q., Fang, Y.Y., Hua, C.L., Ding, S.W. & Guo, H.S. (2016). Cotton plants export microRNAs to inhibit virulence gene expression in a fungal pathogen. *Nature Plants*, 2(10), 1-6.

Zhang, W., Corwin, J. A., Copeland, D. H., Feusier, J., Eshbaugh, R., Cook, D. E., Atwell, S., & Kliebenstein, D. J. (2019). Plant-necrotroph co-transcriptome networks illuminate a metabolic battlefield. *elife*, 8, e44279.

Zhang, X., Han, X., Shi, R., Yang, G., Qi, L., Wang, R., & Li, G. (2013). Arabidopsis cysteine-rich receptor-like kinase 45 positively regulates disease resistance to *Pseudomonas syringae*. *Plant Physiology and Biochemistry*, 73, 383–391.

Zhang, Y., Zhang, Y., Qiu, D., Zeng, H., Guo, L., & Yang, X. (2015). BcGs1, a glycoprotein from *Botrytis cinerea*, elicits defence response and improves disease resistance in host plants. *Biochemical and Biophysical Research Communications*, 457(4), 627–634.

Zhao, J., Sauvage, C., Zhao, J., Bitton, F., Bauchet, G., Liu, D., Huang, S., Tieman, D. M., Klee, H. J., & Causse, M. (2019). Meta-analysis of genome-wide association studies provides insights into genetic control of tomato flavor. *Nature Communications*, 10(1), 1534.

Zhu, W., Ronen, M., Gur, Y., Minz-Dub, A., Masrati, G., Ben-Tal, N., Savidor, A., Sharon, I., Eizner, E., Valerius, O., Braus, G. H., Bowler, K., Bar-Peled, M., & Sharon, A. (2017). BcXYG1, a secreted xyloglucanase from *Botrytis cinerea*, triggers both cell death and plant immune responses. *Plant Physiology*, 175, 438–456.

Zhu, W., Wei, W., Wu, Y., Zhou, Y., Peng, F., Zhang, S., Chen, P., & Xu, X. (2017). BcCFEM1, a CFEM domain-containing protein with putative GPI-anchored site, is involved in pathogenicity, conidial production, and stress tolerance in *Botrytis cinerea*. *Frontiers in Microbiology*, 8, 1807.

Summary

Plant pathogens deploy multiple distinct strategies in order to enable them to colonize their hosts. Among these strategies, the secretion of molecules which are referred to as "effectors" can effectively facilitate the infection of the hosts by pathogens. **Chapter 1** defines the term effector as any secreted molecules from filamentous plant pathogens that can suppress or induce plant defense responses and modulate plant physiology. Plant pathogens can produce four different categories of effectors: secreted cysteine-rich small proteins; small RNAs (sRNAs) that can be translocated into host cells and interfere with the expression of genes involved in plant immunity; secondary metabolites (SMs) that modulate host immunity and physiology; and plant hormones produced by a pathogen. The broad-host range necrotrophic fungus *Botrytis cinerea* produces and secretes all four types of effectors. The molecular basis of the interactions between *B. cinerea* effectors and their (potential) plant targets are discussed. The advances in studying and utilizing the effectors of *B. cinerea*, and future perspectives for identifying plant genotypes as natural sources of resistance are summarized.

The natural occurring sRNA warfare between *B. cinerea* and *Solanum lycopersicum* (tomato) has been studied as described in **Chapter 2** and **Chapter 3**. sRNAs and mRNAs from *B. cinerea* and tomato during early phases of interaction were identified by high-throughput sequencing. Massive numbers of *B. cinerea* sRNAs were predicted to target massive numbers of mRNAs in tomato, and vice versa. In **Chapter 2**, the causal relation between *B. cinerea* sRNAs and their predicted mRNA targets in tomato were investigated. Correlations between the high production of *B. cinerea* sRNAs and the down-regulation of predicted target genes in tomato were observed for eight out of nine selected fungal sRNA – host mRNA pairs. Moreover, in order to investigate the contribution of fungal sRNAs to the virulence, two types of *B. cinerea* mutants were generated. The first type of mutants lacks a transposon region which is the source of about 10% of the fungal sRNAs; and the second type of mutants lacks either one or both Dicer-like genes (*Bcdcl1* and *Bcdcl2*) which are responsible for the production of most transposon-derived sRNAs. However, neither of these mutants showed a significant reduction in virulence on any tested plant species, indicating that the role of *B. cinerea* sRNAs in fungal virulence was undetectable under the tested conditions.

In **Chapter 3**, we examined the effect of plant sRNAs on suppressing the expression of their predicted mRNA targets in *B. cinerea*. The correlations between the abundance of three specific plant sRNAs and their respective three target mRNAs in the fungus were examined. A unique tomato sRNA, which was produced at high levels during infection by *B. cinerea*,

was predicted to target a sole fungal gene, named *Bcspl1*. The BcSPL1 protein had been reported to be important for the virulence, and its transcript showed a transient decrease around 20 hours post inoculation and contained a unique target site for the tomato sRNA. We generated a fungal mutant that contained a 5-nucleotide substitution in *Bcspl1,* which would abolish the interaction between the transcript and the sRNA without changing the encoded protein sequence. A transient downregulation of the *Bcspl1* transcript was observed in both the mutant and the wild type fungus, and the virulence of the *Bcspl1* target site mutant was similar to the wild type fungus.

The contribution of the two major phytotoxins botrydial (BOT) and botcinic acid (BOA) to the virulence of *B. cinerea* has been assessed as described in **Chapter 4.** Different levels of reduction in the virulence of *B. cinerea* mutants lacking the capacity to produce BOT and/or BOA were observed on five different plant species. We showed that BOT was essential for *B. cinerea* to infect Arabidopsis successfully, whereas deficiency in BOA production did not affect the virulence of *B. cinerea* on Arabidopsis. Mutants that do not produce BOT or BOA were slightly less virulent as compared to the wild type fungus on tomato, while the *ΔBcbot2ΔBcboa6* mutant lacking both phytotoxins showed a more prominent reduction in virulence on this host. The same *B. cinerea* double mutant displayed subtly but significantly reduced virulence on *Nicotiana benthamiana* and cowpea but not on French bean. Moreover, this chapter presents the phytotoxic activity of BOT on these five different dicotyledons and shows for the first time that BOT also induces cell death in monocotyledons.

Chapter 5 describes the quantitative variation in cell death responses to BOT between the different tissues (leaves and tepals) sampled from four different lily cultivars. BOT production is demonstrated in the specialized lily pathogen *B. elliptica* during *in vitro* cultures, and we analyzed the transcriptional activity of the BOT biosynthetic gene *Bebot2* during infection in lily. CRISPR/Cas9-mediated transformation enabled us to obtain *B. elliptica ΔBebot2* knockout mutants, which lost the capacity to produce BOT . We observed a significant reduction in lesion size upon inoculation with the *B. elliptica ΔBebot2* mutants as compared to the wild type fungus on all tested lily cultivars. In addition, the levels of reduction in virulence of *ΔBebot2* mutants were different between lily cultivars, suggesting that BOT contributes to fungal virulence in the *B. elliptica*-lily interaction.

In **Chapter 6**, we show that the *B. cinerea ΔBcbot2ΔBcboa6* double mutant was almost avirulent on tomato leaves when Gamborg B5 medium was used for the infection assay. However, the virulence of this mutant was restored when yeast extract was added to the inoculation medium.We performed a transcriptome analysis to identify *B. cinerea* genes

that contribute to the restoration of the virulence of this *ΔBcbot2ΔBcboa6* mutant on tomato. A co-expression analysis resulted in the identification of three modules containing genes with similar expression profiles that were positively correlated with the successful infection. One of the three modules contained four cell death-inducing effector genes that were upregulated in *B. cinerea* by the addition of yeast extract. These four genes were individually overexpressed in the *Δbot2Δboa6* background, to examine whether this could restore successful infection in the absence of yeast extract.

Traits conferring resistance and susceptibility to pathogens are naturally present in populations of plant accessions. To cope with the grey mold disease caused by *B. cinerea,* introducing resistance (*R*) genes and eliminating susceptibility (*S*) genes in host plants can provide a dual path for breeding against the pathogen. Host genes conferring sensitivity to BOT are presumed to function as *S* genes to this necrotrophic pathogen. In **Chapter 7**, we screened a large panel of Arabidopsis accessions for their sensitivity to BOT, and subsequently performed a genome-wide association study (GWAS). This approach resulted in a list of 36 candidate genes associated with the BOT-sensitivity. From these 36 genes, we validated their function in response to BOT by assessing the BOT-sensitivity of Arabidopsis T-DNA insertion mutants for each individual gene. We identified three genes positively contributing to the BOT-sensitivity and one gene functioning in suppressing host response to BOT. The Arabidopsis mutant of a *Serine/threonine kinase* (*STK*) gene that acts as a negative regulator of the BOT-triggered cell death was also more susceptible to *B. cinerea*, indicating that *STK* is an *R* gene against the fungus. The experiments described in this chapter unravel novel molecular mechanisms underlying the host programmed cell death induced by BOT, and provide (potential) *S* and *R* genes against *B. cinerea*.

Chapter 8 provides a general discussion of the main results in this thesis and presents a model illustrating the (potential) multiple modes of action of BOT during the infection of hosts by *B. cinerea*. It pinpoints several issues encountered during this PhD project and makes a number of recommendations for to be adopted by the plant sciences community.

Acknowledgements

As my journey as a PhD candidate draws to a close, I would like to take this opportunity to express my gratitude to all those who have been with me throughout this academic trajectory and have contributed to this thesis.

First of all, I'd like to thank my daily supervisor and promoter Jan, for your supports in different aspects of this PhD thesis and for coaching me to write the proposal before starting my PhD. I am deeply grateful for your constant accessibility and inspiring guidance whenever I sought your help. I was initially drawn to your enthusiasm in research and teaching when I was a MSc student and now I still admire your passion as a teacher, which I have learned a lot and will keep on learning from.

Secondly, I want to thank my co-promoter Joost. I sincerely appreciated your significant contribution to the main research project of this thesis. Many thanks to your advice in experimental design and interpretation of the results, and rapid responses to my questions and feedback to my manuscript.

Maikel, thank you for being my benchmate in the lab for over a half of my PhD life. I derived immense pleasure from our daily exchanges, encompassing both scientific and non-scientific subjects. It was such a nice trip to Kaiserslauten with you and Laura, during which we created a lot of cherished memories together. It was my pleasure to be your paranymph in 2021, and thank you to be my paranymph this year.

Laura (Vilanova), I really enjoyed the interactions with you in the lab and I want to thank you a lot, not only for being an exceptional lab mate, but also for acting as an older sister who provided me with invaluable personal support. I guess you agree that the joyful trip to Kaiserslauten has forged an everlasting bond between you, Maikel, and me, solidifying our friendship.

Javier, I've gained a lot of knowledges from you during my MSc and PhD thesis. It is highly appreciated that you are always very patient and kind to answer all kinds of questions related to science from me.

Yaohua, Xiaoqian and Lorena, I've received substantial support from you during my PhD research. Thank you for the inspiring conversations between us regarding work, and also for the cheerful personal interactions outside of working time with nice food and drinks. Yaohua, thank you for sharing so many stimulating and encouraging words when we were in the lab and also for doing the outing together with Wen and Hua. Xiaoqian, in addition to your expertise in bioinformatic analysis which contributed a lot to this thesis, you are so

kind to organize delightful dinners at your place and to introduce me to bouldering. Lorena, thank you for offering generous help in the lab and your kindness in daily life.

I'd like to also thank other (current and former) *Botrytis* group members, Michele, Henriek, Suraj, Claudio, Dian and Victor, for your daily companionship in the lab. Thank you Michele, for your initiative for the *B. elliptica* – botrydial experiments which eventually became a shared Chapter between us. Thank you Henriek, for your accurate work in helping with many experiments and impactful contributions to this thesis.

Wen, Jelmer and Gabriel, thank you for the inspiring work-related discussions and many good moments we had together beyond work. It was my pleasure to have gathered and preserved all the unforgettable memories with you. Wen, I have to especially thank you for having accepted this invitation to be my paranymph.

I have to thank all MSc students that I've supervised: Jelmer, Tim, Sabine, Sanna and Haris. It was my pleasure to have worked with you for your MSc these as well as parts of my PhD thesis, during which I learned a lot from you and had fun with you.

I enjoyed to be a member of the Phytopathology group during my PhD project. Therefore, I'd like to thank all PIs and lecturers in Phyto: Gert, Matthieu, Francine, Sander, Lotje, Eduard, Like, and Desalegn, for your valuable comments after my PSS presentations and our chats at Phyto. It has been a lot of fun to share the lab and conversations with other Phyto PhDs and Postdocs: Hui, Nick, Martin, Michiel, Sergio, Einar, David, Edgar, Katharina, Carolina, Jinling, Jingbin, Kiki, Lisanne, Chris, Huan, Sen, Esranur, Nicat, Anouk, Jie, Yinping and Ruifang. Thanks to the Phyto Technician team: Henriek, Laurens, Grardy, Ciska, Giuliana and Tijmen, without you the lab would not have been functioning so smoothly. I also want to thank other Phyto staff members: Ali, Petra, Anneke, Arwen and Hanneke.

I have to thank Bert and your colleagues from Unifarm for filling thousands of pots for me to grow Arabidopsis and taking care of our plants in the greenhouse.

I'd like to thank all collaborators from outside of WUR. Isidro and Inmaculada from Cádiz, thank you for your supervision on the purification of botrydial and offering other toxins; thank Matthias, Thomas Leisen and Janina from Kaiserslautern for teaching us the CRISPR-mediated *Botrytis* transformation in detail; and thank Thorsten and Lisha from Tübingen for our forthcoming collaborations after this thesis has been submitted.

Leónie, thank you for being my external advisor of my PhD thesis and the discussions we had during the last few years.

My precious friends Li, Zihan, Ziyang, Yiyuan, Chengcheng, Xulan, Xiaotian (Alexander), Saskia, Laura (Terzi) and Ami, with you I never felt alone during my stay in the Netherlands. We have started to know each other since our master projects or early phases of our PhDs, and the stories between us can be written down into hundreds of pages. Although I cannot fully expand these stories in this thesis book, I do remember and will remember the happy time we spent together and your supports at difficult moments during my PhD.

Yixin, Zhirong, Linjun, Jing, Siqi, Yanrong, Yueying, Zilei, Yufei and Lu, I'm grateful to be constantly in touch with you girls even though we are physically so far from each other. I have been mentally charging from the nice chats and calls among us, and I will keep treasuring our friendships for more decades.

I'm thankful for the chance that the China Scholarship Council (CSC) offered to me to perform this PhD project with my desired supervisors at this adorable lab. Thank EPS graduate school for organizing all kinds of activities for PhD candidates and helping me with keeping the project on track.

In the end, I would like to say greatest thanks to my parents Qingchuan Qin and Lingyan Zhang, as you are the best parents in the world. Thank you both for your eternal love, solicitude and unwavering support. 我想把最诚挚的感恩给我的爸爸妈妈，感谢你们不求回报的爱与支持，你们是全天下最好的父母。

About the author

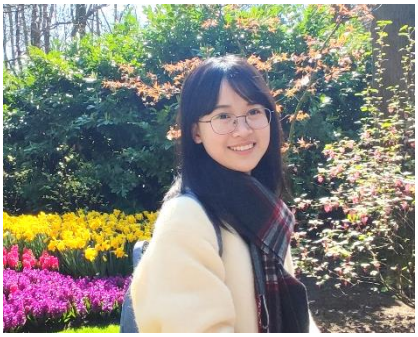

Si Qin was born on May 25th, 1994 in Guilin, China. She pursued her bachelor's degree in Plant Protection as the major at China Agricultural University in Beijing from 2012 to 2016. In the autumn of 2016, she moved to The Netherlands and started her MSc program in Plant Biotechnology at Wageningen University (WU). During her master's study, she conducted her major thesis under the supervision of Dr. Jan van Kan and Dr. Javier Veloso at the Laboratory of Phytopathology in WU, and later on she completed an internship project supervised by Prof. Dr. Thorsten Nürnberger and Dr. Lisha Zhang at the Plant Biochemistry group in the University of Tübingen, Germany. In 2018, she wrote a PhD proposal coached by Dr. Jan van Kan, which was ultimately granted by China Scholarship Council (CSC). Thanks to the CSC fellowship, she carried out the PhD research described in this thesis with Dr. Jan van Kan since October 2018 till July 2023.

List of publications

Qin, S., Veloso, J., Puccetti, G. & van Kan, J. A. L. (2023). Molecular characterization of cross-kingdom RNA interference in *Botrytis cinerea* by tomato small RNAs. *Frontiers in Plant Science*, *14*, 792.

Qin, S., Veloso, J., Baak, M., Boogmans, B., Bosman, T., Puccetti, G., Shi‐Kunne, X., Smit, S., Grant‐Downton, R., Leisen, T., Hahn, M. & van Kan, J. A. L. (2023). Molecular characterization reveals no functional evidence for naturally occurring cross-kingdom RNA interference in the early stages of *Botrytis cinerea*–tomato interaction. *Molecular Plant Pathology*. 24(1), 3-15.

Zhang, L., Hua, C., Pruitt, R. N., **Qin, S.**, Wang, L., Albert, I., Albert, M., van Kan, J. A. L. & Nürnberger, T. (2021). Distinct immune sensor systems for fungal endopolygalacturonases in closely related Brassicaceae. *Nature Plants*, *7*(9), 1254-1263.

Education Statement of the Graduate School

Experimental Plant Sciences

Issued to: Si Qin
Date: 04 July 2023
Group: Laboratory of Phytopathology
University: Wageningen University & Research

1) Start-Up Phase	date	cp
► **First presentation of your project**		
Identification of receptors in Arabidopsis that recognize phytotoxic metabolites of *Botrytis cinerea*	14 Dec 2018	1.5
► **Writing or rewriting a project proposal**		
Identification of receptors in Arabidopsis that recognize phytotoxic metabolites of *Botrytis cinerea*	Jan - Mar 2019	1.0
► **MSc courses**		
Subtotal Start-Up Phase		2.5

2) Scientific Exposure	date	cp
► **EPS PhD days**		
EPS PhD days 'Get2Gether', Soest (NL)	11 - 12 Feb 2019	0.6
EPS PhD days 'Get2Gether', Soest (NL)	10 - 11 Feb 2020	0.6
► **EPS theme symposia**		
EPS Theme 2 Symposium & Willie Commelin Scholten Day 'Interactions between Plants and Biotic Agents', Wageningen (NL)	01 Feb 2019	0.3
EPS Theme 2 Symposium & Willie Commelin Scholten Day 'Interactions between Plants and Biotic Agents', Utrecht (NL)	04 Feb 2020	0.3
EPS Theme 2 Symposium 'Interactions between Plants and Biotic Agents', Online	09 Feb 2021	0.2
EPS Theme 2 Symposium & Willie Commelin Scholten Day 'Interactions between Plants and Biotic Agents', Online	08 Feb 2022	0.2
EPS Theme 2 Symposium 'Interactions between Plants and Biotic Agents', Amsterdam (NL)	19 Jan 2023	0.3
► **Lunteren Days and other national platforms**		
Annual Meeting Experimental Plant Sciences, Lunteren (NL)	08-09 Apr 2019	0.6
Annual Meeting Experimental Plant Sciences, Online	12-13 Apr 2021	0.5
Annual Meeting Experimental Plant Sciences, Lunteren (NL)	11-12 Apr 2022	0.6
Annual Meeting Experimental Plant Sciences, Lunteren (NL)	17-18 Apr 2023	0.6
► **Seminars (series), workshops and symposia**		
Seminar Prof. David Geiser 'A phylogenomic view of Fusarium oxysporum taxonomy and evolution'	30 Oct 2018	0.1
Seminar Dr. Theo van der Lee 'From genomes to function: bioinformatics to disclose the obligate biotrophic soilborne fungus Synchytrium endobioticum'	18 Jan 2019	0.1
Seminar Daniela Sueldo 'Mining the plant-pathogen interface using activity-based proteomics'	08 Feb 2019	0.1
Seminar Ronnie de Jonge 'Microbial small molecules – weapons of plant subversion'	20 Feb 2019	0.1
Seminar Andrea Sanchez-Vallet 'Competition ability of fungal pathogens'	20 Feb 2019	0.1
Seminar Luigi Faino	20 Feb 2019	0.1
Ritzema Bos lecture Nick Talbot 'Investigating the biology of plant infection by rice blast fungus'	02 Apr 2019	0.1
Seminar Yuling Bai 'Activities and perspectives of the research group 'Breeding for resistance in Solanaceae'	05 Apr 2019	0.1
Seminar Daniel Croll 'Parasites within parasites: how transposable elements drive the evolution of plant pathogenic fungi'	21 Jun 2019	0.1
Seminar Rays Jiang 'Using cutting-edge genomics tools to study host-microbe interactions'	05 Jul 2019	0.1
Seminar Eva Stukenbrock 'Causes and consequences of chromosome instability in a fungal plant pathogen'	12 Dec 2019	0.1
Seminar Thorsten Nuernberger 'Microbial virulence and plant immunity-stimulating activities of microbial cytolysins'	03 Feb 2019	0.1
Seminar Eveline Snelders 'The evolution of antifungal resistance'	12 Jun 2020	0.1
Seminar Vivian Valencia 'Investigating the impacts of coffee leaf rust on coffee growers in southwest Mexico'	03 Jul 2020	0.1
Seminar Duur Aanen 'Fusion deficiency causes reproductive parasitism in a fungus'	10 Jul 2020	0.1
Seminar Sarah Gurr	15 Jan 2021	0.1
Seminar José Lozano 'The key for my VENI and VIDI grants: Proline-rich extension-like receptor kinases mediate damage-triggered immune responses to nematode infections'	12 Feb 2021	0.1
Seminar James Brown 'Evolution and genetics of pathogen insensitivity to fungicides'	05 Mar 2021	0.1
Sminar Harrold van den Burg	19 Mar 2021	0.1
Seminar Viviane Cordovez	23 Apr 2021	0.1
Sminar Lisha Zhang	28 May 2021	0.1
Seminar Guido van den Ackerveken	25 Jun 2021	0.1
Seminar David Guest 'Smallholder farmers in tropical horticulture that limit adoption of improved crop management and family livelihoods'	03 Sep 2021	0.1
Seminar Antonio di Pietro 'Mechanisms of adaptation in a clonally evolving fungal pathogen'	15 Oct 2021	0.1
Seminar Gero Steinberg 'Fungal cell biology: From fundamental research to practical application'	05 Nov 2021	0.1
Seminar Frank Takken 'Molecular aspects of Endophyte-Mediated Resistance induced by Fusarium oxysporum'	26 Nov 2021	0.1
Seminar Andre Drenth	18 Feb 2022	0.1
Seminar Mark Sterken	01 Apr 2022	0.1
Seminar Darcy Jones	03 Jun 2022	0.1
Seminar Sebastian Schornack	28 Oct 2022	0.1
Seminar Honour McCann	04 Nov 2022	0.1
Masterclass Anne Osbourn	01 Dec 2022	0.1
Masterclass Cyril Zipfel	16 Dec 2022	0.1
► **Seminar plus**		
► **International symposia and congresses**		
Joint International Botrytis Symposium & Sclerotinia International Symposium - BotrySclero2021, Online	08-11 Jun 2021	1.2
31st Fungal Genetics Conference, Online	15-19 Mar 2022	1.5
Joint International Botrytis Symposium & Sclerotinia International Symposium - BotrySclero2022, Avignon (FR)	13-17 Jun 2022	1.3
► **Presentations**		
Oral presentation at Annual Meeting Experimental Plant Sciences 2021 (virtual)	13 Apr 2021	1.0
Oral presentation at EPS Theme 2 Symposium 2022 (virtual)	08 Feb 2022	1.0
Poster presentation at the 31st Fungal Genetics Conference (virtual)	15 Mar 2022	1.0
Flash Talk at Annual Meeting Experimental Plant Sciences 2022	12 Apr 2022	1.0
Oral presentation at BotrySclero2022	16 Jun 2022	1.0
► **Interviews**		
► **Excursions**		
Subtotal Scientific Exposure		17.1

3) In-Depth Studies	date	cp
► **Advanced scientific courses & workshops**		
EPS Course: Transcription Factors and Transcriptional Regulation, Wageningen (NL)	10-12 Dec 2018	1.0
PE&RC/SENSE Course: Introduction to R for Statistical Analysis, Wageningen (NL)	20-21 Feb 2019	0.6
10th EPS-UU Summer School 'Environmental Signaling in Plants', Utrecht (NL)	26-28 Aug 2019	0.9
IS-MPMI Workshop: Taking MPMI Discoveries To the Field, Online	02 Dec 2020	0.2
► **Journal club**		
Literature discussion workshop (Botrytis group and Phytopathology Laboratory)	2018 -2021	1.0
► **Individual research training**		
Training "CRISPR-Cas for gene knock-out in *Botrytis* ", Technische Universität Kaiserslautern (DE)	19-23 Aug 2019	1.5
Training "Botrydial production and purification", University of Cadiz (ES)	18 Nov-10 Dec 2019	1.5
Subtotal In-Depth Studies		6.7

4) Personal Development	date	cp
► **General skill training courses**		
WGS Course: The Essentials of Scientific Writing and Presenting, Wageningen (NL)	10-20 May 2019	1.2
EPS Course: EPS Introduction Course, Wageningen (NL)	11 Jun 2019	0.3
WGS Course: Critical Thinking and Argumentation, Wageningen (NL)	19 Sep 2019	0.3
Wageningen in'to Languages Course: Basic Dutch 1, Wageningen (NL)	02 Mar-30 Jun 2020	1.5
WGS Course: Adobe InDesign Essential Training, Online	09 - 10 Nov 2020	0.6
WGS Course: Project and Time Management, Wageningen (NL)	28 Sep - 09 Nov 2021	1.5
WGS Course: Posters and Pitching, Wageningen (NL)	10 Mar - 07 Apr 2022	1.0
► **Organisation of meetings, PhD courses or outreach activities**		
Organisation of the Phytopathology PhD meetings	2019-2021	1.0
PhD representative in the Phytopathology Management Team	Nov 2021 - Feb 2022	0.4
► **Membership of EPS PhD Council**		
Subtotal Personal Development		7.8

5) Teaching & Supervision Duties	date	cp
► **Courses**		
Molecular aspects of bio-interactions (supervision of a mini-project)	Nov - Dec 2018	1.0
Genomics	Mar - Apr 2019	0.8
Genomics	Oct - Nov 2019	0.7
Plant-microbe interactions	May 2022	0.5
► **Supervision of BSc/MSc students**		
MSc major thesis-Jelmer Dijkstra	Jul 2019 - Dec 2019	0.5
MSc major thesis-Tim Bosman	Jul 2020 - Aug 2021	0.7
MSc minor thesis-Haris Spyridis	Jan 2022 - Jul 2022	0.6
MSc major thesis-Sabine de Graauw	Feb 2022 - Aug 2022	0.7
MSc major thesis-Sanna Henriquez	Sep 2022 - Mar 2023	0.5
Subtotal Teaching & Supervision Duties		6.0

TOTAL NUMBER OF CREDIT POINTS*	**40.1**

Herewith the Graduate School declares that the PhD candidate has complied with the educational requirements set by the Educational Committee of EPS with a minimum total of 30 ECTS credits.

** A credit represents a normative study load of 28 hours of study.*

Si Qin was sponsored by the China Scholarship Council (CSC).

The research described in this thesis and the printing of this thesis were supported by The Laboratory of Phytopathology, Wageningen University.

Cover design by Si Qin and Xingzi

Layout by Si Qin

Printed by Ridderprint | https://www.ridderprint.nl